Polymeric Delivery of siRNA for Breast Cancer Therapy

by

Manoj B. Parmar

A thesis submitted in partial fulfillment of the requirements for the degree of

Doctor of Philosophy

in

Pharmaceutical Sciences

Faculty of Pharmacy and Pharmaceutical Sciences

University of Alberta

Abstract

Breast cancer is the second most common cancer in women, and the leading cause of cancer-related deaths among women. Conventional breast cancer therapeutic strategies such as surgical removal of tumor, radiation therapy and chemotherapy have several limitations and non-specific effects on non-malignant cells, which warrant a search for alternative and specific therapeutic strategies. RNA interference (RNAi) holds a great promise as more specific and targeted therapy for breast cancer. RNAi using short-interfering RNA (siRNA) could silence a specific gene critical for the uncontrolled growth of cancer cells. Since the delivery of siRNA is a main barrier for implementation of RNAi therapy, we explored the potential of a non-viral delivery system using low-molecular weight polyethylenimines (PEIs) substituted with lipidic moieties. Among the library of modified PEIs, linoleic acid substituted PEI (PEI-LA) delivered siRNAs successfully and higher uptake of siRNA/polymer complexes was observed compared to native PEI. Using PEI-LA delivery system, we first identified potential cell cycle protein targets from the library of 169 siRNAs, and cell division cycle protein 20 (CDC20), a recombinase RAD51, and serine/threonine protein kinase CHEK1 have emerged as promising targets in breast cancer cells. After validating all identified cell cycle proteins *in vitro*, CDC20 siRNA was delivered *in vivo*. The tumor growth was successfully decreased with CDC20 siRNA delivery. We then explored the potential of combinational siRNA delivery against cell cycle and anti-apoptotic proteins as these proteins are essential for cancer cell growth and survival, and targeting both proteins simultaneously may result into synergism of therapy. After delivering two cell cycle proteins (TTK protein kinase and CDC20) and an anti-apoptotic protein (survivin), we observed synergistic effects of combinational siRNA

therapy in breast cancer cells for selected siRNAs. We also determined the potential non-specific effects of combinational siRNA delivery in non-malignant cells *in vitro*. Non-specific effects of siRNA could be minimized with specific formulation of siRNA/polymer complexes. We then focused on to tackle metastasis of breast cancer. Several reports confirmed overexpression of protein phosphatases in metastatic breast cancer, which laid the foundation of our hypothesis to target cell cycle and phosphatase proteins simultaneously to decrease not only breast cancer cell growth, but also metastasis. We performed a library screen consisting of 267 phosphatase siRNAs, and identified PPP1R7, PTPN1, PTPN22, LHPP, PPP1R12A and DUPD1 as potential phosphatase targets to decrease migration of breast cancer cells. Down-regulation of CDC20 and identified phosphatase by siRNA inhibited breast cancer cell growth as well as migration. Here we used hyaluronic acid modified siRNA/PEI-LA polyplexes that showed higher siRNA efficacy compared to non-modified complexes. The higher efficacy of siRNA was due to improved physicochemical characteristics of polyplexes, such as better dissociation of siRNA from its carrier and better availability of siRNA in the cytoplasm. These polyplexes were also used to deliver CDC20 and survivin siRNAs, which inhibited breast cancer cell growth significantly regardless of its phenotype. However, these siRNAs inhibited non-malignant cell growth as well. A careful formulation of siRNA polyplexes is needed to minimize side-effects of siRNA delivery to normal cells. Overall, we established an importance of targeting cell cycle proteins in breast cancer as well as formulation of siRNA polyplexes with a functional and non-toxic siRNA delivery carrier (PEI-LA). The effects of siRNA therapy seem to be independent of breast cancer phenotypes, so that this therapy could be functional for a range of breast cancers and additionally in other types of cancers.

Preface

Parts of this thesis have previously been published, as described below. All chapters presented here are conceptualized, researched and written by me with the involvement of supervisory author, Dr. Hasan Uludag. Specific contribution of other authors in each chapter are acknowledged and outlined below. Additional acknowledgements are listed at the end of respective chapter.

Chapter 1 is a literature review that summarizes cell cycle, anti-apoptotic and phosphatase protein targets for RNAi therapy, and highlights the important of the research work. This chapter includes portions about cell cycle and RNAi reagents from a previously published book chapter (Parmar MB, Uludağ H. Targeting cyclins and cyclin-dependent kinases involved in cell cycle regulation by RNAi as a potential cancer therapy. pp 23-45. *In:* Braddock M. (ed.), *Nanomedicines: design, delivery and detection*, 2016, Royal Society of Chemistry, London, UK). As the lead author of this book chapter, I was responsible for concept formation, conducting the literature review and writing the manuscript.

A version of **Chapter 2** is published as Parmar MB, Aliabadi HM, Mahdipoor P, Kucharski C, Maranchuk R, Hugh JC, Uludağ H. Targeting cell cycle proteins in breast cancer cells with siRNA by using lipid-substituted polyethylenimines. *Front Bioeng Biotechnol*, 2015, 3:14. This chapter summarizes the newly identified cell cycle proteins targets for breast cancer therapy as well as *in vivo* study performed for specific cell cycle protein target. The ethics approval to use animals in this chapter was obtained from Animal Care and Use Committee: Health Sciences at the University of Alberta (File no. AUP00000423) in accordance with the directions of the Canadian Council on Animal Care. As the primary author, I was responsible for concept formation, executing all the

experiments and writing manuscript. H. Aliabadi and C. Kucharski assisted to carry out *in vivo* experiments, while P. Mahdipoor and R. Maranchuk were involved in *in vitro* experiments. J. Hugh assisted in interpreting the results and editing the manuscript.

Chapter 3 is a research article focused on combinational siRNA therapy against cell cycle and anti-apoptotic proteins (Parmar MB, Arteaga Ballesteros BE, Fu T, K.C. RB, Montazeri Aliabadi H, Hugh JC, Löbenberg R, Uludağ H. Multiple siRNA delivery against cell cycle and anti-apoptosis proteins using lipid-substituted polyethylenimine in triple-negative breast cancer and nonmalignant cells. *J Biomed Mater Res A*, 2016, 104:3031-3044). B. Arteaga Ballesteros and T. Fu were undergraduate students, who worked on this project under my guidance. As the first author, I was responsible for concept formation, executing most of the experiments and writing manuscript. R. KC synthesized polymers for siRNA delivery, while H. Montazeri Aliabadi, J. Hugh and R. Löbenberg helped in the concept formation and manuscript editing.

Chapter 4 is a research paper that was published as Parmar MB, Meenakshi Sundaram DN, K.C. RB, Maranchuk R, Montazeri Aliabadi H, Hugh JC, Löbenberg R, Uludağ H. Combinational siRNA delivery using hyaluronic acid modified amphiphilic polyplexes against cell cycle and phosphatase proteins to inhibit growth and migration of triple-negative breast cancer cells. *Acta Biomater*, 2018, 66:294-309. This chapter is focused on combinational siRNA therapy to target metastatic breast cancer. As the lead author, I designed, performed and analyzed the studies, and wrote the manuscript. D. Meenakshi Sundaram and R. Maranchuk assisted in siRNA library screening, while R. KC synthesized polymers for siRNA delivery. H. Montazeri Aliabadi, J. Hugh and R. Löbenberg helped in the concept formation and manuscript writing.

A version of **Chapter 5** is accepted for publication as Parmar MB, K.C. RB, Löbenberg R, Uludağ H. Additive polyplexes to undertake siRNA therapy against CDC20 and survivin in breast cancer cells. *Biomacromolecules*, 2018, 19:4193–4206. As the lead author, I designed, performed and analyzed the studies, and wrote the manuscript. R. KC synthesized polymers for siRNA delivery, while R. Löbenberg helped in the concept formation and manuscript editing.

Chapter 6 consists of overall discussion, conclusions and future directions. This chapter mainly derived from the discussion and conclusions of above five chapters and knowledge gained from the work presented here.

Acknowledgements

Over the course of my PhD studies, I have had the privilege to work with many talented researchers and wonderful colleagues, and I would like to thank them for their valuable inputs to further my personal as well as professional life. I would, first, like to express my deepest gratitude towards my supervisors, Dr. Hasan Uludağ and Dr. Raimar Löbenberg, for their invaluable guidance and support throughout my program. Last five and half years couldn't be more enjoyable and fruitful to develop myself as an independent researcher without their company. I would also like to acknowledge my committee member, Dr. Michael Weinfeld for his useful comments by taking interest in my projects. Many thanks to Dr. Hamidreza Montazeri Aliabadi and Cezary Kucharski for their advice and help in many experimental techniques. I would specifically like to show my gratitude towards my colleagues, Dr. Remant KC, Dr. Juliana Valencia-Serna, Dr. Deniz Meneksedag-Erol, Eleni Tsekoura, Anyeld Ubeda, Bindu Thapa, Daniel Nisakar, Aysha Ansari and Mahsa Mohseni, to whom I enjoyed working with as their different educational background brought many skills to the lab that created a positive research environment.

I would like to extend my thanks to all the funding agencies that have supported me during my doctoral studies, particularly Women and Children's Health Research Institute (WCHRI) and Alberta Innovates-Health Solutions (AIHS) for granting Graduate Studentships. I was also supported with several scholarships and travel awards to attend conferences by Faculty of Pharmacy and Pharmaceutical Sciences, and Faculty of Graduate Studies and Research. As well, my PhD projects were supported by operating grants from Canadian Breast Cancer Foundation (CBCF) and Natural Sciences and Engineering Council of Canada (NSERC).

A special thanks to my M.Sc. supervisor, Prof. Jonathan Wright from Dalhousie University for inviting me to Canada, and furthering my research skills. My work on Molecular Biology at the Wright Lab has laid the foundation for my PhD thesis. Many thanks to my undergraduate mentor, Dr. Shivani Patel, Shree M. & N. Virani Science College, India for always motivating me to pursue my career in research.

A huge thanks to my parents, my brother Hiren and my sister-in-law Archita for always providing moral support and motivating me to finish the journey of PhD studies with flying colors. Special heartfelt thanks to my beloved wife, Snehal for always standing by my side and replenishing me with cheers all the time. Thanks for always boosting my moral to achieve the highest educational degree that is being offered in the world. Thanks to my closest friends, Virendrabhai and Bhavnabhabhi who became a second family away from family. Without unconditional friendship and support from family and friends, none of this would have been possible.

Lastly, a warm gratitude to my spiritual guru, P.P. Hariprasad Swamiji for his continuous inspiration and guidance to follow righteous path.

Table of Contents

List of Tables

List of Figures

List of Abbreviations

APC	Anaphase Promoting Complex
AR	Androgen Receptor
BCL2	B-cell lymphoma 2
BCR	B-cell receptor
bFGF	Basic Fibroblast Growth Factor
BRCA1/2	Breast Cancer Type 1/2
CA	Caprylic Acid
CCNB1	Cyclin B1
CD44	Cluster of Differentiation-44
CDC2	Cell Division Cycle 2
CDC20	Cell Division Cycle Protein 20
CDKs	Cyclin-Dependent Kinases
c-FLIP	Cellular FLICE-inhibitory proteins
CLL	Chronic Lymphocytic Leukemia
CPC	Chromosomal Passenger Complex
CsiRNA	Scrambled Control siRNA
ddPCR	Droplet Digital Polymerase Chain Reaction
DLS	Dynamic Light Scattering
DMSO	Dimethyl Sulfoxide
DOX	Doxorubicin
DS	Dextran Sulfate
DsiRNA	Dicer-Substrate siRNA
dsRNA	Double-Stranded RNA
DUSP27	Dual Specificity Phosphatase 27
EDTA	Ethylene diamine tetra acetic acid
ELS	Electrophoretic Light Scattering
ER	Estrogen Receptor
FADD	Fas-associated protein with death domain
FBS	Fetal Bovine Serum
FZR1	Fizzy-related protein 1
HA	Hyaluronic Acid
hBMSC	Human bone marrow stromal cells
HBSS	Hank’s Balanced Salt Solution
HER2	Human Epidermal Growth Factor Receptor 2-Neu
HUVEC	Human umbilical vein endothelial cells
IAP	Inhibitor of Apoptosis Proteins
KSP	Kinesin Spindle Protein
LA	Linoleic Acid

LHPP	phospholysine phosphohistidine inorganic pyrophosphate phosphatase
M phase	Mitotic Phase
MC	Methyl Cellulose
miRNA	microRNA
MPF	M-phase promoting factor
MPS1	Monopolar Spindle 1
mRNA	messenger RNA
MYPT1	Myosin Phosphatase Target Subunit 1
NSCLC	Non-Small-Cell Lung Carcinoma
NTC	No Template Control
OD	Optical Density
PA	Poly(acrylic) Acid
PARP	Poly(ADP-Ribose) Polymerase
PDI	Polydispersity Index
pDNA	Plasmid DNA
PEG	Polyethylene Glycol
PEI	Polyethylenimine
PEI-LA	Polyethylenimine substituted with linoleic acid
PLK1	Polo-Like Kinase 1
POC	Percent of Control
PR	Progesterone Receptor
pre-miRNA	Precursor miRNA
pri-miRNA	Primary miRNA
PRL3	Phosphatase of regenerating liver 3
PTP	Protein Tyrosine Phosphatase
PTP1B	Protein-Tyrosine Phosphatase 1B
PTTG1	Pituitary Tumor-Transforming Gene 1
QNBC	Quadruple Negative Breast Cancer
RISC	RNA-Inducing Silencing Complex
RLC	Regulatory Light Chain
RNAi	RNA interference
RT-qPCR	Reverse transcription – quantitative PCR
shRNA	Short Hairpin RNA
siRNA	Short-interfering RNA, Small-interfering RNA
TAME	Tosyl-L-Arginine Methyl Ester
TNBC	Triple-Negative Breast Cancer
TOP2A	Topoisomerase II A
TRAIL	TNF-related apoptosis-inducing ligand
αLA	α-Linoleic Acid

Scope

The main objectives of my thesis were (i) to identify novel and establish effective therapeutic targets; and (ii) to develop effective delivery systems for siRNA-mediated breast cancer therapy. Current breast cancer therapies come with significant limitations and side-effects, which warrant a search for alterative breast cancer therapies. RNAi-mediated targeting of deregulated proteins is a specific therapy as siRNA silences a specific targeted protein at mRNA levels. Since siRNA delivery needs a carrier, we synthesized, characterized and formulated polyethylenimine (PEI) based siRNA delivery carrier to improve the transfection efficiency. Our endeavor in this thesis was to establish a potential of siRNA-mediated targeting of deregulated cell cycle proteins. We hypothesized that silencing deregulated or overexpressed cell cycle proteins with siRNA may decrease the growth of breast cancer cells. We further hypothesized that combinational siRNA therapy against cell cycle and anti-apoptotic proteins may lead to synergistic effects of siRNA delivery, and simultaneous siRNA-mediated silencing of cell cycle and phosphatase proteins may decrease breast cancer cell growth as well as metastasis.

We first performed a literature review (**Chapter 1**) to bring the importance of targeting cell cycle proteins in cancer. We specifically focused on cell division cycle protein 20 (CDC20) as it was a lead target in other chapters. We also explored literature to observe the feasibility of combinational siRNA targeting against cell cycle proteins and anti-apoptotic/phosphatase proteins to tackle metastatic cancer. We then focused on nanoparticles engineering to efficiently deliver siRNA in cancer cells.

The aims of **Chapter 2** were to identify potential cell cycle protein targets for siRNA therapy in breast cancer cells as well as to establish the best PEI-based siRNA

delivery system to exert a maximum therapeutic effect. After screening siRNA library targeting cell cycle proteins, we validated identified targets followed by combinational siRNA therapy against multiple cell cycle proteins. CDC20 emerged as the most promising target, and we determined the validity of CDC20 siRNA *in vivo* for therapeutic purpose in this study. Here we synthesized PEI substituted with linoleic acid (PEI-LA) for siRNA delivery and determined its efficacy compared to other commercially available carriers.

We further explored the combinational siRNA therapy against cell cycle and anti-apoptotic proteins in **Chapter 3**. We first evaluated a siRNA delivery efficiency using polymers with different degree of LA substitution in PEI, and characterized these polymers by determining the size and charge of nanoparticles as well as siRNA uptake efficiency of delivery carrier. We then optimized combinational siRNA therapy in breast cancer cells, and determined its outcome in non-malignant cells such as endothelial, bone marrow stromal and normal breast cells.

The objective of **Chapter 4** was to tackle metastatic breast cancer by delivering combinational siRNA against cell cycle and phosphatase proteins. We formulated and characterized hyaluronic acid modified siRNA/PEI-LA polyplexes to improve siRNA transfection efficiency. The specific aim of this study was to identify potential protein phosphatases that contribute to metastasis of breast cancer cells. Silencing these protein phosphatase targets by siRNA could decrease the migration of breast cancer cells. Once the phosphatases were identified and validated, those were targeted along with CDC20 to decrease breast cancer cell migration as well as growth simultaneously.

Chapter 5 was carried out to reveal the main mechanism by which hyaluronic acid modified siRNA/PEI-LA nanoparticles showed improved siRNA efficacy. We also

determined whether different nucleic acid therapeutics could be delivered with the same delivery system that was developed for siRNA delivery. Other aims of this study were to determine whether siRNA therapy could applied to different phenotypic breast cancers, and to compare the effects of siRNA delivery in breast cancer vs. non-malignant cells.

We conclude this thesis with **Chapter 6**, where we specifically discussed about targeting cell cycle, anti-apoptotic and phosphatase proteins in breast cancer by siRNA therapy. We also outlined the future studies that are needed to further clarify the importance of targeting these proteins in breast cancer. We then summarized how nanoparticles engineering helped to improve siRNA transfection and how we can improvise further.

Overall, we established the importance of targeting cell cycle proteins in breast cancer and developed a novel siRNA delivery system. The original contributions of this thesis in the field were: (i) identified and established CDC20 as a promising target in breast cancer; (ii) established the combinational siRNA therapy against cell cycle and anti-apoptotic proteins for improved efficacy of siRNA delivery; (iii) identified novel protein phosphatase targets to tackle metastasis of breast cancer by siRNA therapy; (iv) developed novel siRNA delivery system using PEI and polyanionic polymer that improved the efficacy of siRNA; (v) determined mechanistic understanding of higher efficacy of additive polyplexes; (vi) determined non-specific effects of siRNA delivery in non-malignant cells.

1. RNAi-mediated targeting of cell cycle proteins for breast cancer therapy

Parts of this chapter were published in:

Parmar MB, Uludağ H. Targeting cyclins and cyclin-dependent kinases involved in cell cycle regulation by RNAi as a potential cancer therapy. pp 23-45. *In:* Braddock M. (ed.), *Nanomedicines: design, delivery and detection*, 2016, Royal Society of Chemistry, London, UK.

1.1 Background

Cancer is the second leading cause of death worldwide with nearly 1 in 6 deaths occurring due to this deadly disease (World Health Organization, Geneva, Switzerland). Despite significant advancements in the understanding of fundamental cancer biology, diagnostics and treatments, the overall mortality still remains high with 8.8 million deaths globally in 2015. One of the major reasons behind high mortality by cancer is the lack of target-specific administration of therapeutic agents, which leads to significant side effects of treatment by affecting healthy cells and tissues [1]. The conventional therapeutic strategies such as surgical removal of tumor, radiation therapy and chemotherapy have their own limitations and non-specific effects on non-malignant cells [2]. Therefore, there is an urgent need to search for an alternate, more specific and targeted therapy for cancer.

RNA Interference (RNAi) has emerged as a potential targeted therapy for cancer over the past decade, where double-stranded RNA (dsRNA) is introduced to the cancer cells leading to the translational arrest or degradation of a specific mRNA, resulting in the silencing of specific targeted protein [3]. Targeting overexpressed or critical cell survival protein by RNAi may lead to inhibition of cancer cell growth. Over the past decade, several lines of proteins were targeted by RNAi and a high promising outcome of RNAi therapy have been produced, leading to several clinical trials of this therapy [4].

In this chapter, we review the potential of targeting cell cycle, anti-apoptotic and phosphatase proteins by RNAi therapy specifically in breast cancer along with the current therapies of breast cancer. We also discuss the mechanism of RNAi therapy with the formulation of RNAi therapeutic agents and its delivery carrier.

1.2 Breast cancer and its current therapies

Breast cancer is the second most common cancer in women (World Cancer Research Fund International, London, UK), and the leading cause of cancer-related deaths among women (World Health Organization). Breast cancer is impacting over 1.5 million women each year with nearly 570,000 deaths by breast cancer alone in 2015, which is approximately 15% of all cancer-related deaths among women. Breast cancer risk increases twice each decade until menopause, and the risk decreases after. However, breast cancer is diagnosed after menopause in women as well [5]. Survival rates for breast cancer have generally improved worldwide due to better detection strategies of early diagnosis and screening [6]. The detection of early stage breast cancer leads to high survival rate compared to detection at more advanced stage breast cancer. Breast cancer stage is usually referred to a number on a scale of 0 to IV. Stage 0 describes the non-invasive breast cancer that typically remains within its origin of location. Breast cancer that has invaded the surrounding tissue refers as Stage I breast cancer. Stage II describes the invasive breast cancer that has spread to lymph nodes. Breast cancer that has invaded axillary lymph nodes or lymph nodes near the breastbone refers as Stage III. Stage IV describes invasive breast cancer that has spread to other organs of the body such as the lungs, distant lymph nodes, skin, bone, or liver, which oftentimes refers as metastatic breast cancer.

Breast cancer is a heterogeneous disease comprising several molecular subtypes, which carries important predictive and prognostic values, resulting into incorporation of these subtypes to initial breast cancer diagnosis process. Commonly exploited molecular subtypes of breast cancer are based on the presence of estrogen receptor (ER), progesterone receptor (PR), and human epidermal growth factor receptor 2-neu (HER2). Recently, androgen receptor (AR) has found to be the forth key receptor in breast cancer [7]. Several

targeted therapies have been developed for HER2-positive breast cancer based on the interaction of a therapeutic molecule with this receptor, which can extend survival by many years [8]. Endocrine therapies are also available for ER- and PR-positive subtype [8]. However, these therapies have failed for triple-negative breast cancer (TNBC) that lacks ER, PR and HER2 receptors as well as quadruple negative breast cancer (QNBC) that lacks all four receptors. In addition, receptor targeted therapies have poor outcome when breast cancer has already metastasized.

1.2.1 Current therapies for breast cancer

Current breast cancer therapies can be classified as local and systemic treatments. Local treatments include surgical removal of diseased tissue and radiation therapy, while systemic treatments comprise of chemotherapy, hormone therapy and targeted therapy [9]. By virtue of early detection and screening, early stage breast cancer can be completely resected by surgery. The disease, however, may come back over time even after complete resection, which has prompted the development of adjuvant and neoadjuvant chemo and hormone therapies [10]. Surgery followed by adjuvant or neoadjuvant therapy accounts for the standard breast cancer treatment for a long time.

1.2.1.1 Local treatments for breast cancer

Surgical removal of diseased breast tissue (lumpectomy) or entire breast (mastectomy) is more common to remove as much of the cancer as possible [11]. The lumpectomy is preferable for early staged breast cancer, while mastectomy is needed for advanced breast cancer. Metastasized lymph nodes are often considered to be removed while performing surgery. While surgery does not cure the disease and chances of cancer coming back is higher, adjuvant or neoadjuvant therapy is more advised after surgery,

which would actually increase the long-term survival of a patient. Breast cancer patient also has an option of breast reconstructive surgery after removal of diseased tissue [11].

Another localized treatment for breast cancer is radiation therapy, which is determined based on the type of surgery and stage of cancer [12]. Radiation therapy is mostly required after breast-conserving surgery or mastectomy. It can broadly be divided into two categories of external beam radiation and brachytherapy [13,14]. External beam radiation is the most common type of radiation therapy, where an externally generated radiation is focused on the affected area of breast. In brachytherapy, a device containing radioactive seeds or pellets is placed into the breast tissue for a short time in the area where diseased tissue had been removed. Swelling in the breast, fatigue and skin changes such as redness, peeling, darkening are the short-term side effects of radiation therapy. Breast pain and stiffness, limited options for breast reconstruction, problems with breastfeeding, damage to nerves of the arm, and a rare complication of angiosarcoma [15] are the common side effects of radiation therapy.

1.2.1.2 Systemic treatments for breast cancer

Systemic treatments are often used to treat breast cancer by delivering drugs mostly intravenously. Adjuvant and neoadjuvant chemotherapies are the most common systemic treatment, where small molecule drugs are delivered after or before surgical removal of breast tumor to decrease the recurrence of cancer or to decrease the burden of locally advanced tumor [16]. Chemotherapy is also well-outlined for metastatic breast cancer, where the treatment may be given for longer time depending on the tolerance of patient. Commonly used adjuvant and neoadjuvant chemotherapeutic drugs are anthracyclines (doxorubicin and epirubicin), taxanes (paclitaxel and docetaxel), 5-fluorouracil,

cyclophosphamide and carboplatin [17]. Combination of 2-3 drugs are usually administered in early stages of breast cancer, while a single drug is more preferred in advanced metastatic breast cancer, which includes commonly used drugs as well as cisplatin, vinorelbine, capecitabine, gemcitabine, ixabepilone and eribulin. Chemotherapy comes with significant side effects such as hair loss, mouth sores, loss of appetite, body weight changes, nausea, vomiting and diarrhea. The major affected tissue is blood, where blood cells count decreases, leading to higher chances of infections due to low white blood cells, easy bruising or bleeding because of low platelets and fatigue due to low red blood cells [18]. All these temporary side effects wear off as the doses of chemotherapy is finished. However, certain long-term and permanent side effects are also associated with this treatment. There is a high risk of changes in menstrual periods, premature menopause and infertility in women due to chemotherapy, which may lead to bone loss and osteoporosis [18]. Pregnancies during chemotherapy may lead to birth defects. There is a high risk of cardiomyopathy and neuropathy as a long-term side effects of chemotherapy, which may often become permanent. Moreover, there are some reports of a slight decrease in mental functioning with concentration and memory, which may last for a long time in the patient. Since bone marrow is also greatly affected by chemotherapeutic agents, a rare condition called, myelodysplastic syndromes or acute myeloid leukemia may occur after relatively long period of treatment [18].

Another common systemic treatment of breast cancer is hormone therapy, where overexpressed ER and PR are blocked, or estrogen/progesterone hormone levels are lowered down to contain uncontrolled breast cancer cell growth [19]. Several lines of therapies have been developed that block ER or PR. Tamoxifen is a widely used ER

blocking drug that is mostly administered as adjuvant or neoadjuvant therapy [20]. Oftentimes, tamoxifen is also given to women at high risk of breast cancer. Another ER blocker, toremifene is given orally for metastatic breast cancer [21]. Side effects of ER blocker drugs include hot flashes, nausea, vomiting, vaginal discharge and vaginal bleeding. Uncommon and rare side effects of tamoxifen and toremifene are blood clots and strokes. Hormone therapy that lowers estrogen production also helps to decrease cancer cell growth. Aromatase inhibitors are used to inhibit the activity of aromatase, an important enzyme for estrogen production in fat tissues [22]. However, the main source of estrogen is ovary so that ovarian suppression by surgically removing ovaries is performed followed by aromatase inhibitor therapy. The common side effects of these inhibitors are muscle pain, joint stiffness and rare blood clots. Osteoporosis is one of the major concerns of these inhibitors, where bone density should regularly be checked and drugs to strengthen bones should be taken.

Targeted therapies are chosen based on the overexpression of several proteins in breast cancer cells. HER2 targeted drugs are frequently prescribed due to aggressive growth and spread of HER2-positive breast cancer. Trastuzumab and pretuzumab are monoclonal antibodies that target HER2 [23]. There are reports of heart damage during or after HER2 targeted therapies that may lead to congestive heart failure. The cyclin-dependent kinases (CDKs) inhibitors are targeting cell cycle to inhibit cell proliferation [24]. Several drugs that inhibit CDK4/6 are taken orally, whose side effects are reported to be low blood cell counts, fatigue, nausea, vomiting, hair loss and diarrhea. DNA repair proteins, PolyADP-ribose polymerase (PARP) and breast cancer type 1/2 (BRCA1/2) are targeted to stop DNA repair, resulting in breast cancer cell death [25]. The side effects of

DNA repair protein inhibitors include nausea, vomiting, diarrhea, fatigue, loss of appetite, anemia and muscle/ joint pain.

Owing to tremendous side effects of well-established therapies to treat breast cancer, a novel treatment is urgently warranted that mainly targets cancer cells without affecting normal cells. Our endeavor here in this thesis is to establish a potential of RNAi-based therapeutics against cell cycle, anti-apoptotic and phosphatase proteins to address some of the challenges of breast cancer therapies.

1.3 Targeting cell cycle proteins in malignant cells

The cell cycle is the complex, tightly regulated process of cell division [26]. When cell-cycle is deregulated, normal cells could transform into cancer cells with enhanced potential to migrate and proliferate. In such cases, proteins involved in cell cycle progression may no longer appropriately regulate different stages of events critical for cell division, leading to decoupling of various integrated processes. Transformed cells typically proliferate at a rate faster than the normally tightly regulated reproduction of normal cells without any (or less) quality control, which could lead to a tumor formation [27,28]. The cell cycle is usually arrested upon detecting the presence of damaged DNA in normal cells, where DNA repair process kick-starts the repair of damaged genetic information. Transformed cells, on the other hand, can proceed for synthesis of damaged DNA followed by their division without arresting the cell cycle, resulting in an unregulated proliferation of cells. The altered genetic information that appears in the progeny is sometimes benign with no functional consequences, but could often impart undesired properties to daughter cells [28-30]. The essential cell cycle proteins that are up-regulated and are capable of imparting undesired properties to transformed cells would be potential targets for cancer

therapy; the inhibition of their expression could be pursued in order to arrest cells at quality control checkpoints and/or to induce apoptosis of transformed cells [27,30].

1.3.1 Overview of cell cycle

The cell cycle constitutes a series of complex events that lead to physical division and multiplication of a cell [26]. Cell cycle is broadly defined by two phases: *interphase*, where the cell prepares itself for a division, and *mitosis*, where the cell divides its nuclear materials into two separate daughter cells [26,31]. Several checkpoints exist in the cell cycle to ensure that the cell is ready to divide. If severe damage is detected during the checkpoints, cell division is arrested at that checkpoint and the apoptotic pathway is immediately activated to eradicate the cell. The cell cycle is a continuous process for certain types of cells, and cells are continually entering and exiting this process in their lifetime [26,31].

The interphase includes G1, S and G2 phases, where the first gap phase (G1) occupies the longest time of the cell cycle **(Fig 1.1)**. G1 phase comes immediately after finishing previous cell division during the active stage of cell proliferation. It is the phase where the cell prepares itself for the next cell division by synthesizing the new proteins and organelles needed for daughter cells, resulting in the growth of cell size. During the G1 phase, the cell must decide whether to stay in this phase and commit for a division or leave this phase and remain in the G0 phase. If the cell is not ready for division, it enters the latent G0 phase, which can last for a longer period until enough growth factors and other essential elements become available. Once the required amount of nutrients is available, cell re-enters the G1 phase and starts synthesizing proteins needed for DNA replication.

The duration of G1 is different depending on the cell type and, for human somatic cells, it may take approximately 40% of a complete cell cycle [32,33].

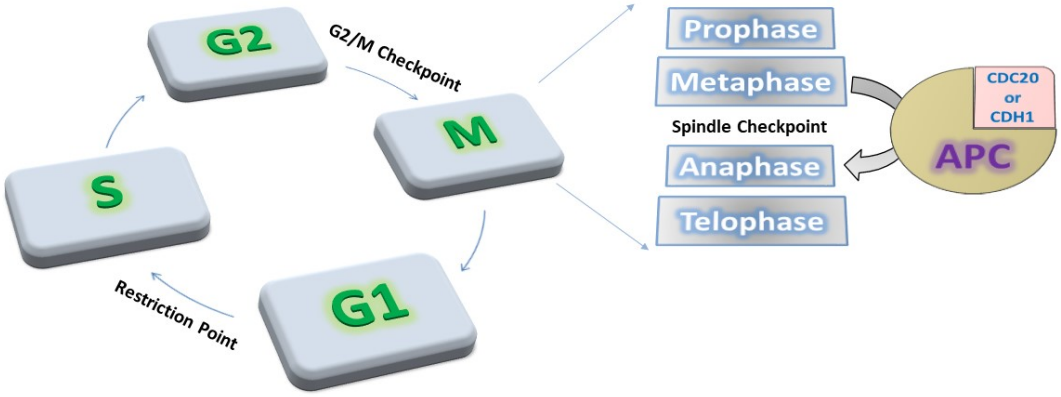

Fig 1.1: Schematic representation of cell cycle with restriction point and checkpoints.

Anaphase Promoting Complex (APC) with co-activator CDC20/CDH1 facilitates the entry of cell into anaphase from metaphase.

After necessary proteins are synthesized in the G1 phase, cell proceeds into the S phase, where the DNA replication is the major event. However, proteins and enzymes that are required for DNA replication are also synthesized in this phase. DNA replication is a very tightly regulated process. Only a single replication is ensured by loading pre-initiation complex on the DNA, which duplicates the entire genome for the two daughter cells. If DNA damage occurs in this phase, it is repaired by initiating several DNA damage strategies depending on the type of damage. In case of un-repairable DNA damage, expression of apoptotic proteins increases to eliminate the mutated cell [32,33].

The last and the shortest gap phase is G2, where the proteins that are required for mitosis are synthesized. The G2 phase ends with the prophase of mitosis, where cellular chromatin condenses into chromosomes. Some transformed cells can directly enter mitosis from S phase as G2 phase is least important in cell cycle [34]. Since this is the last phase

before entering mitosis, it also allows a checkpoint to ensure the correctness of DNA replication and synthesis of organelles. G2 phase ends with the mitosis (M phase) that is division of chromosomes into two identical nuclei followed by division of cytoplasm and cell membrane. The stages of M phase include prophase, metaphase, anaphase, telophase and cytokinesis. At the end of a 'normal' cell cycle, two identical daughter cells are expected to be formed.

1.3.2 Restriction point and checkpoints

The concept of checkpoints in cell cycle regulation was first introduced by Hartwell and Weinert in 1989 [35]. The mechanism of sending an inhibitory signal to later cell cycle events in response to current incomplete event is called as checkpoint. There are three checkpoints in the eukaryotic cell cycle: G1/S, G2/M and metaphase/anaphase checkpoints **(Fig 1.1)**. If the conditions of each phase are not met at these points, cell cycle progression can be halted. The point of no return during G1 phase of cell cycle is called restriction point [36,37]. Cell determines whether to exit cell cycle and remain in quiescent (G0) phase at this checkpoint. If the environmental factors favor replication of the entire genome, cell commits to enter the S phase. After the restriction point is cleared, the cell has the capacity to complete cell cycle with limited nutrient availability following a slow rate of protein synthesis [37].

The G2/M checkpoint ensures that the whole genome is replicated, and the newly synthesized DNA is undamaged before going for chromosome condensation and division of nuclear material in the M phase. The M-phase promoting factor (MPF) plays a key role at this checkpoint [38]. If the cell detects a DNA damage, the phosphorylation of MPF at the tyrosine and threonine residues halt the entry of a cell into the M phase. The

metaphase/anaphase checkpoint is also known as spindle checkpoint, which prevents separation of sister chromatids until all chromosomes aligned at the mitotic plate and attached to the bipolar spindle through their kinetochores. The activation of anaphase promoting complex (APC) through MPF makes the entry of cell into anaphase. Once cell passes spindle checkpoint, completion of the cell cycle is assured.

1.3.3 Regulation of cell cycle by APC^{CDC20}/APC^{CDH1}

APC has a critical role at spindle checkpoint, which is being activated by the substrate recruiting module CDC20 (cell division cycle 20 homologue, also called Fizzy) or CDH1 (CDC20 homologue 1, also known as Fizzy-related protein 1, FZR1; **Fig 1.1**) [39,40]. APC^{CDC20}/APC^{CDH1} leads to ubiquitination-mediated destruction of mitotic cyclins as well as securin [41]. A protease separase is being released upon downregulation of securin, which cleaves cohesion of sister chromatids. Sister chromatids then start migrating towards respective poles, ultimately leading the cell into anaphase.

APC is a multi-subunit E3 ubiquitin ligase that has emerged as one of the major driving forces for cell cycle progression. APC consists of 14 subunits, namely APC1/TSG24, APC2, APC3/CDC27, APC4, APC5, APC6/CDC6, APC7, APC8/CDC23, APC10/DOC1, APC11, APC13/SWM1, APC15/MND2, APC16 and CDC26 along with its co-activator CDC20/CDH1 [42,43]. The large complex structure of APC remains poorly understood until recently when Chang et al. (2014) has mapped its structure using cryo-electron microscopy [44]. The complex structure of APC can be divided into several segments, a scaffolding subunit made up of APC1/APC4/APC5, a catalytic and substrate recognition subunit consist of APC2/APC11/APC10, a tetratricopeptide repeat arm of APC3/APC6/APC8, and an accessory subunit of APC13/CDC26/APC16.

1.3.3.1 Role of CDC20/CDH1

The main role of CDC20 or CDH1 is to activate APC, and serve as the substrate recognizing subunit by mediating WD40 domain dependent protein-protein interaction [45]. Once APC is activated by CDC20/CDH1, it recruits its substrate proteins for its degradation. The substrate specificity depends on the APC activating moiety as different substrate recruiting motifs are available in CDC20 and CDH1. Typically, destruction box (D-box) on targeted substrate is recognized by APC^{CDC20}/APC^{CDH1} that leads to the destruction of protein [46]. However, TEK and ABBA motifs in APC^{CDC20}, and KEN-box, A-box, O-box and CRY-box in APC^{CDH1} are also recognized for the recruitment of substrate proteins [47-52]. Several downstream substrates of CDC20 are involved in the progression of mitosis, including securin, cyclin B1, cyclin A, NEK2A, p21 and MCL1. Centrosomal kinase NEK2A that is required to form bipolar spindle is degraded by APC^{CDC20} upon entry of a cell to anaphase [53]. A well-characterized CDK inhibitor p21 is destroyed by CDC20 activation, leading to activation of CDKs necessary for mitosis [54]. In addition to regulating mitotic progression, CDC20 governs cellular apoptosis through regulating the stability of MCL1 and Bim [55,56].

Even though CDC20 and CDH1 activates APC, both have different biological functions. CDC20 activated APC helps to transit from metaphase to anaphase after degrading securin and cyclins, while CDH1 helps exiting mitosis and maintains G1 phase by inhibiting CDK activity [57,58]. CDH1 contributes to maintain genomic stability and acts as tumor suppressor [59]. On the contrary, CDC20 is considered to promote oncogenesis as it has been found to be upregulated in many cancers [60]. However, CDC20

is an essential developmental gene as embryonic lethality has been reported in mice upon disrupting the expression of CDC20 [61].

1.3.4 CDC20 in human malignancies

Recent evidence suggests an oncogenic role of CDC20 in several types of malignancies [60,62]. CDC20 has consistently found to be overexpressed in variety of cancers such as pancreatic, breast, lung, colorectal, gastric and liver cancers. In pancreatic, colorectal, gastric and hepatocellular malignant tumor tissues, high expression of CDC20 is evident compared to adjacent non-malignant tissues [63-66]. CDC20 has also been identified as a prognostic biomarker, and cell growth inhibition by spindle checkpoint arrest was evident upon depletion of CDC20 in human lung and pancreatic cancer cells [67,68]. Overexpression of CDC20 was evident in metastatic colorectal cancer and a shorter overall survival of patients [64]. CDC20 is also found to be having an oncogenic role in bladder, oral and cervical cancer [69-71]. Furthermore, G2/M cell cycle arrest upon downregulating CDC20 is reported that led to melanoma cancer cell growth inhibition [72].

Besides other types of cancer, CDC20 has also been demonstrated to play an essential role in breast cancer progression. The transcript and protein levels of CDC20 were significantly higher in not only breast cancer cell-lines, but also in primary breast cancer tissues compared to non-malignant breast cell-lines, normal mammary epithelial cells and normal breast tissues, suggesting a potential role of CDC20 to make breast cancer cells genetically unstable [73,74]. After following up with 445 breast cancer patients for up to 20 years, Karra et al. concluded a prognostic value of overexpressed CDC20 that may have contributed in aggressive course of disease with very high risk of death [75]. Breast cancer survival is reported to be extremely poor that is associated with high CDC20 expression.

Owing to the oncogenic role of CDC20 in tumorigenesis, the high promise of targeting CDC20 as a cancer therapy has recently been outlined [60,62]. Therefore, additional scientific investigation is necessary to advocate a promise with this cell cycle protein target, and clinical benefits of targeting CDC20 is also needed to be outlined in various cancers.

1.3.4.1 Targeting CDC20 with small molecular drugs

Since CDC20 has recently been established as a promising cancer therapeutic target, very few drugs have been tested to block the activity of CDC20 during cell cycle. A small molecule, TAME (tosyl-L-arginine methyl ester) has been reported to bind APC, occupying the CDC20/CDH1 binding site that leads to prevention of APC activation by CDC20/CDH1 [76]. However, TAME is not readily cell penetrable so that pro-TAME was developed that can penetrate through cell membrane and be processed by intercellular esterase [76]. Pro-TAME seems to be disrupting APC^{CDC20}/APC^{CDH1} that leads to mitotic arrest in the absence of spindle damage. Another small molecule, apcin binds CDC20 at the D-box binding site within WD40 domain, preventing CDC20 to activate APC during cell cycle [77]. On the contrary, withaferin-A enhances the degradation of CDC20 leading to mitotic delay [78]. Early investigations with other small molecular drugs such as NAHA, CFM4 and BCHHD7c revealed inhibition of CDC20 expression in various cancer cells [79-81]. All small molecules targeting CDC20 have only been tested *in vitro* and *in vivo*, clearly indicating an urgent need to pursue further investigation on these drugs that could lead to possible clinical application. However, there is always a threat to have unacceptable side effects by the small molecules. Therefore, a new strategy to target CDC20 may be a fruitful pursuit to decrease the malignant cell growth.

1.3.4.2 Targeting CDC20 with RNAi

CDC20 has recently been identified as a promising cancer therapeutic target, but only few RNAi-mediated studies have been reported that specifically silence CDC20 expression **(Table 1.1)**. Different siRNA carriers have been used for CDC20 siRNA delivery including commercially available lipid-based carriers, liposome and polyethylenimine-based carriers [82-91]. CDC20 downregulation by siRNA led to cell cycle arrest, and malignant cell growth and proliferation inhibition. Successful silencing of CDC20 not only affected malignant cell growth *in vitro*, but also decreased tumor growth *in vivo*. Liposomally encapsulated CDC20 siRNA has decreased melanoma tumor growth and its metastasis to lung in balb/c mice [86]. Several other studies reported successful tumor growth inhibition with CDC20 siRNA as well as reduced metastasis of cancer to other organs *in vivo* [84-88]. In addition, the sensitization to chemoradiation was found to be increased after silencing CDC20 siRNA [82]. Similarly, chemosensitivity to taxane drugs has increased significantly with CDC20 silencing in xenografted mice, and tumor growth has decreased effectively when taxane was delivered with CDC20 siRNA [85,87].

CDC20 shRNA was also able to decrease malignant cell growth and proliferation. Mostly, commercially available lipid-based carriers were used to deliver plasmid DNA (pDNA) that expresses shRNA [92-95]. While there was no report of *in vivo* study using CDC20 shRNA, Wang et al. showed increased sensitization of glioma cells with CDC20 shRNA, when those were treated with rottlerin, a natural plant product [93]. Several reports have confirmed a critical role of CDC20 during cell cycle and depletion of CDC20 in cells led to cell cycle arrest, ultimately leading to cell death. However, no effects of CDC20 downregulation by shRNA was reported in human somatic cells [95].

The miR-494 was found to decrease CDC20 levels in cancer that led to G2/M arrest [96]. Several other genes such as polo-like kinase 1 (PLK1), pituitary tumor-transforming gene 1 (PTTG1), Cyclin B1 (CCNB1), cell-division cycle 2 (CDC2) and topoisomerase II α (TOP2A) have also been reported to be downregulated by miR-494 microRNA (miRNA).

1.3.4.3 Combinational therapy with CDC20 targeting

Oftentimes combining multiple therapies leads to higher therapeutic effects and less side-effects due to simultaneous activation of multiple ways of targeting and lower doses. RNAi-mediated targeting of CDC20 along with other critical cell cycle protein or any conventional cancer treatments may lead to higher beneficial role of therapy. Silencing CDC20 with siRNA along with kinesin spindle protein (KSP) shows synergism in breast cancer cell growth inhibition [89]. Similarly, Taniguchi et al. showed that combining CDC20 siRNA with chemotherapy and radiation treatment has a significant beneficial role to decrease pancreatic cancer cell growth [82]. Chemotherapeutic agents such as paclitaxel and docetaxel have higher effects on malignant cells when those were treated in conjunction with CDC20 siRNA [85,87].

Overall, CDC20 has proven to be a very promising target for RNAi therapy against several cancer-types, although there are still more validation studies needed to be done in order to determine the magnitude of therapeutic beneficial role of CDC20 targeting in cancer cells. Furthermore, side-effects of CDC20 targeting in normal cells has not been explored carefully; this should be determined carefully since CDC20 could be silenced in normal cells with same RNAi reagents that is intended for just cancer cells.

Table 1.1: RNAi-mediated targeting of CDC20.

Cancer type	Vector/miRNA-type	Transfection reagent	Reference
siRNA Delivery			
Pancreatic cancer	-	RNAiFect (Qiagen)	Taniguchi et al., 2008 [82]
Lung, glioma and breast cancer	-	Lipofectamine 2000 (Invitrogen)	Kidokoro et al., 2008 [83]
Liver cancer	-	Lipofectamine 2000 (Invitrogen)	Liu et al., 2015 [84]
Prostate cancer	-	RNAiMAX (Invitrogen)	Li et al., 2016 [85]
Melanoma	-	Liposome	Mukherjee et al., 2013 [86]
Melanoma	-	Liposome	Majumder et al., 2014 [72]
Neuroblastoma	-	Liposome	Bhunia et al., 2017 [87]
Liver cancer	-	INTERFERin (Polyplus)	Li et al., 2014 [66]
Breast cancer	-	Polyethylenimine-linoleic acid	Parmar et al., 2015-2018 [88-91]
shRNA Delivery			
Lung, glioma and breast cancer	psiU6BX	Lipofectamine 2000 (Invitrogen)	Kidokoro et al., 2008 [83]
Glioblastoma	pCMV-dR8.2, pCI-VSVG	Lipofectamine 2000 (Invitrogen)	Xie et al., 2015 [92]
Glioma	Not-Specified	Lipofectamine 2000 (Invitrogen)	Wang et al., 2016 [93]
Colorectal and breast cancer	pCMV-HA	Lipofectamine 2000 (Invitrogen)	Paul et al., 2017 [94]
Osteosarcoma	pSUPER	Calcium phosphate/chloroquine	Baumgarten et al., 2009 [95]
miRNA Delivery			
Bile duct cancer	miR-494	Lipofectamine 2000 (Invitrogen)	Yamanaka et al., 2012 [96]

1.4 Targeting anti-apoptotic proteins along with cell cycle proteins in human malignancies

Targeting multiple cell survival pathways may be more beneficial to decrease the malignant cell growth compared to targeting one pathway alone. Several reports have clearly confirmed overexpression of anti-apoptotic proteins in many malignancies [97,98], thus holding a great promise as targets to decrease the tumor growth. Simultaneous targeting of anti-apoptotic and cell cycle proteins attacks not only cancer cell proliferation, but cell survival pathway as well, which increases the chances of cancer cell death with the dual targeting.

Anti-apoptotic proteins are mainly divided into three families: Cellular FLICE-inhibitory proteins (c-FLIPs), B-cell lymphoma 2 (BCL2) family and inhibitors of apoptosis proteins (IAPs). The c-FLIPs are mainly inhibiting apoptosis by binding to Fas-associated protein with death domain (FADD), caspase 8/10 and TRAIL (TNF-related apoptosis-inducing ligand) receptor 5 [99,100]. c-FLIP is expressed as long (c-$FLIP_L$), short (c-$FLIP_S$), and c-$FLIP_R$ splice variants. Anti-apoptotic proteins of BCL2 family include BCL2, MCL1 (Induced myeloid leukemia cell differentiation protein) and BCL-XL (also termed BCL2L1; BCL2-like 1). The main function of the anti-apoptotic BCL2 family is to inhibit directly or indirectly the activities of pro-apoptotic BCL2 proteins [101]. Third family is IAPs that are also known as Baculoviral IAP repeat-containing proteins (BIRC), which comprise of NAIP (BIRC1), cIAP1 (BIRC2), cIAP2 (BIRC3), XIAP (BIRC4), survivin (BIRC5), Bruce (BIRC6), ML-IAP (BIRC7) and ILP2 (BIRC8). IAPs serve as endogenous inhibitors of programmed cell death by mainly targeting caspases,

which prevents apoptosis to occur and cell survives the apoptotic signal that has been induced by the internal machinery [102].

Among all anti-apoptotic proteins, survivin has been found to be a key regulator of mitosis during cell cycle [103]. In addition, survivin has been found to be upregulated in many cancer types [104], leading to several studies focusing survivin-targeted cancer therapies. Therefore, we will mainly be discussing about targeting this critical anti-apoptotic protein, survivin in breast cancer along with cell cycle proteins.

1.4.1 Role of survivin in cell cycle

Although survivin has the main role as an anti-apoptotic protein, considerable evidences suggest an essential role in cell cycle progression. During mitosis, survivin forms a multi-protein complex with Aurora B kinase, INCENP and Borealin, called as chromosomal passenger complex (CPC) that is essential for proper chromosome segregation and cytokinesis [105,106]. Survivin is directly associated with polymerized tubulin during metaphase and anaphase, and contributes to the regulation of microtubule dynamics [107,108]. Furthermore, survivin expression is predominantly controlled by a cell cycle dependent regulation, which leads to its maximum expression during the mitotic phase of the cell cycle.

Being an anti-apoptotic protein, survivin inhibits both intrinsic and extrinsic mediators of apoptosis, including FAS, TRAIL, BAX, caspase-3, caspase-7 and caspase-8 [109]. In addition, survivin is found to be a key regulator of cell cycle during embryonic development stages [103], but rarely detectable in normal differentiated adult tissues except thymus, placenta, CD34+ stem cells, and basal colonic epithelial cells [110-113].

1.4.2 Survivin: an attractive target for cancer therapy

Survivin is found to be upregulated in many cancers, but barely detectable in most of the terminally differentiated cells, making it an excellent target to decrease malignant cell growth with less side-effects on normal cells. Survivin is also considered as a nodal protein due to its involvement in multiple signaling mechanisms that enhance and maintain tumor integrity [114]. Considerable evidences also suggest role of survivin in angiogenesis that is necessary for tumor expansion and progression [115,116]. Furthermore, survivin seems to play its part for the resistance to anti-cancer therapies [117] as many drugs ultimately induce apoptosis in cancer cells and overexpression of survivin may hinder the apoptotic signal induced by these therapeutic drugs.

Owing to established oncogenic involvement of survivin in malignant cell growth and progression, several strategies have been developed to target survivin at transcriptional and post-transcriptional levels [118,119]. Anti-sense oligonucleotides, ribozymes and siRNAs have been used to target survivin at transcript levels, while several small molecule inhibitors and immunotherapies have been developed that specifically target survivin at protein level, and some of them have already been to clinics [118,119].

1.4.3 Combinational therapy against survivin and cell cycle protein

Since survivin has been established as an oncogene and several cell cycle proteins such as CDC20 have emerged as an oncogenic protein, targeting both proteins simultaneously may put higher pressure on malignant cells and survival chances may become negligible. Depletion of cell cycle protein by targeted therapy usually interrupts cell cycle progression in malignant cells, and cell cycle is halted until the emerged concern has not been resolved [27]. If the downregulated cell cycle protein has not been replenished, the halted cell cycle usually induces apoptotic response, leading to cell death.

However, overexpression of some anti-apoptotic proteins may suppress the apoptotic response induced by halted cell cycle [120], resulting in minimal response of targeted therapy to cancer cells. Therefore, targeting cell cycle and anti-apoptotic proteins simultaneously may result into synergism of therapy, and doses of therapy could also be lowered to decrease side-effects of therapy to normal cells.

Small molecule drugs such as doxorubicin and paclitaxel have been approved for cancer therapy, which mainly inhibit the activities of cell cycle proteins such as topoisomerase II and tubulin, respectively, leading to cancer cell death [121,122]. The reports have emerged stating that survivin expression becomes higher while giving the doses of these small molecules, leading to the resistance to chemotherapy [123,124]. To overcome this barrier, survivin was silenced by siRNA along with paclitaxel, which have led to enhanced sensitivity of breast cancer cells to chemotherapeutics and higher efficacy of treatment [125].

PLK1 is established as an important cell cycle mediator, which is found to liaise with survivin for cell survival [126]. Therefore, targeting PLK1 and survivin simultaneously has led to improved efficacy of siRNA delivery in bladder cancer [127]. Similarly, siRNA-mediated targeting of an important cell cycle regulator, cyclin B1 along with survivin showed enhanced antitumor effects of melanoma xenografts [128]. We have also targeted survivin and CDC20 with respective siRNAs together in breast cancer cells *in vitro*, and observed synergistic effects of dual targeting with siRNA [89,91]. Thus, there is a significant correlation between cell cycle proteins and survivin, which facilitate the cancer cell progression, and combinational therapy against cell cycle protein and survivin

may improve the outcome of therapy. However, the validity of dual targeting still needed to be further explored to establish the importance of this therapeutic strategy.

1.5 Targeting protein phosphatases along with cell cycle proteins in human malignancies

The oncogenic role of protein phosphatases has recently emerged due to their frequent genetic alteration and deregulation in cancer [129,130]. In addition, protein phosphatases have been found not only to promote the uncontrolled cell growth, but also the metastasis [131,132], suggesting these proteins as potential targets to treat metastatic cancer. Since cell cycle proteins are excellent targets to decrease cancer cell growth, protein phosphatases could be targeted along with cell cycle protein to decrease metastasis of cancer, which may be ideal to inhibit cancer cell growth and migration simultaneously.

The main role of a protein phosphatase is to dephosphorylate its substrate protein. Protein phosphorylation and dephosphorylation are complex enzymatic reactions that are essential to perform several cellular processes, including cell growth, adhesion, motility, and apoptosis [133]. Phosphorylation is usually carried out by protein kinases that act in conjunctions with protein phosphatases to maintain cellular processes. Protein phosphatases can be divided into four major families based on their structure and function: (i) tyrosinespecific phosphatases [134], (ii) serine/threonine-specific phosphatases [135] (iii) dualspecificity phosphatases (DUSP) [136], and (iv) histidine phosphatases [137]. Protein phosphatases recognize either tyrosine or serine/threonine on substrate proteins and dephosphorylate them. However, there are some protein phosphatases that recognize both substrates, generally called as dualspecificity phosphatases. Histidine phosphatases, on the other hand, dephosphorylate substrates that has histidine molecules.

Several protein phosphatases play essential roles to regulate the cell cycle. The key cell cycle regulatory kinases, CDKs dephosphorylate by protein phosphatases as cell passes through different stages of cell cycle [138,139]. In addition, protein phosphatases have been found to regulate mitosis by activating/deactivating several mitotic proteins [140].

1.5.1 Protein phosphatases in cancer

It was initially assumed that protein phosphatases may act as tumor suppressors due to their contrasting activity (*i.e.,* phosphate removal) to protein kinases (*i.e.,* phosphate addition) that have been shown to support oncogenic transformation. However, protein phosphatases have recently been recognized as potential contributors to oncogenesis due to their deregulation in many critical signal transduction pathways [141,142]. Genetic and epigenetic alterations in protein phosphatases also attributed to deregulation of signaling pathways [141]. The deregulation or overexpression of several protein phosphatases is evident in many cancer types, including breast cancer [143-146]. Recently, the role of protein tyrosine phosphatases in colorectal and prostate cancer biology was defined due to evidences showing that dephosphorylation events induced by some protein tyrosine phosphatases may stimulate tumor formation [145,146].

Protein phosphatases have also been suggested to support tumor microenvironment that serve as drivers of tumorigenesis [147]. The support and growth of tumor microenvironment influence metastasis and defeat immune surveillance. Considerable evidences have suggested involvement of protein phosphatases in the metastasis of several types of cancers as well [148,149]. Due to oncogenic role of several protein phosphatases, small molecule inhibitors have been developed to inhibit the expression of specific protein

phosphatase, and several clinical trials are ongoing that specifically target protein tyrosine phosphatases in cancer [150-152].

1.5.2 Combinational therapy against protein phosphatase and cell cycle protein

Since protein phosphatases have been found to contribute in cancer progression and metastasis, those are promising targets to decrease migration of metastatic cancer cells. The deregulated cell cycle proteins, on the other hand, mainly involved in tumor growth. Therefore, targeting protein phosphatase along with cell cycle proteins inhibits metastasis as well as cell growth, which may be an exciting strategy to treat metastatic cancer **(Fig 1.2)**.

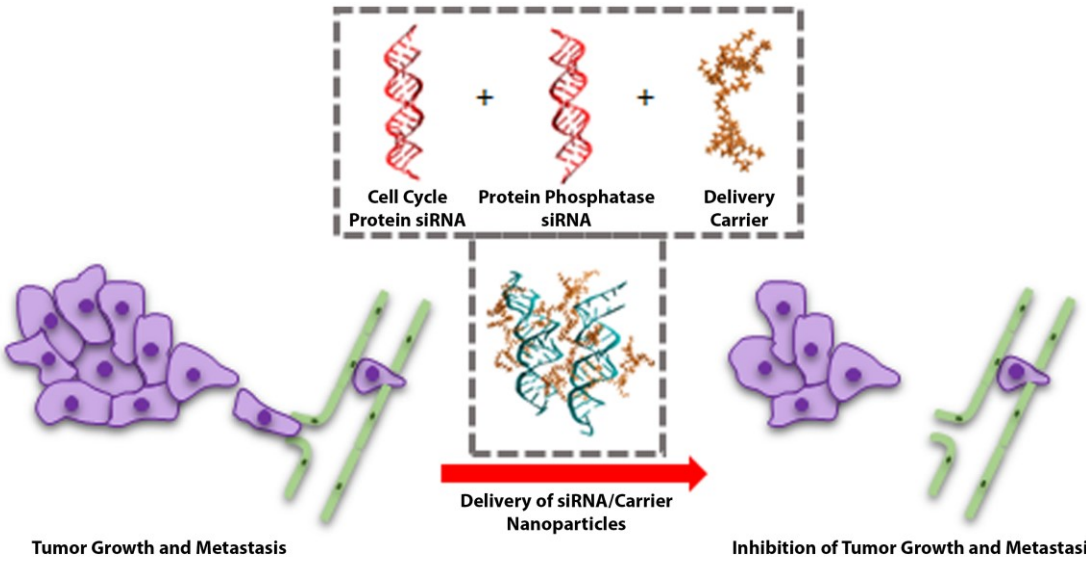

Fig 1.2: A schematic representation of a strategy to inhibit cancer cell growth and metastasis by targeting cell cycle and phosphatase proteins simultaneously.

Phosphatase of regenerating liver 3 (PRL3) family is known to contribute in tumor growth and metastasis [153]. Commonly used chemotherapeutic agents such as doxorubicin, paclitaxel, cisplatin *etc.* have been found to induce PRL3 expression that

promotes cancer growth [154]. Targeting PRL3 along with chemotherapeutic agents that mainly disrupt cell cycle in cancer cells has, therefore, a great potential to increase the efficacy of treatment. Furthermore, silencing protein phosphatase 2C (also known as WIP1) by siRNA seems to be increasing chemosensitivity of human colon cancer cells [155], and combinational targeting of WIP1 and doxorubicin has increased the efficacy of treatment.

Since protein phosphatases were found to have a role in metastasis, several studies were performed to inhibit the expression of these phosphatases, resulting in successful inhibition in cancer cell invasion and migration [156-158]. However, only we have targeted protein phosphatases along with cell cycle proteins to inhibit cancer cell growth as well as migration simultaneously [90]. Even though our initial attempt of targeting cell cycle and phosphatase proteins has given positive outcome *in vitro*, more studies need to be performed to further establish this strategy to tackle metastatic cancer.

1.6 RNA Interference

The post-transcriptional gene silencing mediated by double-stranded RNA (dsRNA) is referred as RNA interference (RNAi). Fire et al. (1998) first discovered RNAi in *Caenorhabditis elegans* as homology-dependent gene silencing [159]. They were able to show that the introduction of dsRNA was effective and specific to knockdown a targeted gene, whereas the effect of single-stranded RNA was negligible to decrease the copies of the targeted mRNA. In recent years, RNAi has been established unequivocally as a promising approach to silence sequence-specific targets, especially for targets that are up-regulated in abnormal conditions such as cancer. The translation arrest or degradation of specific mRNA is mediated by RNAi as a regulation of post-transcription of a gene. The

RNAi can be mediated by three means: i) synthetic small interfering RNA (siRNA) that is 20-25 nucleotides long with few overhang bases can interfere with the expression of specific genes with complementary nucleotide sequence in the mRNA transcript [160]; ii) miRNA, an endogenously expressed non-coding nuclear transcript, is processed by intracellular enzymes to yield 20-25 nucleotides sequences for mRNA silencing [161] and; iii) short hairpin RNA (shRNA) which is expressed from vectors that are artificially transfected into cells [162].

The endogenous RNAi can be broadly divided into two steps: cleavage of pri-miRNA into mature miRNA and transport of mature miRNA to its intracellular target [163,164]. A complex hairpin structure of endogenously expressed primary miRNA (pri-miRNA) is cleaved to small hairpin structures, the precursor miRNA (pre-miRNA), in the nucleus. The ribonuclease enzyme dicer cleaves the hairpin structure once the pre-miRNA is transported to the cytoplasm, which, in turn, forms 20-25 nucleotides long mature miRNA with 2-3 overhang nucleotides. An ectopically expressed shRNA from a vector and synthetically designed siRNA can be introduced directly to cells since the nuclear processing can be avoided with the appropriate design **(Fig 1.3)**. The siRNA is incorporated into the RNA-inducing silencing complex (RISC) following the release of the passenger strand and leaving the guide strand of siRNA to target the mRNA of interest, which is followed by cleavage of the target mRNA via endonuclease activity or translational arrest depending on the nature of base pairing between the mRNA and the guide strand [165,166]. Because of high specificity and minimal side-effects, RNAi using siRNA is gaining the upper hand as a useful approach for the treatment of cancer [167]. In this case, siRNA could be visualized as a ‘drug’, but one that is distinct from conventional drugs in the sense

that its delivery requires special attention due to its hydrophilic and anionic nature that makes it practically non-permeable to cell membrane [168].

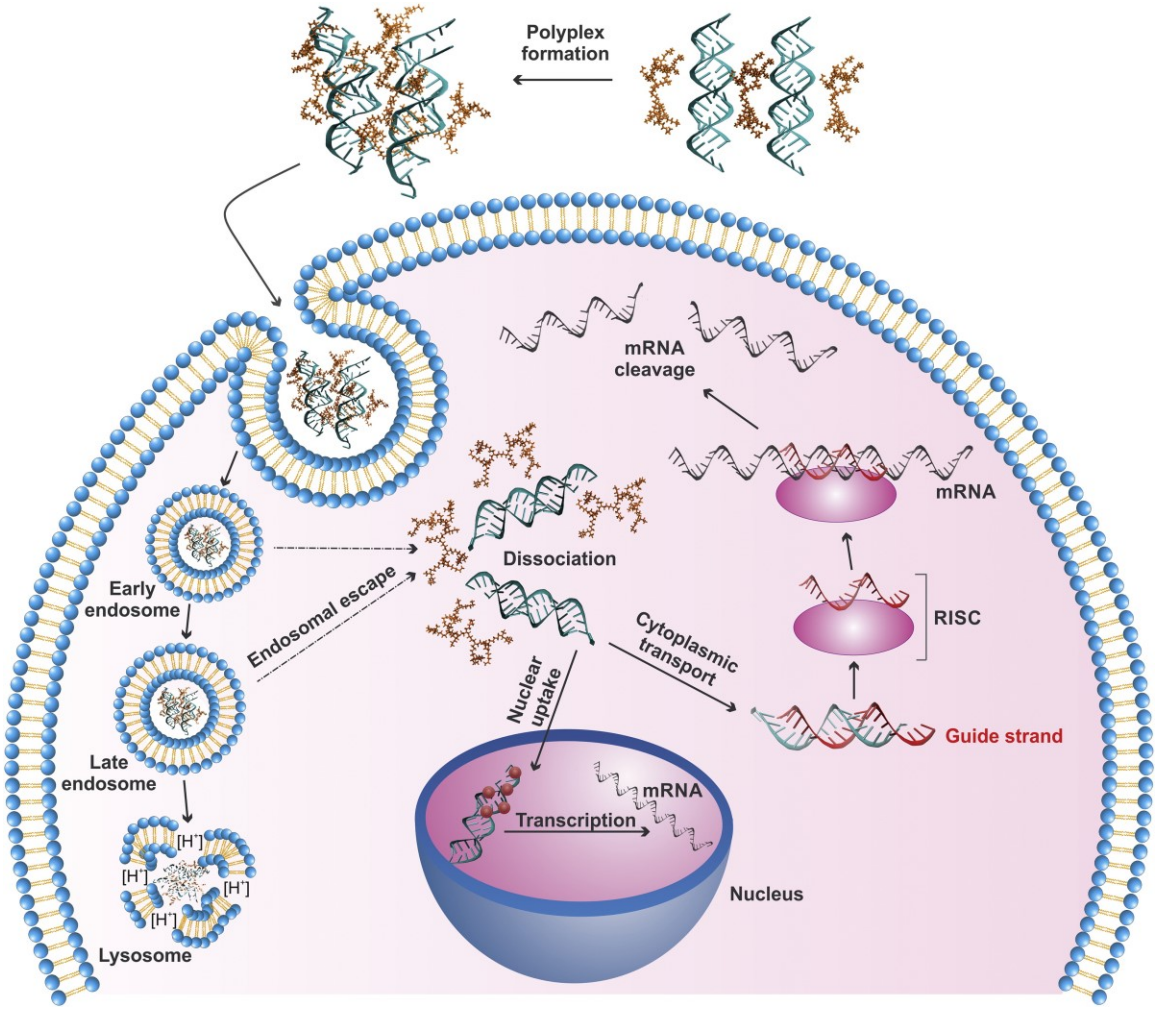

Fig 1.3: An illustration for the delivery of siRNA, miRNA and shRNA.

The siRNA, miRNA or shRNA is complexed with its delivery carrier. Nucleic acid/carrier nanoparticles are usually uptaken by endocytosis. After endosomal escape, siRNA/miRNA is transported directly for RNA-inducing silencing complex (RISC) assembly, while shRNA is trafficked to nucleus for its expression. Reproduced with permission from Meneksedag-Erol et al, 2014 [169].

1.6.1 Nucleic acids for RNAi

1.6.1.1 siRNA delivery

The binding of siRNA to cell membranes and subsequent uptake is nearly impossible due to its highly labile and anionic nature, as well as large (~14 kDa) molecular weight [168]. siRNA can be transported into the cells using cationic carriers which form cationic (or neutral) nanoparticles as the carrier interacts with the siRNA through ionic interactions to form the nanoparticles [168,170]. Biodegradable and biocompatible carriers are desirable not to display any adverse effects on the cells while leaving no trace of the 'passive' carrier in the cells [171]. Among different carriers used for siRNA delivery, commercially available lipid-based carriers are more popular. Lipid-based carriers form liposomal structures with a lipid bilayer envelope and an aqueous core [168,171]. Cationic lipids in the lipid bilayer structure interact with negatively charged siRNA to form an ionic complex, and immobilize siRNA on the envelope structure (either internal or external). The siRNA could also be entrapped in the core of the liposome. Some carriers form 'solid' lipidic nanoparticles of homogenous siRNA-lipid complexes. Cationic lipids display more disruptive activity on cell membranes (*i.e.,* more toxic) compared to neutral lipids and may have higher immunogenicity due to enhanced liposomal uptake by macrophages [172]. Certain cationic polymers such as PEI have also been used to deliver siRNA. Polymers condense siRNA into positively charged polymeric micelles (believed to be homogenous structures) that are subsequently internalized through the anionic cell membrane by endocytosis. In the case of PEI, osmotic imbalance bursts the endosomal vesicles (so called proton-sponge effect of PEI), releasing polymer-siRNA complexes into cytoplasm [173]. Cationic polymers are also toxic due to their ability to disrupt cell membrane and mitochondrial membrane and their toxicity usually increases with their molecular weight. The efficacy of siRNA critically depends on the release of siRNA from the carrier in the

cytoplasm so that it is available in free form for RISC incorporation, and its efficient intracellular transport to the site(s) of silencing.

Oftentimes, nucleofection or electrofection is used to deliver siRNA into cells. The amount required to transfect siRNA by this method is usually higher. The higher amount of siRNA could lead to non-specific effects, resulting in poor specificity for a 'therapeutic' siRNA. Additionally, nucleofection or electrofection is nearly impossible to use at the clinical stage, which make them just an experimental tool. Gong et al. (2007) have targeted cell cycle proteins using a new unconventional dicer-substrate siRNA (DsiRNA) that are synthetically designed siRNA to be optimally processed by dicer before engaging the RISC complex [174]. The potency of DsiRNA seems to be higher than traditional siRNA as it goes through natural processing pathway in the cell.

1.6.1.2 shRNA expression for RNAi

The shRNA is mainly delivered with non-viral vectors, mostly pDNA. The main concern with shRNA is its limited duration of expression in the eukaryotic cells resulting in the silencing of a target for short period of time, which is the same drawback facing the siRNA itself. Although non-viral vectors are more popular over viral vectors for shRNA delivery because of their superior safety profile, non-viral vectors have certain limitations and disadvantages. As in siRNA, the major issue is the delivery of pDNA into the cells, which requires a carrier as well. Though many commercially available lipid-based carriers and polymers have been used for successful transfection of pDNA *in vitro*, the carrier and/or pDNA complexes may induce an immune response *in vivo*, mainly innate immune response by causing tissue damage [175-177]. Intracellular trafficking affects the expression of shRNA from pDNA. pDNA must dissociate from its carrier in the cytoplasm

and must be transported to the nucleus for transcription (unlike siRNA that needs to be remained in the cytoplasm), and exposes itself to the transcriptional machinery by decondensation of double-stranded DNA [178]. Being a foreign DNA, activities such as inhibition of transcription, nuclease-mediated degradation of pDNA, induced mutation in the pDNA or induction of apoptosis may be associated with the delivery of pDNA [179,180]. Moreover, adaptive immune response may be activated because of the sensitivity of the pathogen recognition *in vivo* [181,182]. As plasmid lacks the mechanism of maintaining its copy number in the eukaryotic cells, the plasmid concentration decreases in the daughter cells, and eventually shRNA expression diminishes [183]. Some of these limitations can be avoided by designing vector that can complement the mammalian DNA sequence such as the mammalian tissue-specific promoters and enhancer sequences. The positive charge of the carriers can be reduced by substitution of the amine groups, so that pDNA can easily dissociate after transfection into cells.

1.6.1.3 miRNA

As the synthesis of several genes are endogenously controlled by miRNAs [184], its delivery can be used to target some proteins to decrease the proliferation rate of cancer cells. The miRNA can be delivered using a pDNA as a vector for *in situ* expression. However, naked miRNA delivery is easier and common using cationic carriers [185]. The advantage of using miRNA over siRNA or shRNA is the wide range of potential targets that can be silenced with the introduction of a specific miRNA. The siRNA or shRNA would be very specific to silence just single target, while miRNA can silence more than one targets based on its complementary sequence to different genes [185].

1.6.2 Overcoming RNAi intended for gene silencing

Although RNAi seems to be a powerful approach to regulate specific protein expression, there might be specific mechanisms employed by malignant cells in order to overcome its inhibitory activities. If mutated copies of a specific gene are amplified in the genome or over-expressed, these mutated transcripts might not be recognized by siRNA and escape the processing by the RISC complex. Chromosomal instability may also lead to mutations in essential survival pathways [186], and malignant cells may nullify the RNAi treatment by utilizing the mutated survival pathway. Since miRNAs silence more than one targets based on its complementary sequence to different mRNAs, off-targets effects of miRNA often tags along [187]. The miRNAs targeting some overexpressed genes may have complementary sequences to indigenous cell growth inhibitors such as pro-apoptotic proteins, which may decrease the expression of inhibitors and amplify cell proliferation. In such instances, these miRNAs will not be appropriate for RNAi treatment. Sometimes, targeting just one gene may not be enough to stop unscheduled cell proliferation, and targeting multiple proteins might be required to inhibit the cell growth drastically. The choice of the RNAi mediator (siRNA vs. shRNA vs. miRNA) will be critical for this purpose. Furthermore, transcript copy number of different targets varies in a specific cancer-type [188,189], which also determines the functional outcome of nucleic acid therapeutics. The low transcript copy number genes crucial for cell progression would be more effective to target than those with high copy number. Any dynamics regulation of transcript copy number by malignant cells might also provide a means to overcome therapeutic RNAi. These are un-resolved issues at this stage and it will require careful studies to reveal their impact in targeting cell growth regulators.

1.6.3 Nanoparticles engineering

Apart from several biological challenges for RNAi, effective delivery of nucleic acid-therapeutics always remains a major concerning factor. There is a continuous development of new/modified delivery carriers with some expert formulation of nucleic acid and carrier using specific amount and method due to constant pressure to improve the transfection as well as silencing efficiency. The size, shape and charge are the first-line of nanoparticle features that is being manipulated based on transfected cell-types. Small nanoparticles (<10 nm) are mainly cleared by kidney, while larger particles are processed by liver and spleen [190]. The size of nanoparticles is critically affecting the pharmacokinetics, transport, penetration in tumor vasculature and cellular uptake of nanoparticles. The cellular uptake of 50 nm nanoparticles in HeLa cells were found to be higher compared to 14 and 74 nm nanoparticles [191], clearly indicates the importance of specific size of nanoparticles. Similarly, nanoparticle shape has an influence on how it flows in blood circulation and how it internalizes in the cell. Spherical shape is the most common and preferable, but recent advancements in nanoparticle engineering provided several other shapes as well, such as rod, prism, cube, disk etc. [192]. Asymmetry of nanoparticles enhances cell penetration and distribution in tumor microenvironment as nanodisks were found to be uptaken more compared to nanorods [193]. In addition, different inflammatory cytokines were released with the delivery of spheres and rod-shaped nanoparticles [194]. The surface charge of nanoparticles is equally important as size and shape. Cationic lipids and polymers are widely used for nucleic acid delivery as it can easily bind to anionic nucleic acids and bring positive change to the nanoparticles. Positive surface charge of nanoparticles can easily interact with anionic cell membrane and the availability of nanoparticles increases. As cationic carriers derived from polymers such as

PEI typically possess high density of positive charges, it is difficult for nucleic acid and cationic carrier complexes to easily dissociate in the cytoplasm. The efficiency for nucleic acid release can be improved by decreasing the surface charge density of nanoparticles by introducing anionic lipids or polymers. We have successfully increased the transfection efficiency as well as functional outcomes of siRNA delivery using an additive polyplexes, where nanoparticles were formed with PEI and hyaluronic acid/polyacrylic acid [90,91]. The improved efficacy of siRNA delivery with additive polyplexes was likely due to higher dissociation of siRNA once the nanoparticles were in the cytoplasm.

The surface of nanoparticles could be engineered as well to deliver them to specific cell-type or tissue. Shen et al (2015) has coated paclitaxel loaded lipid nanoparticles with hyaluronic acid, and showed improved efficacy of chemotherapy in melanoma cells [195]. The higher uptake of nanoparticles in melanoma cells is likely due to receptor-mediated uptake of hyaluronic acid-coated nanoparticles as hyaluronic acid can bind to overexpressed CD44 receptor present in several cancer-types. Nanoparticles surfaces are often coated with popular polyethylene glycol (PEG). PEG is also covalently attached to delivery carrier so that PEG remain on the surface when nanoparticles are formed using this carrier. PEG is known to reduce immunogenicity, antigenicity and renal clearance, while improving pharmacokinetics of nanoparticles [196]. Similarly, tumor-penetrating peptides can be used to modify nanoparticles surfaces as well. Well-studied RGD peptides increases tumor-homing of nanoparticles due to binding-specificity to overexpressing integrin in cancer cells [197]. Antibody-conjugated nanoparticles have also been tested to improve cell penetration by inducing receptor-mediated endocytosis of nanoparticles. In addition, altering and tailoring basic antibody structure based on the specificity and

functionality have also been facilitated due to recent advancement in antibody engineering [198].

The nanoparticles engineering could be done by chemically modifying nucleic acid delivery carriers, which may improve the transfection efficiency. Recently, we reported silencing of cell cycle proteins using engineered PEIs that is substituted with lipid molecules [88-91]. Such tailored carriers are expected to be preferable to commercially available alternatives, since they can offer superior delivery kinetics and can be tailored depending on the cell type and chosen target. Molecular weight of a nucleic acid delivery carrier play an important role as higher cellular toxicity tags along with the high molecular weight carriers. High molecular weight PEIs, in such cases, possess higher cellular toxicity, making it an unreliable delivery carrier. On the other hand, low molecular weight PEIs shows poor transfection efficiency. In order to increase the transfection efficiency, we substituted some tertiary amines with lipidic moieties in PEI as the substituted lipids are believed to be helping in cell membrane penetration.

1.7 Concluding remarks and prospective

Breast cancer is a heterogeneous disease that clearly needs a therapeutic attention. Current breast cancer therapies have their own limitations and side-effects, resulting in an urgent need for alternative therapies. RNAi targeting of critical cell cycle regulators seems to be a promising approach to tackle this deadly disease, and we specifically discussed here to target APC activator, CDC20 that has recently been emerged as an oncogenic protein in cancer. Several other proteins contributing to cell cycle regulation, such as CDKs, cyclins, kinesin protein family, cell division cycle proteins, checkpoint kinases, centromere proteins, RAD homolog proteins, *etc.* have also been found to be deregulated in many

cancer types, and these proteins could also serve as potential targets for cancer treatment. Therefore, these regulators should be taken into account for RNAi therapy as well.

Other potential cancer therapeutic targets that act in conjunction with cell cycle regulators are anti-apoptotic proteins. Targeting critical cell cycle regulator along with an anti-apoptotic protein may result into synergistic effect of dual therapy as multiple cell survival pathways may have been targeted simultaneously. An anti-apoptotic protein, survivin is an attractive cancer therapeutic target that has a role in cell cycle progression as well. Many other anti-apoptotic proteins have found to be upregulated in cancer, and those could be explored as potential targets for combinational therapy along with cell cycle proteins. Similarly, protein phosphatases could be targeted along with cell cycle proteins to tackle metastatic cancer. The role of protein phosphatases in cancer has recently been defined and those are found to be upregulated in metastatic cancer, indicating these proteins as potential cancer therapeutic targets.

Finally, carrier design to deliver effective anti-cancer agents is an ongoing activity as more effective carriers is constantly needed for nucleic acid-based therapies. The size, shape, charge and surface of nanoparticles could be tailored according to transfected cell-type. In addition, the carrier could also be modified chemically to potentially increase transfection efficiency in cancer cells. We reported transfection of siRNA with engineered PEIs that showed superior delivery compared to native PEI [88-91]. However, nanoparticles made with siRNA and modified PEI also transfected non-malignant cells at some extent [91], and RNAi delivery agent that transfects cancer cells solely still remains to be conceptualized, designed and synthesized. Studies for such systematic investigations remain to be conducted for deploying siRNA-based RNAi therapy for breast cancer.

1.8 Acknowledgements

The siRNA research in the authors' laboratory was financially supported by operating grants from Canadian Breast Cancer Foundation (CBCF), Alberta Innovates Health Sciences (AIHS) and Natural Sciences and Engineering Council of Canada (NSERC), and equipment support from Alberta Heritage Foundation for Medical Research (AHFMR) and Edmonton Civic Employees Charitable Assistance Fund (ECE-CAF). The authors declare that there are no competing financial interests in relation to the work described. We are grateful to numerous past trainees in the Uludag laboratory who contributed to the development of non-viral delivery systems, in particular Dr. Vanessa Incani, Dr. Meysam Abbasi, Dr. Hamidreza M. Aliabadi, Dr. Charlie Hsu, Dr. Aws Alshamsan and Dr. Remant K.C. We also acknowledge our long-term collaborators Dr. Afsaneh Lavasanifar, Dr. Tian Tang, Dr. Michael Weinfeld and Dr. Xiaoyan Jiang for their valuable contributions to our RNAi research.

1.9 References

1. Joo WD, Visintin I, Mor G. Targeted cancer therapy - are the days of systemic chemotherapy numbered? *Maturitas*, 2013, 76:308-314.
2. Tannock IF. Conventional cancer therapy: promise broken or promise delayed? *Lancet*, 1998, 351 Suppl 2:SII9-SII16.
3. Abdelrahim M, Safe S, Baker C, Abudayyeh A. RNAi and cancer: Implications and applications. *J RNAi Gene Silencing*, 2006, 2:136-145.
4. Chakraborty C, Sharma AR, Sharma G, Doss CGP, Lee SS. Therapeutic miRNA and siRNA: moving from bench to clinic as next generation medicine. *Mol Ther Nucleic Acids*, 2017, 8:132-143.
5. Surakasula A, Nagarjunapu GC, Raghavaiah KV. A comparative study of pre- and post-menopausal breast cancer: Risk factors, presentation, characteristics and management. *J Res Pharm Pract*, 2014, 3:12-18.
6. Singh V, Saunders C, Wylie L, Bourke A. New diagnostic techniques for breast cancer detection. *Future Oncol*, 2008, 4:501-513.
7. Hon JD, Singh B, et al. Breast cancer molecular subtypes: from TNBC to QNBC. *Am J Cancer Res*, 2016, 6:1864-1872.

8. Mohamed A, Krajewski K, Cakar B, Ma CX. Targeted therapy for breast cancer. *Am J Pathol*, 2013, 183:1096-1112.

9. Aydiner A, Sen F, Karanlik H, Aslay I, Dincer M, İğci A. A Review of Local and Systemic Therapy in Breast Cancer. In: Aydiner A, İgci A, Soran A. (ed.) *Breast Disease*, 2016, Springer, Cham, Switzerland.

10. Miller E, Lee HJ, Lulla A, Hernandez L, Gokare P, Lim B. Current treatment of early breast cancer: adjuvant and neoadjuvant therapy. *F1000Res*, 2014, 3:198.

11. Karam A. Update on breast cancer surgery approaches. *Curr Opin Obstet Gynecol*, 2013, 25:74-80.

12. Joshi SC, Khan FA, Pant I, Shukla A. Role of radiotherapy in early breast cancer: an overview. *Int J Health Sci (Qassim)*, 2007, 1:259-264.

13. Brown LC, Mutter RW, Halyard MY. Benefits, risks, and safety of external beam radiation therapy for breast cancer. *Int J Womens Health*, 2015, 7:449-458.

14. Deng X, Wu H, Gao F, Su Y, Li Q, Liu S, Cai J. Brachytherapy in the treatment of breast cancer. *Int J Clin Oncol*, 2017, 22:641-650.

15. Monroe AT, Feigenberg SJ, Mendenhall NP. Angiosarcoma after breast-conserving therapy. *Cancer*, 2003, 97:1832-1840.

16. Apuri S. Neoadjuvant and Adjuvant Therapies for Breast Cancer. *South Med J*, 2017, 110:638-642.

17. Hassan MS, Ansari J, Spooner D, Hussain SA. Chemotherapy for breast cancer (Review). *Oncol Rep*, 2010, 24:1121-1131.

18. Partridge AH, Burstein HJ, Winer EP. Side effects of chemotherapy and combined chemohormonal therapy in women with early-stage breast cancer. *J Natl Cancer Inst Monogr*, 2001, 2001:135-142.

19. Abdulkareem IH, Zurmi IB. Review of hormonal treatment of breast cancer. *Niger J Clin Pract*, 2012, 15:9-14.

20. Tremont A, Lu J, Cole JT. Endocrine Therapy for Early Breast Cancer: Updated Review. *Ochsner J*, 2017, 17:405-411.

21. Wiseman LR, Goa KL. Toremifene. A review of its pharmacological properties and clinical efficacy in the management of advanced breast cancer. *Drugs*, 1997, 54:141-160.

22. Riemsma R, Forbes CA, Kessels A, Lykopoulos K, Amonkar MM, Rea DW, Kleijnen J. Systematic review of aromatase inhibitors in the first-line treatment for hormone sensitive advanced or metastatic breast cancer. *Breast Cancer Res Treat*, 2010, 123:9-24.

23. Loibl S, Gianni L. HER2-positive breast cancer. *Lancet*, 2017, 389:2415-2429.

24. Mayer EL. Targeting breast cancer with CDK inhibitors. *Curr Oncol Rep*, 2015, 17:443.

25. Amir E, Seruga B, Serrano R, Ocana A. Targeting DNA repair in breast cancer: a clinical and translational update. *Cancer Treat Rev*, 2010, 36:557-565.

26. Schafer KA. The cell cycle: a review. *Vet Pathol*, 1998, 35:461-478.

27. Vermeulen K, Van Bockstaele DR, Berneman ZN. The cell cycle: a review of regulation, deregulation and therapeutic targets in cancer. *Cell Prolif*, 2003, 36:131-149.

28. Ahmad A, Wang Z, Ali R, Bitar B, Logna FT, Maitah MY, Bao B, Ali S, Kong D, Li Y, Sarkar FH. Cell cycle regulatory proteins in breast cancer: molecular determinants of drug resistance and targets

for anticancer therapies. In: Aft RL. (ed.) *Targeting New Pathways and Cell Death in Breast Cancer*, 2012, InTech, Rijeka, Croatia.

29. Stewart ZA, Westfall MD, Pietenpol JA. Cell-cycle dysregulation and anticancer therapy. *Trends Pharmacol Sci*, 2003, 24:139-145.

30. Maya-Mendoza A, Tang CW, Pombo A, Jackson DA. Mechanisms regulating S phase progression in mammalian cells. *Front Biosci*, 2009, 14:4199-4213.

31. Norbury C, Nurse P. Animal cell cycles and their control. *Annu Rev Biochem*, 1992, 61:441-470.

32. Lodish H, Berk A, Kaiser CA, Krieger M, Scott MP, Bretscher A, Ploegh H, Matsudaira P. *Molecular Cell Biology (6th edition)*, 2008, W.H. Freeman, New York, USA.

33. Morgan D. *Cell Cycle: Principles of Control*, 2007, New Science Press, London, UK.

34. Liskay RM. Absence of a measurable G2 phase in two Chinese hamster cell lines. *PNAS*, 1977, 74:1622-1625.

35. Hartwell LH, Weinert TA. Checkpoints: controls that ensure the order of cell cycle events. *Science*, 1989, 246:629-634.

36. Pardee AB. G1 events and regulation of cell proliferation. *Science*, 1989, 246:603-608.

37. Zetterberg A, Larsson O, Wiman KG. What is the restriction point? *Curr Opin Cell Biol*, 7:835-842.

38. Maller Jl, Gautier J, Langan TA, Lohka MJ, Shenoy S, Shalloway D, Nurse P. Maturation-promoting factor and the regulation of the cell cycle. *J Cell Sci Suppl*, 1989, 12:53-63.

39. Castro A, Bernis C, Vigneron S, Labbé JC, Lorca T. The anaphase-promoting complex: a key factor in the regulation of cell cycle. *Oncogene*, 2005, 24:314-325.

40. Kramer ER, Scheuringer N, Podtelejnikov AV, Mann M, Peters JM. Mitotic regulation of the APC activator proteins CDC20 and CDH1. *Mol Biol Cell*, 2000, 11:1555-1569.

41. Peters JM. SCF and APC: the Yin and Yang of cell cycle regulated proteolysis. *Curr Opin Cell Biol*, 1998, 10:759-768.

42. Foe I, Toczyski D. Structural biology: a new look for the APC. *Nature*, 2011, 470:182-183.

43. Chang L, Barford D. Insights into the anaphase-promoting complex: a molecular machine that regulates mitosis. *Curr Opin Struct Biol*, 2014, 29:1-9.

44. Chang LF, Zhang Z, Yang J, McLaughlin SH, Barford D. Molecular architecture and mechanism of the anaphase-promoting complex. *Nature*, 2014, 513:388-393.

45. Hartwell LH, Mortimer RK, Culotti J, Culotti M. Genetic control of the cell division cycle in yeast: v. genetic analysis of CDC mutants. *Genetics*, 1973, 74:267-286.

46. Morgan DO. The D box meets its match. *Mol Cell*, 2013, 50:609-610.

47. Jin L, Williamson A, Banerjee S, Philipp I, Rape M. Mechanism of ubiquitin-chain formation by the human anaphase-promoting complex. *Cell*, 2008, 133:653-665.

48. Di Fiore B, Davey NE, Hagting A, Izawa D, Mansfeld J, Gibson TJ, Pines J. The ABBA motif binds APC/C activators and is shared by APC/C substrates and regulators. *Dev Cell*, 2015, 32:358-372.

49. Petersen BO, Wagener C, et al. Cell cycle- and cell growth-regulated proteolysis ofmammalian CDC6 is dependent on APC-CDH1. *Genes Dev*, 2000, 14:2330–2343.

50. Littlepage LE, Ruderman JV. Identification of a new APC/C recognition domain, the A box, which is required for the Cdh1-dependent destruction of the kinase Aurora-A during mitotic exit. *Genes Dev*, 2002, 16:2274–2285.

51. Araki M, Wharton RP, Tang Z, Yu H, Asano M. Degradation of origin recognition complex large subunit by the anaphase-promoting complex in Drosophila. *EMBO J*, 2003, 22:6115–6126.

52. Reis A, Levasseur M, Chang HY, Elliott DJ, Jones KT. The CRY box: a second APCcdh1-dependent degron in mammalian cdc20. *EMBO Rep*, 2006, 7:1040–1045.

53. Hames RS, Wattam SL, Yamano H, Bacchieri R, Fry AM. APC/C-mediated destruction of the centrosomal kinase Nek2A occurs in early mitosis and depends upon a cyclin A-type D-box. *EMBO J*, 2001, 20:7117–7127.

54. Amador V, Ge S, Santamaria PG, Guardavaccaro D, Pagano M. APC/C(Cdc20) controls the ubiquitin-mediated degradation of p21 in prometaphase. *Mol Cell*, 2007, 27:462–473.

55. Harley ME, Allan LA, Sanderson HS, Clarke PR. Phosphorylation of Mcl-1 by CDK1-cyclin B1 initiates its Cdc20-dependent destruction during mitotic arrest. *EMBO J*, 2010, 29:2407–2420.

56. Wan L, Tan M, et al. APC(Cdc20) suppresses apoptosis through targeting Bim for ubiquitination and destruction. *Dev Cell*, 2014, 29:377–391.

57. Yu H. Cdc20: a WD40 activator for a cell cycle degradation machine. *Mol Cell*, 2007, 27:3–16.

58. Hu D, Qiao X, Wu G, Wan Y. The emerging role of APC/CCdh1 in development. *Semin Cell Dev Biol*, 2011, 22:579–585.

59. Penas C, Ramachandran V, Ayad NG. The APC/C ubiquitin ligase: from cell biology to tumorigenesis. *Front Oncol*, 2011, 1:60.

60. Wang Z, Wan L, et al. Cdc20: a potential novel therapeutic target for cancer treatment. *Curr Pharm Des*, 2013, 19:3210–3214.

61. Li M, York JP, Zhang P. Loss of Cdc20 causes a securin-dependent metaphase arrest in two-cell mouse embryos. *Mol Cell Biol*, 2007, 27:3481–3488.

62. Wang L, Zhang J, Wan L, Zhou X, Wang Z, Wei W. Targeting Cdc20 as a novel cancer therapeutic strategy. *Pharmacol Ther*, 2015, 151:141-151.

63. Li D, Zhu J, et al. Overexpression of oncogenic STK15/BTAK/Aurora A kinase in human pancreatic cancer. *Clin Cancer Res*, 2003, 9:991–997.

64. Wu WJ, Hu KS, et al. CDC20 overexpression predicts a poor prognosis for patients with colorectal cancer. *J Transl Med*, 2013, 11:142.

65. Kim JM, Sohn HY, et al. Identification of gastric cancer-related genes using a cDNA microarray containing novel expressed sequence tags expressed in gastric cancer cells. *Clin Cancer Res*, 2005, 11:473–482.

66. Li J, Gao JZ, Du JL, Huang ZX, Wei LX. Increased CDC20 expression is associated with development and progression of hepatocellular carcinoma. *Int J Oncol*, 2014, 45:1547-1555.

67. Chang DZ, Ma Y, et al. Increased CDC20 expression is associated with pancreatic ductal adenocarcinoma differentiation and progression. *J Hematol Oncol*, 2012, 5:15.

68. Kato T, Daigo Y, Aragaki M, Ishikawa K, Sato M, Kaji M. Overexpression of CDC20 predicts poor prognosis in primary non-small cell lung cancer patients. *J Surg Oncol*, 2012, 106:423–430.

69. Zaravinos A, Lambrou GI, Boulalas I, Delakas D, Spandidos DA. Identification of common differentially expressed genes in urinary bladder cancer. *PLoS One*, 2011, 6:e18135.

70. Mondal G, Sengupta S, Panda CK, Gollin SM, Saunders WS, Roychoudhury S. Overexpression of Cdc20 leads to impairment of the spindle assembly checkpoint and aneuploidization in oral cancer. *Carcinogenesis*, 2007, 28:81–92.

71. Rajkumar T, Sabitha K, et al. Identification and validation of genes involved in cervical tumourigenesis. *BMC Cancer*, 2011, 11:80.

72. Majumder P, Bhunia S, Bhattacharyya J, Chaudhuri A. Inhibiting tumor growth by targeting liposomally encapsulated CDC20 siRNA to tumor vasculature: therapeutic RNA interference. *J Control Release*, 2014, 180:100–108.

73. Yuan B, Xu Y, et al. Increased expression of mitotic checkpoint genes in breast cancer cells with chromosomal instability. *Clin Cancer Res*, 2006, 12:405–410.

74. Bièche I, Vacher S, et al. Expression analysis of mitotic spindle checkpoint genes in breast carcinoma: role of NDC80/HEC1 in early breast tumorigenicity, and a two-gene signature for aneuploidy. *Mol Cancer*, 2011, 10:23.

75. Karra H, Repo H, et al. Cdc20 and securin overexpression predict short-term breast cancer survival. *Br J Cancer*, 2014, 110:2905–2913.

76. Zeng X, Sigoillot F, et al. Pharmacologic inhibition of the anaphase-promoting complex induces a spindle checkpoint dependent mitotic arrest in the absence of spindle damage. *Cancer Cell*, 2010, 18:382–395.

77. Sackton KL, Dimova N, et al. Synergistic blockade of mitotic exit by two chemical inhibitors of the APC/C. *Nature*, 2014, 514:646–649.

78. Das T, Roy KS, Chakrabarti T, Mukhopadhyay S, Roychoudhury S. Withaferin A modulates the spindle assembly checkpoint by degradation of Mad2-Cdc20 complex in colorectal cancer cell lines. *Biochem Pharmacol*, 2014, 91:31–39.

79. Jiang J, Thyagarajan-Sahu A, Krchnak V, Jedinak A, Sandusky GE, Sliva D. NAHA, a novel hydroxamic acid-derivative, inhibits growth and angiogenesis of breast cancer *in vitro* and *in vivo*. *PLoS One*, 2012, 7:e34283.

80. Puliyappadamba VT, Wu W, et al. Antagonists of anaphase-promoting complex (APC)-2-cell cycle and apoptosis regulatory protein (CARP)-1 interaction are novel regulators of cell growth and apoptosis. *J Biol Chem*, 2011, 286:38000–38017.

81. Nasr T, Bondock S, Youns M. Anticancer activity of new coumarin substituted hydrazide–hydrazone derivatives. *Eur J Med Chem*, 2014, 76:539–548.

82. Taniguchi K, Momiyama N, Ueda M, Matsuyama R, Mori R, Fujii Y, Ichikawa Y, Endo I, Togo S, Shimada H. Targeting of CDC20 via small interfering RNA causes enhancement of the cytotoxicity of chemoradiation. *Anticancer Res*, 2008, 28:1559-1563.

83. Kidokoro T, Tanikawa C, Furukawa Y, Katagiri T, Nakamura Y, Matsuda K. CDC20, a potential cancer therapeutic target, is negatively regulated by p53. *Oncogene*, 2008, 27:1562-1571.

84. Liu M, Zhang Y, Liao Y, Chen Y, Pan Y, Tian H, Zhan Y, Liu D. Evaluation of the antitumor efficacy of RNAi-mediated inhibition of CDC20 and heparanase in an orthotopic liver tumor model. *Cancer Biother Radiopharm*, 2015, 30:233-239.

85. Li K, Mao Y, et al. Silencing of CDC20 suppresses metastatic castration-resistant prostate cancer growth and enhances chemosensitivity to docetaxel. *Int J Oncol*, 2016, 49:1679-1685.

86. Mukherjee A, Bhattacharyya J, Sagar MV, Chaudhuri A. Liposomally encapsulated CDC20 siRNA inhibits both solid melanoma tumor growth and spontaneous growth of intravenously injected melanoma cells on mouse lung. *Drug Deliv Transl Res*, 2013, 3:224-234.

87. Bhunia S, Radha V, Chaudhuri A. CDC20 siRNA and paclitaxel co-loaded nanometric liposomes of a nipecotic acid-derived cationic amphiphile inhibit xenografted neuroblastoma. *Nanoscale*, 2017, 9:1201-1212.

88. Parmar MB, Aliabadi HM, Mahdipoor P, Kucharski C, Maranchuk R, Hugh JC, Uludağ H. Targeting cell cycle proteins in breast cancer cells with siRNA by using lipid-substituted polyethylenimines. *Front Bioeng Biotechnol*, 2015, 3:14.

89. Parmar MB, Arteaga Ballesteros BE, Fu T, K.C. RB, Montazeri Aliabadi H, Hugh JC, Löbenberg R, Uludağ H. Multiple siRNA delivery against cell cycle and anti-apoptosis proteins using lipid-substituted polyethylenimine in triple-negative breast cancer and nonmalignant cells. *J Biomed Mater Res A*, 2016, 104:3031-3044.

90. Parmar MB, Meenakshi Sundaram DN, K.C. RB, Maranchuk R, Montazeri Aliabadi H, Hugh JC, Löbenberg R, Uludağ H. Combinational siRNA delivery using hyaluronic acid modified amphiphilic polyplexes against cell cycle and phosphatase proteins to inhibit growth and migration of triple-negative breast cancer cells. *Acta Biomater*, 2018, 66:294-309.

91. Parmar MB, K.C. RB, Löbenberg R, Uludağ H. Additive polyplexes to undertake siRNA therapy against CDC20 and survivin in breast cancer cells. *Biomacromolecules*, 2018, 19:4193–4206.

92. Xie Q, Wu Q, et al. CDC20 maintains tumor initiating cells. *Oncotarget*, 2015, 6:13241-13254.

93. Wang L, Hou Y, Yin X, Su J, Zhao Z, Ye X, Zhou X, Zhou L, Wang Z. Rottlerin inhibits cell growth and invasion via down-regulation of Cdc20 in glioma cells. *Oncotarget*, 2016, 7:69770-69782.

94. Paul D, Ghorai S, Dinesh US, Shetty P, Chattopadhyay S, Santra MK. Cdc20 directs proteasome-mediated degradation of the tumor suppressor SMAR1 in higher grades of cancer through the anaphase promoting complex. *Cell Death Dis*, 2017, 8:e2882.

95. Baumgarten AJ, Felthaus J, Wäsch R. Strong inducible knockdown of APC/C^{CDC20} does not cause mitotic arrest in human somatic cells. *Cell Cycle*, 2009, 8:643-646.

96. Yamanaka S, Campbell NR, An F, Kuo SC, Potter JJ, Mezey E, Maitra A, Selaru FM. Coordinated effects of microRNA-494 induce G_2/M arrest in human cholangiocarcinoma. *Cell Cycle*, 2012, 11:2729-2738.

97. Frenzel A, Grespi F, Chmelewskij W, Villunger A. Bcl2 family proteins in carcinogenesis and the treatment of cancer. *Apoptosis*, 2009, 14:584-596.

98. Wang S, Bai L, Lu J, Liu L, Yang CY, Sun H. Targeting inhibitors of apoptosis proteins (IAPs) for new breast cancer therapeutics. *J Mammary Gland Biol Neoplasia*, 2012, 17:217-228.

99. Krueger A, Baumann S, Krammer PH, Kirchhoff S. FLICE-inhibitory proteins: regulators of death receptor-mediated apoptosis. *Mol Cell Biol*, 2001, 21:8247-8254.

100. Safa AR. c-FLIP, a master anti-apoptotic regulator. *Exp Oncol*, 2012, 34:176-184.

101. Shamas-Din A, Kale J, Leber B, Andrews DW. Mechanisms of action of Bcl-2 family proteins. *Cold Spring Harb Perspect Biol*, 2013, 5:a008714.

102. Oberoi-Khanuja TK, Murali A, Rajalingam K. IAPs on the move: role of inhibitors of apoptosis proteins in cell migration. *Cell Death Dis*, 2013, 4:e784.

103. Mita AC, Mita MM, Nawrocki ST, Giles FJ. Survivin: key regulator of mitosis and apoptosis and novel target for cancer therapeutics. *Clin Cancer Res*, 2008, 14:5000-5005.

104. Khan S, Ferguson Bennit H, et al. Localization and upregulation of survivin in cancer health disparities: a clinical perspective. *Biologics*, 2015, 9:57-67.

105. Vader G, Kauw JJ, Medema RH, Lens SM. Survivin mediates targeting of the chromosomal passenger complex to the centromere and midbody. *EMBO Rep*, 2006, 71:85-92.

106. Sampath SC, Ohi R, Leismann O, Salic A, Pozniakovski A, Funabiki H. The chromosomal passenger complex is required for chromatin-induced microtubule stabilization and spindle assembly. *Cell*, 2004, 118:187-202.

107. Giodini A, Kallio MJ, et al. Regulation of microtubule stability and mitotic progression by survivin. *Cancer Res*, 2002, 62:2462-2467.

108. Altieri DC. The case for survivin as a regulator of microtubule dynamics and cell-death decisions. *Curr Opin Cell Biol*, 2006, 18:609-615.

109. Tamm I, Wang Y, et al. IAP-family protein survivin inhibits caspase activity and apoptosis induced by Fas (CD95), Bax, caspases, and anticancer drugs. *Cancer Res*, 1998, 5823:5315-5320.

110. Adida C, Berrebi D, Peuchmaur M, Reyes-Mugica M, Altieri DC. Anti-apoptosis gene, survivin, and prognosis of neuroblastoma. *Lancet*, 1998, 351:882-883.

111. ZhangT, Otevrel T, et al. Evidence that APC regulates survivin expression: a possible mechanism contributing to the stem cell origin of colon cancer. *Cancer Res*, 2001, 61:8664-8667.

112. Fukuda S, Pelus LM. Regulation of the inhibitorof- apoptosis family member survivin in normal cord blood and bone marrow CD34(+) cells by hematopoietic growth factors: implication of survivin expression in normal hematopoiesis. *Blood*, 2001, 98:2091-2100.

113. Gianani R, Jarboe E, et al. Expression of survivin innormal, hyperplastic, and neoplastic colonic mucosa. *Hum Pathol*, 2001, 32:119-125.

114. Altieri DC. Survivin, cancer networks and pathway-directed drug discovery. *Nat Rev Cancer*, 2008, 81:61-70.

115. Blanc-Brude OP, Mesri M, Wall NR, Plescia J, Dohi T, Altieri DC. Therapeutic targeting of the survivin pathway in cancer: initiation of mitochondrial apoptosis and suppression of tumor-associated angiogenesis. *Clin Cancer Res*, 2003, 97:2683-2692.

116. Tu SP, Jiang XH, et al. Suppression of survivin expression inhibits *in vivo* tumorigenicity and angiogenesis in gastric cancer. Cancer Res, 2003, 6322:7724-7732.

117. Pennati M, Folini M, Zaffaroni N. Targeting survivin in cancer therapy: fulfilled promises and open questions. *Carcinogenesis*, 2007, 286:1133-1139.

118. Ryan BM, O'Donovan N, Duffy MJ. Survivin: a new target for anti-cancer therapy. *Cancer Treat Rev*, 2009, 35:553-562.

119. Peery RC, Liu JY, Zhang JT. Targeting survivin for therapeutic discovery: past, present, and future promises. *Drug Discov Today*, 2017, 22:1466-1477.

120. Fernald K, Kurokawa M. Evading apoptosis in cancer. *Trends Cell Biol*, 2013, 23:620-633.

121. Tacar O, Sriamornsak P, Dass CR. Doxorubicin: an update on anticancer molecular action, toxicity and novel drug delivery systems. *J Pharm Pharmacol*, 2013, 65:157-170.

122. Horwitz SB. Taxol (paclitaxel): mechanisms of action. *Ann Oncol*, 1994, 5 Suppl 6:S3-S6.

123. Lee BS, Kim SH, Jin T, Choi EY, Oh J, Park S, Lee SH, Chung JH, Kang SM. Protective effect of survivin in Doxorubicin-induced cell death in h9c2 cardiac myocytes. *Korean Circ J*, 2013, 43:400-407.

124. Xiong H, Yu S, Zhuang L, Xiong H. Changes of survivin mRNA and protein expression during paclitaxel treatment in breast cancer cells. *J Huazhong Univ Sci Technolog Med Sci*, 2007, 27:65-67.

125. Dong H, Yao L, Bi W, Wang F, Song W, Lv Y. Combination of survivin siRNA with neoadjuvant chemotherapy enhances apoptosis and reverses drug resistance in breast cancer MCF-7 cells. J Cancer Res Ther, 2015, 11:717-722.

126. Colnaghi R, Wheatley SP. Liaisons between survivin and Plk1 during cell division and cell death. *J Biol Chem*, 2010, 285:22592-22604.

127. Seth S, Matsui Y, et al. RNAi-based therapeutics targeting survivin and PLK1 for treatment of bladder cancer. *Mol Ther*, 2011, 19:928-935.

128. Kedinger V, Meulle A, et al. Sticky siRNAs targeting survivin and cyclin B1 exert an antitumoral effect on melanoma subcutaneous xenografts and lung metastases. *BMC Cancer*, 2013, 13:338.

129. Zhao S, Sedwick D, Wang Z. Genetic alterations of protein tyrosine phosphatases in human cancers. *Oncogene*, 2015, 34:3885-3894.

130. Hardy S, Julien SG, Tremblay ML. Impact of oncogenic protein tyrosine phosphatases in cancer. *Anticancer Agents Med Chem*, 2012, 12:4-18.

131. Yu S, Li L, Wu Q, Dou N, Li Y, Gao Y. PPP2R2D, a regulatory subunit of protein phosphatase 2A, promotes gastric cancer growth and metastasis via mechanistic target of rapamycin activation. *Int J Oncol*, 2018, 52:2011-2020.

132. Luo W, Xu C, Ayello J, Dela Cruz F, Rosenblum JM, Lessnick SL, Cairo MS. Protein phosphatase 1 regulatory subunit 1A in ewing sarcoma tumorigenesis and metastasis. *Oncogene*, 2018, 37:798-809.

133. Tonks NK. Protein tyrosine phosphatases: from genes, to function, to disease. *Nat Rev Mol Cell Biol*, 2006, 7:833-846.

134. Zhang ZY. Protein tyrosine phosphatases: structure and function, substrate specificity, and inhibitor development. *Annu Rev Pharmacol Toxicol*, 2002, 42:209-234.

135. Mumby MC, Walter G. Protein serine/threonine phosphatases: structure, regulation, and functions in cell growth. *Physiol Rev*, 1993, 73:673-699.

136. Camps M, Nichols A, Arkinstall S. Dual specificity phosphatases: a gene family for control of MAP kinase function. *FASEB J*, 2000, 14:6-16.

137. Bäumer N, Mäurer A, Krieglstein J, Klumpp S. Expression of protein histidine phosphatase in *Escherichia coli*, purification, and determination of enzyme activity. *Methods Mol Biol*, 2007, 365:247-260.

138. Jiang Y. Regulation of the cell cycle by protein phosphatase 2A in *Saccharomyces cerevisiae*. *Microbiol Mol Biol Rev*, 2006, 70:440-449.

139. Cheng A, Ross KE, Kaldis P, Solomon MJ. Dephosphorylation of cyclin-dependent kinases by type 2C protein phosphatases. *Genes Dev*, 1999, 13:2946-2957.

140. Kim HS, Fernandes G, Lee CW. Protein Phosphatases Involved in Regulating Mitosis: Facts and Hypotheses. *Mol Cells*, 2016, 39:654-662.

141. Motiwala T, Jacob ST. Role of protein tyrosine phosphatases in cancer. *Prog Nucleic Acid Res Mol Biol*, 2006, 81:297-329.

142. Figueiredo J, da Cruz E Silva OA, Fardilha M. Protein phosphatase 1 and its complexes in carcinogenesis. *Curr Cancer Drug Targets*, 2014, 14:2-29.

143. Lee ST, Feng M, et al. Protein tyrosine phosphatase UBASH3B is overexpressed in triple-negative breast cancer and promotes invasion and metastasis. *Proc Natl Acad Sci USA*, 2013, 110:11121-11126.

144. Spring K, Fournier P, Lapointe L, Chabot C, Roussy J, Pommey S, Stagg J, Royal I. The protein tyrosine phosphatase DEP-1/PTPRJ promotes breast cancer cell invasion and metastasis. *Oncogene*, 2015, 34:5536-5547.

145. Hoekstra E, Peppelenbosch MP, Fuhler GM. The role of protein tyrosine phosphatases in colorectal cancer. *Biochim Biophys Acta*, 2012, 1826:179-188.

146. Nunes-Xavier CE, Mingo J, López JI, Pulido R. The role of protein tyrosine phosphatases in prostate cancer biology. *Biochim Biophys Acta Mol Cell Res*, 2019, 1866:102-113.

147. Ruvolo PP. Role of protein phosphatases in the cancer microenvironment. *Biochim Biophys Acta Mol Cell Res*, 2019, 1866:144-152.

148. Al-Aidaroos AQ, Zeng Q. PRL-3 phosphatase and cancer metastasis. *J Cell Biochem*, 2010, 111:1087-1098.

149. Feng X, Wu Z, Wu Y, Hankey W, Prior TW, Li L, Ganju RK, Shen R, Zou X. Cdc25A regulates matrix metalloprotease 1 through Foxo1 and mediates metastasis of breast cancer cells. *Mol Cell Biol*, 2011, 31:3457-3471.

150. Bollu LR, Mazumdar A, Savage MI, Brown PH. Molecular pathways: targeting protein tyrosine phosphatases in cancer. *Clin Cancer Res*, 2017, 23:2136-2142.

151. Scott LM, Lawrence HR, Sebti SM, Lawrence NJ, Wu J. Targeting protein tyrosine phosphatases for anticancer drug discovery. *Curr Pharm Des*, 2010, 16:1843-1862.

152. McConnell JL, Wadzinski BE. Targeting protein serine/threonine phosphatases for drug development. *Mol Pharmacol*, 2009, 75:1249-1261.

153. Liang F, Liang J, Wang WQ, Sun JP, Udho E, Zhang ZY. PRL3 promotes cell invasion and proliferation by down-regulation of Csk leading to Src activation. *J Biol Chem*, 2007, 282:5413-5419.

154. Csoboz B, Gombos I, Tatrai E, Tovari J, Kiss AL, Horvath I, Vigh L. Chemotherapy induced PRL3 expression promotes cancer growth via plasma membrane remodeling and specific alterations of caveolae-associated signaling. *Cell Commun Signal*, 2018, 16:51.

155. Xia ZS, Wu D, Zhong W, Lu XJ, Yu T, Chen QK. Wip1 gene silencing enhances the chemosensitivity of human colon cancer cells. *Oncol Lett*, 2017, 14:1875-1883.

156. Cao Y, Tu Y, Mei J, Li Z, Jie Z, Xu S, Xu L, Wang S, Xiong Y. RNAi-mediated knockdown of PRL-3 inhibits cell invasion and downregulates ERK 1/2 expression in the human gastric cancer cell line, SGC-7901. *Mol Med Rep*, 2013, 7:1805-1811.

157. Zimmerman MW, Homanics GE, Lazo JS. Targeted deletion of the metastasis-associated phosphatase Ptp4a3 (PRL-3) suppresses murine colon cancer. *PLoS One*, 2013, 8:e58300.

158. Wei M, Korotkov KV, Blackburn JS. Targeting phosphatases of regenerating liver (PRLs) in cancer. *Pharmacol Ther*, 2018, 2018, 190:128-138.

159. Fire A, Xu S, Montgomery MK, Kostas SA, Driver SE, Mello CC. Potent and specific genetic interference by double-stranded RNA in *Caenorhabditis elegans*. *Nature*, 1998, 391:806-811.

160. Hamilton AJ, Baulcombe DC. A species of small antisense RNA in posttranscriptional gene silencing in plants. *Science*, 1999, 286:950-952.

161. Bentwich I, et al. Identification of hundreds of conserved and nonconserved human microRNAs. *Nature Genet*, 2005, 37:766-770.

162. Moore CB, Guthrie EH, Huang MT, Taxman DJ. Short hairpin RNA (shRNA): design, delivery, and assessment of gene knockdown. *Methods Mol Biol*, 2010, 629:141-158.

163. Kim DH, Rossi JJ. Strategies for silencing human disease using RNA interference. *Nature Rev Genet*, 2007, 8:173-184.

164. Wilson RC, Doudna JA. Molecular mechanisms of RNA interference. *Annu Rev Biophys*, 2013, 42:217-239.

165. Leuschner PJ, Ameres SL, Kueng S, Martinez J. Cleavage of the siRNA passenger strand during RISC assembly in human cells. *EMBO Rep*, 2006, 7:314-320.

166. Preall JB, Sontheimer EJ. RNAi: RISC gets loaded. *Cell*, 2005, 123:543-545.

167. Wang Z, Rao DD, Senzer N, Nemunaitis J. RNA interference and cancer therapy. *Pharm Res*, 2011, 28:2983-2995.

168. Aliabadi HM, Landry B, Sun C, Tang T, Uludağ H. Supramolecular assemblies in functional siRNA delivery: where do we stand? *Biomaterials*, 2012, 33:2546-2569.

169. Meneksedag-Erol D, Tang T, Uludağ H. Molecular modeling of polynucleotide complexes. Biomaterials, 2014, 35:7068-7076.

170. Aliabadi HM, Landry B, Bahadur RK, Neamnark A, Suwantong O, Uludağ H. Impact of lipid substitution on assembly and delivery of siRNA by cationic polymers. *Macromol Biosci*, 2011, 11:662-672.

171. Wang J, Lu Z, Wientjes MG, Au JL. Delivery of siRNA therapeutics: barriers and carriers. *AAPS J*, 2010, 12:492-503.

172. Hashida M, Kawakami S, Yamashita F. Lipid carrier systems for targeted drug and gene delivery. *Chem Pharm Bull*, 2005, 53:871-880.

173. Boussif O, Lezoualc'h F, Zanta MA, Mergny MD, Scherman D, Demeneix B, Behr JP. A versatile vector for gene and oligonucleotide transfer into cells in culture and *in vivo*: polyethylenimine. *Proc Natl Acad Sci USA*, 1995, 92:7297-7303.

174. Gong D et al. Cyclin A2 regulates nuclear-envelope breakdown and the nuclear accumulation of cyclin B1. *Curr Biol*, 2007, 17:85-91.

175. Sakurai H et al. Comparison of gene expression efficiency and innate immune response induced by Ad vector and lipoplex. *J Control Release*, 2007, 117:430-437.

176. Gautam A, Densmore CL, Waldrep JC. Pulmonary cytokine responses associated with PEI-DNA aerosol gene therapy. *Gene Ther*, 2001, 8:254-257.

177. Sakurai H, Kawabata K, Sakurai F, Nakagawa S, Mizuguchi H. Innate immune response induced by gene delivery vectors. *Int J Pharm*, 2008 354:9-15.

178. Lechardeur D, Lukacs GL. Nucleocytoplasmic transport of plasmid DNA: a perilous journey from the cytoplasm to the nucleus. *Hum Gene Ther*, 2006, 17:882-889.

179. Zang L, Nishikawa M, Machida K, Ando M, Takahashi Y, Watanabe Y, Takakura Y. Inhibition of nuclear delivery of plasmid DNA and transcription by interferon γ: hurdles to be overcome for sustained gene therapy. *Gene Ther*, 2011, 18:891-897.

180. Ribeiro SC, Monteiro GA, Prazeres DM. The role of polyadenylation signal secondary structures on the resistance of plasmid vectors to nucleases. *J Gene Med*, 2004, 6:565-573.

181. Whitehead KA, Dahlman JE, Langer RS, Anderson DG. Silencing or stimulation? siRNA delivery and the immune system. *Annu Rev Chem Biomol Eng*, 2011, 2:77-96.

182. Bessis N, GarciaCozar FJ, Boissier MC. Immune responses to gene therapy vectors: influence on vector function and effector mechanisms. *Gene Ther*, 2004, 11:S10-S17.

183. Riu E, Chen ZY, Xu H, He CY, Kay MA. Histone modifications are associated with the persistence or silencing of vector-mediated transgene expression *in vivo*. *Mol Ther*, 2007, 15:1348-1355.

184. Pillai RS. MicroRNA function: multiple mechanisms for a tiny RNA? *RNA*, 2005, 11:1753-1761.

185. Baumann V, Winkler J. miRNA-based therapies: strategies and delivery platforms for oligonucleotide and non-oligonucleotide agents. *Future Med Chem*, 2014, 6:1967-1984.

186. Shaukat Z, Liu D, Choo A, Hussain R, O'Keefe L, Richards R, Saint R, Gregory SL. Chromosomal instability causes sensitivity to metabolic stress. *Oncogene*, 2015, 34:4044-4055.

187. Aagaard L, Rossi JJ. RNAi therapeutics: principles, prospects and challenges. *Adv Drug Deliv Rev*, 2007, 59:75-86.

188. Carter MG, Sharov AA, VanBuren V, Dudekula DB, Carmack CE, Nelson C, Ko MS. Transcript copy number estimation using a mouse whole-genome oligonucleotide microarray. *Genome Biol*, 2005, 6:R61.

189. Bao T, Davidson NE. Gene expression profiling of breast cancer. *Adv Surg*, 2008, 42:249-260.

190. Owens DE III, Peppas NA. Opsonization, biodistribution, and pharmacokinetics of polymeric nanoparticles. *Int J Pharm*, 2006, 307:93-102.

191. Chithrani BD, Ghazani AA, Chan WC. Determining the size and shape dependence of gold nanoparticle uptake into mammalian cells. *Nano Lett*, 2006, 6:662-668.

192. Toy R, Peiris PM, Ghaghada KB, Karathanasis E. Shaping cancer nanomedicine: the effect of particle shape on the *in vivo* journey of nanoparticles. *Nanomedicine (Lond)*, 2014, 9:121–134.

193. Agarwal R, Jurney P, Raythatha M, et al. Effect of shape, size, and aspect ratio on nanoparticle penetration and distribution inside solid tissues using 3D spheroid models. *Adv Healthc Mater*, 2015, 4:2269–2280.

194. Sun B, Ji Z, Liao YP, et al. Engineering an effective immune adjuvant by designed control of shape and crystallinity of aluminum oxyhydroxide nanoparticles. *ACS Nano*, 2013, 7:10834–10849.

195. Shen H, Shi S, Zhang Z, Gong T, Sun X. Coating solid lipid nanoparticles with hyaluronic acid enhances antitumor activity against melanoma stem-like cells. *Theranostics*, 2015, 5:755-771.

196. Veronese FM, Mero A. The impact of PEGylation on biological therapies. *BioDrugs*, 2008, 22:315-329.

197. Teesalu T, Sugahara KN, Ruoslahti E. Tumor-penetrating peptides. *Front Oncol*, 2013, 3:216.

198. Cardoso MM, Peça IN, Roque AC. Antibody-conjugated nanoparticles for therapeutic applications. *Curr Med Chem*, 2012, 19:3103-3127.

2. Targeting cell cycle proteins in breast cancer cells with siRNA by using lipid-substituted polyethylenimines

A version of this chapter was published in:

Parmar MB, Aliabadi HM, Mahdipoor P, Kucharski C, Maranchuk R, Hugh JC, Uludağ H. Targeting cell cycle proteins in breast cancer cells with siRNA by using lipid-substituted polyethylenimines. *Front Bioeng Biotechnol*, 2015, 3:14.

2.1 Introduction

There are significant limitations and side-effects to conventional chemotherapy employed in management of breast cancers. Malignant cells can additionally develop resistance to chemotherapy by changing their molecular (genetic) makeup [1,2]. The development of drug resistance in particular warrants a search for alternative and more effective therapies in breast cancers. The treatment of cancer based on RNA interference (RNAi) using small interfering RNA (siRNA) has been a promising approach and it is actively explored as an alternative to chemotherapy [3,4]. Double-stranded synthetic siRNA can be incorporated into the RNA inducing silencing complex (RISC) following the release of the passenger strand and leaving the guide strand of siRNA bound to RISC [4,5]. The guide strand directs the siRNA-RISC complex to a targeted mRNA. The siRNA-RISC complex can bind and either cleave the target mRNA via endonuclease activity or block the translation of mRNA, resulting in the 'silencing' of a specific target [5]. However, the binding of siRNA on its own to cell membranes and subsequent uptake is nearly impossible due to its highly anionic nature [6,7]. The naked siRNA is, moreover, instantly degraded by RNase A in extracellular milieu, resulting in a poor pharmacokinetics profile [8]. Well-designed carriers are, therefore, necessary to neutralize the anionic charge of siRNA to facilitate its intracellular delivery and inhibit extracellular degradation. We reported a library of cationic polymers based on low molecular weight (2 kDa) polyethylenimine (PEI) that are substituted with different hydrophobic moieties and have shown effective transfection efficiency without significant toxicity [9-12]. Cationic PEI binds to siRNA to provide effective protection against enzymatic degradation, and delivers siRNA into the cells for assembly into the RISC [13].

The cell cycle constitutes a series of events that leads to controlled cell division and multiplication [14]. Since de-regulation of cell cycle events leads to uncontrolled cell proliferation and is a hallmark of malignancy [15,16], the molecular mediators responsible for abnormal cell cycle regulation are viable targets for siRNA therapy. There are several factors that can deregulate a cell cycle; mutation of a regulatory protein might lead to a loss of binding to its target, or overexpression of a critical protein might lead to constitutive activation of cell cycle. In such cases, malignant cells could proliferate at faster rate than the normal cells, and/or lose the efficiency to detect DNA damage and arrest the progression of cell cycle [15,16]. Overexpressed or mutated cell cycle proteins can, therefore, be targeted as the basis of a breast cancer therapy. Many proteins have been found de-regulated during the progression of cell cycle such as the cyclins and cyclin dependent kinases (CDKs) [17,18], and some efforts have been directed to regulate the uncontrolled malignant cell proliferation by delivering siRNA specific to such proteins.

To explore the role of cell cycle proteins as the basis of a breast cancer therapy, this study has undertaken a general approach to identify therapeutically useful targets with polymer-mediated siRNA delivery. Several in-house prepared lipophilic PEIs and a library of siRNAs against cell cycle proteins were screened for this purpose in breast cancer cells. Kinesin spindle protein (KSP), which is required to form a bipolar spindle in mitosis by separating the emerging spindle poles [19,20], was employed as a reference target since an siRNA against KSP is at early stages of clinical trials [21,22]. We hypothesized that silencing critical cell cycle proteins by RNAi would result in reduced cell growth and decreased viability of malignant cells. We further hypothesize that polymeric delivery of siRNA is an effective approach to silence cell cycle proteins in breast cancer cells. The

objectives of this study were to find the optimal siRNA delivery system and to identify most effective cell cycle protein target(s) for therapeutic silencing in breast cancer cells. Moreover, we explored the efficacy of siRNA and dicer-substrate siRNA (DsiRNA) against *in vitro* and *in vivo*. Unlike the conventional 21-bp double-stranded siRNA, longer DsiRNA can incorporate into the Dicer enzyme in RISC complex, leading to improved silencing efficacies [23].

2.2 Materials and Methods

2.2.1 Cell-lines

The wild-type (WT) and drug-resistant (R) breast cancer MDA-MB-435* cells were cultured in RPMI 1640 medium, while MDA-MB-231 (WT and R phenotypes) and MCF7 breast cancer cells were cultured in DMEM medium with 10% FBS, 100 U/mL penicillin and 100 µg/mL streptomycin, and maintained at 37 °C and 5% CO2. The drug resistance in MDA-MB-435 and MDA-MB-231 cells was developed as described in [11,12], and was confirmed periodically by evaluating the IC50 (*i.e.,* concentration for 50% cell kill) of doxorubicin in both cell-lines.

2.2.2 Polymeric carriers and siRNA-polymer complex preparation

Polyethylenimines (PEI, 2 kDa branched) modified with linoleic acid (LA, 1.65 substitutions/PEI), caprylic acid (CA, 6.0 substitutions/PEI) and α-linoleic acid (αLA, 0.5

*MDA-MB-435 cells have been debated scientifically about its true origin [50]. Originally, these cells were described as breast cancer cells, but recent expression array profile indicated them melanoma cells due to expression of melanoma-specific markers in these cells [51]. Due to this controversy about MDA-MB-435 cells, we stopped using these cells in our subsequent studies. However, we still reported the studies that we performed using these cells here.

substitutions/PEI) were synthesized according to our established protocol [24,25] and the degree of substitution was determined by ^{1}H-NMR. The siRNA-polymer complexes were prepared in 150 mM NaCl, and were added to the cells after 30 min of incubation. The siRNA:polymer ratio in the complexes were either 1:2, 1:4 or 1:8 (w/w), and complexes were added to the cells at desired siRNA concentrations (see Figure legends for exact ratios and concentrations). The lipid-based commercial carriers, HiperFect (Qiagen, Valencia, CA) and TurboFect (Thermo Fisher Scientific, Waltham, MA) were included in the screening with the synthesized polymers, and they were used to make complexes as suggested by the manufacturers.

2.2.3 Cellular uptake of siRNA by flow cytometry and confocal microscopy

To investigate quantitative uptake of siRNA, MDA-MB-435WT were seeded in 24-well plates, and transfected with 6-carboxyfluorescein (FAM)-labeled scrambled siRNA (Cat. No. AM4620; Life Technologies) at 20 nM and 40 nM concentrations with 1:2, 1:4 and 1:8 siRNA:PEILA ratios. Non-labeled scrambled siRNA was used as a negative control. After 24 hrs of treatment, cells were washed with Hank's Balanced Salt Solution (HBSS), treated with trypsin/ Ethylene diamine tetra acetic acid (EDTA), and the recovered cells were fixed with 3.7% formaldehyde. The uptake of siRNA was quantified using Cell Lab Quanta SC flow cytometer (Beckman Coulter, Brea, CA, USA). The mean fluorescence of the recovered cell population and the percentage of cells showing FAM-fluorescence were determined. Gating of the cell population was such that auto-fluorescence of untreated cells represented 1-2% of the total cell population.

To further investigate qualitative uptake of siRNA, MDA-MB-435WT were grown on glass cover slips (Thermo Fisher Scientific) for 24 hrs and transfected by non-labeled

scrambled siRNA and FAM-labeled scrambled siRNA complexes at 40 nM with 1:2 and 1:8 siRNA to PEI-LA ratios. After 24 hrs, cells were washed with HBSS, fixed with 3.7% formaldehyde and mounted on a slide using in-house prepared mounting medium (poly vinyl alcohol in glycerol) with 4',6-diamidino-2- phenylindole (DAPI, Life Technologies) to stain nuclei and wheat germ agglutinin, tetramethylrhodamine conjugate (Invitrogen) to stain cytoplasmic membrane. Prepared slides were studied using 40x 1.3 oil plan-Apochromat lens in Laser Scanning Confocal Microscope (LSM710, Carl Zeiss AG, Oberkochen, Germany), and using ZEN 2011 software. The number of siRNApolymer complexes per cell was determined by Imaris software (Bitplane, Belfast, UK). The similar uptake study was performed using MCF7 cells **(Fig 2.S1)**.

2.2.4 Screening of cell cycle proteins

The human siGENOME siRNA Library on Cell Cycle Regulation (Dharmacon, Lafayette, CO, USA) was used to screen 169 siRNAs to determine the potential cell cycle proteins that can be used as siRNA targets in breast cancer cells. The siRNAs were formulated as a mixture of four different sequences in the library targeting specific protein at four different sites. MDA-MB-435R and MDA-MB-231R cells were cultured in 96-well plate and transfected with 54 nM of each cell cycle protein siRNA at 1:4 siRNA:PEI-LA ratio. In order to assess the sensitizing effect of a drug, doxorubicin (Sigma-Aldrich) was added after 48 hrs of siRNA treatment at 5 μg/mL concentration. The MTT (3-(4 5-dimethylthiazol-2-yl)-2 5-diphenyltetrazolium) assay was performed after 72 hrs of treatment. The MTT (Sigma-Aldrich, St. Louis, MO, USA) was added to the cells at 1 mg/mL final concentration in HBSS and the cells were incubated for 45 min at 37 °C and 5% CO2. Soluble MTT is transformed into insoluble formazan crystals during this time by

the activity of mitochondrial dehydrogenase enzymes, giving a measure of cellular activity [26]. Dimethyl sulfoxide (DMSO) was added to the well to dissolve the crystals of MTT dye and the optical density was measured at 570 nm. The percentage viability was calculated as follows: 100% x (absorbance of cells treated with an siRNA complex/absorbance of untreated cells), where the activity of untreated cells was taken as 100% cell growth.

2.2.5 Validation of identified targets and combinational siRNA therapy

The CDC20, RAD51 and CHEK1 were identified as potential targets based on an initial screening of siRNAs against cell cycle proteins. For validation, individual siRNAs against these cell cycle proteins were obtained from Dharmacon (CDC20: Cat. No. D-003225-10; RAD51: Cat. No. D-003530-02, and; CHEK1: Cat. No. D-003255-06) and delivered to cells at 20 and 40 nM of siRNA concentrations and 1:2, 1:4 and 1:8 siRNA:carrier ratios (in triplicate). Another well-studied cell cycle protein, KSP (siRNA against KSP: Cat. No. AM16706, Life Technologies) and a scrambled siRNA (Cat. No. AM4635, Life Technologies) was included in the validation study. The siRNAs were evaluated in MDA-MB-231WT, MDA-MB-231R and MCF7 cells by using PEI-LA and PEI-CA as indicated in Figure legends **(Fig 2.S2, 2.S3)**. The combinational siRNA therapy was performed using 20 nM of each CDC20, RAD51, CHEK1, KSP and scrambled siRNA with the final siRNA concentration of 40 nM. The siRNA to PEI-LA ratio was 1:2 in MDA-MB-435WT and 1:8 in MDA-MB-435R cells at 40 nM of combinational siRNA. The MTT assay was performed after 72 hrs of combinational treatment as indicated above. The sensitizing effect of siRNA for doxorubicin was determined using MDA-MB-435R cells at 20, 40 and 60 nM concentrations of siRNA with 1:2, 1:4 and 1:8 siRNA: PEI-LA ratios.

Doxorubicin (5 μg/mL) was added to cells after 48 hrs of treatment with siRNAs and inhibition of cell growth was assessed by the MTT after a further 72 hrs of incubation.

2.2.6 Quantification of transcripts by droplet digital PCR (ddPCR)

The MDA-MB-435WT were seeded in 6-well plates, and transfected with siRNA complexes at 40 nM (1:2 siRNA:PEI-LA ratios) and 60 nM (1:8 siRNA:PEI-LA ratios), respectively. Total RNA was isolated from MDA-MB-435WT after 24 hrs and 48 hrs of treatment using TRIzol (Invitrogen). Two micrograms of total RNA were converted into cDNA using M-MLV reverse transcriptase (Invitrogen) according to manufacturer's instruction. The ddPCR was performed using 10 ng of each cDNA sample and ddPCR supermix for probes by employing QX100 droplet digital PCR system (Bio-Rad, Hercules, CA, USA). The PrimeTime qPCR assays for CDC20 (Assay ID: Hs.PT.58.41063796), RAD51 (Assay ID: Hs.PT.58.38809475) and CHEK1 (Assay ID: Hs.PT.58.3518318) were ordered from IDT (Coralville, Iowa), while TaqMan gene expression assays for KSP (Assay ID: Hs00189698_m1) and a reference gene, β-actin (Assay ID: Hs01060665_g1) were purchased from Life Technologies. The ddPCR conditions comprised of an initial denaturation for 10 min at 95 °C followed by 45 cycles of denaturation for 30 s at 94 °C and annealing for 1 min at 60 °C, and the final extension for 10 min at 98 °C. Template DNA was omitted from the ddPCR reaction as a no template control (NTC) and the results of ddPCR were analyzed using the QuantaSoft Software (Bio-Rad). The absolute copy number of targeted gene was divided by the absolute copy number of a reference gene β-actin and presented as percentage based on untreated cells (100%).

2.2.7 Targeting cell cycle proteins with DsiRNA

The DsiRNA, having displayed superior efficacy (*i.e.,* sub-nM concentrations) in previous studies [27] was also explored to confirm the validity of chosen targets and improve therapeutic efficacy with our carriers. Three DsiRNAs targeting different locations of the mRNA transcript for CDC20, RAD51 and CHEK1 were obtained from IDT, namely CDC20-1 (Cat. No. HSC.RNAi.N001255.12.1), CDC20-2 (Cat. No. HSC.RNAi.N001255.12.2), CDC20-3 (Cat. No. HSC.RNAi.N001255.12.3), RAD51-1 (Cat. No. HSC.RNAi.N001164269.12.1), RAD51-2 (Cat. No. HSC.RNAi.N001164269. 12.2), RAD51-3 (Cat. No. HSC.RNAi.N001164269.12.3), CHEK1-1 (Cat. No. HSC.RNAi .N001114121.12.1), CHEK1-2 (Cat. No. HSC.RNAi.N001114121.12.2) and CHEK1-3 (Cat. No. HSC.RNAi.N001114121.12.3) with scrambled DsiRNA (Cat. No. DS NC1). The MDA-MB-435WT and MDA-MB-435R cells were transfected with 20 and 40 nM of DsiRNAs at 1:2, 1:4 and 1:8 DsiRNA:PEI-LA ratios. The sensitizing effect of DsiRNAs for doxorubicin was determined in MDA-MB-435R with the same DsiRNA concentrations by adding doxorubicin (5 μg/mL) after 48 hrs of DsiRNA treatment. The MTT assay was performed after 72 hrs of DsiRNA treatment (24 hrs of doxorubicin treatment). The inhibition of cell growth by DsiRNAs against these cell cycle protein targets were additionally determined in MDA-MB-231WT and MCF7 cells at 40 nM and 60 nM of DsiRNA using various ratios of DsiRNA:PEI-LA **(Fig 2.S4)**.

2.2.8 Animal Study

All experimental protocols using animals were approved by the Animal Care and Use Committee: Health Sciences at the University of Alberta in accordance with the directions of the Canadian Council on Animal Care. The athymic NCRNU nude mice (4-6 weeks old male) to be used as a xenograft model were obtained from Taconic Biosciences

Inc. (Hudson, NY). Approximately three million MDA-MB-435WT cells were injected subcutaneously into the right flank of the mice, and tumor growth was monitored every three days. When the tumor volume reached 60-100 mm3 (measured by external calibers as indicated in [12]), mice were put on the study by injecting DsiRNA and polymer complexes subcutaneously in the vicinity of the tumors. The mice were treated by 2 μg of DsiRNA/mouse (scrambled or CDC20-1) with 1:8 DsiRNA:PEI-LA ratio. All mice were divided into two groups. First group of mice received weekly injections of scrambled DsiRNA and CDC20-1 DsiRNA (n = 7 in each study group) for three weeks. The second group of mice received the same siRNA treatment, but at bi-weekly injection intervals (n = 7 in each study group). The subsequent tumor volumes were measured twice a week with 3- and 4-day intervals. Any mouse with large tumor volume (>1500 mm^3), necrotic spot on tumor, or excessive (>20%) weight loss was euthanized before the end-time point of the study for humane considerations and excluded from the entire study. Relative tumor volumes were calculated normalizing the tumor volumes at different time points with the initial tumor volume (*i.e.,* at the time a mouse is included in the study; taken at 100% initially).

2.2.9 Statistical analysis

All results were presented as mean ± standard deviation and analyzed by unpaired student's t-test. The significance ($p<0.05$) was typically determined by comparing specific siRNA-treated groups to that of scrambled siRNA treated groups. The significantly different treatment groups are indicated with an asterisk (*) in Figures, with reference groups indicated in the Legend.

2.3 Results

2.3.1 Initial screening of carriers

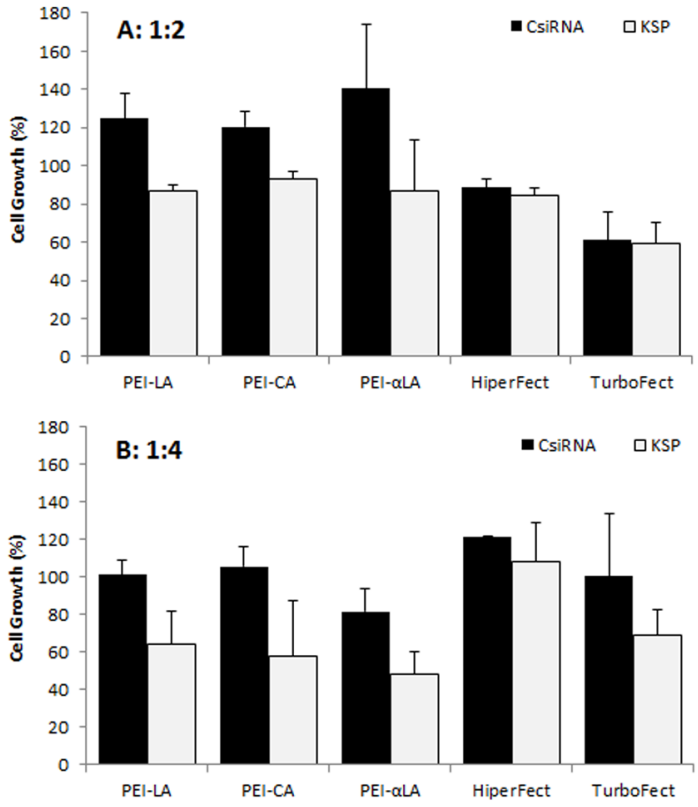

Fig 2.1: Screening of polymeric and commercial carriers.

Screening of carriers in MDA-MB-435WT cells at 1:2 (A) and 1:4 (B) siRNA to carrier ratios with 20 nM of scrambled siRNA (control; CsiRNA) and KSP siRNA. PEI substituted with linoleic acid (LA), caprylic acid (CA) and α-linoleic acid (αLA) were used in the initial screen along with two commercially available carriers.

We previously reported successful delivery of siRNA for specific targets in breast cancer cells using low molecular weight PEI-based polymers [9-12]. As the efficacy of polymers and designed siRNAs was different for each targeted protein, we screened several polymers to identify effective carrier for cell cycle proteins. We screened the PEIs substituted with LA, CA and αLA and used siRNA against KSP in MDA-MB-435WT cells for this purpose. All chosen polymers were effective for the delivery of KSP siRNA at 1:2

and 1:4 siRNA:polymer ratios employed **(Fig 2.1)**. The effectiveness of commercial carriers HiperFect and TurboFect was not evident under similar conditions. Among the polymers, PEI-LA was chosen for further studies since (i) this polymer was equivalent in potency to other polymers, and (ii) it was previously used with other targets and in animal models with success [12].

2.3.2 Cellular uptake of siRNA

The cellular uptake of FAM-labeled scrambled siRNA was performed by flow cytometry to determine the efficiency of PEI-LA to deliver siRNA in MDA-MB-435WT cells **(Fig 2.2A)**. An equivalent mean fluorescence and FAM-positive cell population was observed between non-treated cell and cells exposed to non-labeled siRNA (data not shown), indicating no cellular autofluorescence as a result of siRNA delivery. The siRNA uptake (mean fluorescence) and FAM-labeled siRNA positive cells were dependent on siRNA:PEI-LA ratios, and they were both higher at 40 nM siRNA as compared to 20 nM siRNA concentration, as expected **(Fig 2.2A)**. A significant difference was found in FAM-labeled siRNA positive cells between 1:4 and 1:8 ratios at 40 nM despite a similar mean fluorescence, suggesting that a higher fraction of MDA-MB-435WT cells were transfected at 1:8 ratio. In order to quantify the number of siRNA-polymer complexes per cell, confocal microscopy was employed, and the number of particles was calculated in each cell after taking image by z-stacking **(Fig 2.2B)**. Non-labeled siRNA was delivered in MDA-MB-435WT **(Fig 2.2Bi)** as a control to observe any auto-fluorescent particles; no fluorescent particles were found which confirmed a lack of auto-fluorescence in confocal microscopy as well. The number of siRNA-polymer complexes per cell was significantly different between 1:2 **(Fig 2.2Bii)** and 1:8 **(Fig 2.2Biii)** siRNA:polymer ratios **(Fig 2.2C)**.

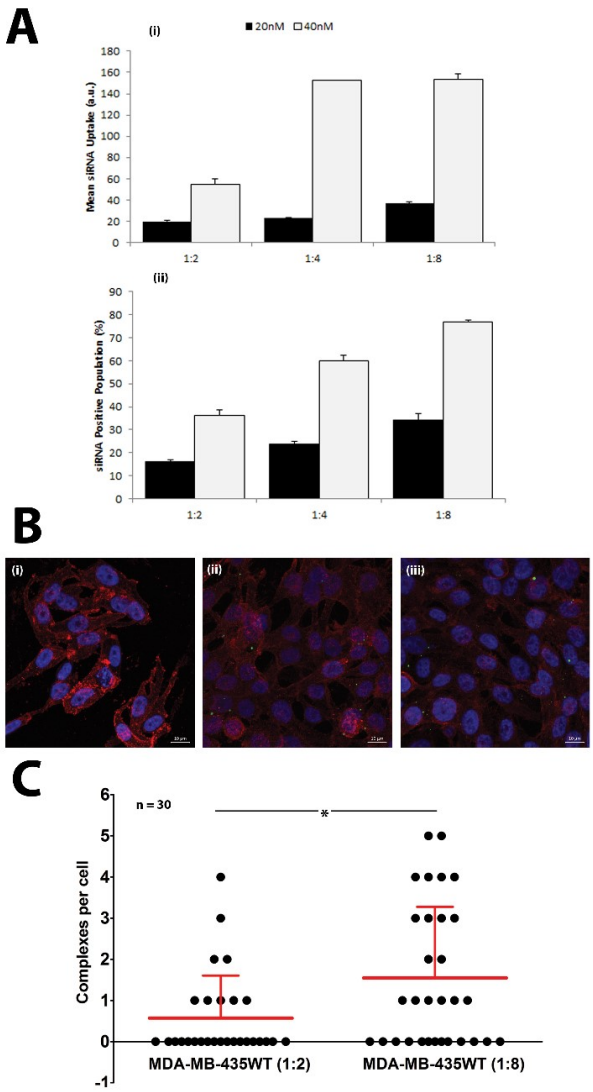

Fig 2.2: Cellular uptake of FAM-labeled siRNA in MDA-MB-435WT cells.

(A) Uptake of FAM-labeled siRNA complexes at 20 nM and 40 nM siRNA using 1:2, 1:4 and 1:8 siRNA:PEI-LA ratios. The MDA-MB-435WT cells were incubated with the complexes for 24 hrs and recovered for flow cytometry analysis. The results were summarized as mean FAMsiRNA per cell (top) and FAM-siRNA positive cell population (bottom). **(B)** Confocal microscopy to determine the uptake of FAM-labeled siRNA complexes at 40 nM siRNA with 1:2 (ii) and 1:8 (iii) siRNA:PEI-LA ratios after 24 hrs treatment. Purple, red and green colors represent nuclei, cytoplasm and siRNA complexes, respectively. Non-labeled scrambled siRNA was transfected as a control in MDA-MB-435WT (i). **(C)** The number of visible complexes per cell (as quantitated from confocal microscopy images) at 1:2 and 1:8 siRNA:PEI-LA ratios. The uptake was significantly different between 1:2 and 1:8 ratios (*p<0.05).

Both flow cytometry and confocal microscopy indicated a better delivery by PEI-LA at higher ratio of siRNA:PEI-LA. A similar uptake study using flow cytometry and confocal microscopy was additionally performed with MCF7 cells **(Fig 2.S1)** and the results again indicated a better delivery with a higher siRNA:PEI-LA ratio.

2.3.3 Screening of cell cycle proteins

A screening of 169 siRNAs against cell cycle proteins was performed using PEI-LA for delivery. The outcome was based on inhibition of cell growth as assessed by the MTT assay **(Fig 2.3A)**. The growth inhibition was more significant in MDA-MB-435R cells (up to >50% of control) compared to MDA-MB-231R cells (typically <25% of control). Based on the response of MDA-MB-435R cells, cell division cycle protein 20 (CDC20), the recombinase RAD51, and the serine/threonine protein kinase CHEK1 were identified as potential targets as >50% inhibition of cell growth was achieved by the treatment of siRNA alone for these targets **(Fig 2.3A)**. In a subsequent study, doxorubicin was added to the cells after 48 hrs of siRNA addition to determine whether siRNA treatment resulted in sensitizing the cells to doxorubicin. The cell growth of MDA-MB-231R was >70% after dual therapy of siRNA and doxorubicin, except silencing of cyclin D3 (62%; **Fig 2.3B**). The MDA-MB-435R cells were more responsive to siRNA therapy, but the sensitizing effect of doxorubicin was not immediately clear in these cells **(Fig 2.3C)**. The difference in cell growth between siRNA treatment alone and the dual therapy of siRNA/doxorubicin is presented in **Fig 2.3D**. The difference in cell growth was 10 to 25% for many cell cycle proteins in MDA-MB-231R, except homeodomain interacting protein kinase 2 (HIPK2, 46%), which indicates a sensitizing effect for doxorubicin.

However, the cell growth of MDA-MB-231R after siRNA/doxorubicin therapy was again >75% (**Fig 2.3B)**, which was equivalent to siRNA alone.

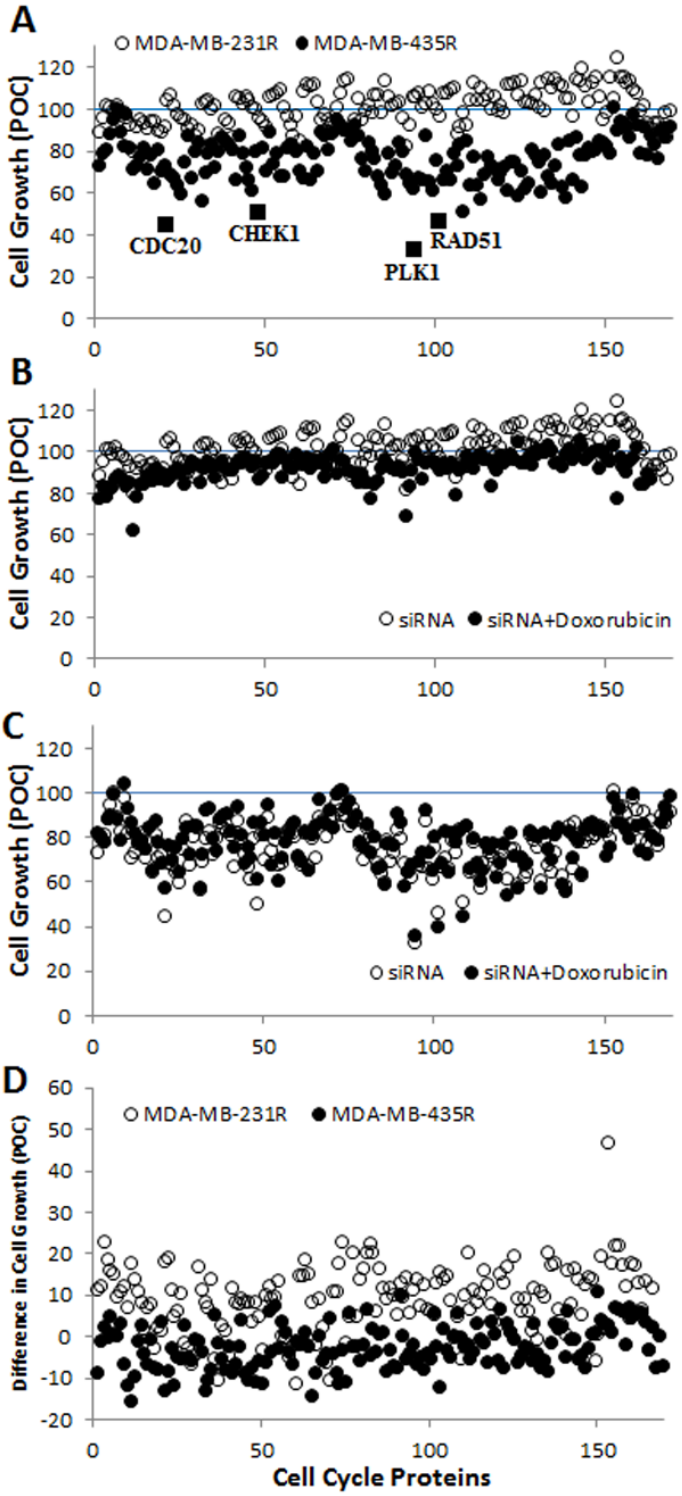

Fig 2.3: siRNA library screening in breast cancer cells.

(A) Screening of the library of siRNAs against cell cycle proteins using MDA-MB-231R and MDA-MB-435R cells. The identified cell cycle proteins, CDC20, RAD51 and CHEK1 are indicated along with the positive control, PLK1. A specific siRNA against PLK1 (Polo-like kinase 1) was provided along with the cell cycle proteins; it was meant to assure the functioning of siRNA delivery but was not pursued in this study. **(B** and **C)** The results of siRNA treatment alone and siRNA/doxorubicin combinational treatment in MDA-MB-231R (B) and MDA-MB-435R (C). **(D)** The difference in cell growth between siRNA treatment alone and the combinational treatment. Inhibition of cell growth in all cases was expressed as a percentage of control (POC), which was calculated as a percentage of cell growth (from MTT Assay) for scrambled siRNA treated cells.

2.3.4 Validation and further evaluation of identified targets

The individually prepared siRNAs against the selected cell cycle proteins were used to better determine the effectiveness of siRNA therapy. Different siRNA concentrations and siRNA:PEI-LA ratios were explored for this purpose. The inhibition of cell growth was 77% and 62% by delivering KSP siRNA to MDA-MB-435WT cells at 20 nM (1:8) and 40 nM (1:2) siRNA compared to scrambled siRNA using PEI-LA, respectively **(Fig 2.4A**,**B)**. However, 1:4 and 1:8 siRNA:polymer ratios at 40 nM siRNA were found more toxic based on the inhibition of cell growth of scrambled siRNA **(Fig 2.4B)**. Significant decrease in cell growth was observed with 20 nM and 40 nM CHEK1 siRNA at 1:8 and 1:2 ratios compared to scrambled siRNA, respectively, while cell growth was not significantly decreased with CDC20 and RAD51 siRNA in MDA-MB-435WT cells **(Fig 2.4A,B)**. This study was repeated with PEI-CA as the delivery agent and the obtained results were similar **(Fig 2.4C,D)**; a significant inhibition of cell growth was found upon KSP and CHEK1 siRNA treatment at 40 nM siRNA concentration. Consistent with the library screens, the siRNA treatment was not effective in MDA-MB-231WT and MDA-

MB-231R cells at 54 nM siRNA using PEI-LA and PEI-CA at 1:2, 1:4 and 1:8 siRNA:polymer ratios **(Fig 2.S2, 2.S3)**. Similarly, inhibition of cell growth was not significant by delivering these siRNAs to MCF7 cells using PEI-LA (40 nM and 60 nM siRNA) and PEI-CA (20 nM and 40 nM siRNA) at 1:2, 1:4 and 1:8 siRNA:polymer ratios **(Fig 2.S2, 2.S3)**.

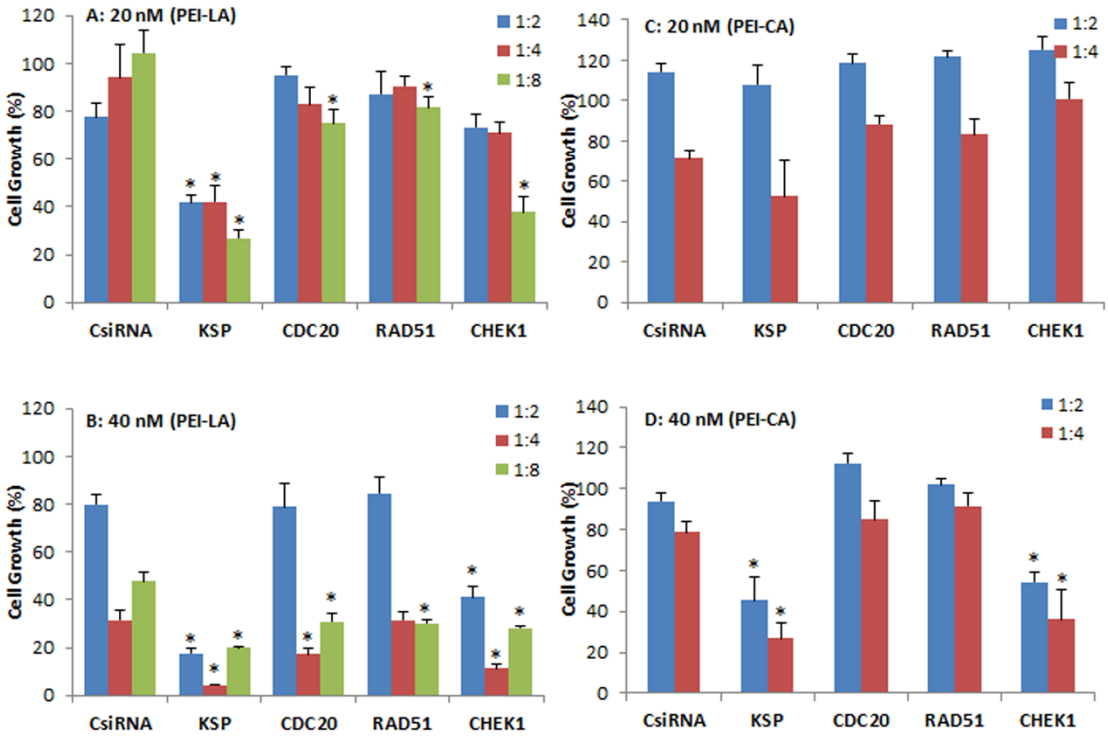

Fig 2.4: Validation of targets in MDA-MB-435WT cells.

Validation of KSP, CDC20, RAD51 and CHEK1 in MDA-MB-435WT cells at 20 nM (**A** and **C**) and 40 nM (**B** and **D**) siRNA concentrations. The results from PEI-LA were summarized in **A** and **B** (siRNA:polymer ratios of 1:2, 1:4 and 1:8) while the results from PEI-CA were summarized in **C** and **D** (siRNA:polymer ratios of 1:2 and 1:4). Scrambled siRNA (CsiRNA) was used as a control. Significant (*p<0.05) decreases in the cell growth were observed in specific siRNA treated group compared to CsiRNA.

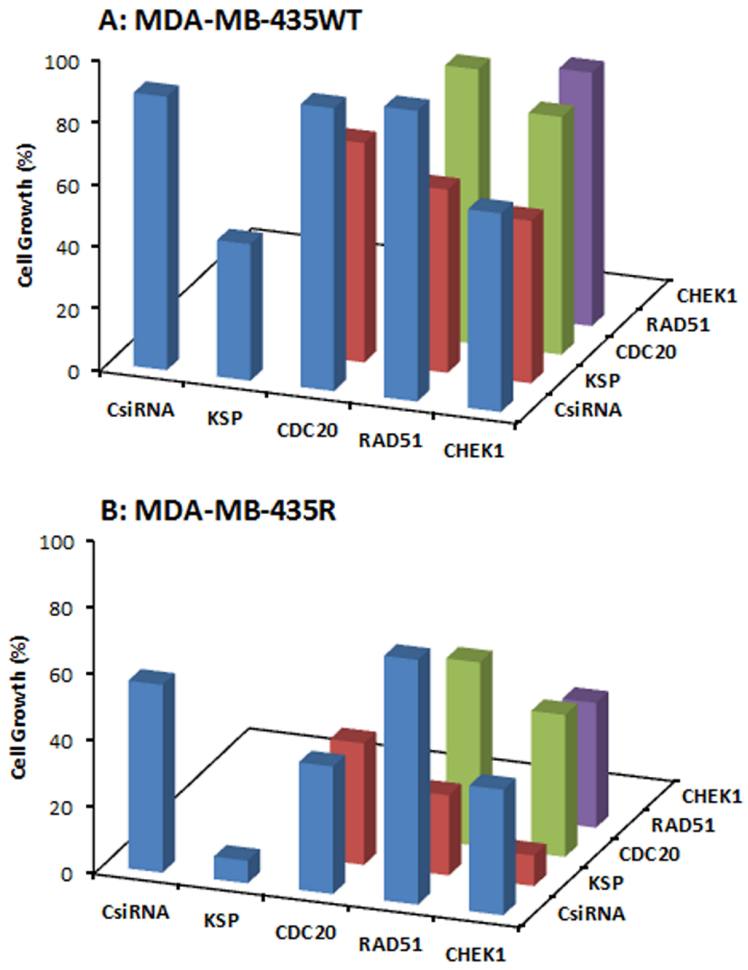

Fig 2.5: Combinational siRNA delivery in MDA-MB-435WT and MDA-MB-435R cells.

Combinations of siRNA (20+20 nM) treatments among KSP, CDC20, RAD51 and CHEK1 siRNA in MDA-MB-435WT (**A**; siRNA:PEI-LA ratio of 1:2) and MDA-MB-435R (**B**; siRNA:PEI-LA ratio of 1:8). Scrambled siRNA (CsiRNA) was used as a control on its own as well as in combination with other siRNAs. The standard deviation (not shown) was <5% for all groups.

We next explored dual delivery of siRNAs with the expectation that if two essential cell cycle proteins are down-regulated simultaneously, cell cycle could be disrupted more significantly with a more pronounced treatment effect. The combinational siRNA therapy was performed using MDA-MB-435WT and MDA-MB-435R cells with 40 nM total siRNA concentration **(Fig 2.5)**. KSP siRNA, on its own, was highly effective to achieve

significant cell death compared to scrambled siRNA. However, cell growth was not drastically decreased using KSP siRNA when co-delivered with CDC20, RAD51 and CHEK1 siRNAs compared to KSP siRNA delivery alone. Similar results were observed with the combinations of CDC20, RAD51 and CHEK1 siRNAs; (i) combining CDC20 with KSP siRNA did not lead to any more inhibition of cell growth with either siRNAs alone, (ii) a combination of RAD51 and CDC20 siRNAs led to a greater inhibition of cell growth than RAD51 siRNA alone, but not CDC20 siRNA alone, and (iii) CHEK1 siRNA combinations with RAD51 and CDC20 siRNA did not lead to greater inhibition of cell growth than CHEK1 siRNA alone. Taking together, these results indicated no synergistic effect with combinational siRNA therapy.

We next explored the effect of siRNA delivery on the doxorubicin response of the cells, with the purpose of assessing whether silencing the chosen targets could sensitize the cells to doxorubicin treatment (*i.e.,* further inhibit cell growth compared to doxorubicin treatment alone). A range of siRNA doses was employed (20, 40 and 60 nM) as well as siRNA:carrier ratios (1:2, 1:4 and 1:8) for a full silencing effect. The MDA-MB-435R cells were subsequently exposed to doxorubicin after 48 hrs of siRNA treatment targeting the cell cycle proteins. No significant effect of the siRNA treatment was observed at 20 nM siRNA, resulting in no sensitizing effect of doxorubicin in MDA-MB-435R cells **(Fig 2.6A,D)**. KSP siRNA was the most effective siRNA at 40 nM with 1:8 siRNA:polymer ratio compared to CDC20, RAD51 and CHEK1 siRNAs **(Fig 2.6B)**. However, the sensitizing effect on doxorubicin was again not observed in the combinational therapy of siRNA (40 nM) and doxorubicin **(Fig 2.6E)**. Similarly, no sensitizing effect of doxorubicin

was observed at 60 nM siRNA concentrations with the drug treatment compared to no drug treated group at the same siRNA concentration **(Fig 2.6C,F)**.

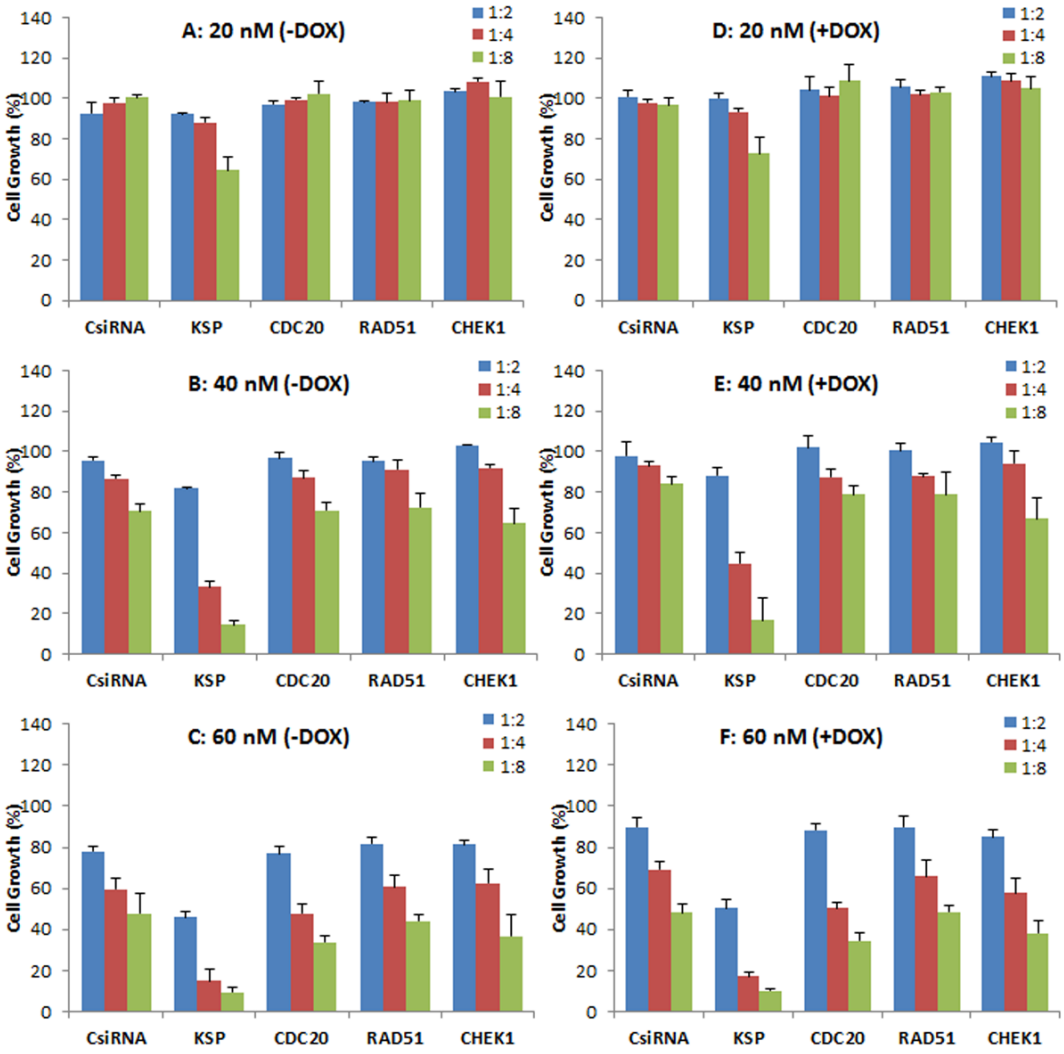

Fig 2.6: Effect of siRNA on doxorubicin cytotoxicity in MDA-MB-435R cells.

The cells were first treated with siRNA at 20 nM (**A, D**), 40 nM (**B, E**) and 60 nM (**C, F**) and 1:2, 1:4 and 1:8 siRNA:PEI-LA ratios, followed by treatment with buffer (**A, B, C**; -DOX) or doxorubicin (**D, E, F**; +DOX). Scrambled siRNA (CsiRNA) was used as a control.

2.3.5 Down-regulation of targeted protein transcripts

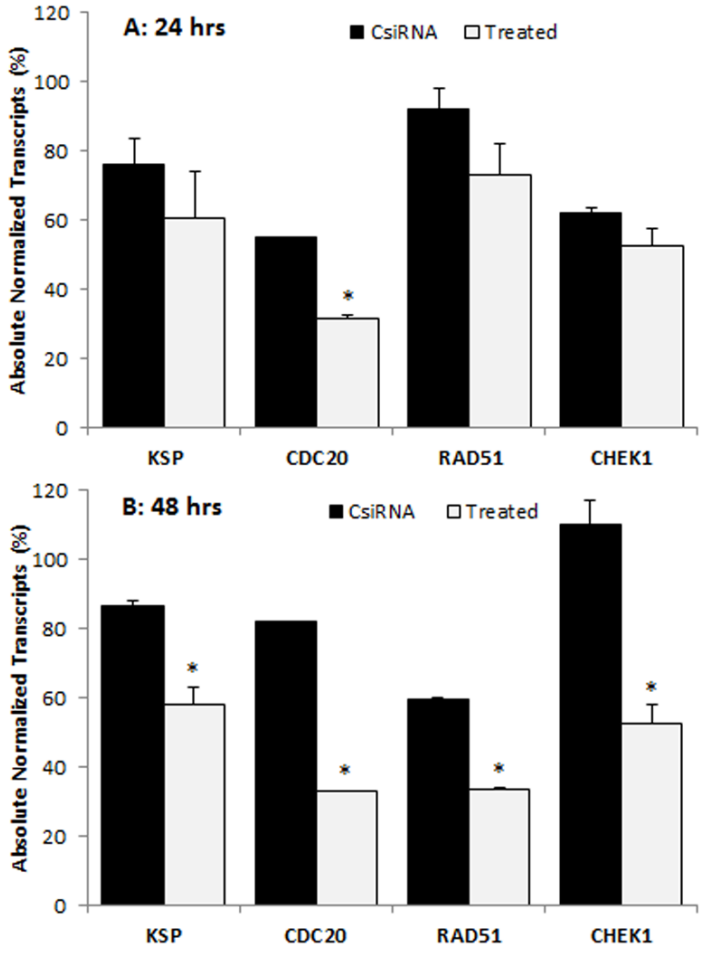

Fig 2.7: Digital droplet PCR (ddPCR) analysis.

ddPCR was performed in MDA-MB-435WT cells after 24 hrs (**A**) and 48 hrs (**B**) of treatment with indicated siRNAs. The percentage of quantity of transcripts was calculated based on the transcripts level of untreated cells (100%). The significance (*p<0.05) was calculated for specific siRNA treated group based on CsiRNA.

The down-regulation in the levels of mRNA transcripts of targeted proteins was analyzed with ddPCR in MDA-MB-435WT by determining absolute transcripts quantities. The levels of KSP transcripts were not significantly decreased in KSP siRNA treated cells after 24 hrs of siRNA treatment **(Fig 2.7A)**; however, a significant decrease was obtained after 48 hrs of treatment **(Fig 2.7B)**. The amount of KSP transcripts in treated cells was ~60%, indicating that a relatively small change in levels of KSP transcripts inhibited cell

growth drastically as KSP siRNA decreased the cell growth >70% **(Fig 2.4)**. The CDC20 and RAD51 siRNAs silenced their mRNA targets more effectively compared to other cell cycle proteins as only ~30% transcripts were found in the siRNA treated cells **(Fig 2.7B)**. However, MDA-MB-435WT cells had escaped the effect of CDC20 and RAD51 siRNA treatment and survived with low copy numbers of CDC20 and RAD51 transcripts **(Fig 2.4)**. A significant difference in the levels of CHEK1 transcripts was also found between scrambled siRNA and CHEK1 siRNA treated cells after 48 hrs **(Fig 2.7B)**. It was interesting to note that the levels of gene transcripts were variable among the chosen targets after the control siRNA treatment; while some transcripts were not affected (*e.g.,* RAD51 at 24 hrs and CHEK1 at 48 hrs), others displayed as much as ~40% reduction in transcript levels as compared to untreated control cells (*e.g.,* CDC20 at 24 hrs and RAD51 at 48 hrs). The reason(s) for such a variation is not known.

2.3.6 DsiRNA delivery against cell cycle proteins

To explore the effectiveness of alternative RNAi reagents, three DsiRNAs targeting different locations in mRNA was delivered against CDC20, RAD51 and CHEK1 in MDA-MB- 435WT and MDA-MB-435R using PEI-LA. The siRNA concentrations were 20 and 40 nM and 1:2, 1:4 and 1:8 DsiRNA:polymer ratios were used **(Fig 2.8)**. The CDC20-1 DsiRNA was the most effective among three DsiRNAs as the inhibition of cell growth was >80% at 20 nM and 40 nM concentrations in MDA-MB-435WT. The CDC20-2 and CDC20-3 DsiRNAs were not effective in MDA-MB-435WT cells. The DsiRNA:PEI-LA ratios 1:4 and 1:8 at 40 nM were toxic as only ~30% cell growth was found in scramble DsiRNA treated cells **(Fig 2.8B)**. Similarly, a significant decrease in cell growth was observed by delivering CDC20-1 DsiRNA to MDA-MB-435R, and CDC20-2 and CDC20-

3 DsiRNAs were again not as effective as CDC20-1 in this cell at 20 nM **(Fig 2.8C)** and 40 nM **(Fig 2.8D)**. Again, CDC20-1 inhibited the growth of MDA-MB-231WT cells significantly, and CDC20-2 and CDC20-3 were unable to decrease the cell growth **(Fig 2.S4)**. All three DsiRNAs against CDC20 were effective in MCF7 cells at 40 nM and 60 nM DsiRNAs **(Fig 2.S4)**. However, the DsiRNA:polymer ratio 1:4 inhibited more MCF7 growth compared to 1:2 and 1:8 ratios, which was different from MDA-MB-435 cells, where the higher ratios inhibited cell growth more effectively.

The DsiRNAs against RAD51 were not as effective as CDC20-1 **(Fig 2.8)**. RAD51-1 inhibited the MDA-MB-435WT cell growth ~20% compared to scrambled DsiRNA at 20 nM with 1:4 and 1:8 DsiRNA to PEI-LA ratios. No drastic decrease in the cell growth was detected by delivering RAD51-2 and RAD51-3 to MDA-MB-435WT cells at 20 nM and 40 nM. The significant decrease in the MDA-MB-435R cell growth was only observed at 40 nM of DsiRNA at 1:8 ratio with all three DsiRNAs **(Fig 2.8D)**. RAD51 DsiRNAs were not effective in MDA-MB-231WT cells **(Fig 2.S4)**. However, MCF7 cells were more sensitive to all three RAD51 DsiRNAs, which inhibited cell growth drastically at 60 nM of DsiRNA **(Fig 2.S4)**.

All CHEK1 DsiRNAs decreased the MDA-MB-435WT cell growth significantly compared to scrambled DsiRNA at 20 nM with various ratios **(Fig 2.8A)**. However, 1:8 DsiRNA:PEI-LA ratio at 20 nM was the most effective ratio in MDA-MB-435WT as ~40% cell growth was inhibited. Since the higher ratios at 40 nM of DsiRNA were toxic, the inhibition of cell growth by CHEK1 DsiRNAs alone was quite low at 40 nM **(Fig 2.8B)**. Only the higher CHEK1 DsiRNA:polymer ratios inhibited the MDA-MB-435R cells significantly at 20 nM and 40 nM of DsiRNAs **(Fig 2.8D)**. The CHEK1 DsiRNAs were

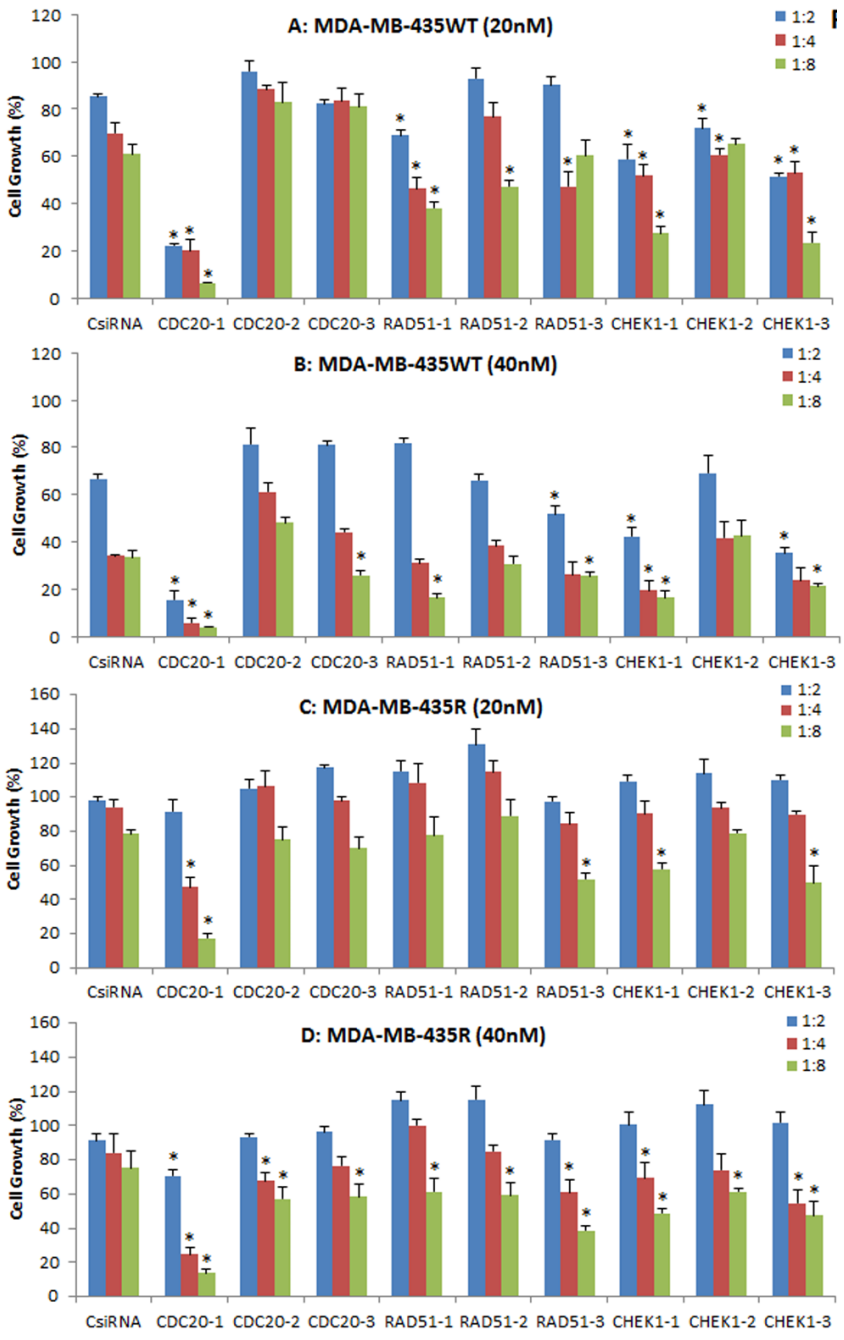

Fig 2.8: Breast cancer cell growth inhibition by DsiRNAs.

Inhibition of cell growth using DsiRNAs against CDC20, RAD51 and CHEK1 at 20 nM and 40 nM DsiRNA concentrations with different DsiRNA:PEI-LA ratios in MDA-MB-435WT (**A** and **B**) and MDA-MB-435R (**C** and **D**). For each target proteins, three different DsiRNA isoforms were used. The significance (*p<0.05) was calculated for specific DsiRNA treated group compared to scrambled DsiRNA (CsiRNA) at the equivalent concentration/ratio used.

not effective in MDA-MB-231WT cells **(Fig 2.S4)**. CHEK1-1 decreased the MCF7 cell growth drastically at 40 nM and 60 nM of DsiRNA at different ratios. CHEK1-2 and CHEK1-3 DsiRNAs failed to inhibit the cell growth drastically in MCF7 cells **(Fig 2.S4)**.

The sensitizing effect of DsiRNAs for doxorubicin was not observed in MDA-MB-435R at 20 nM and 40 nM, as a similar inhibition of cell growth was observed between DsiRNA/ doxorubicin treated and DsiRNA treated cells (data not shown).

2.3.7 *In vivo* CDC20 DsiRNA therapy

Since the CDC20-1 DsiRNA led to >80% growth inhibition in MDA-MB-435WT cells *in vitro* (more so than the CDC20 siRNA from library screens), we further evaluated its efficacy *in vivo* by injecting DsiRNA/PEI-LA complexes to breast cancer xenografts weekly and bi-weekly subcutaneously in the vicinity of tumor. In the weekly injection group, the initial growth of scrambled and CDC20-1 DsiRNA treated tumor was similar **(Fig 2.9A)**. However, the growth of tumor was suppressed after the second injection of CDC20-1 DsiRNA and a significant difference compared to scrambled DsiRNA treated tumor was achieved on day 14. Similarly, the third injection also decreased the growth of CDC20-1 DsiRNA treated tumor significantly on day 17. In the bi-weekly injection groups, the slower growth was evident with CDC20-1 DsiRNA treated group from the beginning of the study, where the differences between the CDC20-1 and scrambled DsiRNA were significant on day 7 and 14 **(Fig 2.9B)**. The tumor growth was retarded significantly after the second injection of CDC20-1 DsiRNA on day 17 and the difference in growth rate between scrambled and CDC20-1 DsiRNA treated tumor started decreasing gradually thereafter.

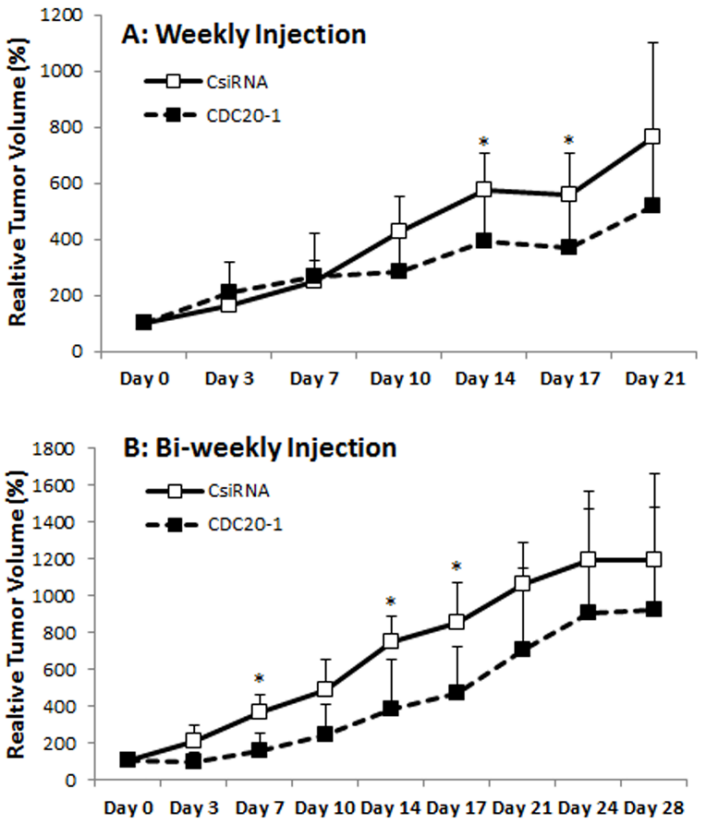

Fig 2.9: Effect of CDC20 DsiRNA treatment *in vivo*.

Xenografts of MDA-MB-435WT were established in nude mice, and were treated with a scrambled DsiRNA (CsiRNA) and CDC20-1 DsiRNA. Relative tumor volume for weekly injection **(A**; n=6 and n=5 in CsiRNA and CDC20-1 groups, respectively**)** and bi-weekly injection **(B**; n=3 and n=4 in CsiRNA and CDC20-1, respectively) groups, are summarized (only positive SDs are shown for clarity). The time points that showed a significant decrease in the volume of CDC20-1 DsiRNA treated tumors compared to CsiRNA treated tumor are indicated with an asterisk ($p<0.05$).

2.4 Discussion

The siRNA mediated RNAi has become a powerful tool for its specificity and efficiency to knock-down targets that cannot be readily down-regulated by conventional chemotherapy [3,4]. However, an efficient delivery system has to be developed for a functional siRNA effect [6,7]. Here, we report polymeric delivery systems, PEI-LA and

PEI-CA for siRNA therapy against cell cycle proteins in breast cancer cells. Lipid moieties that have been used to substitute amines of PEI were speculated to increase the interaction of anionic cell membrane with complexes (nanoparticles) of siRNA formed with cationic polymers, which, in turn, facilitate the entry of anionic siRNA into the cell. The optimal ratio of polymer to siRNA for each cell-line needs to be determined as a balance between the cytotoxicity of the polymer (lower cytotoxicity at lower ratios) and effective siRNA delivery (increased siRNA delivery at higher ratios). The current study mostly utilized *in vitro* cell models since, at the onset of study, little was known about the feasibility of silencing the newly explored targets to obtain a therapeutic effect. Detailed studies on dose-response relationships, relative potency of silencing each identified target, and details of siRNA delivery system (efficiency and undesired cytotoxicity) were thoroughly explored *in vitro*. With the critical insight generated in this study, further *in vivo* studies are warranted to better explore the potential of the identified targets.

The arrest of cell cycle by knocking out or inhibiting specific proteins was explored previously by others [28,29]. Our results (based on PCR analysis and inhibition of cell growth) highlighted three specific mediators, namely CDC20, RAD51, and CHEK1, as therapeutic targets in breast cancer cells. Western blot analysis to assess protein levels as a result of specific siRNA delivery would have been additionally useful to better validate these targets, but the inhibition of cell growth by specific siRNAs was considered a strong indication for their importance and a practical end-point to identify leads. The CDC20 activates the anaphase-promoting complex in the cell cycle, which initiates chromatid separation and entrance into anaphase [30]. RAD51 repairs the DNA double strand break during homologous recombination [31]. CHEK1 has kinase activity and phosphorylates

CDC25, an important phosphatase for entry of the cell into mitosis [32]. There are already a precedent for the roles of unregulated CDC20, RAD51 and CHEK1 in cancer development and progression. CDC20 has been found to be overexpressed in many cancer types [33-37], which may deregulate activation process of anaphase promoting complex (APC) and often result in multinucleation, premature anaphase promotion and mis-segregation of chromosomes, and leads to chromosomal instability and defect in spindle assembly checkpoint response [38,39]. Given the role of RAD51 in DNA double-strand break repair [31], RAD51 up-regulation increases the number of recombination events that may lead to defective DNA strands [40]. In addition, spontaneous recombination frequency may increase in mammalian cells because of overexpression of RAD51, which ultimately provides resistance to chemotherapy [41,42]. CHEK1, on the other hand, is an essential cell cycle protein to maintain genomic stability. Syljuåsen et al. suggested that CHEK1 is a required protein to avoid uncontrolled increase in DNA replication, thereby protecting against DNA breakage [43]. Although this literature supported all three targets for RNAi based cancer therapy, only a few studies attempted to silence CDC20, RAD51 and CHEK1 expression by siRNA [43-45]. Commercial carriers such as RNAiFect reagent (Qiagen), Lipofectamine 2000 and Oligofectamine (Invitrogen) were used to deliver CDC20, RAD51 and CHEK1 siRNA, respectively, and these studies were conducted in pancreatic, non-small-cell lung carcinoma (NSCLC) and osteosarcoma cell-lines. The breast cancer therapy investigated here might be an additional indication for these targets in RNAi therapy.

Our studies indicated that MDA-MB-435R cells were more responsive to siRNA treatment as compared to MDA-MB-231R. One possible reason might be that the polymeric carrier has not delivered siRNAs effectively to MDA-MB-231R cells. We

previously reported that MDA-MB- 231R cells displayed lower uptake compared to MDA-MB-435R cells under identical culture conditions [12], so that lower quantitative delivery of intracellular siRNA could be one of the reasons for lower efficacy in these cells. Another possibility is that the targeted cell cycle proteins may not be as crucial for the survival of MDA-MB-231R, unlike the MDA-MB-435R cells, and the MDA-MB-231R cells may have circumvented the effect of siRNA treatment by recruiting alternative mediators. However, individually prepared siRNAs against three cell cycle proteins showed lower efficacy in MDA-MB-435WT **(Fig 2.4, 2.7)** and MDA-MB-435R **(Fig 2.6)**, and these siRNAs were not effective at all in MDA-MB-231WT, MDA-MB-231R and MCF7 cells **(Fig 2.S2 and 2.S3)**, which might be an indication of these siRNAs not being efficiently incorporated into the RISC assembly. In order to address this possibility, we determined the efficacy of DsiRNAs against the three cell cycle proteins. DsiRNA (27 base pairs) interacts with the dicer enzyme before its incorporation into RISC assembly, leading to increased potency by engaging to the natural siRNA processing pathway [46]. Three 27 base pairs DsiRNAs for each target were not uniformly effective than the 21 base pairs siRNA used in this study, but we are cognizant of the fact that different regions of mRNA were targeted with each RNAi reagent and this might have contributed to variation in their efficacy. However, the CDC20-1 DsiRNA was clearly the most effective among the tested reagents, which led us to determine its efficacy in a xenograft model. The CDC20-1 DsiRNA was able to decrease the tumor growth in both weekly and bi-weekly injection groups. The retardation of tumor growth with CDC20-1 DsiRNA was not as robust as other studies in the literature. However, the DsiRNA dose used here was 2 μg (~0.08 mg/kg/day), which was quite low compared to 4-10 μg of siRNA used in intratumoral injections in

previous studies and some higher doses (up to 40 μg of siRNA) used in other modes of administrations [47]. We did not employ intratumoral injections since that might alter tumor growth patterns and complicate the interpretation of tumor growth data. Moreover, we reduced the number of injections in our study to weekly and bi-weekly, leading to a large interval between the injections as 1-5 day durations were frequently employed in previous *in vivo* studies [47]. Even though the dose of DsiRNA and frequency of injections were low, the CDC20-1 DsiRNA was effective to slow down the growth of tumor compared to scrambled DsiRNA **(Fig 2.9)**. We must, however, note that no buffer injection group was employed in the animal study, so that we could not evaluate if the scrambled DsiRNA complexes had any effect on tumor growth due to non-specific toxicity.

The resistance to the chemotherapy arises due to molecular (protein) changes in cancer cells [1]. If a protein associated with drug resistance was to be down-regulated by siRNA therapy, cells could be sensitized to chemotherapy. This issue was explored in several experiments with cell cycle proteins in this study, where the silencing of particular proteins was first attempted to investigate subsequent drug (doxorubicin) response. Since doxorubicin action involves DNA intercalation to inhibit DNA replication and ultimately cell cycle arrest, we initially reasoned that protein controlling the cell cycle could be altered in doxorubicin-treated cells, as observed in MCF-7 cells [48]. The drug-resistant MDA-MB-231R and MDA-MB-435R cells were not sensitized to doxorubicin after siRNA therapy (either as a single or dual siRNA delivery), indicating that the targeted cell cycle proteins may not be contributing to resistance against doxorubicin in breast cancer cells. Our previous studies with siRNA delivery were able to sensitize breast cancer cells by targeting anti-apoptotic proteins survivin [10] and Mcl-1 [11], so that this class of proteins

(rather than cell cycle proteins) might be more suitable to target for chemo-sensitization. However, beyond chemosensitization, cell cycle proteins could serve as targets to inhibit metastasis, since delivering specific siRNAs against survivin and cyclin B1 (with linear PEI) were found to be effective to prevent lung metastasis in a mammary adenocarcinoma model in mice [49].

Another cell cycle protein, KSP, has been investigated as a target for RNAi therapy and currently it is being evaluated at clinics [22]. As KSP is a microtubule-based motor protein and plays a critical role during mitosis to separate centrosome and to assemble bipolar spindle, knock-down of KSP expression leads to cell cycle arrest and ultimately to cell death. KSP was another effective target with the described polymeric delivery system. We previously observed that silencing multiple targets by delivering multiple siRNAs simultaneously led to improved therapeutic responses [11,12]; however, this was not the case here when KSP was combined with siRNAs targeting one of the cell cycle proteins. KSP on its own seemed to be effective enough to eradicate >70% cells. KSP with vascular endothelial growth factor (VEGF) siRNA is in clinical use [22], so that other targets beyond the cell cycle proteins might still be suitable for combinational therapy with KSP siRNA. Lipid nanoparticles (LNP) are used to deliver KSP-VEGF siRNAs intravenously, which form micelles around siRNA to protect its extracellular degradation. The modified PEI used for delivery of KSP siRNA here interacts electrostatically with siRNA and might provide an alternative delivery system for this clinically useful siRNA.

2.5 Conclusions

We report effective polymers derived from lipid-substituted 2 kDa PEI to target proteins involved in cell cycle regulation in breast cancer cells. No clear difference was

evident in our study whether a caprylic acid or linoleic acid modification of PEI was more effective. The proteins CDC20, RAD51 and CHEK1 were identified as promising targets among the cell cycle proteins for non-viral RNAi therapy. The specific type of RNAi reagent, siRNA (21 base pairs) or DsiRNA (27 base pairs), was found to influence the efficacy of therapy for individual targets, but more studies are needed to clarify the exact reason for the differences. Although we expected the siRNA therapy against cell cycle proteins to sensitize the cells with chemotherapy, no such effect was evident when doxorubicin was employed as a sensitizing drug. Nevertheless, a DsiRNA against CDC20 was the most potent RNAi reagent in our hands, and it also effectively slowed the growth of breast cancer xenografts in an animal model. The present study highlighted the importance of cell cycle protein targets in breast cancer therapy, and demonstrated an effective delivery system for down-regulation of cell cycle proteins.

2.6 Acknowledgments

We thank Ms. Juliana Valencia-Serna for the technical assistance in confocal microscopy. Manoj Parmar is a recipient of Dorothy Whiteman Scholarship, Women and Children's Health Research Institute (WCHRI) Graduate Studentship Grant, and Alberta Innovates-Health Solutions (AIHS) Graduate Studentship. This study was supported by operating grants from Canadian Breast Cancer Foundation (CBCF) and Natural Sciences and Engineering Council of Canada (NSERC).

2.7 References

1. Luqmani YA. Mechanisms of drug resistance in cancer chemotherapy. *Med Princ Pract*, 2005, 14:35-48.
2. Gillet JP, Gottesman MM. Mechanisms of multidrug resistance in cancer. *Methods Mol Biol,* 2010, 596:47-76.

3. McManus MT, Sharp PA. Gene silencing in mammals by small interfering RNAs. *Nat Rev Genet*, 2002, 3:737-747.

4. Kim DH, Rossi JJ. Strategies for silencing human disease using RNA interference. *Nat Rev Genet*, 2007, 8:173-184.

5. Wilson RC, Doudna JA. Molecular mechanisms of RNA interference. *Ann. Rev. Biophys,* 2013, 42:217-239.

6. Pecot CV, Calin GA, Coleman RL, Lopez-Berestein G, Sood AK. RNA interference in the clinic: challenges and future directions. *Nat Rev Cancer*, 2011, 11: 59-67.

7. Bora RS, Gupta D, Mukkur TK, Saini KS. RNA interference therapeutics for cancer: challenges and opportunities. *Mol Med Rep*, 2012, 6:9-15.

8. Haupenthal J, Baehr C, Kiermayer S, Zeuzem S, Piiper A. Inhibition of RNAse A family enzymes prevents degradation and loss of silencing activity of siRNAs in serum. *Biochem Pharmacol,* 2006, 71: 702-710.

9. Aliabadi HM, Landry B, Bahadur RK, Neamnark A, Suwantong O, Uludağ H. Impact of lipid substitution on assembly and delivery of siRNA by cationic polymers. *Macromol Biosci*, 2011, 11:662-672.

10. Montazeri Aliabadi H, Landry B, Mahdipoor P, Uludağ H. Induction of apoptosis by survivin silencing through siRNA delivery in a human breast cancer cell line. *Mol Pharm*, 2011, 8:1821-1830.

11. Aliabadi HM, Mahdipoor P, Uludağ H. Polymeric delivery of siRNA for dual silencing of Mcl-1 and P-glycoprotein and apoptosis induction in drug-resistant breast cancer cells. *Cancer Gene Ther*, 2013, 20:169-177.

12. Aliabadi HM, Maranchuk R, Kucharski C, Mahdipoor P, Hugh J, Uludağ H. Effective response of doxorubicin-sensitive and -resistant breast cancer cells to combinational siRNA therapy. *J Cont Rel*, 2013, 172:219-228.

13. Aliabadi HM, Landry B, Sun C, Tang T, Uludağ H. Supramolecular assemblies in functional siRNA delivery: where do we stand? *Biomaterials,* 2012, 33:2546-2569.

14. Cooper GM. *The Cell: A Molecular Approach (2nd Ed.)*, 2000, ASM Press, Washington, DC.

15. Malumbres M, Carnero A. Cell cycle deregulation: a common motif in cancer. *Prog Cell Cycle Res,* 2003, 5:5-18.

16. Sandhu C, Slingerland J. Deregulation of the cell cycle in cancer. *Cancer Detect Prev,* 2000, 24:107-118.

17. Vermeulen K, Van Bockstaele DR, Berneman ZN. The cell cycle: a review of regulation, deregulation and therapeutic targets in cancer. *Cell Prolif*, 2003, 36:131-149.

18. Parmar MB, Uludağ H. Targeting cyclins and cyclin-dependent kinases involved in cell cycle regulation by RNAi as a potential cancer therapy. pp 23-45. In: Braddock M. (ed.) *Nanomedicines: Design, Delivery and Detection,* 2016, Royal Society of Chemistry, London, UK.

19. Blangy A, Lane HA, d'Hérin P, Harper M, Kress M, Nigg EA. Phosphorylation by p34cdc2 regulates spindle association of human Eg5, a kinesin-related motor essential for bipolar spindle formation *in vivo. Cell*, 1995, 83:1159-1169.

20. Dagenbach EM, Endow SA. A new kinesin tree. *J Cell Sci*, 2004, 117:3-7.

21. Marra E, Palombo F, Ciliberto G, Aurisicchio L. Kinesin spindle protein siRNA slows tumor progression. *J Cell Physiol*, 2013, 228:58-64.

22. Tabernero J, Shapiro GI, LoRusso PM, Cervantes A, Schwartz GK, Weiss GJ, et al. First-in-humans trial of an RNA interference therapeutic targeting VEGF and KSP in cancer patients with liver involvement. *Cancer Discovery,* 2013, 3:406-417.

23. Amarzguioui M, Rossi JJ. Principles of dicer substrate (D-siRNA) design and function. *Methods Mol Biol*, 2008, 442:3-10.

24. Bahadur KC, Landry B, Aliabadi HM, Lavasanifar A, Uludağ H. Lipid substitution on low molecular weight (0.6-2.0 kDa) polyethylenimine leads to a higher zeta potential of plasmid DNA and enhances transgene expression. *Acta Biomater,* 2011, 7:2209 2217.

25. Remant Bahadur KC, Uludağ H. A comparative evaluation of disulfide-linked and hydrophobically-modified PEI for plasmid delivery. *J Biomater Sci Polym Ed*, 2011, 22:873-892.

26. Sumantran VN. Cellular chemosensitivity assays: an overview. *Methods Mol Biol*, 2011, 731:219-236.

27. Snead NM, Wu X, Li A, Cui Q, Sakurai K, Burnett JC, Rossi JJ. Molecular basis for improved gene silencing by Dicer substrate interfering RNA compared with other siRNA variants. *Nucleic Acids Res*, 2013, 41:6209-6221.

28. Satyanarayana A, Kaldis P. Mammalian cell-cycle regulation: several Cdks, numerous cyclins and diverse compensatory mechanisms. *Oncogene,* 2009, 28:2925-2939.

29. Schwartz GK, Shah MA. Targeting the cell cycle: a new approach to cancer therapy. *J Clin Oncol,* 2005, 23:9408-9421.

30. Weinstein J. Cell cycle-regulated expression, phosphorylation, and degradation of p55Cdc. A mammalian homolog of CDC20/Fizzy/slp1. *J Biol Chem,* 1997, 272:28501-28511.

31. Galkin VE, Wu Y, Zhang XP, Qian X, He Y, Yu X, Heyer WD, Luo Y, Egelman EH. The Rad51/RadA N-terminal domain activates nucleoprotein filament ATPase activity. *Structure,* 2006, 14:983-992.

32. Chen MS, Ryan CE, Piwnica-Worms H. Chk1 kinase negatively regulates mitotic function of Cdc25A phosphatase through 14-3-3 binding. *Mol Cell Biol,* 2003, 23:7488-7497.

33. Iacomino G, Medici MC, Napoli D, Russo GL. Effects of histone deacetylase inhibitors on p55CDC/Cdc20 expression in HT29 cell line. *J Cell Biochem*, 2006, 99:1122-1131.

34. Kim JM, Sohn HY, Yoon SY, Oh JH, Yang JO, Kim JH, et al. Identification of gastric cancer-related genes using a cDNA microarray containing novel expressed sequence tags expressed in gastric cancer cells. *Clin Cancer Res*, 2005, 11:473-482.

35. Ouellet V, Guyot MC, Le Page C, Filali-Mouhim A, Lussier C, Tonin PN, Provencher DM, Mes-Masson AM. Tissue array analysis of expression microarray candidates identifies markers associated with tumor grade and outcome in serous epithelial ovarian cancer. *Int J Cancer,* 2006, 119:599-607.

36. Kidokoro T, Tanikawa C, Furukawa Y, Katagiri T, Nakamura Y, Matsuda K. CDC20, a potential cancer therapeutic target, is negatively regulated by p53. *Oncogene,* 2008, 27:1562-1571.

37. Takahashi T, Haruki N, Nomoto S, Masuda A, Saji S, Osada H, Takahashi T. Identification of frequent impairment of the mitotic checkpoint and molecular analysis of the mitotic checkpoint genes, hsMAD2 and p55CDC, in human lung cancers. *Oncogene,* 1999, 18: 4295-4300.

38. Wang Z, Wan L, Zhong J, Inuzuka H, Liu P, Sarkar FH, Wei W. Cdc20: a potential novel therapeutic target for cancer treatment. *Curr Pharm Des*, 2013, 19:3210-3214.

39. Mondal G, Sengupta S, Panda CK, Gollin SM, Saunders WS, Roychoudhury S. Overexpression of Cdc20 leads to impairment of the spindle assembly checkpoint and aneuploidization in oral cancer. *Carcinogenesis*, 2007, 28:81-92.

40. Richardson C, Stark JM, Ommundsen M, Jasin M. Rad51 overexpression promotes alternative double-strand break repair pathways and genome instability. *Oncogene,* 200423:546-553.

41. Vispé S, Cazaux C, Lesca C, Defais M. Overexpression of Rad51 protein stimulates homologous recombination and increases resistance of mammalian cells to ionizing radiation. *Nucleic Acids Res*, 1998, 26:2859-2864.

42. Klein HL. The consequences of Rad51 overexpression for normal and tumor cells. *DNA Repair,* 2008, 7:686-693.

43. Syljuåsen RG, Sørensen CS, Hansen LT, Fugger K, Lundin C, Johansson F, et al. Inhibition of human Chk1 causes increased initiation of DNA replication, phosphorylation of ATR targets, and DNA breakage. *Mol Cell Biol*, 2005, 25:3553-3562.

44. Taniguchi K, Momiyama N, Ueda M, Matsuyama R, Mori R, Fujii Y, et al. Targeting of CDC20 via small interfering RNA causes enhancement of the cytotoxicity of chemoradiation. *Anticancer Res*, 2008, 28:1559-1563.

45. Tsai MS, Kuo YH, Chiu YF, Su YC, Lin YW. Down-regulation of Rad51 expression overcomes drug resistance to gemcitabine in human non-small-cell lung cancer cells. *J Pharmacol Exp Ther*, 2010, 335:830-840.

46. Kim DH, Behlke MA, Rose SD, Chang MS, Choi S, Rossi JJ. Synthetic dsRNA Dicer substrates enhance RNAi potency and efficacy. *Nat Biotechnol*, 2005, 23:222-226.

47. Behlke MA. Progress towards *in vivo* use of siRNAs. *Mol Ther.* 2006, 13:644-670.

48. AbuHammad S, Zihlif M. Gene expression alterations in doxorubicin resistant MCF7 breast cancer cell line. *Genomics,* 2013, 101:213-220.

49. Bonnet ME, Gossart JB, Benoit E, Messmer M, Zounib O, Moreau V, Behr JP, Lenne- Samuel N, Kedinger V, Meulle A, Erbacher P, Bolcato-Bellemin AL. Systemic delivery of sticky siRNAs targeting the cell cycle for lung tumor metastasis inhibition. *J Control Rel*, 2013, 170:183-190.

50. Christgen M, Lehmann U. MDA-MB-435: the questionable use of a melanoma cell line as a model for human breast cancer is ongoing. *Cancer Biol Ther*, 2007, 6:1355-1357.

51. Chambers AF. MDA-MB-435 and M14 cell lines: identical but not M14 melanoma? *Cancer Res*, 2009, 69:5292-5293.

3. Multiple siRNA delivery against cell cycle and anti-apoptosis proteins using lipid-substituted polyethylenimine in triple-negative breast cancer and non-malignant cells

A version of this chapter was published in:

Parmar MB, Arteaga Ballesteros BE, Fu T, K.C. RB, Montazeri Aliabadi H, Hugh JC, Löbenberg R, Uludağ H. Multiple siRNA delivery against cell cycle and anti-apoptosis proteins using lipid-substituted polyethylenimine in triple-negative breast cancer and nonmalignant cells. *J Biomed Mater Res A*, 2016, 104:3031-3044.

3.1 Introduction

Conventional breast cancer therapies, based on broadly acting chemotherapeutic agents, have significant limitations and side effects due to their non-specificity. More recently developed therapies mainly target estrogen receptors, progesterone receptors and human epidermal growth factor receptor 2 (HER2) of breast cancer cells to decrease the tumor growth [1-3]. However, the common subtype of breast cancer, triple-negative breast cancer, occurs in 12-17% of patients, which has no expression of these receptors and will not be responsive to such therapies [4]. Triple-negative breast cancer is highly metastatic, display low response to chemotherapy, has a very high recurrence rates and poor prognoses for patient survival [5,6]. Targeted therapies for triple-negative breast cancer currently do not exist, so that search for novel avenues to fight against this deadly disease is warranted. A promising therapy in this regard is based on RNA interference (RNAi), where small interfering RNA (siRNA) is introduced into cells to silence the expression of aberrant genes. The latter may include proteins important for prolonged cell survival and/or causing un-checked tumor growth [7,8]. Upon introduction of siRNA to a cell, siRNA is incorporated into an RNA inducing silencing complex (RISC). RISC hydrolyses the double-stranded synthetic siRNA and degrades passenger strand while having the guide strand into the RISC assembly [8,9]. The guide strand of siRNA directs the whole complex specifically towards its targeted mRNA. The siRNA-RISC complex binds to the targeted mRNA, and either cleave the mRNA or block the translation process, which results into silencing of specific target [9]. The major issue associated with siRNA therapy is the delivery. Since the siRNA is highly labile due to endogenous nucleases and its negative charge, its entry into the cell on its own is almost impossible [10,11]. The siRNA, therefore,

needs a carrier that can deliver it into the cells by neutralizing its anionic charge, and protect it from extracellular degradation. We have synthesized a library of cationic polymeric carriers for such purpose, which is based on low molecular weight polyethylenimines (PEI) [12,13]. PEIs were substituted with different lipidic moieties that help siRNA/polymer complexes to penetrate the plasma membrane and improve the uptake of complexes [13,14]. Cationic lipid-substituted PEIs provide protection to siRNA as well as facilitate its delivery into the cell so that siRNA can be assembled with RISC.

Controlled cell division and multiplication involve many proteins in a series of events, commonly known as the cell cycle. The deregulation of the cell cycle is one of the hallmarks of cancer, where cell cycle proteins are mostly upregulated [15,16]. Due to aberrant expression of cell cycle proteins, control over proliferation and multiplication of the cells is lost, resulting in a cancerous growth. If the expression of these up-regulated cell cycle proteins is silenced by siRNA therapy, the proliferation of malignant cells may be decreased, and tumor growth can be halted. Here, we have targeted two cell cycle proteins, monopolar spindle 1 (MPS1) and cell division cycle protein 20 (CDC20) to silence their expression by siRNA. MPS1 is more commonly known as TTK protein kinase since it can phosphorylate tyrosine, serine and threonine residues of a substrate. It is exclusively associated with the cell proliferation [17]. It aligns chromosomes at the centromere and is required for the duplication of centrosome during mitosis [18]. TTK is a critical mitotic checkpoint protein for accurate segregation of chromosomes during mitosis, and it is up-regulated in tumorigenesis [19-22]. A related cell cycle protein, CDC20, activates the anaphase-promoting complex (APC) in the cell cycle during mitosis, which initiates chromatid separation and entrance of the cell division into anaphase [23]. The reports have

shown that inhibition of TTK protein disrupts the CDC20-MAD2 (mitotic arrest deficient 2; inhibitor of CDC20) complexation, causing premature activation of APC that accelerates anaphase during mitosis [24,25]. Therefore, silencing TTK along with CDC20 could be a promising strategy to achieve a synergistic reduction in malignant cell growth by combinational siRNA therapy.

The cell cycle process is often coordinated with the apoptosis machinery to maintain tissue homeostasis [26]. Apoptosis is a tightly regulated process of programed cell death that is executed by activation of caspases [27]. The delicate balance between pro-apoptotic and anti-apoptotic proteins maintains the integrity of normal cell, and this balance is often shifted in favor of anti-apoptotic proteins in transformed cells to allow cells to resist drug therapy and to maintain an over-proliferative state [28-30]. The member of inhibitor of apoptosis proteins (IAP), survivin is known to inhibit caspase activation and block apoptosis. Survivin is up-regulated in many cancer types, but is completely absent in terminally differentiated cells [31]. Transcriptional silencing of survivin may provide an excellent therapeutic opportunity as the discrimination between malignant and normal cells can be achieved. The evidences suggest a role for survivin in spindle checkpoint [32,33]. and, therefore, targeting survivin along with cell cycle proteins by siRNA may lead to additive effect(s) to retard tumor growth.

In this study, we first determined the most effective polymeric carrier for siRNA delivery, and evaluated the efficacy of various TTK siRNAs targeting different locations of TTK transcripts using that effective polymeric carrier. We then evaluated the combinational siRNA therapy with TTK, CDC20 and survivin siRNAs in breast cancer cells. We hypothesize that siRNA combinations targeting mediators of abnormal cell cycle

progression such as TTK, CDC20 and survivin may provide synergistic therapeutic effect on breast cancer cells. The effect of this combinational siRNA therapy was also evaluated in normal cells, including breast, endothelial and bone marrow stromal cells.

3.2 Materials and Methods

3.2.1 Materials

The amines of low molecular weight PEIs (0.6, 1.2 and 2.0 kDa) were substituted with linoleic acid via N-acylation (PEI-LA) and the degree of substitution was determined by NMR Spectroscopy as previously described [34,35]. MTT [3-(4 5-dimethylthiazol-2-yl)-2 5-diphenyltetrazolium] and dimethyl sulfoxide (DMSO) were purchased from Sigma-Aldrich (St. Louis, MO). Hank's Balanced Salt Solution (HBSS) was prepared in-house.

TTK-1 (Cat. No. SI02223207), TTK-2 (Cat. No. SI02223214), TTK-3 (Cat. No. SI03062745) and TTK-4 (Cat. No. SI04898747) siRNAs were ordered from Qiagen (Valencia, CA), and TTK-5 (Cat. No. HSC.RNAI.N001166691.12.1) and TTK-6 siRNAs (Cat. No. HSC.RNAI.N001166691.12.2) were purchased from IDT (Coralville, IA). Negative control scrambled siRNA (Cat. No. DS NC1), CDC20 siRNA (Cat. No. HSC.RNAi.N001255.12.1) and survivin siRNA (Cat. No. HSC.RNAI.N001012271.12.1) were ordered from IDT. The 6-Carboxyfluorescein (FAM) labeled scrambled siRNA was purchased from IDT. Primers for TTK (forward: GCCCGAAAAGTTAATACAGAG CAGA; reverse: GATGTTGATATTGGTGGTGACTGT), CDC20 (forward: CGCTA TATCCCCCATCGCAG; reverse: GATGTTCCTTCTTGGTGGGC), survivin (forward: TGAGAACGAGCCAGACTTGG; reverse: ATGTTCCTCTATGGGGTCGT) and Glyceraldehyde 3-phosphate dehydrogenase (GAPDH; forward: TCACTGTTCTCTC CCTCCGC; reverse: TACGACCAAATCCGTTGACTCC) were supplied by IDT.

3.2.2 Cell models

The triple-negative breast cancer MDA-MB-231 cells and MCF7 (estrogen- and progesterone-positive) cells were cultured in DMEM medium with 10% fetal bovine serum (FBS), 100 U/mL penicillin and 100 µg/mL streptomycin. MDA-MB-231 and MCF7 cells were generous gifts from Dr. Michael Weinfeld, Department of Oncology, University of Alberta, and Dr. Afsaneh Lavasanifar, Faculty of Pharmacy and Pharmaceutical Sciences, University of Alberta, respectively. The normal breast cells MCF10A were cultured in DMEM/F12 medium with 500 ng/mL hydrocortisone, 20 ng/mL human epidermal growth factor (hEGF), 0.01 mg/mL human insulin, 100 ng/mL cholera toxin, 5% horse serum, 100 U/mL penicillin and 100 µg/mL streptomycin. MCF10A cells were gift from Dr. Judith Hugh, Department of Laboratory Medicine and Pathology, University of Alberta. Human umbilical vein endothelial cells (HUVEC), generous gift from Dr. Janet A. W. Elliott, Department of Chemical and Materials Engineering, University of Alberta, were cultured on rat tail type I collagen coated culture flask with EGM-2 medium that was supplied with manufacturer's growth factor bulletkit, 10% FBS, 100 U/mL penicillin and 100 µg/mL streptomycin. Human bone marrow stromal cells (hBMSC) were isolated from 29 years old female patient as previously described [36] with informed consent and approval from the Research Ethics Board, University of Alberta. hBMSC cells were cultured in DMEM/F12 medium with 10% FBS, 20 ng/mL basic fibroblast growth factor (bFGF), 100 U/mL penicillin and 100 µg/mL streptomycin. All cell-lines were maintained at 37°C and 95/5% air/CO_2.

3.2.3 Screening of polymers and preparation of siRNA/polymer complexes

To determine most effective polymeric carrier for siRNA delivery, a library of synthesized polymers **(Table 3.S1)** was screened with TTK-1 and CDC20 siRNAs, and scrambled siRNA as a negative control. The inhibition of cell growth was assessed with the MTT assay after 72 hrs of siRNA transfection. The siRNAs were typically used at 40 nM concentration with 1:6 siRNA:polymer ratio. The lipid-based commercial carrier, Lipofectamine® 2000 (Thermo Fisher Scientific, Waltham, MA) was also used in the screening with 1:1 siRNA:Lipofectamine ratio. The siRNA/polymer complexes were prepared in 150 mM NaCl by allowing 30 min of incubation time after adding polymer into siRNA for their interaction with each other to form complexes. The complexes were added to cells after 30 min of incubation at room temperature. After 72 hrs of treatment, MTT was added to the cells at 1 mg/mL final concentration in HBSS. The cells were incubated for 1 hr at 37 °C and 5% CO_2. During this incubation, soluble MTT is transformed into insoluble formazan crystals due to the activity of mitochondrial dehydrogenase enzymes, giving a measure of cellular activity [37]. DMSO was added to the well to dissolve the formazan crystals formed because of cellular activity of live cells. The optical density (OD) was measured at 570 nm and the ODs were summarized as a percentage of cell growth based on non-treated cells (taken as 100% cell growth).

3.2.4 Size and ζ-potential of siRNA/polymer complexes

To characterize siRNA/polymer complexes based on different degree of lipid-substitutions in 1.2 kDa PEI, hydrodynamic diameter (Z-average) and surface charge (ζ-potential) of these complexes were determined in ddH_2O through dynamic light scattering (DLS) and electrophoretic light scattering (ELS) using Zetasizer Nano ZS (Malvern, UK). The complexes were prepared as described above with 0.6 μg of scrambled siRNA at 1:6

and 1:1 siRNA:polymer and siRNA:Lipofectamine ratio, respectively, and were diluted to 1 mL ddH_2O before each measurement. The size and ζ-potential of siRNA/polymer complexes were characterized based on different siRNA:polymer ratios as well. Native 1.2 kDa PEI and 1.2PEI-LA6 were employed at 1:2, 1:4 and 1:8 siRNA:polymer ratios to determine the size and ζ-potential of complexes as described above.

3.2.5 siRNA uptake by flow cytometry

To determine the delivery efficiency of lipid-substituted PEIs based on different degree of LA substitutions, MDA-MB-231 cells were transfected with FAM-labeled siRNA at 40 nM with 1:6 siRNA:polymer ratio. Lipofectamine® 2000 (Thermo Fisher Scientific) was used at 1:1 siRNA:Lipofectamine ratio. Non-labeled scrambled siRNA was used as a negative control. Cells were trypsinized after 24 hrs of siRNA transfection and fixed with 3.7% formaldehyde. The uptake of siRNA was quantified using BD LSRFortessa™ cell analyzer (Becton Dickinson, Franklin Lakes, NJ). The mean fluorescence of the recovered cell population and the percentage of cells showing FAM-fluorescence were determined after gating of the cell population as such that auto-fluorescence of untreated cells represented ~1% of the total cell population.

To investigate the potential of the lead polymer 1.2PEI-LA6 to deliver siRNA, MDA-MB-231 and MCF7 cells were transfected with FAM-labeled siRNA at 30 nM with 1:2, 1:4, and 1:8 siRNA:1.2PEI-LA6 ratios. The uptake study by flow cytometry was also performed in normal cells, MCF10A, HUVEC and hBMSC as described above to determine how effectively siRNA was delivered by the polymer to normal cells.

3.2.6 Targeting TTK with various siRNAs

TTK siRNAs targeting different locations of the gene were used to determine their efficacy by MTT assay in MDA-MB-231 and MCF7 cells using 20, 40 and 60 nM siRNA concentrations with 1:4 siRNA:polymer ratio. After 72 hrs of siRNA transfections, MTT assay was performed as described above to measure the inhibition of MDA-MB-231 and MCF7 cells growth by various TTK siRNAs.

3.2.7 Reverse transcription – quantitative PCR (RT-qPCR)

The MDA-MB-231 and MCF7 cells were transfected by TTK-1 and CDC20 siRNAs at 60 nM with 1:4 siRNA:1.2PEI-LA6 ratio. Total RNA was isolated from cells after 24 and 48 hrs of treatment using TRIzol reagent (Invitrogen, Carlsbad, CA). One microgram of total RNA was converted into cDNA using M-MLV reverse transcriptase (Invitrogen) according to manufacturer's instruction. The quantitative PCR (qPCR) was performed by taking 15 ng of cDNA from each sample using SYBR Green qPCR Mastermix (Molecular Biology Service Unit, Department of Biological Sciences, University of Alberta, Edmonton, AB) and StepOne Real-Time PCR System (Applied Biosystems, Foster City, CA) based on the recommendations of manufacturer. Primers were designed using NCBI Primer-BLAST (http://www.ncbi.nlm.nih.gov/tools/primer-blast/) in such a way that at least one primer (forward or reverse) spans the exon-exon junction of a gene so that the amplification of contaminating genomic DNA or hetero-nuclear RNA by PCR can be avoided. GAPDH was used as a reference gene in RT-qPCR and template cDNA was omitted from qPCR reaction as a negative control. The qPCR results were analyzed using $2^{-\Delta\Delta C_T}$ method and presented as relative quantity of transcripts. The qPCR conditions comprised an initial denaturation step for 10 min at 95.0 ºC, followed

by 40 cycles at 95.0 ºC for 15 s (denaturation), and annealing and elongation at 60 ºC for 1 min.

3.2.8 Combinational siRNA therapy

Combinational siRNA delivery was performed in MDA-MB-231 and MCF7 using TTK-1, CDC20 and survivin siRNAs at 30 nM (15 nM each) total siRNA concentration with 1:2, 1:4 and 1:8 siRNA:1.2PEI-LA6 ratio. After 72 hrs of siRNA transfection, MTT assay was performed as described above to determine the efficacy of combinational siRNA therapy. Induction of apoptosis in MDA-MD-231 cells by combinational siRNA therapy was determined by caspase activity assay. To investigate caspase activity, total protein from MDA-MB-231 cells was isolated by applying freeze-thaw cycle 3-times after 72 hrs of combinational siRNA transfection. Cell-debris was removed from isolated protein by centrifugation at 10,000g for 5 min. Total protein was incubated for 2 hrs with the fluorogenic substrate (Ac-DEVD-AFC; Cat. No. ALX-260-032, Enzo Life Sciences, Farmingdale, NY) at 37ºC and the fluorescence of the substrate was measured at 390/510 nm excitation/emission. The fluorescence was normalized per µg of protein after determining the concentration of total protein for each sample by Pierce™ BCA Protein Assay Kit (Cat. No. 23227, Thermo Fisher Scientific) according to manufacturer's instructions. The caspase activity was presented as a percentage of activity based on non-treated cells (taken as 100% activity).

The validity of combinational siRNA therapy at mRNA transcript levels was determined by RT-qPCR. MDA-MB-231 and MCF7 cells were transfected with 30 and 60 nM total combinational siRNA concentration at 1:4 siRNA:1.2PEI-LA6 ratio. After 24 hrs

of transfection, RNA was isolated and converted into cDNA as described above, which was used to perform qPCR.

3.2.9 siRNA delivery to non-malignant cells

Combinational siRNAs against TTK-1, CDC20 and survivin were also delivered to normal cells, MCF10A, HUVEC and hBMSC to determine the side effects of siRNA therapy. MTT assay was performed to determine the inhibition of normal cell growth by siRNA transfection at 30 nM (15 nM each) total siRNA concentration with 1:2, 1:4 and 1:8 siRNA:1.2PEI-LA6 ratio. Specific cell growth inhibition by combinational siRNA therapy compared to scrambled siRNA in all cell-lines was calculated by removing cell growth inhibition of scrambled siRNA from specific siRNA treated cells and the values were presented as a heat-map.

3.2.10 Statistical analysis

All results were presented as mean + standard deviation. Results were analyzed by unpaired Student's t–test, where an asterisk (*) indicated significantly different groups in figures. The significance ($p < 0.05$) was typically determined by comparing specific siRNA-treated groups to that of scrambled siRNA-treated groups.

3.3 Results

3.3.1 Screening for effective carriers

Several LA-substituted PEIs were used to screen for the best polymeric carrier by determining inhibition of MDA-MB-231 cell growth with the TTK-1 and CDC20 siRNAs **(Fig 3.1)**. The synthesized polymers were designated based on the molecular weight of PEI (0.6, 1.2 and 2.0 kDa) backbone used for modification, followed by the substituted lipid

moiety and the feed ratio of lipid/PEI during the synthesis of the polymers (see **Table 3.S1** for more detailed info). Lipofectamine® 2000, a widely used commercial carrier, was employed as a reference carrier that was unable to inhibit cell growth with TTK-1 siRNA while it inhibited cell growth ~50% with the CDC20 siRNA. Many synthesized polymeric carriers were not effective to inhibit cell growth with TTK-1 siRNA, except 1.2PEI-LA6 that inhibited cell growth significantly **(Fig 3.1A)**. With CDC20 siRNA delivery, 1.2PEI-LA6, 2.0PEI-LA6 and 2.0PEI-LA9 polymers were able to decrease cell growth significantly **(Fig 3.1B)**. The 1.2PEI-LA6 was the most effective polymer as it inhibited ~80% of cell growth with CDC20 siRNA and, since it was also effective with TTK-1 siRNA, it was used to carry out the rest of the studies. The 1.2PEI-LA8 was quite toxic in MDA-MB-231 cells as the growth of scrambled siRNA treated cells was inhibited drastically.

siRNA/polymer complexes were characterized based on different degree of lipid-substitutions in 1.2 kDa PEI by measuring size and surface charge **(Fig 3.2A)**. The size of complexes with Lipofectamine® 2000 was ~100 nm, while it was less with native 1.2 kDa PEI without any modification (~70 nm). Substitution of PEI with linoleic acid (1.2PEI-LA0.5) increased the complex size (~127 nm), and complex size gradually decreased as the LA substitution in PEI was increased from 1.2PEI-LA0.5 to 1.2PEI-LA8 (~70 nm). On the other hand, ζ-potential of complexes with Lipofectamine® 2000 was -21 mV, and initial (minimal) substitution of LA in PEI decreased surface charge from ~17 mV (1.2PEI-LA0) to 10 mV (1.2PEI-LA0.5). The ζ-potential of complexes gradually increased as the substitution of LA has increased in PEI from 1.2PEI-LA0.5 (~10 mV) to 1.2PEI-LA6 (28.8 mV), after which 1.2PEI-LA8 showed a significant drop in the surface charge (~15 mV).

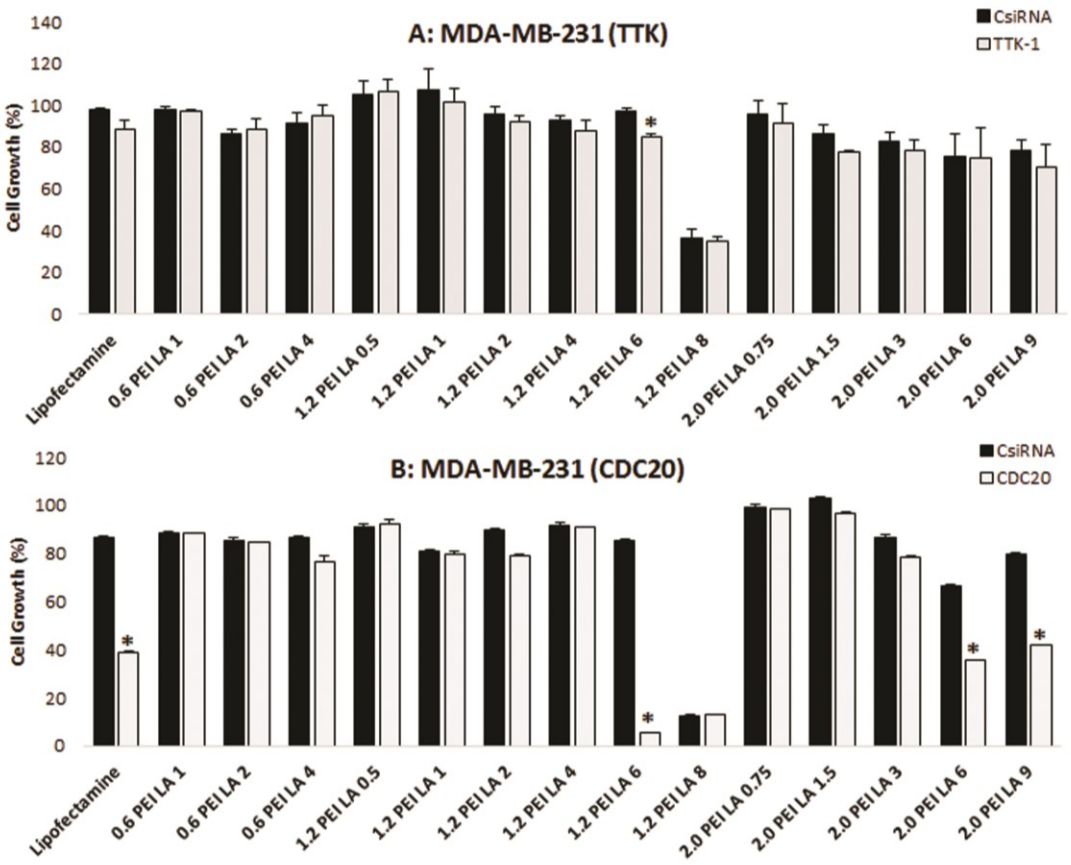

Fig 3.1: Screening of polymeric carriers using lipid-substituted PEIs in MDA-MB-231 cells.

Modified PEIs were synthesized using linoleic acid (LA) with different feed ratios. The synthesized polymers were designated based on the molecular weight of PEI (0.6, 1.2 and 2.0 kDa) backbone used for modification, followed by the substituted lipid moiety and the feed ratio of lipid/PEI during the synthesis of the polymers. The inhibition of cell growth by 40 nM siRNA against TTK-1 **(A)** and CDC20 **(B)** at 1:6 siRNA:polymer ratio was assessed with MTT assay. Lipofectamine® 2000 (Thermo Fisher Scientific) was used as a positive control with 1:1 siRNA:lipofectamine ratio. Scrambled siRNA (CsiRNA) was used as a negative control. The results were presented by taking non-treated cells as 100% cell growth. Asterisks represent the significant cell growth inhibition by TTK-1 or CDC20 siRNA compared to CsiRNA ($p < 0.05$).

The uptake of siRNA/polymer complexes was determined for different LA substituted PEIs **(Fig 3.2B)**. Lipofectamine® 2000 successfully delivered siRNA to MDA-MB-231 cells and transfected ~80% cell population. As expected, non-modified 1.2 kDa

PEI was not able to deliver siRNA at all to MDA-MB-231 cells. Similarly, siRNA uptake was not observed when it was delivered with 1.2PEI-LA0.5, 1.2PEI-LA2 and 1.2PEI-LA4. Polymers 1.2PEI-LA1 and 1.2PEI-LA8 delivered siRNA at some extent as higher mean fluorescence compared to 1.2PEI-LA0.5, 1.2PEI-LA2 and 1.2PEI-LA4 was observed in these cells. However, the transfection efficiency was lower as only 53 and 38% of cells were transfected with 1.2PEI-LA1 and 1.2PEI-LA8, respectively. The 1.2PEI-LA6 was the most effective polymer as the highest mean fluorescence was detected and 97% cell population were transfected with this polymer.

3.3.2 Delivery of TTK siRNAs to breast cancer cells

The efficacy of various TTK siRNAs targeting different locations of the mRNA was determined by inhibition of MDA-MB-231 and MCF7 cell growth **(Fig 3.3)**. TTK-1, TTK-2, TTK-3 and TTK-4 siRNAs at 20 nM has decreased the MDA-MB-231 cell growth by 10-40%, while 40 nM of siRNA inhibited cell growth by 70-90%. Similarly, 60 nM of TTK siRNAs decreased MDA-MB-231 cell growth significantly compared to scrambled siRNA. CDC20 siRNA was able to inhibit the MDA-MB-231 cell growth drastically at all the concentrations used. Furthermore, MCF7 cells were not responsive to TTK-1, TTK-2, TTK-3, TTK-4 and CDC20 siRNAs at all concentrations.

The TTK-5 and TTK-6 siRNAs decreased the MDA-MB-231 cell growth ~90% at 40 nM siRNA, while no significant difference between TTK-5 and TTK-6 siRNA treated cells and scrambled siRNA treated cells was found at 60 nM siRNA **(Fig 3.3)**. TTK-5 siRNA decreased MCF7 cell growth 20-40% at 40 and 60 nM, while TTK-6 siRNA was not able to inhibit the cell growth significantly compared to scrambled siRNA.

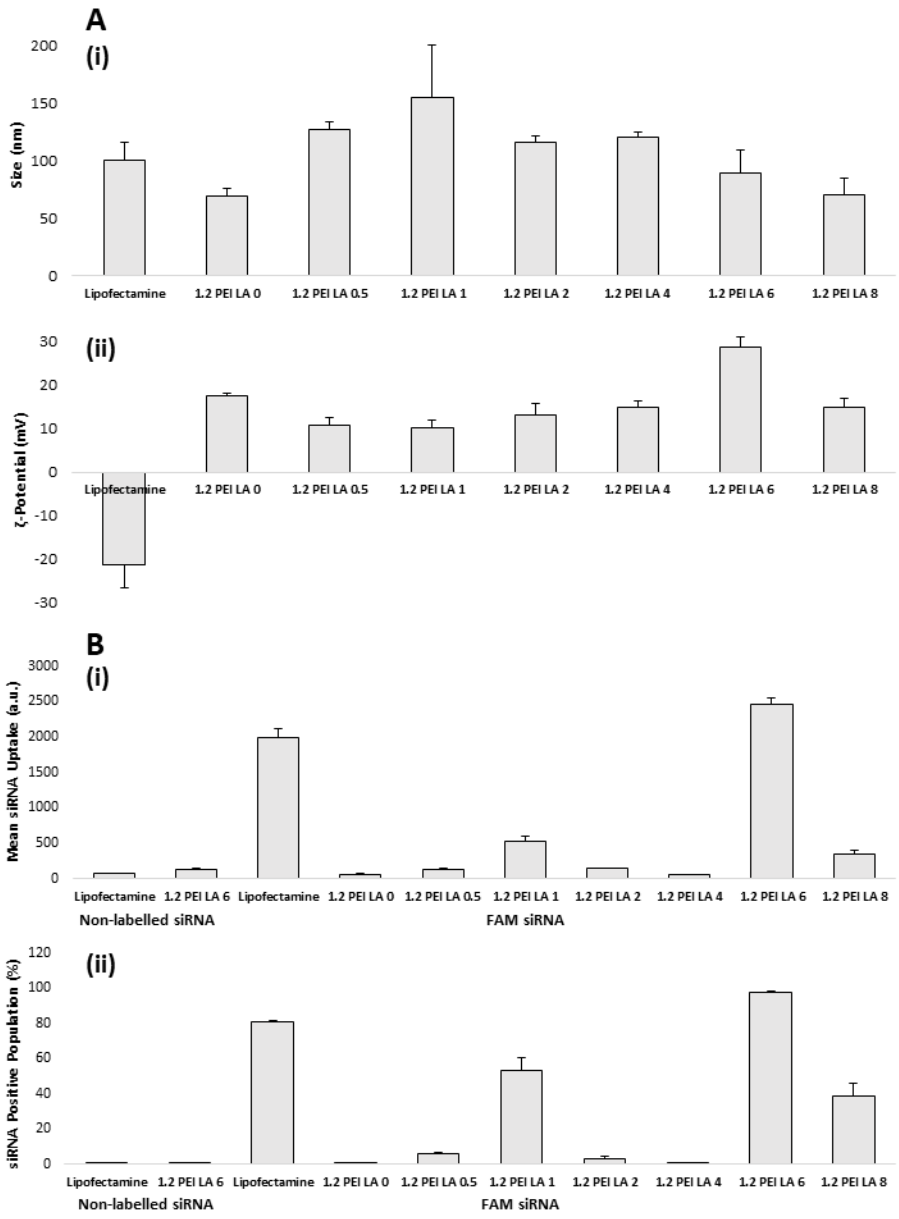

Fig 3.2: Physicochemical characterization and cellular uptake of siRNA by flow cytometry.

(A) Size **(i)** and surface charge **(ii**; **ζ**-potential) of siRNA/polymer complexes were determined using polymers with different degree of lipid-substitutions in 1.2 kDa PEI. The complexes were prepared with 0.6 µg of scrambled siRNA at 1:6 and 1:1 siRNA:polymer and siRNA:Lipofectamine ratios, respectively. **(B)** FAM-labeled scrambled siRNA was used to determine cellular uptake of siRNA/polymer complexes at 40 nM siRNA with 1:6 and 1:1 siRNA:polymer and siRNA:Lipofectamine ratios, respectively. Non-labeled scrambled siRNA was used as a control to investigate auto-fluorescence of complexes. The mean fluorescence **(i)** and FAM-positive cell population **(ii)** was determined for all siRNA carriers.

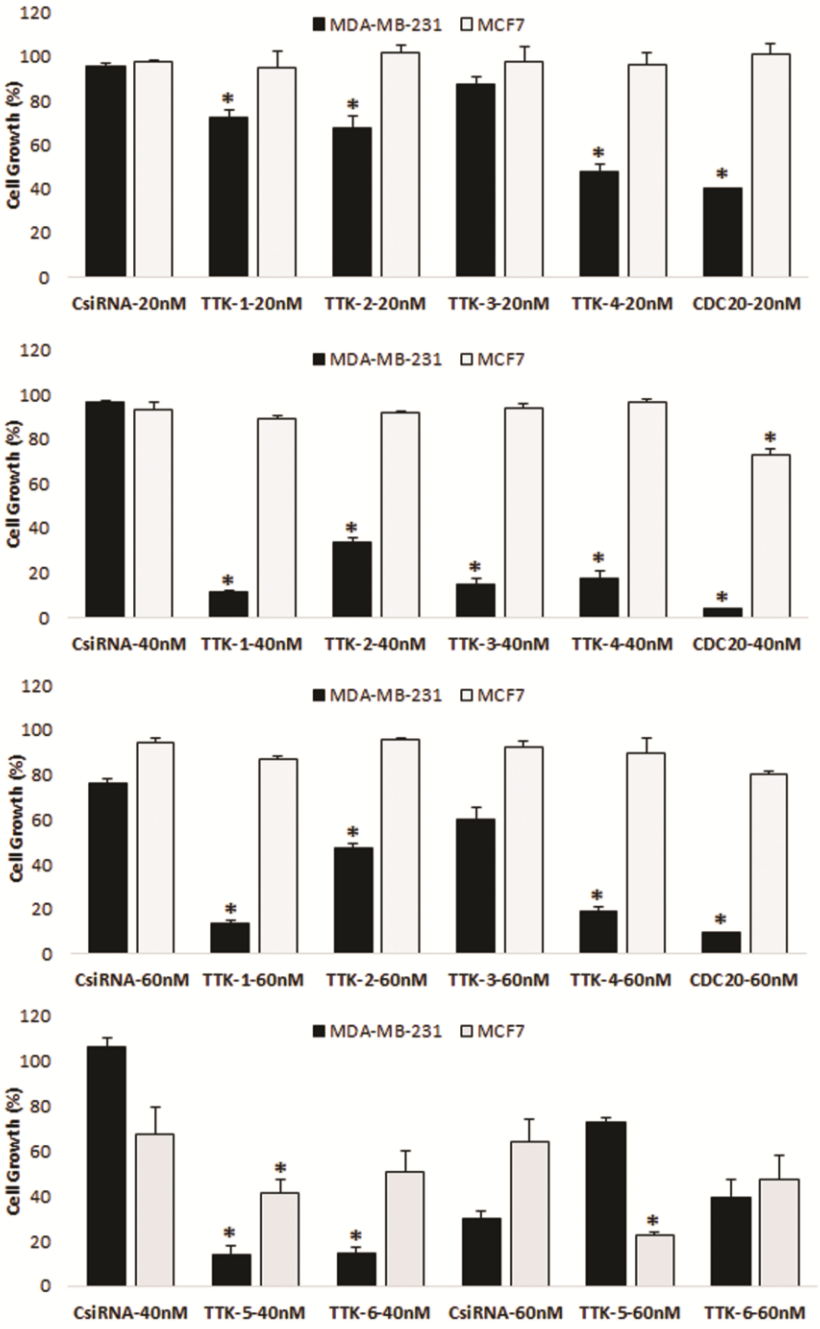

Fig 3.3: Targeting TTK with various siRNAs in MDA-MB-231 and MCF7 cells.

TTK-1, TTK-2, TTK-3 and TTK-4 siRNAs were delivered with 20 **(A)**, 40 **(B)** and 60 nM **(C)** siRNA, while TTK-5 and TTK-6 siRNAs **(D)** were delivered with 40 and 60 nM siRNA at 1:4 siRNA:1.2PEI-LA6 ratios. The inhibition of cell growth was assessed by MTT assay and scrambled siRNA (CsiRNA) was used as a negative control. Asterisks represent the significant cell growth inhibition by specific siRNA compared to CsiRNA ($p < 0.05$).

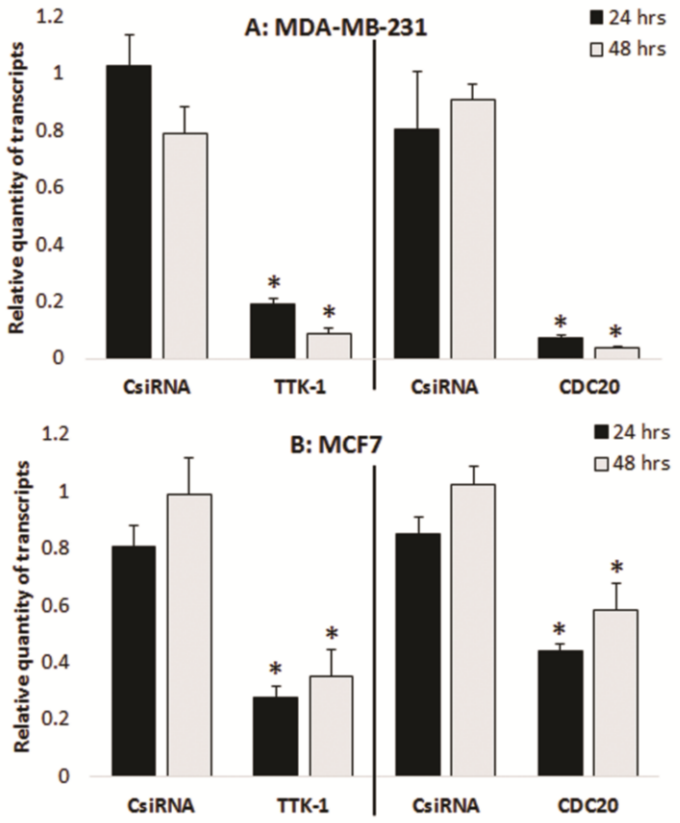

Fig 3.4: RT-qPCR for MDA-MB-231 (A) and MCF7 (B) cells treated with TTK-1 and CDC20 siRNAs. TTK-1 and CDC20 were targeted with 60 nM siRNA at 1:4 siRNA:1.2PEI-LA6 ratio. RT-qPCR was performed after 24 and 48 hrs of transfection. Scrambled siRNA (CsiRNA) was used as a negative control. Asterisks represent the significant reduction in the quantity of transcripts compared to CsiRNA ($p < 0.05$).

To determine the functionality of TTK-1 and CDC20 siRNAs at the transcripts level, RT-qPCR was performed for MDA-MB-231 and MCF7 cells. Significant reduction in the levels of TTK and CDC20 mRNA transcripts was found using TTK-1 and CDC20 siRNAs after 24 and 48 hrs of siRNA transfection **(Fig 3.4)**. RT-qPCR confirmed that the siRNAs against TTK protein were effective in obtaining the desired silencing and the polymeric carrier was able to deliver siRNAs successfully into the cells.

3.3.3 Combinational siRNA delivery against TTK, CDC20 and survivin

Combinational siRNA therapy was performed in MDA-MB-231 and MCF7 cells to determine if a synergistic effect can be achieved with carefully selected combination of siRNAs. A relatively low concentration of siRNA (total 30 nM; 15 nM siRNA each) was chosen for this purpose. The siRNA delivery against single targets at these concentrations (15 nM specific siRNA + 15 nM scrambled siRNA) served as a reference treatment. The siRNA against TTK (using TTK-1 siRNA; referred as TTK siRNA hereafter) and CDC20 alone was not effective in MDA-MB-231 as no inhibition of cell growth was found due to very low concentration of siRNA. However, survivin siRNA alone decreased cell growth by ~25% at 1:4 siRNA:polymer ratio. The synergistic effect of dual therapy was detected with TTK-CDC20 and CDC20-survivin siRNA combination in MDA-MB-231 cells at 1:4 ratio as the cell growth was inhibited by ~30% and ~45%, respectively compared to scrambled siRNA as well as individual targeted siRNAs **(Fig 3.5A)**. The synergism was not detected for dual therapy at 1:2 and 1:8 siRNA:polymer ratios. Caspase activity assay was performed using MDA-MB-231 cells to investigate the initiation of apoptosis in the cell by combinational siRNA therapy. No increase in the caspase activity was found with TTK siRNA alone, while CDC20 and survivin siRNAs showed drastic increase in the caspase activity **(Fig 3.S1)**. Similarly, all siRNA combinations confirmed the initiation of apoptosis in MDA-MB-231 cells as caspase activity was found significantly higher.

No significant decrease in MCF7 cell growth was found by individual siRNA against TTK, CDC20 and survivin at 30 nM total concentration. TTK-CDC20 combination has shown synergistic effect as ~25% of cell growth was inhibited by these siRNAs at 1:4 ratio in MCF7 cells compared to scrambled siRNA as well as individual TTK and CDC20 siRNAs **(Fig 3.5B)**.

The efficacy of the combinational siRNA therapy was also determined by RT-qPCR in MDA-MB-231 and MCF7 cells at 30 and 60 nM total siRNAs **(Fig 3.6)**. The amount of mRNA transcripts for each targeted protein was significantly decreased after individual and dual siRNA delivery, which confirmed that TTK, CDC20 and survivin siRNAs were able to silence its target upon successfully delivered by polymeric carrier.

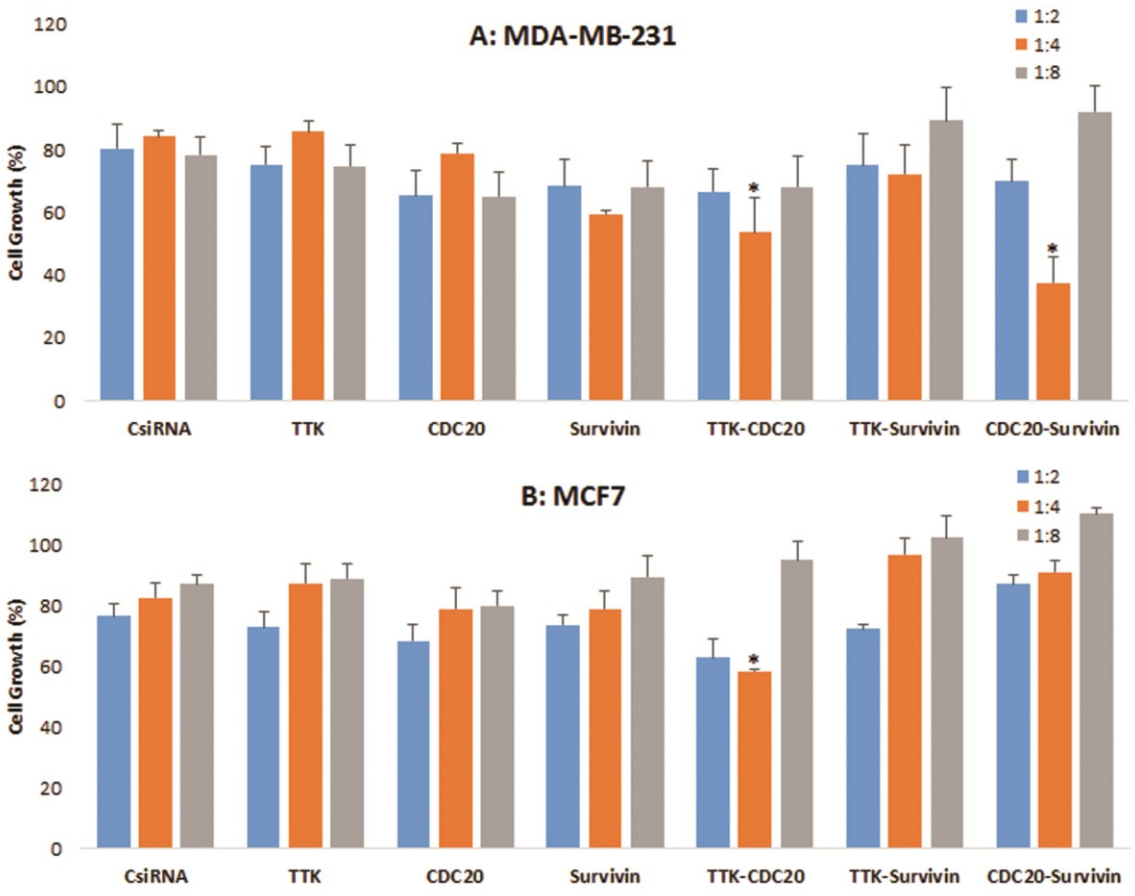

Fig 3.5: Combinational siRNA delivery against TTK-1 (referred as TTK), CDC20 and survivin in MDA-MB-231 (A) and MCF7 (B) cells.

Combination was performed with total 30 nM (15+15 nM each) siRNA at 1:2, 1:4 and 1:8 siRNA:1.2PEI-LA6 ratio. Scrambled siRNA (CsiRNA) was used as a negative control. Asterisks represent the significant cell growth inhibition with combinational siRNA therapy compared to CsiRNA and specific siRNA alone ($p < 0.05$).

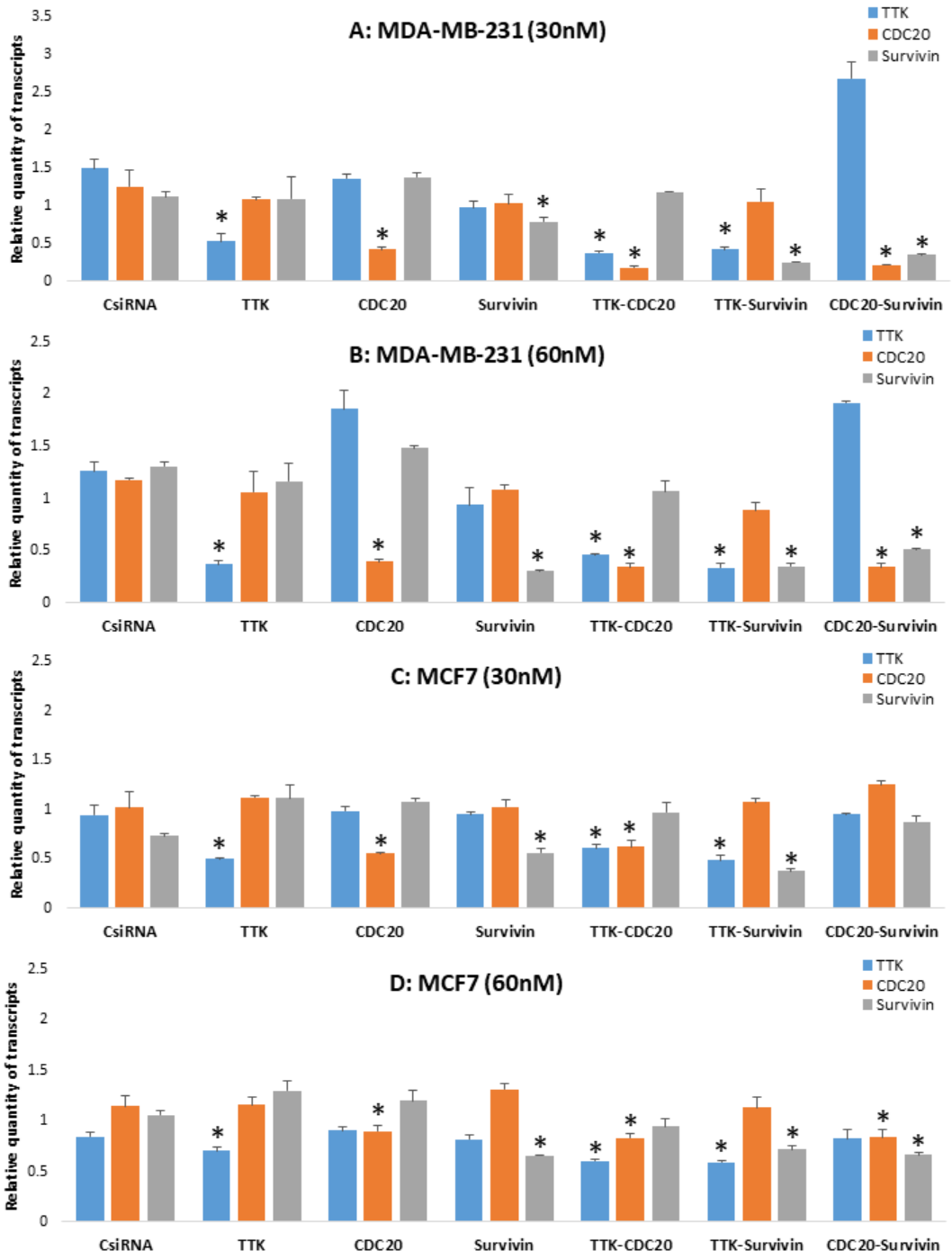

Fig 3.6: RT-qPCR for MDA-MB-231 and MCF7 cells treated with combinational siRNAs.

Cells were transfected with total 30 nM (15+15 nM each) and 60 nM (30+30 nM each) siRNA at 1:4 siRNA:1.2PEI-LA6 ratio. RT-qPCR was performed after 24 hrs of transfection. Scrambled siRNA (CsiRNA) was used as a negative control. Asterisks represent the significant reduction in the quantity of transcripts compared to CsiRNA ($p < 0.05$).

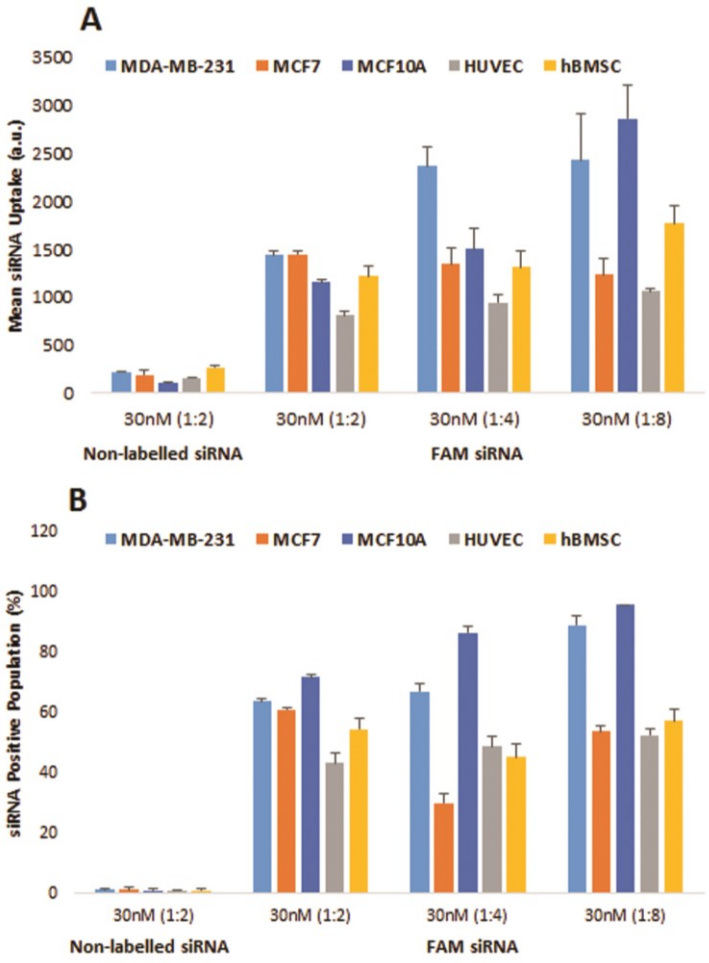

Fig 3.7: Cellular uptake of siRNA by flow cytometry.

FAM-labeled scrambled siRNA was used to determine cellular uptake of siRNA/polymer complexes at 30 nM siRNA with 1:2, 1:4 and 1:8 siRNA:polymer ratios. Non-labeled scrambled siRNA was used as a control to investigate auto-fluorescence of complexes at 30 nM siRNA with 1:2 ratio. The mean fluorescence **(A)** and FAM-positive cell population **(B)** was determined for breast cancer and normal cells.

3.3.4 Cellular uptake of siRNA in breast cancer and non-malignant cells

To investigate how effectively 1.2PEI-LA6 delivers siRNA into the cells, the uptake of FAM-labeled siRNA was performed in breast cancer MDA-MB-231 and MCF7 cells and normal cells, MCF10A, HUVEC, hBMSC **(Fig 3.7)**. No autofluorescence of the complexes was detected as the mean fluorescence and FAM-positive population of non-

treated and non-labeled scrambled siRNA treated cells were similar (data not shown). Based on the mean fluorescence of MDA-MB-231 cells, the cellular uptake of siRNA increased with higher siRNA:polymer ratio (1:4 and 1:8) compared to lower ratio (1:2). However, no major difference was found in MDA-MB-231 cellular uptake between 1:4 and 1:8 ratio. Similarly, an equivalent uptake of siRNA was found at all ratios in MCF7 cells, which was quite low compared to MDA-MB-231 cells.

The cellular uptake of siRNA at 1:2 and 1:4 siRNA:polymer ratios was similar in normal breast MCF10A cells, while the uptake was significantly increased at 1:8 ratio **(Fig 3.7)**. No difference was evident among all siRNA:polymer ratios in the cellular uptake of HUVEC and hBMSC cells. Considering the cellular uptake by breast cancer and normal cells, 1:4 siRNA:polymer ratio could be better formulation of siRNA and 1.2PEI-LA6 due to quite low siRNA delivery efficiency of polymer at this ratio in normal cells compared to MDA-MB-231 cells.

3.3.5 Targeting TTK, CDC20 and survivin in non-malignant cells

The TTK, CDC20 and survivin siRNAs were delivered to normal cells to determine possible effects of siRNA therapy on non-malignant cells. Normal breast cells MCF10A were quite responsive to siRNAs at 1:2 and 1:4 ratios as 20-40% of cell growth was inhibited with individual or combinational siRNAs **(Fig 3.8A)**. However, 1:8 ratio of siRNA was not at all effective to MCF10A cells. No inhibition of HUVEC cell growth was found with complexes formed at higher ratios (1:4 and 1:8). However, complexes at 1:2 ratio inhibited HUVEC cell growth by 20-50% with individual/combined CDC20 and survivin siRNAs **(Fig 3.8B)**. The hBMSC cell growth was significantly inhibited by the CDC20 siRNA at 1:2 and 1:4 ratios whether it was delivered individually or in combination

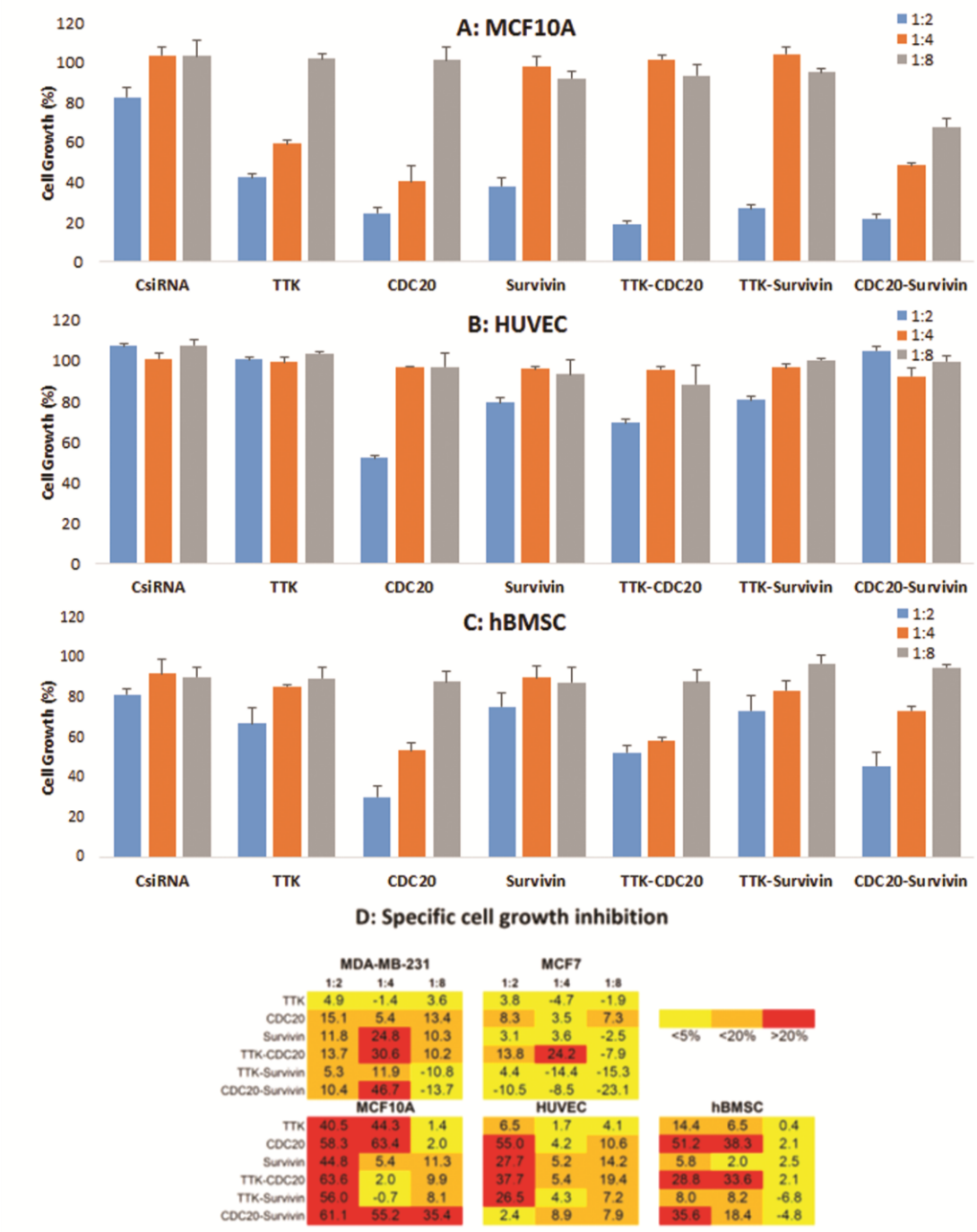

Fig 3.8: Combinational siRNA delivery against TTK, CDC20 and survivin in non-malignant cells.

Combination was performed with total 30 nM (15+15 nM each) siRNA at 1:2, 1:4 and 1:8 siRNA:1.2PEI-LA6 ratio in MCF10A **(A)**, HUVEC **(B)** and hBMSC **(C)** cells. Scrambled siRNA (CsiRNA) was used as a negative control. A heat-map **(D)** represents specific cell growth inhibition by combinational siRNA therapy compared to CsiRNA in breast cancer and normal cells.

(Fig 3.8C). However, 1:8 ratio was unable to decrease the cell growth by all siRNAs. Specific cell growth inhibition by combinational siRNA therapy is presented for breast cancer and normal cells in **Fig 3.8D**. Overall, complexes formulated at higher siRNA:polymer ratio showed the least siRNA effect on non-malignant cells and, therefore, the ratio of siRNA:polymer will need to be chosen carefully to decrease the side effects of siRNAs on normal cells.

3.4 Discussion

The RNAi has become a viable approach in the last decade to develop a targeted cancer therapy, where a specific protein can be silenced to achieve a reduction in tumor growth [7,8]. The siRNA therapy has its limitations, and one of them is the development of a non-toxic carrier that can successfully deliver siRNA into the cell. We evaluated a library of polymeric carriers based on low molecular weight PEIs (0.6, 1.2 and 2.0 kDa) to deliver siRNA as high molecular weight branched (>25 kDa) and linear (>750 kDa) PEIs possess unacceptable cytotoxicity [38]. PEI can escape the endosomal compartment due to its inherent 'proton-sponge' effect so that siRNA can be effectively delivered into cytoplasm after the cellular uptake of siRNA/polymer complexes [38]. The cellular uptake of siRNA using low molecular weight PEIs is quite low [34,35] and no cellular uptake of siRNA was observed with non-modified 1.2 kDa PEI **(Fig 3.2B)**. Therefore, we substituted the amines of PEIs with lipidic moieties to improve the delivery of siRNA. The lipidic moieties presumably improves chemical compatibility of siRNA/polymer complexes with cell membrane so that siRNA uptake can be increased significantly [14]. In addition, the degree of substitutions in PEI plays a major role for uptake of complexes. No siRNA uptake was observed with low LA substitutions **(Fig 3.2B)**, and high LA substituted PEI showed

higher toxicity **(Fig 3.1)**. The relationship between the uptake and LA substitution was not monotonous, since a critical degree of substitution (>2 LA/1.2 PEI) was required to enable uptake of siRNA complexes. An optimal LA substitution in PEI is necessary to have higher uptake and less cytotoxicity, and 1.2PEI-LA6 seemed to have both characteristics based on cellular uptake and inhibition of cell growth. Moreover, physicochemical characteristics of the complexes play an important role in the uptake of siRNA as well. Hydrodynamic size of complexes with 1.2PEI-LA6 has decreased significantly **(Fig 3.2A)**, while ζ-potential has dramatically increased compared to other LA substituted polymers, which could have contributed to better uptake of siRNA with 1.2PEI-LA6 compared to other polymers. Among many synthesized polymers, 1.2PEI-LA6 was the most effective polymer that inhibited cell growth drastically when it was used to deliver CDC20 siRNA **(Fig 3.1)**, which was consistent with uptake results **(Fig 3.2)**. Several other polymers inhibited MDA-MB-231 cell growth as well with CDC20 siRNA. However, only 1.2PEI-LA6 showed significant decrease in the cell growth with TTK siRNA. The efficacy of growth inhibition by TTK delivery, however, was quite low compared to CDC20 siRNA, which suggests that CDC20 may be more potent target for silencing compared to TTK. This is not surprising since CDC20 was previously identified from a siRNA library screen, where we selected the most efficacious siRNA from a library of 169 siRNAs [39]. The polymers derived from the 0.6 kDa PEI were generally not effective, presumably due to smaller size and relatively less efficient binding to siRNA, and higher LA substitutions on 1.2 and 2.0 kDa PEIs generally led to more effective growth inhibition.

We targeted TTK protein in this study with various siRNAs since the up-regulation of this gene in many cancer types was reported leading to uncontrolled proliferation of

those cancer cells [21,22]. As TTK is associated with cell proliferation, it has been silenced in pancreatic, prostate and liver cancers by siRNA using commercially available carriers to decrease cell proliferation [22,40-42]. In this study, we showed that TTK is also a viable target in breast cancer and delivering the TTK siRNA using polymeric carrier would lead to decrease in the breast cancer cell growth **(Fig 3.3)**. The results were confirmed at transcripts level as well by RT-qPCR **(Fig 3.4)**. We used six different siRNAs against TTK to determine the efficacy of each siRNA. The outcome was expected to depend on how thermodynamically asymmetric siRNA is and where siRNA is targeting in the gene [43]. Based on the thermodynamic asymmetry of siRNA, the components of RISC bind to siRNA and the selection of guide strand is made [44]. The various siRNAs for the same gene, therefore, should have different efficiency of silencing its target. TTK-5 and TTK-6 siRNAs that were supplied by IDT were 27 base pair dicer-substrate siRNA, which has a longer nucleotide sequence compared to regular 21 base pair siRNAs. Dicer-substrate siRNA interacts with the dicer enzyme before its incorporation into the RISC assembly, which may lead to increased potency by engaging to natural siRNA processing pathway [45]. However, no difference in the potency of 21 and 27 base pairs siRNAs was observed for TTK siRNAs, and inhibition of MDA-MB-231 cell growth was found at some extent with all six siRNAs **(Fig 3.3)**. Previously, we have observed high efficacy with dicer-substrate siRNA against CDC20 compared to regular 21 base pair siRNA [39], but it seems that the relative efficiency might depend on the target and/or exact sequence (siRNA binding site in a gene) of the siRNA. MCF7 cells were not as responsive as MDA-MB-231 to TTK siRNAs despite displaying effective silencing **(Fig 3.4)**, which suggests that MCF7

cells may not critically rely on TTK protein for its survival and may have found an alternative protein to undertake cell division.

CDC20 has a key role during mitosis to activate APC that leads cells from metaphase to anaphase. We have validated the efficacy of various siRNAs against CDC20 previously in two breast cancer models (MDA-MB-435 and MDA-MB-231 cells) [39]. CDC20 silencing showed significant cell death at 40 nM of siRNA in MDA-MB-231 cells **(Fig 3.1B)**, while it displayed poor efficacy at 15 nM of siRNA in both MDA-MB-231 and MCF7 cells **(Fig 3.5)**. Survivin siRNAs employed here was dicer-substrate siRNAs and has shown increased potency in MDA-MB-231 cells at 15 nM concentration **(Fig 3.5A)**. Since survivin has been shown to be a critical target for cancer therapy as well, the siRNA against survivin was applied to breast cancer cells and the efficacy of targeting survivin was validated previously [46].

Silencing the expression of two essential proteins simultaneously is a promising strategy as the chances of survival for malignant cells could drastically be decreased. Not only the synergistic effect of the combinational therapy can be achieved, but also the doses of siRNAs can be lowered to have less side effects on non-malignant cells. We have targeted the cell cycle proteins, TTK and CDC20 with siRNAs and observed a synergism in the therapy at low doses of siRNAs. RT-qPCR confirmed the functionality of combinational TTK-CDC20 siRNA therapy at transcripts level **(Fig 3.6)** so that we do not seem to be overloading the RISC-mediated silencing machinery with dual siRNA delivery. Elevation in TTK transcripts was consistently observed in MDA-MB-231 cells upon silencing CDC20 individually or with combination, which suggests that cells may have upregulated TTK expression upon detecting loss of CDC20 protein. Upon depletion of cell

cycle proteins during cell proliferation, cell cycle is arrested until the error in the cell cycle is corrected [47]. If the essential proteins for cell cycles are missing, especially TTK and CDC20 that participate in mitosis, the error cannot be corrected and pathways for cell death is expected to be initiated. The mitotic catastrophe [48] or initiation of apoptotic pathway by caspase activation (cell death mechanisms) may have played role upon depletion of TTK and CDC20 in breast cancer cells as the cell death **(Fig 3.5)** and the elevation in caspase activity **(Fig 3.S1)** were evident with combinational siRNA therapy against these cell cycle proteins. Several lines of evidence suggest that cell cycle and anti-apoptosis proteins have conjunctional roles during cell division [49,50]. Moreover, arrested cell cycle due to inhibition of a specific cell cycle protein could increase the production of anti-apoptosis protein to block the apoptotic pathway that may have been initiated in order to overcome cell cycle arrest. Therefore, targeting anti-apoptosis protein such as survivin with TTK and CDC20 seems appropriate to have a synergism in combinational siRNA delivery. The synergistic effect of the combinational CDC20/survivin siRNA therapy was evident in MDA-MB-231 cells **(Fig 3.5A)**.

The siRNA:polymer ratio plays a major role for the efficacy of siRNA treatment. The synergistic effect of dual siRNA therapy was not observed at lower 1:2 siRNA:polymer ratio in MDA-MB-231 cells **(Fig 3.5A)** due to poor uptake of complexes **(Fig 3.7)**. On the other hand, the synergistic effect was only observed at 1:4 siRNA:polymer ratio even though the uptake of siRNA was similar at 1:4 and 1:8 siRNA:polymer ratios. A possible reason for ineffective siRNA treatment at 1:8 ratio could be the dissociation of complexes in cytoplasm; siRNA may have dissociated poorly from polymer at the higher 1:8 ratio because of strong binding between anionic siRNA and

cationic polymer, resulting in poor efficacy of siRNA **(Fig 3.S2)**. In addition, the size and ζ-potential of complexes at different siRNA:polymer ratios may have contributed for the efficacy of siRNA treatment as well. The size of siRNA/1.2PEI-LA6 complexes decreased from ~130 to ~63 nm as the polymer amount was increased from 1:2 to 1:8 ratios **(Fig 3.S3)**. Similarly, the ζ-potential has increased as the siRNA:polymer ratio increased. No significant difference was observed in size and ζ-potential of complexes at 1:4 and 1:8 ratios, which may support the uptake of siRNA results as similar uptake was found at both of these ratios in MDA-MB-231 cells.

We have also determined how much damage the siRNAs are causing to normal cells since siRNA/polymer complexes will not be restricted to transfect only tumor cells when administered *in vivo*. As the results indicate, normal breast cells (MCF10A) seemed to be more sensitive to these complexes compared to endothelial (HUVEC) and bone marrow stromal cells (hBMSC; **Fig 3.8)**. Moreover, the higher siRNA:polymer ratio used to prepare complexes was not effective to decrease cell growth of normal cells compared to lower ratio that inhibited the cell growth drastically in normal cells, which clearly showed how important it is to determine the specific formulation ratio carefully for siRNA therapy. The employed polymer (1.2PEI-LA6) did not have any cell-targeted moieties so that it is not surprising to observe its functionality in all these adherent cells. Since no growth inhibition was found for the scrambled siRNA treated normal cells with all ratios, it was obvious that the polymeric delivery system was not toxic, and the observed effect was due to specific siRNAs delivered. Furthermore, the cellular uptake of siRNA was found to be similar at all ratios in normal cells **(Fig 3.7)**, which suggests that the polymer had successfully delivered siRNA into the cells at all ratios. However, the dissociation of

polymer from siRNA in cytoplasm may have been higher at lower 1:2 siRNA:polymer ratio so that the effect of siRNA was evident in normal cells, and siRNA may have dissociated poorly from polymer at higher 1:8 ratio, resulting in poor efficacy of siRNA **(Fig 3.S2)**. The 1:4 siRNA:polymer ratio showed synergistic effect with TTK and CDC20 siRNA in breast cancer cells **(Fig 3.5)**, and the same ratio was not effective in normal cells except hBMSC that showed ~30% cell death **(Fig 3.8)**. Therefore, 1:4 ratio at total 30 nM siRNA could be an effective dose to target TTK and CDC20 in breast cancer cells. The siRNA:polymer ratio could play a critical role under *in vivo* conditions at preclinical models, but this issue remains to be addressed at this stage; such an optimization with siRNA:polymer ratio might be necessary with the chosen molecular targets *in vivo*.

The synthesized polymer showed different efficacy in siRNA delivery to breast cancer and normal cells. Comparing the two breast cancer cells, we noted lower uptake of siRNA by MCF7 cells compared to MDA-MB-231 that may explain the lower silencing efficiencies (*i.e.,* mRNA reduction based on RT-qPCR) and reduced response (*i.e.,* cell growth inhibition) to specific siRNA delivery in MCF7 cells. The siRNA uptake was similar in HUVEC and hBMSC, suggesting no particular selectivity of polymer towards these normal cells. MCF10A, however, showed higher uptake of siRNA and were more responsive, leading to the selectivity of employed polymer to transfect breast cells efficiently compared to other cell-types. We have observed in the past that certain polymers can only transfect particular cell-lines, *e.g.* the polymer used to deliver siRNA to breast cancer cells has displayed poor efficacy in leukemia cells [51]. This is expected to some extent since adherent cells probably possess different membrane structure than the non-adherent leukemic cells. For more effective clinical utility, it might be necessary to make

the current polymers (without a targeting moiety) selective towards a particular cell-type. Perhaps, coating of complexes with polyethylene glycol [52] or hyaluronic acid [53] could make the complexes selective for cancer cells (due to reduced uptake by initially encountered normal cells). The selectivity may arise from the choice of siRNA as well (*i.e.,* selection of specific oncotargets), but with the three specific targets explored here, the selectivity was not universal and could only be partially achieved by fine-tuning of siRNA:polymer ratio used in formulating the nucleic acid complexes. Tailored polymers that can exclusively transfect malignant cells remain to be designed, synthesized and tested.

3.5 Conclusions

The proteins TTK, CDC20 and survivin could be promising targets for siRNA therapy to decrease the proliferation of triple-negative breast cancer cells, such as MDA-MB-231 cells employed here. This study has indicated improved therapeutic efficacy of siRNAs by employing combinational siRNAs against cell cycle and anti-apoptosis proteins in breast cancer cells. The lipid-substituted polymers could serve as a viable platform for delivery of multiple siRNAs against critical targets, and co-delivery of siRNAs did not impair the desired silencing efficiency observed with individual siRNAs. However, the siRNA therapy with the chosen targets showed significant effects on non-malignant cells *in vitro*. While the side-effects could be minimized with the optimization of siRNA:polymer ratio, more selective therapies (either polymers or siRNA against therapeutic targets) might be needed to target cancer cells solely.

3.6 Acknowledgments

Manoj Parmar was a recipient of Women and Children's Health Research Institute (WCHRI) Graduate Studentship Grant and Alberta Innovates-Health Solutions (AIHS)

Graduate Studentship. This study was supported by operating grants from Canadian Breast Cancer Foundation (CBCF) and Natural Sciences and Engineering Council of Canada (NSERC).

3.7 References

1. Vici P, Pizzuti L, Natoli C, Gamucci T, Di Lauro L, Barba M, Sergi D, Botti C, Michelotti A, Moscetti L, Mariani L, Izzo F, D'Onofrio L, Sperduti I, Conti F, Rossi V, Cassano A, Maugeri-Saccà M, Mottolese M, Marchetti P. Triple positive breast cancer: a distinct subtype? *Cancer Treat Rev*, 2015, 41:69-76.
2. Hart CD, Migliaccio I, Malorni L, Guarducci C, Biganzoli L, Di Leo A. Challenges in the management of advanced, ER-positive, HER2-negative breast cancer. *Nat Rev Clin Oncol*, 2015, 12:541-552.
3. Tinoco G, Warsch S, Glück S, Avancha K, Montero AJ. Treating breast cancer in the 21st century: emerging biological therapies. *J Cancer*, 2013, 4:117-132.
4. Foulkes WD, Smith IE, Reis-Filho JS. Triple-negative breast cancer. *N Engl J Med*, 2010, 363:1938-1948.
5. Dent R, Trudeau M, Pritchard KI, Hanna WM, Kahn HK, Sawka CA, Lickley LA, Rawlinson E, Sun P, Narod SA. Triple-negative breast cancer: clinical features and patterns of recurrence. *Clin Cancer Res,* 2007, 13:4429-4434.
6. Reis-Filho JS, Tutt AN. Triple negative tumours: a critical review. *Histopathology*, 2008, 52:108-118.
7. McManus MT, Sharp PA. Gene silencing in mammals by small interfering RNAs. *Nat Rev Genet*, 2002, 3:737-747.
8. Kim DH, Rossi JJ. Strategies for silencing human disease using RNA interference. *Nat Rev Genet*, 2007, 8:173-184.
9. Wilson RC, Doudna JA. Molecular mechanisms of RNA interference. *Annu Rev Biophys,* 2013, 42:217-239.
10. Pecot CV, Calin GA, Coleman RL, Lopez-Berestein G, Sood AK. RNA interference in the clinic: challenges and future directions. *Nat Rev Cancer*, 2011, 11:59-67.
11. Bora RS, Gupta D, Mukkur TK, Saini KS. RNA interference therapeutics for cancer: challenges and opportunities. *Mol Med Rep,* 2012, 6:9-15.
12. Aliabadi HM, Landry B, Sun C, Tang T, Uludağ H. Supramolecular assemblies in functional siRNA delivery: where do we stand? *Biomaterials*, 2012, 33:2546-2569.
13. Aliabadi HM, Landry B, Bahadur RK, Neamnark A, Suwantong O, Uludağ H. Impact of lipid substitution on assembly and delivery of siRNA by cationic polymers. *Macromol Biosci*, 2011, 11:662-672.
14. KC RB, Kucharski C, Uludağ H. Additive nanocomplexes of cationic lipopolymers for improved non-viral gene delivery to mesenchymal stem cells. *J Mat Chem B*, 2015, 3:3972-3982.
15. Sandhu C, Slingerland J. Deregulation of the cell cycle in cancer. *Cancer Detect Prev*, 2000, 24:107-118.

16. Malumbres M, Carnero A. Cell cycle deregulation: a common motif in cancer. *Prog Cell Cycle Res*, 2003, 5:5-18.

17. Mills GB, Schmandt R, McGill M, Amendola A, Hill M, Jacobs K, May C, Rodricks AM, Campbell S, Hogg D. Expression of TTK, a novel human protein kinase, is associated with cell proliferation. *J Biol Chem*, 1992, 267:16000-16006.

18. Hiruma Y, Sacristan C, Pachis ST, Adamopoulos A, Kuijt T, Ubbink M, von Castelmur E, Perrakis A, Kops GJ. Competition between MPS1 and microtubules at kinetochores regulates spindle checkpoint signaling. *Science*, 2015, 348:1264-1267.

19. Lo YL, Yu JC, Chen ST, Hsu GC, Mau YC, Yang SL, Wu PE, Shen CY. Breast cancer risk associated with genotypic polymorphism of the mitotic checkpoint genes: a multigenic study on cancer susceptibility. *Carcinogenesis*, 2007, 28:1079-1086.

20. Vaclavicek A, Bermejo JL, Wappenschmidt B, Meindl A, Sutter C, Schmutzler RK, Kiechle M, Bugert P, Burwinkel B, Bartram CR, Hemminki K, Försti A. Genetic variation in the major mitotic checkpoint genes does not affect familial breast cancer risk. *Breast Cancer Res Treat*, 2007, 106:205-213.

21. Ahn CH, Kim YR, Kim SS, Yoo NJ, Lee SH. Mutational analysis of TTK gene in gastric and colorectal cancers with microsatellite instability. *Cancer Res Treat*, 2009, 41:224-228.

22. Kaistha BP, Honstein T, Müller V, Bielak S, Sauer M, Kreider R, Fassan M, Scarpa A, Schmees C, Volkmer H, Gress TM, Buchholz M. Key role of dual specificity kinase TTK in proliferation and survival of pancreatic cancer cells. *Br J Cancer*, 2014, 111:1780-1787.

23. Kimata Y, Baxter JE, Fry AM, Yamano H. A role for the Fizzy/Cdc20 family of proteins in activation of the APC/C distinct from substrate recruitment. *Mol Cell*, 2008, 32:576-583.

24. Tipton AR, Ji W, Sturt-Gillespie B, Bekier ME, Wang K, Taylor WR, Liu ST. Monopolar spindle 1 (MPS1) kinase promotes production of closed MAD2 (C-MAD2) conformer and assembly of the mitotic checkpoint complex. *J Biol Chem*, 2013, 288:35149-35158.

25. Maciejowski J, George KA, Terret ME, Zhang C, Shokat KM, Jallepalli PV. Mps1 directs the assembly of Cdc20 inhibitory complexes during interphase and mitosis to control M phase timing and spindle checkpoint signaling. *J Cell Biol*, 2010, 190:89-100.

26. King KL, Cidlowski JA. Cell cycle regulation and apoptosis. *Annu Rev Physiol*, 1998, 60:601-617.

27. Reed JC. Mechanisms of apoptosis. *Am J Pathol*, 2000, 157:1415-1430.

28. Small S, Keerthivasan G, Huang Z, Gurbuxani S, Crispino JD. Overexpression of survivin initiates hematologic malignancies *in vivo*. *Leukemia,* 2010, 24:1920-1926.

29. Shi Z, Liang YJ, Chen ZS, Wang XH, Ding Y, Chen LM, Fu LW. Overexpression of Survivin and XIAP in MDR cancer cells unrelated to P-glycoprotein. *Oncol Rep*, 2007, 17:969-976.

30. Peroukides S, Bravou V, Alexopoulos A, Varakis J, Kalofonos H, Papadaki H. Survivin overexpression in HCC and liver cirrhosis differentially correlates with p-STAT3 and E-cadherin. *Histol Histopathol*, 2010, 25:299-307.

31. Sah NK, Khan Z, Khan GJ, Bisen PS. Structural, functional and therapeutic biology of survivin. *Cancer Lett*, 2006, 244:164-171.

32. Carvalho A, Carmena M, Sambade C, Earnshaw WC, Wheatley SP. Survivin is required for stable checkpoint activation in taxol-treated HeLa cells. *J Cell Sci*, 2003, 116:2987-2998.

33. Lens SM, Wolthuis RM, Klompmaker R, Kauw J, Agami R, Brummelkamp T, Kops G, Medema RH. Survivin is required for a sustained spindle checkpoint arrest in response to lack of tension. *EMBO J*, 2003, 22:2934-2947.

34. Bahadur KC, Landry B, Aliabadi HM, Lavasanifar A, Uludağ H. Lipid substitution on low molecular weight (0.6-2.0 kDa) polyethylenimine leads to a higher zeta potential of plasmid DNA and enhances transgene expression. *Acta Biomater*, 2011, 7:2209-2217.

35. Remant Bahadur KC, Uludağ H. A comparative evaluation of disulfide-linked and hydrophobically-modified PEI for plasmid delivery. *J Biomater Sci Polym Ed,* 2011, 22:873-892.

36. Jiang H, Secretan C, Gao T, Bagnall K, Korbutt G, Lakey J, Jomha NM. The development of osteoblasts from stem cells to supplement fusion of the spine during surgery for AIS. p 467-472. *In:* Uyttendaele D, Dangerfield PH (ed.). *Studies in Health Technology and Informatics: Research in Spinal Deformities*, 2006, IOS Press, Amsterdam, The Netherlands.

37. Sumantran VN. Cellular chemosensitivity assays: an overview. *Methods Mol Biol*, 2011, 731:219-236.

38. Moghimi SM, Symonds P, Murray JC, Hunter AC, Debska G, Szewczyk A. A two-stage poly(ethylenimine)-mediated cytotoxicity: implications for gene transfer/therapy. *Mol Ther*, 2005, 11:990-995.

39. Parmar MB, Aliabadi HM, Mahdipoor P, Kucharski C, Maranchuk R, Hugh JC, Uludağ H. Targeting cell cycle proteins in breast cancer cells with siRNA by using lipid-substituted polyethylenimines. *Front Bioeng Biotechnol*, 2015, 3:14.

40. Maire V, Baldeyron C, Richardson M, Tesson B, Vincent-Salomon A, Gravier E, Marty-Prouvost B, De Koning L, Rigaill G, Dumont A, Gentien D, Barillot E, Roman-Roman S, Depil S, Cruzalegui F, Pierré A, Tucker GC, Dubois T. TTK/hMPS1 is an attractive therapeutic target for triple-negative breast cancer. *PLoS One*, 2013, 8:e63712.

41. Liang XD, Dai YC, Li ZY, Gan MF, Zhang SR, Yin-Pan, Lu HS, Cao XQ, Zheng BJ, Bao LF, Wang DD, Zhang LM, Ma SL. Expression and function analysis of mitotic checkpoint genes identifies TTK as a potential therapeutic target for human hepatocellular carcinoma. *PLoS One*, 2014, 9:e97739.

42. Dahlman KB, Parker JS, Shamu T, Hieronymus H, Chapinski C, Carver B, Chang K, Hannon GJ, Sawyers CL. Modulators of prostate cancer cell proliferation and viability identified by short-hairpin RNA library screening. *PLoS One*, 2012, 7:e34414.

43. Malefyt AP, Wu M, Vocelle DB, Kappes SJ, Lindeman SD, Chan C, Walton SP. Improved asymmetry prediction for short interfering RNAs. *FEBS J*, 2014, 281:320-330.

44. Noland CL, Doudna JA. Multiple sensors ensure guide strand selection in human RNAi pathways. *RNA*, 2013, 19:639-648.

45. Kim DH, Behlke MA, Rose SD, Chang MS, Choi S, Rossi JJ. Synthetic dsRNA Dicer substrates enhance RNAi potency and efficacy. *Nat Biotechnol*, 2005, 23:222-226.

46. Montazeri Aliabadi H, Landry B, Mahdipoor P, Uludağ H. Induction of apoptosis by survivin silencing through siRNA delivery in a human breast cancer cell line. *Mol Pharm*, 2011, 8:1821-1830.

47. Pietenpol JA, Stewart ZA. Cell cycle checkpoint signaling: cell cycle arrest versus apoptosis. *Toxicology,* 2002, 181-182:475-481.

48. Castedo M, Perfettini JL, Roumier T, Andreau K, Medema R, Kroemer G. Cell death by mitotic catastrophe: a molecular definition. *Oncogene,* 2004, 23:2825-2837.

49. Harley ME, Allan LA, Sanderson HS, Clarke PR. Phosphorylation of Mcl-1 by CDK1-cyclin B1 initiates its Cdc20-dependent destruction during mitotic arrest. *EMBO J*, 2010, 29:2407-2420.

50. Saintigny Y, Dumay A, Lambert S, Lopez BS. A novel role for the Bcl-2 protein family: specific suppression of the RAD51 recombination pathway. *EMBO J*, 2001, 20:2596-2607.

51. Valencia-Serna J, Gul-Uludağ H, Mahdipoor P, Jiang X, Uludağ H. Investigating siRNA delivery to chronic myeloid leukemia K562 cells with lipophilic polymers for therapeutic BCR-ABL down-regulation. *J Control Release*, 2013, 172:495-503.

52. Mishra P, Nayak B, Dey RK. PEGylation in anti-cancer therapy: An overview. *Asian Journal of Pharmaceutical Sciences*, 2015, 11:337-348.

53. Martens TF, Remaut K, Deschout H, Engbersen JF, Hennink WE, van Steenbergen MJ, Demeester J, De Smedt SC, Braeckmans K. Coating nanocarriers with hyaluronic acid facilitates intravitreal drug delivery for retinal gene therapy. *J Control Release*, 2015, 202:83-92.

4. Combinational siRNA delivery using hyaluronic acid modified amphiphilic polyplexes against cell cycle and phosphatase proteins to inhibit growth and migration of triple-negative breast cancer cells

A version of this chapter was published in:

Parmar MB, Meenakshi Sundaram DN, K.C. RB, Maranchuk R, Montazeri Aliabadi H, Hugh JC, Löbenberg R, Uludağ H. Combinational siRNA delivery using hyaluronic acid modified amphiphilic polyplexes against cell cycle and phosphatase proteins to inhibit growth and migration of triple-negative breast cancer cells. *Acta Biomater*, 2018, 66:294-309.

4.1 Introduction

Despite advances in the diagnosis and treatment of breast cancer, the metastasis of breast cancer to distant organs continues to be the major cause of death [1,2]. Having spread to the rest of the body, metastatic breast cancer can only be addressed by systemic chemotherapies that have many toxic side effects due to the non-specificity of their action. Targeted agents developed to block estrogen receptor, progesterone receptor or human epidermal growth factor receptor 2 (HER2), are only of use in tumors that display the corresponding receptors [3]. However, a common sub-type of breast cancer, triple-negative breast cancer, lacks these three receptors and are not candidates for existing targeted therapies because of the lack of utility when the targeted receptors are absent. Triple-negative breast cancer affects 12-17% of patients, and although it initially responds well to primary chemotherapy, has a high recurrence rate with poor survival [4,5]. RNA interference (RNAi) is a relatively recent targeted therapy that is ideal for triple-negative breast cancer cells since it can address aberrant factors specifically associated with these cells. The synthetic pharmacological RNAi agent, small-interfering RNA (siRNA), can target specific mRNA, silencing the expression of the corresponding protein [6]. Once siRNA is introduced to the cell, it incorporates into the RNA inducing silencing complex (RISC) followed by degradation of the passenger strand of double-stranded siRNA. The other "guide" strand of siRNA then guides the RISC assembly to its targeted mRNA that is directing the translation of the corresponding protein. The RISC assembly loaded with the guide strand of siRNA cleaves the mRNA or inhibit the translation, leading to the silencing of that protein in the cell [7].

However, siRNA is a highly labile, anionic and nuclease-sensitive molecule, and needs a carrier that can transport it to the cell and protect it from extracellular degradation [8]. To facilitate the entry of siRNA into the cell, we have previously developed a library of cationic polymeric carriers that are based on low molecular weight polyethylenimines (PEI) [9,10]. High molecular weight PEIs possess excess cationic charge that readily disrupts the plasma membrane, leading to significant toxicity of the carrier itself. In contrast, minimal toxicity has been reported for low molecular weight (<2.0 kDa) PEIs, making them more suitable for the delivery of siRNA. We have shown that modification of these PEIs with lipidic moieties results in efficient uptake of siRNA/PEI complexes [10,11], presumably due to improved chemical compatibility of siRNA/PEI complexes with cell membrane as a result of introduced hydrophobic moieties.

In this study, we introduce hyaluronic acid (HA) to siRNA/PEI complexes and show a drastic increase in cellular uptake. HA is an anionic, nonsulfated glycosaminoglycan distributed widely throughout connective, epithelial, and neural tissues. It is one of the main components of extracellular matrix, and is known to contribute to cell proliferation [12]. In 1990, Aruffo *et al.* identified HA as the primary binding molecule of cluster of differentiation-44 (CD44), a cell-surface glycoprotein that plays a significant role in a number of biological functions, including cell–cell interactions, cell adhesion and migration [13]. Since the CD44 receptor is over-expressed in a variety of solid tumors, and is known to be increased in triple negative breast cancers [14,15], the HA formulated delivery system can potentially bind to over-expressed CD44 receptors selectively, increasing the uptake of siRNA in cancer cells. Thus, the HA-formulated

delivery agent could assist in the discrimination between healthy and malignant cells *in vivo* with a reduction of off-target toxicity.

One of the hallmarks of cancer is the deregulation of the cell cycle due to up-regulation of many essential proteins that control cell division [16]. Targeting and silencing these up-regulated cell cycle proteins could lead to inhibition of cell proliferation, and decrease the growth of cancer cells. One of the cell cycle proteins we identified previously, based on a library screen of siRNAs targeting proteins involved in cell cycle regulation, is cell-division cycle protein 20 (CDC20) [17]. CDC20 activates the anaphase-promoting complex (APC) in the cell cycle during mitosis, which initiates chromatid separation and entrance of the cell division into anaphase [18]. Since CDC20 plays a key role during mitosis, silencing its expression by siRNA could potentially lead to cell cycle arrest, thereby decreasing tumor cell growth.

Since down-regulating a single target involved in cell growth may be ineffective in metastatic cancer, we pursued combinational therapy inhibiting both cell growth as well as migration as a more effective strategy. Several reports have suggested involvement of protein-tyrosine phosphatases in the metastasis of several types of cancer [19-22]. Protein-tyrosine phosphatases function in signal transduction by deactivating kinases with the removal of phosphate group from phosphorylated tyrosine. The de-regulation or over-expression of protein-tyrosine phosphatases is evident in many types of cancers including breast cancer [23-25]. Therefore, we investigated whether silencing phosphatases with siRNA could decrease cellular migration and ultimately contribute to a useful therapeutic development for triple-negative breast cancer.

In this report, we tested the hypothesis that dual siRNA therapy against a cell cycle protein (to decrease cell growth) and a phosphatase (to decrease metastasis) may have a more drastic impact on the growth of triple-negative breast cancers. We first synthesized lipid-substituted low molecular weight PEI followed by a formulation of PEI/HA for the delivery of siRNA. We then characterized the PEI/HA delivery carrier and determined its efficiency at delivering siRNA by cellular uptake and cell growth inhibition. We also determined a potential role of CD44 surface receptor for the uptake of siRNA when siRNA was delivered with PEI/HA. We additionally screened a library of siRNAs against 267 phosphatase targets to identify potential candidates to reduce the migration of tripe-negative breast cancer cells followed by a combinational siRNA therapy targeting cell cycle (CDC20) and identified phosphatase proteins to decrease cell growth as well as migration simultaneously.

4.2 Materials and Methods

4.2.1 Materials

The amines of low molecular weight PEI (1.2 kDa) were substituted with linoleic acid via N-acylation (PEI-LA) and the degree of substitution on the polymer (PEI-LA) was determined by ^{1}H-NMR spectroscopy, as previously described [26,27]. HA (~300 kDa), doxorubicin, MTT [3-(4 5-dimethylthiazol-2-yl)-2 5-diphenyltetrazolium] and dimethyl sulfoxide (DMSO) were purchased from Sigma-Aldrich (St. Louis, MO). Hank's Balanced Salt Solution (HBSS) was prepared in-house.

Silencer® Human Phosphatase siRNA Library V3 (Cat. No. AM80140v3) containing siRNAs against 267 phosphatases was purchased from Ambion (Foster City, CA). All siRNAs against CD44 (Cat. No. HSC.RNAi.N000610.12.1), CDC20 (Cat. No.

HSC.RNAi.N001255.12.1), protein phosphatase 1 regulatory subunit 7 (PPP1R7, Cat. No. HSC.RNAI.N002712.12.1), protein tyrosine phosphatase, non-receptor type 1 (PTPN1, Cat. No. HSC.RNAI.N002827.12.1), protein tyrosine phosphatase, non-receptor type 22 (PTPN22, Cat. No. HSC.RNAI.N015967.12.1), phospholysine phosphohistidine inorganic pyrophosphate phosphatase (LHPP, Cat. No. HSC.RNAI.N022126.12.1), protein phosphatase 1 regulatory subunit 12A (PPP1R12A, Cat. No. HSC.RNAI.N002480.12.1), dual specificity phosphatase and pro isomerase domain containing 1 (DUPD1, Cat. No. HSC.RNAI.N001003892.12.1), and negative control scrambled siRNA (Cat. No. DS NC1) were ordered from IDT (Coralville, IA). The 6-Carboxyfluorescein (FAM) labeled scrambled siRNA was purchased from IDT. Primers for CD44 (forward: GCTTCAATGCTTCAGCTCCAC; reverse: TTTCTGGACATAGCGGGTGC), CDC20 (forward: CGCTATATCCCCCATCGCAG; reverse: GATGTTCCTTCTTGGTGGGC), PPP1R7 (forward: GAAAGGGGAAGAGCAGCCAA; reverse: CGCCTGTCAACCTCC ATCA), PTPN1 (forward: AGAGACGTCAGTCCCTTTGAC; reverse: ACTCCTTTGG GCTTCTTCCATT), PTPN22 (forward: GGGAAAGAAAAAGTGTGAGCG; reverse: CACAGGATACAGAGAAAGGGC), LHPP (forward: CCGTCATGATTGGGGACGA; reverse: CTCGTCACTGGGCCTGAAC), PPP1R12A (forward: CAACAAAGTGGGCC AAACAG; reverse: CCCGTTTTTCACTATGGAGCAG), DUPD1 (forward: AAGCGAC GACCACAGTAAGA; reverse: GTGGATCATCAGGTAGGCCAG), and Glyceral-dehyde 3-phosphate dehydrogenase (GAPDH; forward: TCACTGTTCTCT CCCTCCGC; reverse: TACGACCAAATCCGTTGACTCC) were supplied by IDT. PE Mouse Anti-Human CD44 (Clone 515) and PE Mouse Anti-Human IgG (Clone G18-145) antibodies were purchased from BD Pharmingen (Franklin Lakes, NJ).

4.2.2 Cell culture

The triple-negative breast cancer MDA-MB-231 cells were cultured in DMEM medium with 10% fetal bovine serum (FBS), 100 U/mL penicillin and 100 μg/mL streptomycin. Another triple-negative breast cancer SUM149PT cells, and estrogen/progesterone-positive MCF7 cells were cultured in DMEM/F12 medium with 10% fetal bovine serum (FBS), 100 U/mL penicillin and 100 μg/mL streptomycin. All cells were maintained in a humidified atmosphere at 37 °C and 95/5% air/CO_2. MDA-MB-231 and MCF7 cells were a generous gift from Dr. Judith Hugh, Department of Laboratory Medicine & Pathology, University of Alberta, while SUM149PT cells was a gift from Dr. Afsaneh Lavasanifar, Faculty of Pharmacy and Pharmaceutical Sciences, University of Alberta. All cells were authenticated by STR DNA profiling analysis.

4.2.3 Preparation of siRNA/polymer complexes

The siRNA/polymer complexes were prepared in two different ways **(Fig 4.1)**: 1) HA Additive: HA was first added to siRNA at pre-specified concentrations followed by addition of the required volume of 150 mM NaCl. PEI-LA was then added to the siRNA/HA solution to allow a final complexation process for 30 min. 2) HA Coating: the siRNA/PEI-LA complexes in 150mM NaCl were prepared first by adding PEI-LA to siRNA with 30 min of incubation. Once siRNA/PEI-LA complexes were formed, HA was added to coat the complexes for 30 min.

4.2.4 Size and ζ-potential of siRNA/polymer complexes

To characterize the siRNA/polymer complexes based on different amounts of HA in the complexation process, the hydrodynamic diameter (Z-average) and surface charge (ζ-potential) of these complexes were determined in ddH_2O through dynamic light

scattering (DLS) and electrophoretic light scattering (ELS) using Zetasizer Nano ZS (Malvern, UK), respectively. The complexes were prepared as described above with HA additive and coating using 0.6 µg of scrambled siRNA at 1:6 siRNA:PEI-LA w/w ratio, and 1:0, 1:0.05, 1:0.5, 1:1, 1:4 and 1:8 siRNA:HA w/w ratios. The complexes were diluted to 1 mL ddH_2O before each measurement.

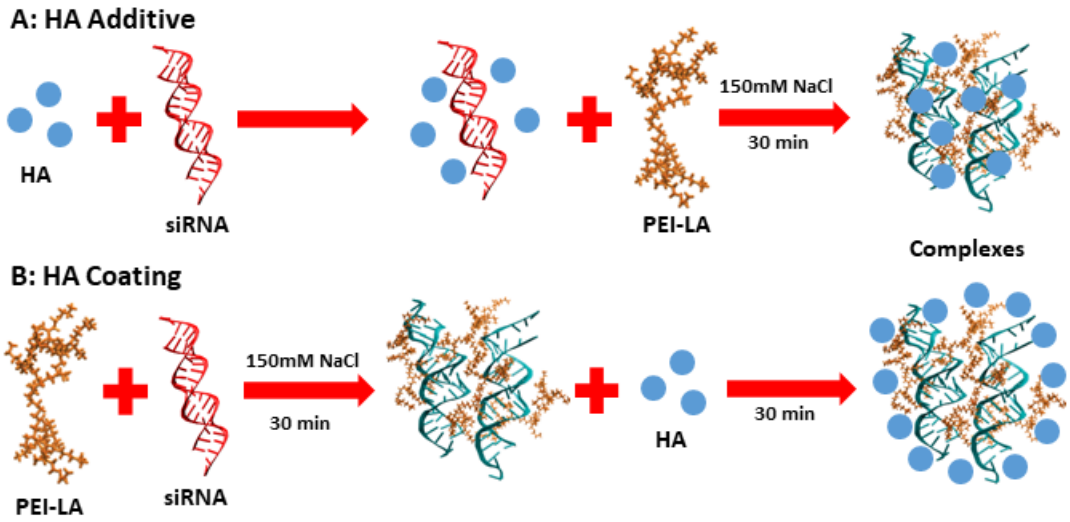

Fig 4.1: Schematic representation of the formulated siRNA/polymer complexes.

The complexes were prepared by two methods. **(A)** HA Additive: siRNA was first mixed with HA followed by the addition of PEI-LA in the presence of 150 mM NaCl with 30 min of incubation to form complexes. **(B)** HA Coating: The complexes of siRNA/PEI-LA were first prepared in the presence of 150 mM NaCl with 30 min of incubation followed by the coating of HA for 30 min to siRNA/PEI-LA complexes.

4.2.5 siRNA uptake by flow cytometry and confocal microscopy

To determine siRNA delivery efficiency of complexes made with different amounts of HA, MDA-MB-231 cells were transfected with FAM-labeled siRNA at 40 nM with 1:6 siRNA:PEI-LA w/w ratio, and 1:0, 1:0.05, 1:0.5, 1:1, 1:4 and 1:8 siRNA:HA w/w ratios. As a negative control, non-labeled scrambled siRNA was used to make complexes at 1:6:1

siRNA:PEI-LA:HA w/w/w ratio. Cells were treated with complexes prepared as HA additive and coating, and were trypsinized after 24 hrs of siRNA transfection. Cell were fixed with 3.7% formaldehyde after washing with HBSS. The uptake of siRNA was quantified using BD LSRFortessa™ cell analyzer (Becton Dickinson, Franklin Lakes, NJ). The mean fluorescence of the recovered cell population and the percentage of cells showing FAM-fluorescence were determined after gating of the cell population as such that auto-fluorescence of non-treated cells represented ~1% of the total cell population.

To further investigate qualitative uptake of siRNA, MDA-MB-231 were grown on glass cover slips (Thermo Fisher Scientific) for 24 hrs and transfected by FAM-labeled scrambled siRNA complexes at 40 nM with 1:6:0, 1:6:0.05, 1:6:1 and 1:6:8 siRNA:PEI-LA:HA w/w/w ratios. As a negative control, non-labeled scrambled siRNA was used to make complexes at 1:6:1 siRNA:PEI-LA:HA w/w/w ratio. After 24 hrs, cells were washed with HBSS, fixed with 4% paraformaldehyde for 20 min at 37°C and mounted on a slide using in-house prepared mounting medium (poly vinyl alcohol in glycerol) with 4',6-diamidino-2-phenylindole (DAPI, Life Technologies) to stain nuclei and wheat germ agglutinin, Texas Red conjugate (Invitrogen) to stain the cytoplasmic membrane. Prepared slides were studied using 40x 1.3 oil plan-Apochromat lens in a Laser Scanning Confocal Microscope (LSM710, Carl Zeiss AG, Oberkochen, Germany), and using ZEN 2011 software.

To determine the retention period of siRNA in the cell, a time-course study was performed using confocal microscopy. MDA-MB-231 cells were transfected by FAM-labeled scrambled siRNA at 40 nM with 1:6:0 and 1:6:1 siRNA:PEI-LA:HA w/w/w ratios, and slides for confocal microscopy were prepared as mentioned above after 4, 24, 48 and

72 hrs of transfection. The number of siRNA-polymer complexes per cell was determined by Imaris software (Bitplane, Belfast, UK).

4.2.6 siRNA uptake after CD44 silencing

To determine the role of CD44 in the uptake of HA-formulated complexes, MDA-MB-231 was transfected with 60 nM CD44 siRNA at 1:6:1 siRNA:PEI-LA:HA w/w/w ratio. After 72 hrs, cells were exposed to FAM-labeled siRNA with 40 nM at 1:6:0 and 1:6:1 siRNA:PEI-LA:HA w/w/w ratio prepared as HA additive and coated complexes. The uptake of FAM-labeled siRNA was determined as described above using a BD Accuri™ C6 Plus Flow Cytometer (BD Biosciences, Franklin Lakes, NJ) after 4 hrs.

To determine the silencing efficiency of CD44 siRNA at the protein level, MDA-MB-231 cells were transfected with 60 nM CD44 siRNA at 1:6:0 and 1:6:1 siRNA:PEI-LA:HA w/w/w ratios. After 72 hrs, cells were washed with HBSS and incubated with PE-labeled anti-human control IgG and anti-human CD44 antibodies for 1 hr at room temperature. Cells were trypsinized and fixed with 3.7% formaldehyde. The surface binding of control IgG and CD44 antibodies were then quantified using BD Accuri™ C6 Plus Flow Cytometer (BD Biosciences).

The silencing efficiency of CD44 specific siRNA at the transcript level was determined by the Reverse Transcription – quantitative PCR (RT-qPCR). MDA-MB-231 cells were transfected with 60 nM CD44 siRNA at 1:6:0 and 1:6:1 siRNA:PEI-LA:HA w/w/w ratios. After 48 hrs, RT-qPCR was performed as described in RT-qPCR section below (Section 2.11).

4.2.7 Comparison of CD44 levels and siRNA uptake among MDA-MB-231, SUM149PT and MCF7 cells

CD44 surface protein and transcripts levels in the cells were determined by immunostaining and RT-qPCR, respectively. MDA-MB-231, SUM149PT and MCF7 cells were stained with PE-labeled anti-human control IgG and anti-human CD44 antibodies for 1 hr at room temperature, and surface binding of antibodies were then quantified as described above (Section 2.6). To determine the levels of CD44 transcripts, total mRNA was isolated from MDA-MB-231, SUM149PT and MCF7 cells, and RT-qPCR was performed as described in section below.

To compare the relative uptake of siRNA by MDA-MB-231 to other cell types, SUM149PT and MCF7 cells were treated with 40 nM FAM-labeled siRNA at 1:6:0 and 1:6:1 siRNA:PEI-LA:HA w/w/w ratio prepared as HA additive and coated complexes. After 24 hrs of siRNA treatment, the uptake of FAM-labeled siRNA was determined as described above using a BD Accuri™ C6 Plus Flow Cytometer (BD Biosciences).

4.2.8 Functional evaluation of different siRNA:HA ratios in siRNA/polymer complexes

Various amounts of HA ranging from 1:0 to 1:12 siRNA:HA w/w ratio was used to make HA additive and coating complexes at 20 nM siRNA with 1:6 siRNA:PEI-LA w/w ratio. Scrambled siRNA was used as a negative control. To evaluate a functional efficacy of siRNA/polymer complexes, MDA-MB-231 cells were treated with CDC20 siRNA and the inhibition of cell growth was determined by MTT assay. The complexes were prepared as described above for HA additive and coating and added to cells. After 72 hrs of treatment, MTT was added to the cells at 1 mg/mL final concentration in HBSS. The cells were incubated for 1 hr at 37 °C and 5% CO_2. During this incubation, soluble MTT is transformed into insoluble formazan crystals due to the activity of mitochondrial

dehydrogenase enzymes, giving a measure of cellular activity [28]. DMSO was added to the well to dissolve the formazan crystals formed because of cellular activity of live cells. The optical density (OD) was measured at 570 nm and the ODs were summarized as a percentage of cell growth based on non-treated cells (taken as 100% cell growth).

4.2.9 Screening of phosphatase proteins

Silencer® Human Phosphatase siRNA Library V3 (Ambion) was used to screen 267 phosphatase proteins to determine the potential phosphatase proteins that can decrease the migration of metastatic breast cancer cells. The siRNAs against each phosphatase was a pool of three siRNAs targeting different locations of the phosphatase mRNA. To assess the efficacy of phosphatase siRNAs, MDA-MB-231 cells were cultured in 96-well plate and transfected with 40 nM of each phosphatase siRNA at 1:6 siRNA:PEI-LA w/w ratio without HA. After 72 hrs of siRNA treatment, inhibition of cell growth was assessed by MTT assay as described above.

To identify potential phosphatase targets that could reduce the migration of MDA-MB-231 cells, a scratch assay [29] was performed for the entire library of phosphatase proteins. Cells were cultured in 96-well plates and transfected with 40 nM of each phosphatase siRNA at 1:6 siRNA:PEI-LA w/w ratio without HA. After 48 hrs of siRNA treatment, a scratch was made in each well using P-200 pipette tips. The cells were allowed to migrate for 24 hrs, and were then stained by coomassie brilliant blue R-250 (Thermo Fisher Scientific). The plates were scanned and grayscale values for each well was determined by ImageJ software [30]. CDC20 siRNA was also used as a control in the library screen, while doxorubicin (5 μg/ml) was used as a positive control as it can not only

decrease the growth of breast cancer cells, but also inhibit migration of cells. The migration of cells and percent of control for the migrated cells was calculated as follows:

$$\boldsymbol{Migration\ of\ cells} = \frac{(\mathrm{A0} - \mathrm{A})}{(\mathrm{A0} - \mathrm{A}\infty)}$$

Where, A_0: Grayscale value at 0 hr

A: Grayscale value after 24 hr of migration

A_∞: Grayscale value of non-migrated cells in a well

$$\boldsymbol{Percent\ of\ Control\ (POC)} = \frac{\text{Migration of cells (Phosphatase siRNA)}}{\text{Migration of cells (Control siRNA)}}\ \%$$

4.2.10 Validation of identified targets

The potential phosphatase targets were identified based on an initial screen of siRNAs against phosphatase proteins. For validation, individual siRNAs against these phosphatase proteins were obtained from IDT, and MTT and scratch assays were performed to determine the inhibition of MDA-MB-231 cell growth and migration, respectively. The siRNAs against CDC20, PPP1R7, PTPN1, PTPN22, LHPP, PPP1R12A and DUPD1 were delivered to MDA-MB-231 cells at 20, 40 and 60 nM concentrations with 1:3 and 1:6 siRNA:PEI-LA w/w ratios. Scrambled siRNA and doxorubicin (2 µg/ml) were also used in the validation study as negative and positive controls, respectively. To determine the migration of cell, scratch was made in each well using P-200 pipette tips after 48 hrs of siRNA treatment and a picture of each well was taken by FSX100 Microscope (Olympus, Tokyo, Japan), which was considered as 0 hr migration. The cells were allowed to migrate for 24 hrs, and pictures of each well were taken again. The migration of cells in each of the 0 hr and 24 hr pictures was calculated by determining the

scratch area by TScratch software [31]. The migration of cells and percent of control for the migrated cells was calculated as follows:

$$\boldsymbol{Migration\ of\ cells} = \frac{(\text{Migration at 0 hr})}{(\text{Migration at 0 hr} - \text{Migration at 24 hrs})}$$

$$\boldsymbol{Percent\ of\ Control\ (POC)} = \frac{\text{Migration of cells (Phosphatase siRNA)}}{\text{Migration of cells (Control siRNA)}}\ \%$$

4.2.11 Transwell migration assay

MDA-MB-231 cells were cultured on 6-well plates, 24 hrs prior to the siRNA treatment. The siRNA/PEI-LA complexes at 40 nM siRNA with 1:6 ratio without HA were then added to the cells and incubated at 37 °C for 48 hrs. The cells were then washed gently with HBSS to remove the serum content and trypsinized. Cells were resuspended in serum-free medium and 1.5×10^5 cells were added to transwell inserts. The lower chamber of the wells containing the inserts was filled with medium containing 20% serum as a chemoattractant. Scrambled siRNA-treated cells were added to the inserts that contained serum as well as serum-free media in the lower bottom well, which served as negative and positive controls, respectively. Doxorubicin-treated cells (5 µg/ml) were also used in this study as a therapeutic positive control. Cells were allowed to migrate from the upper chamber to the bottom surface of the insert for 24 hrs. Cells present on the upper surface of the inserts (non-migrated cells) were removed gently using a cotton swab. The inserts were then fixed with 3.7% formaldehyde for 20 min and stained with 0.1% crystal violet for 1 h. The inserts were washed with HBSS before imaging under FSX100 Microscope (Olympus). The dye was subsequently solubilized with 10% acetic acid, and the optical density (OD) was measured at 570 nm using the EL_x800 Universal Microplate reader (Bio-Tek Instruments, Winooski, VT). The ODs were summarized as a percentage of cell

migration based on non-treated cells with serum in the lower bottom well (taken as 100% cell migration).

4.2.12 Reverse transcription – quantitative PCR (RT-qPCR)

MDA-MB-231 cells were transfected by combinational CDC20/phosphatase siRNAs at total 40 nM (20 nM CDC20 siRNA + 20 nM phosphatase siRNA) as well as individual CDC20 and phosphatase siRNAs (20 nM individual siRNA + 20 nM scrambled siRNA) with 1:6:1 siRNA:PEI-LA:HA w/w/w ratio. After 24 hrs of siRNA treatment, total RNA was isolated from cells using TRIzol reagent (Invitrogen, Carlsbad, CA). One microgram of total RNA was converted into cDNA using M-MLV reverse transcriptase (Invitrogen) according to manufacturer's instruction. StepOne Real-Time PCR System (Applied Biosystems, Foster City, CA) was employed to perform quantitative PCR (qPCR) with 15 ng of cDNA from each sample and a SYBR Green qPCR Mastermix (Molecular Biology Service Unit, Department of Biological Sciences, University of Alberta, Edmonton, AB) based on the manufacturer recommendations. Primers were designed using NCBI Primer-BLAST (http://www.ncbi.nlm.nih.gov/tools/primer-blast/). GAPDH was used as a reference gene in RT-qPCR and template cDNA was omitted from qPCR reaction as a negative control. The qPCR results were analyzed using $2^{-\Delta\Delta C_T}$ method and presented as relative quantity of transcripts [32]. The qPCR conditions comprised an initial denaturation step for 10 min at 95.0 ºC, followed by 40 cycles at 95.0 ºC for 15 s (denaturation), and annealing and elongation at 60 ºC for 1 min.

4.2.13 Combinational siRNA therapy

Combinational siRNA delivery was performed in MDA-MB-231 using CDC20 and phosphatase siRNAs at total 40 nM (20 nM each) siRNA concentration with 1:3:1 and

1:6:1 siRNA:PEI-LA:HA w/w/w ratios. Individual CDC20 or phosphatase siRNA at total 40 nM concentration (20 nM individual siRNA + 20 nM scrambled siRNA) with 1:3:1 and 1:6:1 siRNA:PEI-LA:HA w/w/w ratios was delivered in MDA-MB-231 cells as well. To determine the efficacy of combinational siRNA therapy to inhibit cell growth and migration, MTT and scratch assays were performed as described above, respectively. Scrambled siRNA and doxorubicin (5 μg/ml) were used as negative and positive controls for inhibition of cell growth as well as migration, respectively.

4.2.14 Statistical analysis

All results were presented as mean ± standard deviation. Results were analyzed by one-way ANOVA with tukey's multiple comparison post-hoc test, where an asterisk (*) indicated significantly different groups in figures. The significance ($p < 0.05$) was typically determined by comparing specific siRNA-treated groups to that of scrambled siRNA-treated group.

4.3 Results

4.3.1 Characterization of siRNA/polymer complexes with HA incorporation

We have previously shown effective silencing of aberrant proteins by delivering specific siRNAs by using PEI-LA as a single carrier [17,33]. The PEI-LA used in this study was derived from 1.2 kDa PEI and substituted with linoleic acid to give 2.6 LA per PEI. Here, we additionally introduced HA into the siRNA/polymer complexes to better facilitate the delivery of siRNA. We made siRNA/polymer complexes in two ways **(Fig 4.1)** using HA as an additive and a coating. The complexes were characterized for hydrodynamic diameter (Z-average) and surface charge (ζ-potential). The size of siRNA/PEI-LA complexes without HA was ~200 nm, and it was reduced to ~100 nm as soon as a small

amount of HA (1:0.05 siRNA:HA) was added to the complexes **(Fig 4.2A)**. The size of complexes increased gradually in HA additive from 1:0.05 to 1:4 siRNA:HA ratios, reaching ~180 nm, but excess HA reduced the complex size to ~130 nm at the 1:8 siRNA:HA ratio. In contrast to HA additive complexes, the sizes of HA-coated complexes remained at ~125 nm for all HA ratios used in the complexation process.

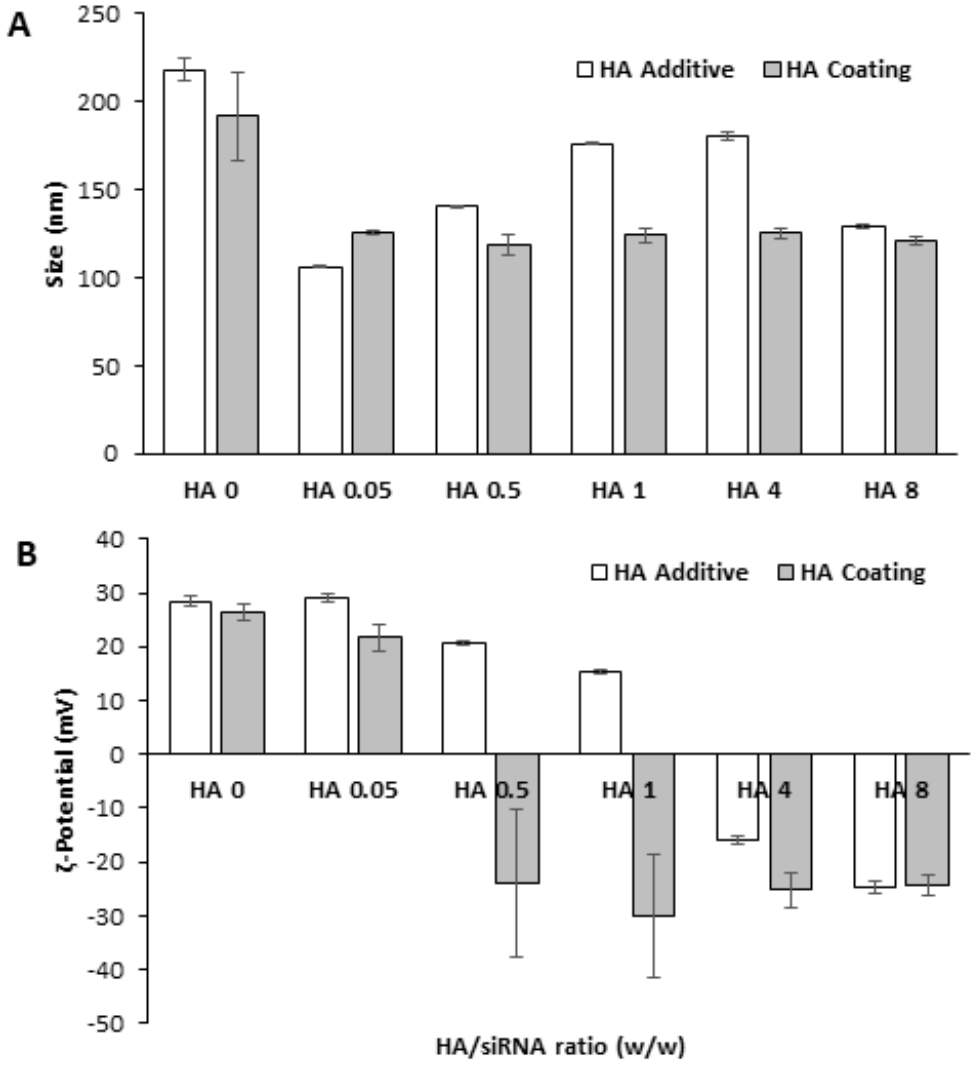

Fig 4.2: Size and ζ-potential of siRNA/polymer complexes.

Size **(A)** and surface charge **(B)** of the complexes were determined for siRNA:PEI-LA (1:6 w/w ratio) complexes with various amounts of HA added to the complexes as additive and coating. The siRNA:HA ratios were 1:0, 1:0.05, 1:0.5, 1:1, 1:4 and 1:8 for the complexes.

The ζ-potential of the complexes was +28 mV in the absence of HA, which decreased gradually as the amount of HA was increased in both approaches **(Fig 4.2B)**. The ζ-potential was still in the positive range up to siRNA:HA ratio of 1:1 (+15 mV) for HA additive complexes, and it turned negative at higher HA ratios. In HA coated complexes, ζ-potential decreased from +28 to +21 mV when a small amount of HA was added (1:0.05 siRNA:HA ratio), after which it was reduced to -25 mV for all other HA coatings.

To determine the stability of siRNA in complexes, the complexes were incubated in culture medium for 0, 4 and 24 hrs at 37 ºC, and uptake of siRNA was determined by flow cytometry. As expected, the mean siRNA uptake decreased dramatically after 4 and 24 hrs of incubation in culture medium compared to fresh complexes **(Fig 4.S1)**, which was due to decreased fluorescence of the FAM-labeled siRNA while incubating at 37 ºC (data not shown). However, the siRNA positive population clearly showed that the more cells were transfected with HA-modified complexes compared to without HA complexes at both 4 and 24 hrs of complexes incubation in culture medium.

4.3.2 Uptake of siRNA/PEI-LA/HA complexes

The uptake of siRNA was determined by flow cytometry for siRNA/polymer complexes with different amounts of HA. The siRNA:PEI-LA complexes without HA was able to deliver siRNA successfully. However, mean fluorescence was markedly less compared to complexes having HA, where ~80% of the cell population was transfected by the complexes **(Fig 4.3A)**. HA additive and coating protocols exhibited a similar pattern of uptake; when a small amount of HA was introduced to complexes (1:0.05 siRNA:HA), the uptake of siRNA was 5 and 2 fold higher for HA additive and coating, respectively,

compared to complexes without HA. Uptake was increased with the addition of more HA to a maximum with the 1:1 siRNA:HA ratio. The uptake of siRNA gradually decreased with higher amounts of HA in the complexes. The cell population positive for siRNA was ~95% for the optimal siRNA/PEI-LA/HA complexes, while a lower percentage was noted in the complexes without HA. No autofluorescence of the complexes was detected as the mean fluorescence of non-treated and non-labeled scrambled siRNA-treated cells was similar.

To further investigate the uptake of siRNA, confocal microscopy was performed for HA additive **(Fig 4.3B)** and HA coated complexes **(Fig 4.3C)**. As expected, no autofluorescence was observed for non-treated cells and non-labeled scrambled siRNA-treated cells **(Fig 4.3Bi** and **Fig 4.3Ci)**. For siRNA/polymer complexes without HA, uptake of FAM-labeled siRNA was quite low compared to complexes with HA **(Fig 4.3Bii** and **Fig 4.3Cii)**. With a small amount of HA in complexes (1:0.05 ratio of siRNA:HA), the transfection of siRNA has increased dramatically **(Fig 4.3Biii** and **Fig 4.3Ciii)**. Confirming the flow cytometry data, the highest uptake was detected with 1:1 ratio of siRNA:HA **(Fig 4.3Biv** and **Fig 4.3Civ)**, with uptake decreasing significantly with 1:8 ratio of siRNA:HA **(Fig 4.3Bv** and **Fig 4.3Cv)**.

The transfection efficiency of siRNA/polymer complexes was also determined by confocal microscopy over 72 hrs of post-transfection. The number of complexes inside cells without HA **(Fig 4.S2A)** and with HA additive **(Fig 4.S2B)** was quantitated **(Fig 4.S2C)**. Some heterogeneity among the cell population was evident, but average number of particles/cell was higher when HA was added into complexes compared to without HA

at all time-points. However, no statistical difference between HA additive and without HA complexes was observed due to heterogeneity of complexes among the cell population.

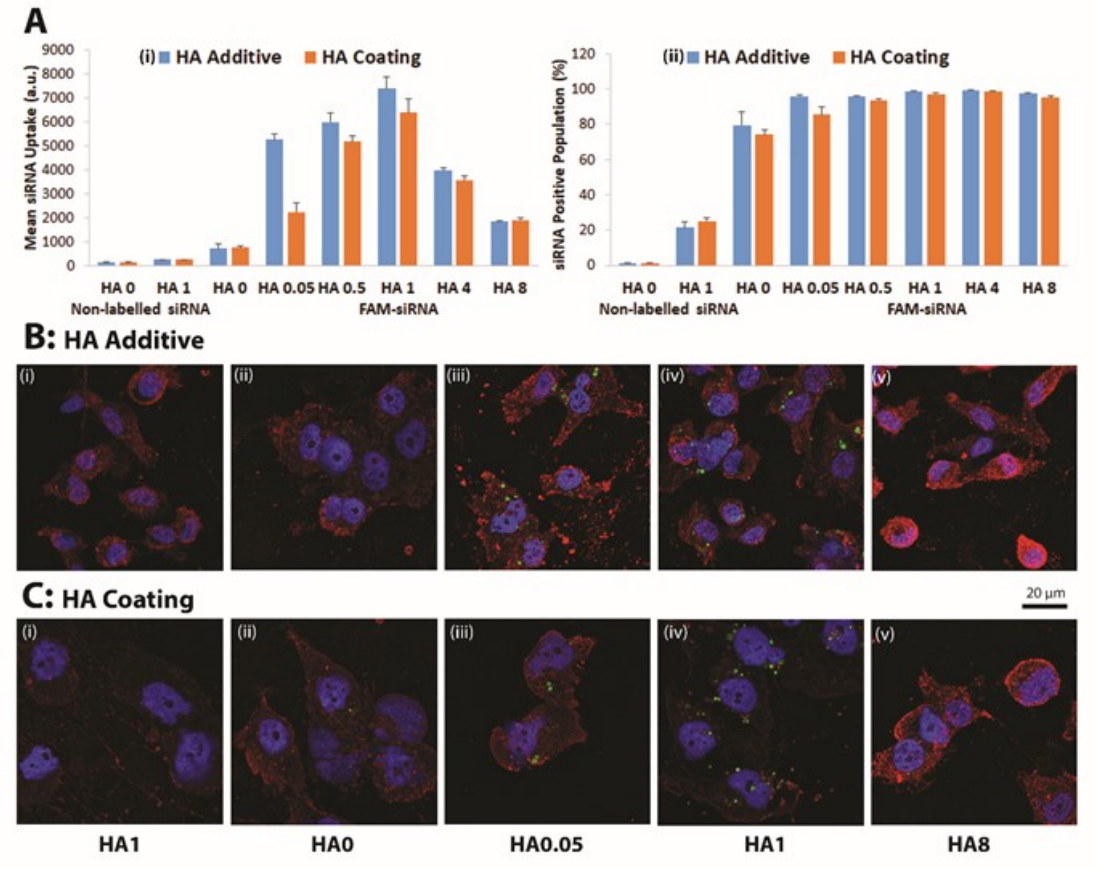

Fig 4.3: Cellular uptake of siRNA/polymer complexes after 24 hr of transfection.

(A) Uptake of FAM-labeled siRNA by flow cytometry was determined using 40 nM siRNA at 1:6 siRNA:PEI-LA w/w ratio with various amounts of HA. The mean fluorescence **(i)** and siRNA positive cell population **(ii)** were calculated for siRNA:HA w/w ratios 1:0, 1:0.05, 1:0.5, 1:1, 1:4 and 1:8. As a negative controls, non-labeled siRNA was delivered to MDA-MB-231 cells with 1:6:0 and 1:6:1 siRNA:PEI-LA:HA w/w/w ratios. **(B)** Uptake of FAM-labeled siRNA by confocal microscopy was determined for HA additive complexes. Non-labeled siRNA was transfected at 1:6:1 siRNA:PEI-LA:HA w/w/w ratio **(i)** as a negative control. Uptake of FAM-labeled siRNA was determined at 1:6:0 **(ii)**, 1:6:0.05 **(iii)**, 1:6:1 **(iv)** and 1:6:8 **(v)** siRNA:PEI-LA:HA w/w/w ratios. **(C)** Cellular uptake of siRNA by confocal microscopy for HA coating with similar groups as in HA additive. Purple, red and green colors represent nuclei, cytoplasm and FAM-labeled siRNA complexes, respectively.

4.3.3 Role of CD44 in uptake of HA-modified complexes

To assess the role of CD44 in the uptake of HA-modified complexes, CD44 was silenced with the specific siRNA, followed by uptake of FAM-labeled siRNA. No effect of CD44 silencing on siRNA uptake was observed for complexes without HA (1:6:0 siRNA:PEI-LA:HA ratio). A significant difference in uptake was found between CD44 siRNA-treated and scrambled siRNA-treated/non-treated cells with both HA additive and coated complexes **(Fig 4.4A)**. Approximately 15% and 30% of decrease in siRNA uptake was observed for HA additive and coated complexes, respectively.

To determine the efficiency of silencing by the CD44 siRNA, CD44 protein and mRNA levels were determined by CD44 antibody staining and RT-qPCR, respectively. The siRNA complexes were formulated with/without HA as well to investigate the influence of HA on silencing efficiency. A significant reduction in the surface CD44 protein was observed with HA additive and coated complexes compared to scrambled siRNA complexes **(Fig 4.4B)**. No reduction in surface CD44 protein was found when complexes were delivered without HA (1:6:0 siRNA:PEI-LA:HA ratio). CD44 transcripts were significantly reduced when CD44 siRNA was delivered with/without HA modified complexes **(Fig 4.4C)**.

To compare siRNA uptake between high CD44 expressing and low CD44 expressing cells, the siRNA uptake in MDA-MB-231, SUM149PT and MCF7 cells were determined using FAM-labeled siRNA. MDA-MB-231 is known to be high CD44 expressing cells, while MCF7 is low CD44 expressing cells [34]. The levels of CD44 surface proteins, as determined by immunostaining **(Fig 4.5A),** clearly suggested overexpression of CD44 in MDA-MB-231 cells, while low-expression of CD44 in MCF7

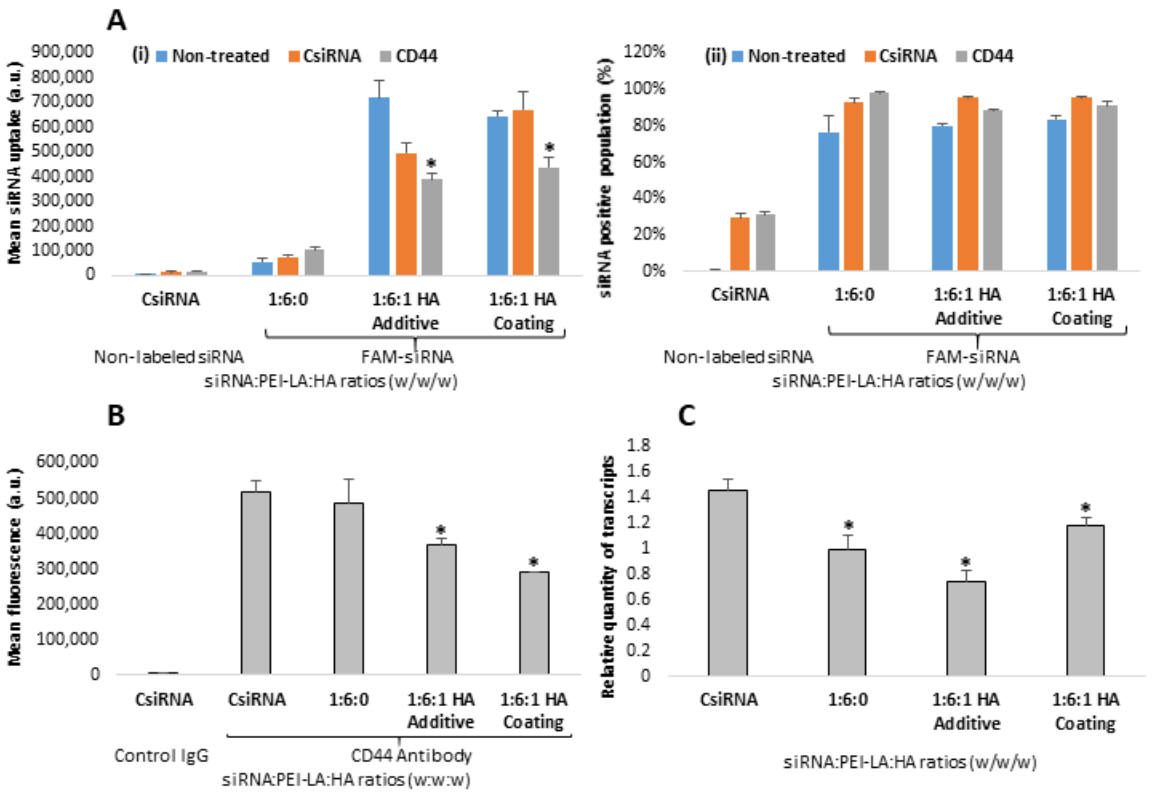

Fig 4.4: Cellular uptake of siRNA/polymer complexes after CD44 silencing.

(A) MDA-MB-231 cells were transfected with 60 nM of CD44 siRNA at 1:6:1 siRNA:PEI-LA:HA w/w/w ratio. After 72 hrs of CD44 siRNA treatment, FAM-labeled siRNA was added to the cells for 4 hrs at 1:6:0 and 1:6:1 siRNA:PEI-LA:HA w/w/w ratios with HA additive and coated complexes, followed by siRNA uptake analysis by flow cytometry. **(B)** CD44 silencing at surface protein levels determined by immunostaining. MDA-MB-231 cells were transfected with 60 nM of CD44 siRNA at 1:6:0 and 1:6:1 siRNA:PEI-LA:HA w/w/w ratios. After 72 hrs of CD44 siRNA treatment, cells were stained with PE-labeled anti-human CD44 antibody for 1 hr followed by flow cytometry. PE-labeled anti-human IgG was used as a negative control antibody. **(C)** CD44 silencing was confirmed by RT-qPCR with 60 nM siRNA at 1:6:0 and 1:6:1 siRNA:PEI-LA:HA w/w/w ratios. Scrambled siRNA (CsiRNA) was used as a negative control. The asterisks represent the significant reduction in cellular uptake of siRNA or CD44 surface protein or CD44 transcripts compared to CsiRNA ($p < 0.05$).

and SUM149PT cells. A similar result was obtained when CD44 mRNA levels were analyzed by RT-qPCR **(Fig 4.5B)**. No significant siRNA uptake difference was observed

among different cells when complexes were delivered without HA **(Fig 4.5C)**. However, approximately 20-30% siRNA uptake difference was evident between the CD44-overexpressing MDA-MB-231 cells and two others low CD44-expressing SUM149PT and MCF7 cells. Compared to complexes without HA, however, 3-4 fold increased siRNA uptake with the HA-modified complexes was observed with all cell-lines.

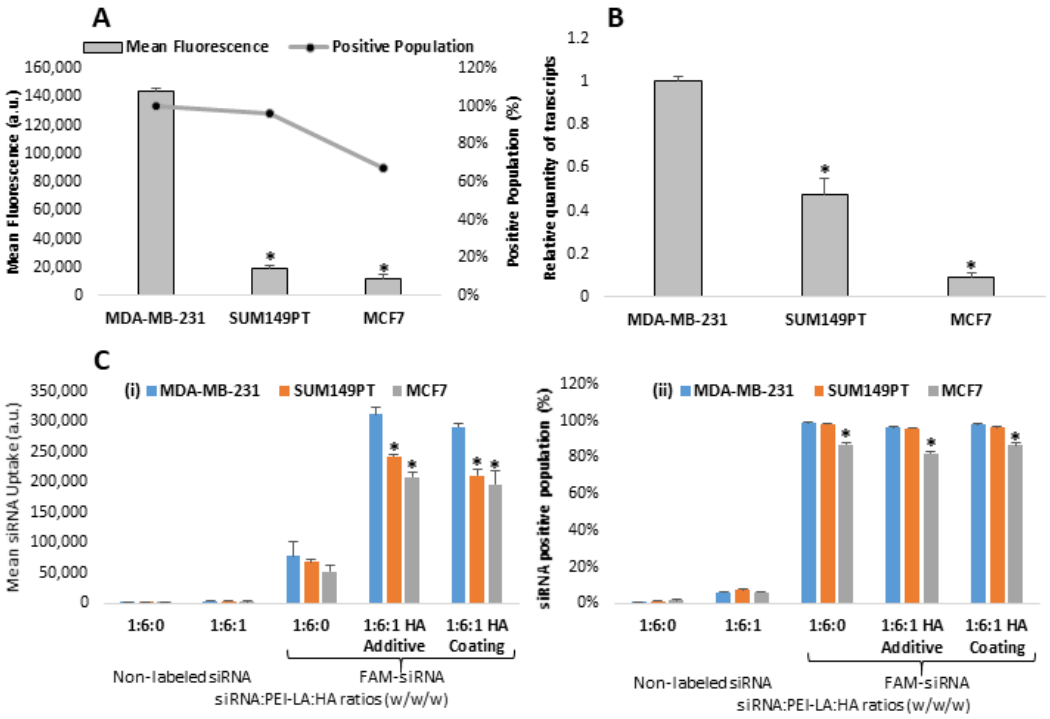

Fig 4.5: The levels of CD44 and cellular uptake of siRNA/polymer complexes.

(A) The levels of CD44 surface protein in MDA-MB-231, SUM149PT and MCF7 cells determined by immunostaining. Cells were stained with PE-labeled anti-human CD44 antibody for 1 hr followed by flow cytometry. PE-labeled anti-human IgG was used as a negative control antibody (not shown). **(B)** The levels of CD44 transcripts determined by RT-qPCR in MDA-MB-231, SUM149PT and MCF7 cells. **(C)** Cellular uptake of siRNA/polymer complexes in MDA-MB-231, SUM149PT and MCF7 cells. Cells were transfected with 40 nM of FAM-labeled siRNA at 1:6:0 and 1:6:1 siRNA:PEI-LA:HA w/w/w ratio. After 24 hrs, siRNA uptake was analyzed by flow cytometry. The asterisks represent the significant decrease in CD44 surface protein or CD44 transcripts or cellular uptake of siRNA in SUM149PT/MCF7 compared to MDA-MB-231 cells ($p < 0.05$).

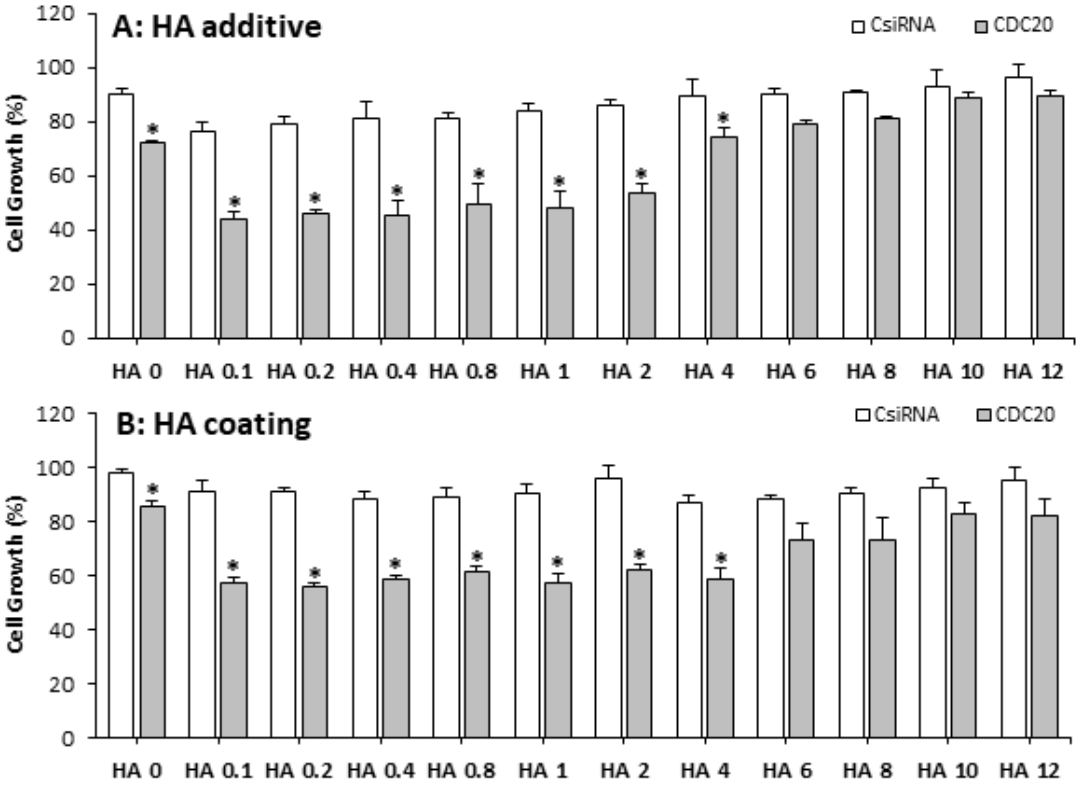

Fig 4.6: Functional evaluation of HA in siRNA/polymer complexes.

The cell growth inhibition by CDC20 siRNA at 20 nM was determined by siRNA/polymer complexes prepared with various amounts of HA, ranging from 1:0.1 to 1:12 siRNA:HA w/w ratios. Complexes were formulated with HA additive **(A)** and HA coating **(B)**. Scrambled siRNA (CsiRNA) was used as a negative control. The asterisks represent the significant cell growth inhibition by CDC20 siRNA compared to CsiRNA ($p < 0.05$).

4.3.4 Cell growth inhibition with CDC20 siRNA/PEI-LA/HA complexes

Functional efficacy of siRNA/PEI-LA/HA complexes was determined by delivering siRNA against CDC20 in MDA-MB-231 cells. CDC20 siRNA was delivered at low concentration of siRNA (20 nM) with various amounts of HA into complexes ranging from 1:0.1 to 1:12 siRNA:HA ratios. Approximately 20% cell growth inhibition was observed when HA was not added to the complexes **(Fig 4.6A** and **4.6B)**. However, the efficacy of siRNA was increased to ~40% cell growth inhibition when a small amount of

HA (1:0.1 siRNA:HA ratio) was introduced into the HA additive **(Fig 4.6A)** and HA coated **(Fig 4.6B)** complexes, which remained constant until 1:1 siRNA:HA ratio. The effect of siRNA gradually diminished with increasing amounts of HA. Very little cell growth inhibition (5-10%) was observed at the highest siRNA:HA ratio of 1:12.

4.3.5 Screening of phosphatases to identify targets for cell migration inhibition

A total 267 phosphatase-specific siRNAs were employed to transfect MDA-MB-231 cells using PEI-LA as a delivery carrier, and the efficacy of siRNAs was determined by inhibition of cell growth **(Fig 4.7A)** and migration **(Fig 4.7B)**. CDC20 siRNA was used as a positive control with the library screen, and ~40% cell growth inhibition was observed with this siRNA during the screen. For the inhibition of migration assay, doxorubicin was additionally used as a positive control in the library screen, which inhibited ~60% cell migration. Overall, more than 20% cell growth inhibition was obtained with 73% of phosphatase siRNAs, with CDC20 providing the most effective inhibition **(Fig 4.7A**). Similarly, numerous phosphatase-specific siRNAs inhibited the cellular migration of MDA-MB-231 **(Fig 4.7B)**, again with CDC20 siRNA and doxorubicin acting as the most effective inhibitors. The effectiveness of the latter treatments was presumed to be due to indirect effects of cell proliferation inhibition. The extent of growth inhibition (POC from **Fig 4.7A**) and inhibition of migration (POC from **Fig 4.7B**) for each phosphatase siRNA was correlated in **Fig 4.7C** to identify specific targets that can inhibit migration of MDA-MB-231 cells specifically. Two groups of phosphatase siRNAs were identified accordingly: first group of phosphatases PPP1R7, PTPN22 and PPP1R12A siRNA inhibited cells migration drastically, but failed to inhibit cell growth. A second group of phosphatases PTPN1, LHPP and DUPD1 inhibited both cell migration and growth.

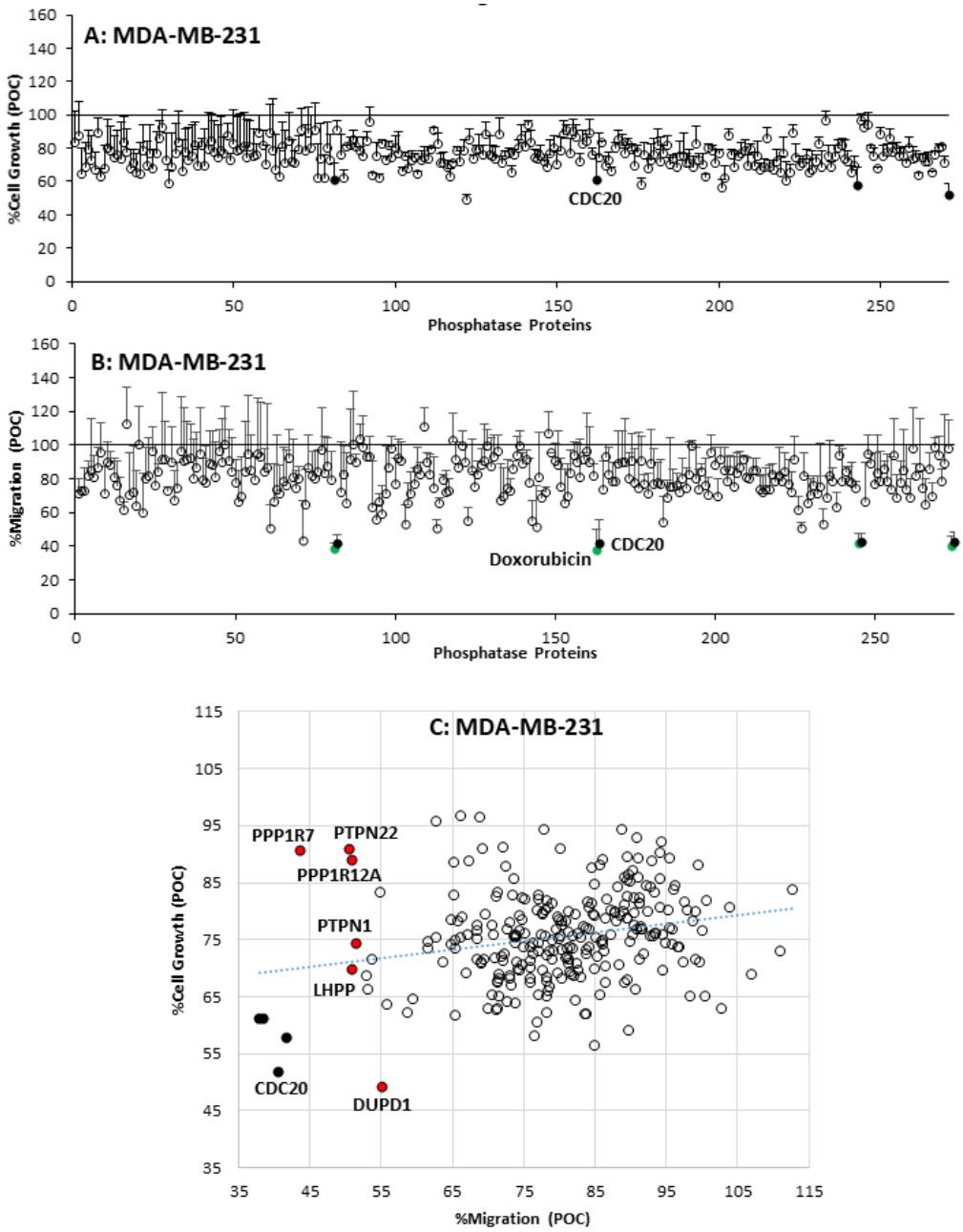

Fig 4.7: Phosphatase siRNA library screening in MDA-MB-231 cells.

(A) Inhibition of cell growth by phosphatase-specific siRNAs at 40 nM with 1:6 siRNA:PEI-LA w/w ratio was determined as percentage of control siRNA-treated cell (POC). Black solid dot represents inhibition of cell growth by CDC20 siRNA delivery. **(B)** Inhibition of cell migration by phosphatase siRNA delivery was determined relative to control siRNA (POC). Green solid dot represents inhibition of cell growth by doxorubicin that was a positive control. **(C)** The correlation between inhibition of cell growth and migration by phosphatase siRNAs to reveal phosphatases that inhibited cell migration drastically (red solid dots).

4.3.6 Validation of identified phosphatase targets

The efficacy of identified phosphatase siRNAs was validated with inhibition of MDA-MB-231 cell growth and migration by delivering individual siRNAs against each phosphatase using PEI-LA as a delivery agent. At 20 nM siRNA, only PTPN1, LHPP and DUPD1 siRNAs inhibited cell migration significantly compared to scrambled siRNA-treated cells **(Fig 4.8A)**. However, no growth inhibition was observed at 20 nM siRNA **(Fig 4.8D)**. MDA-MB-231 cells seemed responsive to all phosphatase siRNAs at 40 nM even though a significant difference in inhibition of cell migration was observed with LHPP and PPP1R12A siRNAs only **(Fig 4.8B)**. Similarly, only CDC20, PPP1R7, LHPP and DUPD1 siRNAs showed significant cell growth inhibition at 40 nM siRNA **(Fig 4.8E)**. The siRNA/PEI-LA complexes were toxic at 60 nM siRNA as ~50% inhibition of cell growth and ~40% inhibition of cell migration was observed with the scrambled siRNA itself. However, the cells showed strong response at higher siRNA concentration as the migration of cells was inhibited completely with CDC20, PTPN1 and PTPN22 siRNAs at 1:3 siRNA:PEI-LA ratios **(Fig 4.8C)**. Cell growth was also decreased significantly with CDC20, PPP1R7, PTPN1, PTPN22, PPP1R12A and DUPD1 siRNAs at higher concentration of siRNA **(Fig 4.8F)**.

To further validate the inhibition of cell migration, Transwell migration assays were performed using phosphatase siRNAs with PEI-LA **(Fig 4.9)**. No inhibition of MDA-MB-231 cell migration was observed with the scrambled siRNA-treated cells. Doxorubicin (5 μg/mL) that was used as a positive control, inhibited ~80% cell migration, while CDC20 siRNA decreased the migration of cells by ~20%. Among all phosphatase siRNAs, PPP1R7, PTPN22 and PPP1R12A siRNAs inhibited the cell migration significantly

compared to scrambled siRNA-treated cells, and PTPN22 inhibited the highest percentage of cell migration (~50%).

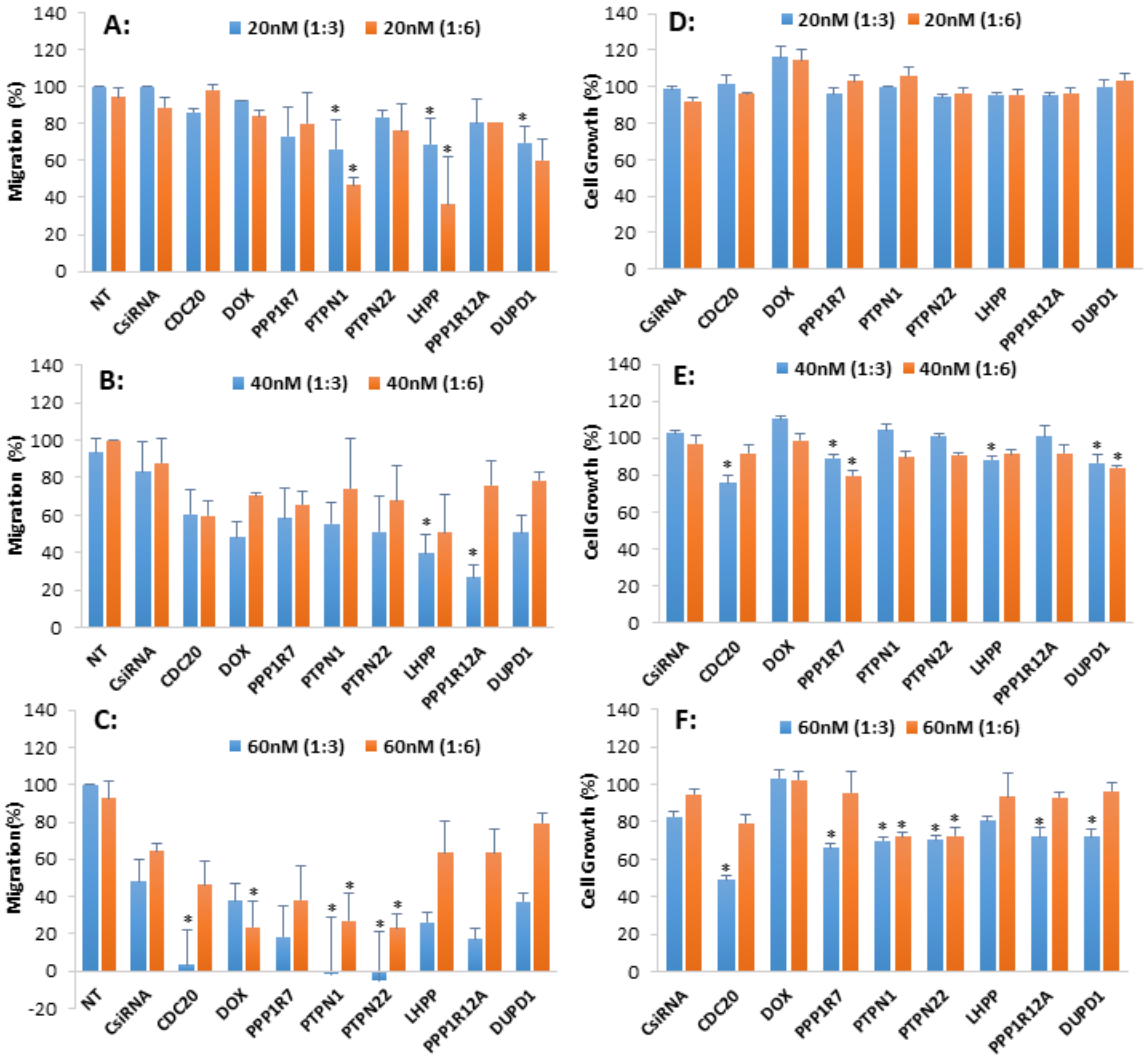

Fig 4.8: Validation of identified phosphatase targets.

Validation of identified phosphatase targets for cell migration **(A, B, C)** and growth **(D, E, F)** inhibitions at 20, 40 and 60 nM siRNA with 1:3 and 1:6 siRNA:PEI-LA w/w ratios. Non-treated cells (NT) and scrambled siRNA-treated cells (CsiRNA) were presented as negative controls, while doxorubicin (DOX) was chosen as a positive control for the validation study. The asterisks represent significant inhibition of cell migration or growth by phosphatase siRNAs compared to CsiRNA ($p < 0.05$).

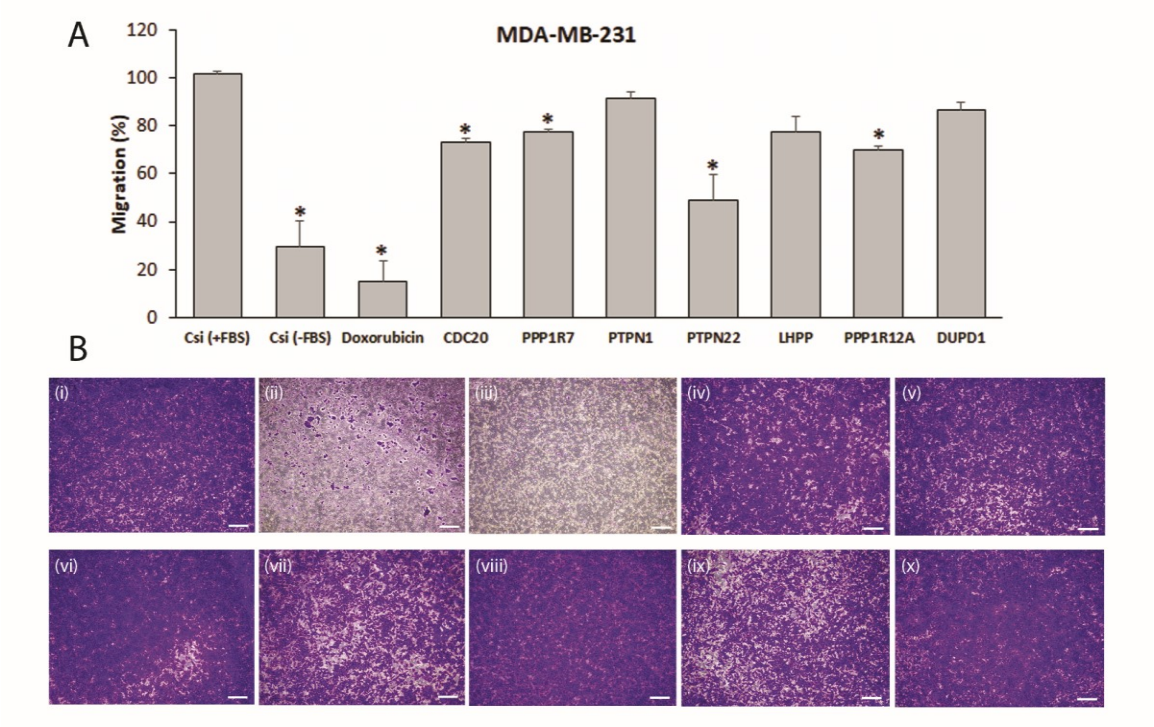

Fig 4.9: Transwell migration assay for MDA-MB-231 cells.

Effects of phosphatase silencing on MDA-MB-231 migration by transwell migration assay at 40 nM siRNA with 1:6 siRNA:PEI-LA w/w ratio. **(A)** Percentage of cell migration was determined based on non-treated cells. Scrambled siRNA-treated cells (CsiRNA) seeded in a well with fetal bovine serum (FBS) was used as a negative control, while incubation without FBS was considered as an additional control for inhibition. Doxorubicin with strong anti-growth activity was also used as a positive control. **(B)** Crystal violate stained migrated cells for scrambled siRNA-treated cells incubated with FBS **(i)**, scrambled siRNA-treated cells without FBS **(ii)**, and for cells treated with doxorubicin **(iii)**, CDC20 **(iv)**, PPP1R7 **(v)**, PTPN1 **(vi)**, PTPN22 **(vii)**, LHPP **(viii)**, PPP1R12A **(ix)** and DUPD1 **(x)** siRNAs. The asterisks represent the significant inhibition of cell migration by phosphatase siRNAs compared to CsiRNA ($p < 0.05$).

4.3.7 Combinational siRNA therapy

Once the identified phosphatase targets were validated, the combinational siRNA delivery of CDC20 and phosphatase siRNAs was performed with HA-formulated complexes. To assess silencing at the mRNA level, the changes in each phosphatase

transcript levels was determined when delivered individually or in combination with CDC20 **(Fig 4.10)**. All phosphatase siRNAs decreased the levels of transcripts significantly compared to scrambled siRNA-treated cells when those were delivered individually or in combination except DUPD1 siRNA. Interestingly, no decrease in the levels of DUPD1 transcripts was observed after siRNA delivery (consistent with a lack of reduction of migration in **Fig 4.9)**, and slight increase in the transcripts levels was found compared to scrambled siRNA-treated transcripts. In contrast, CDC20 siRNA showed the highest amount of inhibition (~80%) of its mRNA among all siRNAs. No change in the efficiency of silencing CDC20 or phosphatase proteins was observed with the combinational siRNA delivery compared to individual siRNA delivery **(Fig 4.10)**.

Finally, the functional evaluation of combinational siRNA delivery was performed for inhibition of cell growth and migration **(Fig 4.11)**. Doxorubicin was used as a positive control and it inhibited the migration as well as growth of MDA-MB-231 cells significantly compared to non-treated cells. The CDC20 siRNA inhibited cell migration and growth (40-60% inhibition) when delivered at 20 or 40 nM concentrations. Individual PPP1R7, PTPN1, LHPP and PPP1R12A siRNAs decreased the migration of cells significantly compared to scrambled siRNA and failed to decrease the cell growth in HA additive complexes **(Fig 4.11A)**. However, all phosphatase siRNAs inhibited cell migration and growth when delivered in combination with CDC20 except DUPD1 that failed to decrease the cell migration **(Fig 4.11A)**. For HA-coated complexes, only PTPN1 siRNA decreased cell migration significantly, while no growth inhibition was found with all phosphatase siRNAs when those were delivered individually **(Fig 4.11B)**. In contrast, cell migration and growth were inhibited significantly in the combinational siRNA delivery of

phosphatase and CDC20 except DUPD1 again **(Fig 4.11B)**. Overall, MDA-MB-231 cells treated with HA additive complexes showed more response compared to HA coated complexes, and both 1:3:1 and 1:6:1 siRNA:PEI-LA:HA ratios have shown similar results.

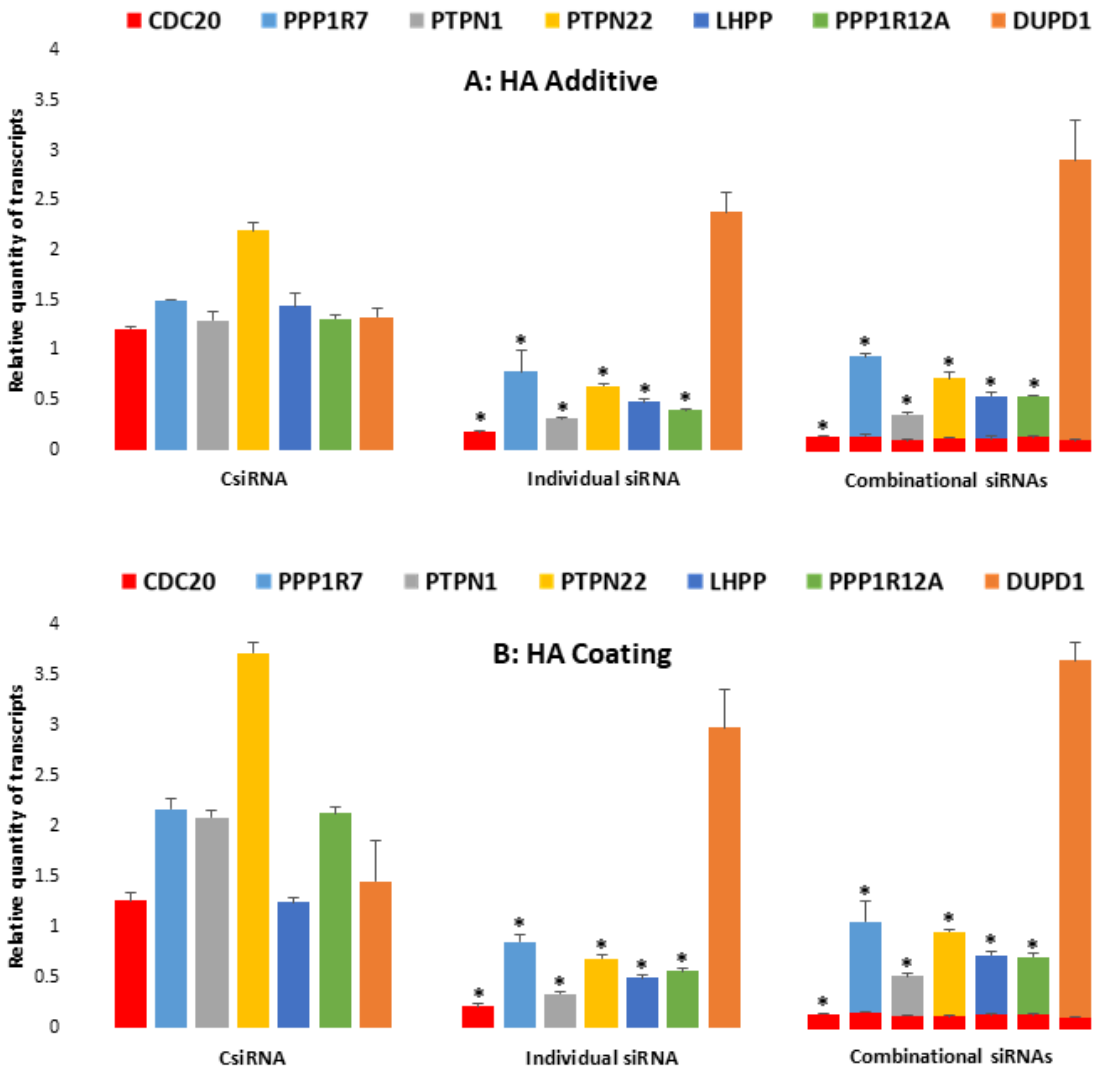

Fig 4.10: RT-qPCR analysis in MDA-MB-231 cells.

RT-qPCR analysis to determine the silencing efficiency of individual and combinational siRNAs at total 40 nM (20 + 20 nM) concentration with 1:3:1 and 1:6:1 siRNA:PEI-LA:HA w/w/w ratios against CDC20 and phosphatases for HA additive **(A)** and coated **(B)** complexes. Scrambled siRNA (CsiRNA) was used as a negative control. The asterisks represent the significant silencing of individual and combinational targets by specific siRNAs compared to CsiRNA ($p < 0.05$).

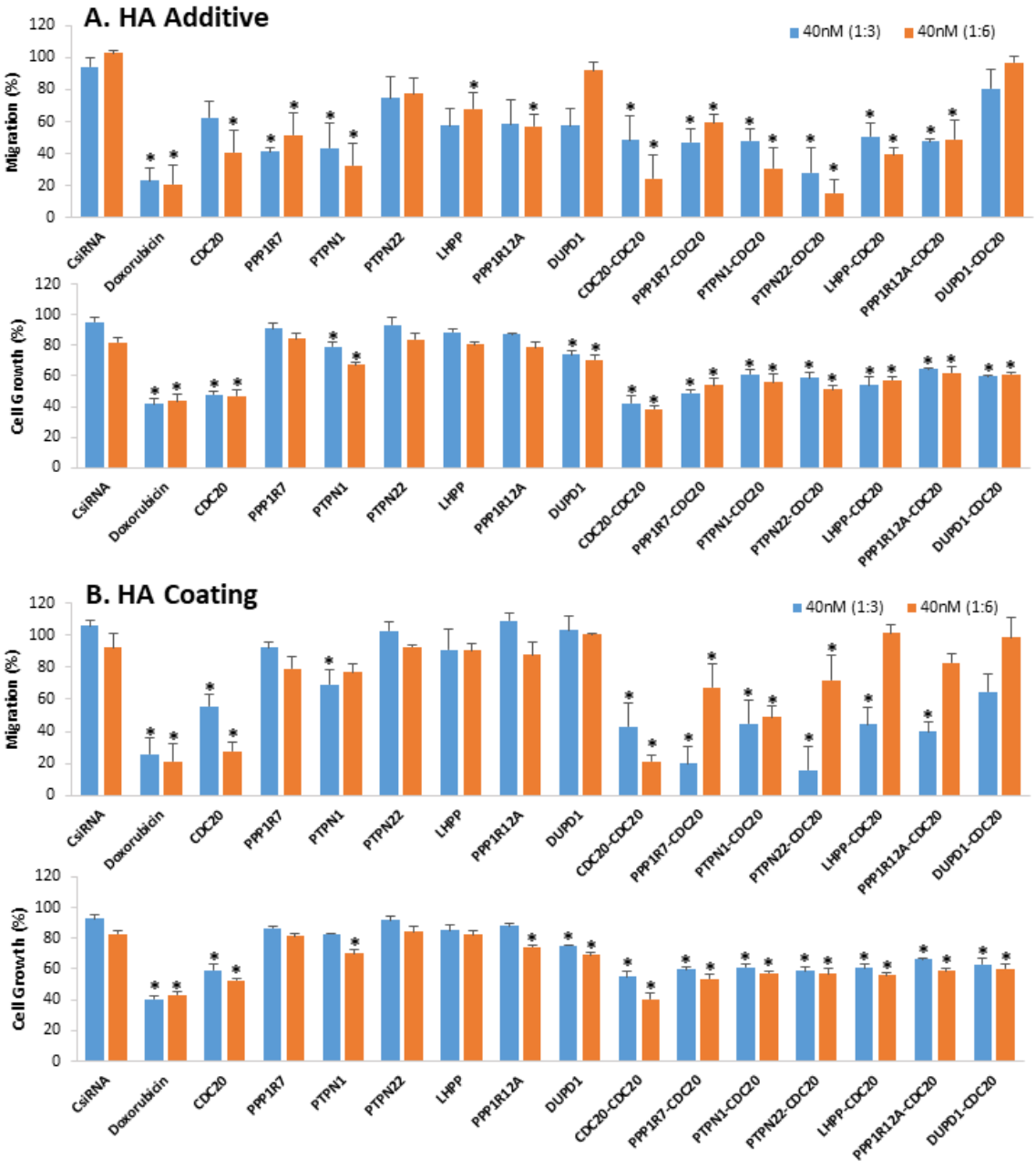

Fig 4.11: Inhibition of cell growth and migration by CDC20 and phosphatase siRNAs.

Inhibition of MDA-MB-231 growth and migration by individual siRNAs (20 nM phosphatase + 20 nM scrambled siRNA) and combinational siRNAs (20 nM CDC20 + 20 nM phosphatase) at 1:3:1 and 1:6:1 siRNA:PEI-LA:HA w/w/w ratios using HA additive **(A)** and coated **(B)** complexes. Percentage of cell migration and growth was determined based on non-treated cells. Scrambled siRNA (CsiRNA) was used as a negative control. The asterisks represent the significant cell growth or migration inhibition by individual and combinational siRNAs compared to CsiRNA ($p < 0.05$).

4.4 Discussion

RNAi-mediated knockdown of specific proteins using siRNA is a promising approach to target deregulated or over-expressed protein that could not be selectively targeted by chemotherapy [6,7]. However, siRNA-mediated silencing of specific targets has its own limitations; one of them is the need for non-toxic carriers that could easily transport siRNA without extracellular degradation, and release siRNA into cytoplasm, so that siRNA could incorporate into the RISC assembly [8]. To this end, we have developed a library of carriers based on lipid-substituted low molecular weight PEIs and have found linoleic acid-substituted 1.2 kDa PEI to be most effective at delivering siRNA to breast cancer cells [17,33]. This report shows that introduction of HA into the complexation process further increases the delivery efficiency to breast cancer cells with higher cellular uptake of FAM-labeled siRNA when the complexes were formulated with HA additive and coating compared with complexes made without HA. Furthermore, confocal microscopy showed that the HA-mediated delivery of siRNA led to more sustained presence of siRNA intracellularly. One of the reasons for increased efficiency of complexes to deliver siRNA could be overexpression of surface receptor CD44 in triple-negative MDA-MB-231 cells [15,34]. Shen *et al.* have successfully shown an enhanced antitumor activity with HA coated lipid nanoparticles loaded with paclitaxel in CD44 over-expressing melanoma cells, and Yang *et al.* reported a targeted paclitaxel delivery by self-assembled HA coated lipid-based nanoparticles in CD44 over-expressing breast cancer cells [35,36], suggesting a high specificity of HA to bind CD44 for increased interactions with cell membrane, leading to increased uptake of siRNA. With the three cell-lines used in this study, we noted 3-4 fold increased siRNA uptake after HA incorporation into complexes, clearly indicating the

beneficial effect of HA addition. A critical issue was whether this increase was solely attributed to CD44 receptors on the cells. Two lines of evidence argued against this; first, the CD44 levels were different between the MDA-MB-231 cells and SUM149PT/MCF7 cells, yet the increased uptake was relatively similar (only 20-30% difference with HA-modified complexes), and second, silencing CD44 in MDA-MB-231 reduced the uptake of siRNA to some extent (15-30%), but did not abolish the uptake to baseline levels (*i.e.,* equivalent to complexes without HA). These observations, while confirming a role of CD44 surface receptor with HA-modified complexes**,** suggested another mechanism(s) of uptake to be responsible for the improved effect of complexes with HA modification. It is likely that improved physicochemical characteristics of complexes with HA addition might have played a role in the uptake of siRNA. Even though others showed CD44 expression to be significant for the efficacy of HA-modified nanoparticles [35,36], our results with PEI-LA/HA polymeric carrier suggests a minor role of CD44 for the uptake of siRNA, and the uptake seems to be mostly increasing by CD44 independent uptake pathway(s). Higher uptake of siRNA when complexed with HA clearly showed higher functional efficacy with CDC20 siRNA, which inhibited MDA-MB-231 cell growth more significantly compared to siRNA complexes without HA. In contrast, when excessive HA was incorporated into complexes, the uptake of siRNA decreased significantly, and this correlated with a reduction in the efficiency of CDC20 siRNA delivered with these complexes to inhibit MDA-MB-231 cell growth. The poor efficacy of siRNA delivery at higher siRNA:HA ratios could be due to high negative ζ-potential of complexes at excess HA incorporation.

The physicochemical characteristics of complexes impact greatly on the efficacy of siRNA treatment. The size of complexes became smaller with the addition of HA, which

indicated a better compaction of siRNA into complexes, possibly due to better shielding of repulsive charges in the polyion complexes. The effect of HA on the ζ-potential of complexes was more significant in decreasing the surface charge as high positive ζ-potential could easily disrupt the cell membrane leading to cell death. Addition of HA into complexes decreased the surface charge of complexes, which may have played a major role during the interaction between complexes and the cell membrane including cell surface receptor CD44, resulting in a higher cellular uptake of siRNA. However, excessive HA into complexes leading to negative ζ-potential might have impeded interactions of complexes with cell membrane, resulting in sub-optimal uptake of the complexes and silencing of the chosen targets. Moreover, addition of HA into complexes increased the stability of complexes in culture medium compared to without HA complexes **(Fig 4.S1)**, given by 2-3 fold increased uptake for complexes incubated for 24 hours before addition to the cells.

Silencing the expression of cell cycle proteins is a promising approach to cancer therapy as the cell cycle is known to be deregulated in malignant cells and many cell cycle proteins are upregulated during malignancy [16]. One of the over-expressed proteins is CDC20, a critical protein for mitosis and cell division. We have previously validated siRNA therapy against CDC20 in breast cancer cells and shown a significant effect of silencing CDC20 in breast cancer cell survival *in vitro* and in an animal model [17]. Here, we observed a significant improvement in the inhibition of MDA-MB-231 cells by CDC20 siRNA delivery with the HA-incorporated complexes. In this study, CDC20 was mainly explored to develop a complementary siRNA therapy in conjunction with targeting phosphatase proteins that could be involved in metastasis. We relied on an unbiased

approach using an siRNA library screen to identify potential phosphatase proteins as potential therapeutic targets for metastatic breast cancer. MDA-MB-231 cells were quite responsive to all phosphatases in terms of inhibition of cell growth and migration compared to non-invasive MDA-MB-435 and MCF7 cell-lines (data not shown), which was a clear indication that MDA-MB-231 cells are relying more on phosphatases for its survival. In contrast, a poor response of MDA-MB-231 cells to a kinase library screen compared to MDA-MB-435 cells [37] clearly suggests independence of MDA-MB-231 cells from kinases for its survival. From the library screen, we identified PPP1R7, PTPN1, PTPN22, LHPP, PPP1R12A and DUPD1 as potential targets for siRNA-mediated inhibition of migration. After evaluating these phosphatases individually, the combinational siRNA therapy with CDC20 was performed to decrease cell growth and migration simultaneously. No interference in the functional effect of inhibiting cell growth by CDC20 siRNA was observed by phosphatase siRNAs when those were delivered in combination. Similarly, no suppression in the functional effect of migration inhibition by phosphatase siRNA was observed by the combination with CDC20 siRNA. The combinational siRNA delivery showed mostly additive effects of CDC20 and phosphatase siRNAs in terms of cell growth inhibition by CDC20 siRNA and migration inhibition by phosphatase siRNAs. However, a synergistic effect in inhibition of migration by PTPN22 and CDC20 siRNAs was observed when those were delivered as HA additive complexes **(Fig 4.11A)**. In addition, PPP1R7, PTPN22 and PPP1R12A siRNAs when combined with CDC20 siRNA showed a synergistic effect in migration inhibition when those were delivered as HA coated complexes **(Fig 4.11B)**.

Among the phosphatases identified, the downregulation of PPP1R7, PTPN22 and PPP1R12A resulted in inhibition of migration only without affecting cell growth. PPP1R7 is a subunit that regulates the activity of protein phosphatase 1. PPP1R7 is required for completion of the mitotic cycle and for targeting protein phosphatase 1 to the mitotic kinetochores. PPP1R7 is over-expressed in several cancers including cervical, lung, colorectal, gastric and ovarian, and has been implicated in carcinogenesis [38,39]. While the PPP1R7 siRNA was effective on its own, the combinational delivery with CDC20 siRNA inhibited cell growth and migration drastically **(Fig 4.11)**, suggesting an important role of PPP1R7 in survival of MDA-MB-231 cells and inhibiting its expression by siRNA may lead to increased therapeutic effect in metastatic breast cancer.

The second identified phosphatase, PTPN22 is a lymphoid-specific intracellular phosphatase that was initially described in the T-cell receptor signaling pathway, and has been reported to promote the survival of antigen stimulated chronic lymphocytic leukemia (CLL) cells by blocking B-cell receptor (BCR) related antigen-induced apoptosis [40]. Mutated PTPN22 has been reported in breast cancer [41], and Fasching *et al.* have listed PTPN22 as one of the predictive genes, whose mutations could potentially play a role in the pathogenesis or prognosis of breast cancer [42]. Inhibition of PTPN22 expression led to a decrease in the migration of MDA-MB-231 cells in both scratch and transwell migration assays in this study. No inhibition of cell growth and migration was observed with PTPN22 siRNA at low 20 nM siRNA concentration when it was delivered individually **(Fig 4.11)**, however, both were inhibited significantly when PTPN22 siRNA was combined with CDC20 siRNA. This is consistent with the ability of combinational

siRNA therapy to lower the required dose of siRNA while obtaining significant inhibition of cell growth and migration simultaneously.

The third phosphatase that inhibited cell migration only was PPP1R12A, also called myosin phosphatase target subunit 1 (MYPT1) as it is one of the subunits of myosin phosphatase. Myosin II plays important roles in many contractile-like cell functions, such as cell migration, adhesion, and retraction [43,44]. Phosphorylation by regulatory light chain (RLC) activates myosin II, while its dephosphorylation by myosin phosphatase containing MYPT1 or PPP1R12A leads to myosin inactivation [43,44]. Phosphorylation of RLC is also involved in regulating aspects of cell migration and spreading [44,45]. Inhibiting the activities of myosin phosphatase by downregulating its subunit PPP1R12A increases the phosphorylation of RLC, which ultimately reduces the turnover of phosphorylation followed by the blocking of peripheral membrane ruffling as well as the assembly of stable focal adhesions, leading to decreased cell migration [46,47]. While targeting PPP1R12A might not be particularly specific for malignant cells (given its normal role in cell migration), PPP1R12A has been found upregulated in various cancer such as breast [48], pancreatic [49] and colorectal [50] cancers. We observed excellent reduction of PPP1R12A transcripts with siRNA and successful migration inhibition of MDA-MB-231 cells during validation studies, supporting its involvement in cell migration and adhesion. There was also improved efficiency of PPP1R12A siRNA in the combinational siRNA therapy with CDC20 siRNA, suggesting a potential candidate for siRNA therapy to inhibit the metastasis of other types of cancers in addition to breast cancer.

A second group of phosphatases, PTPN1, LHPP and DUPD1, inhibited cell migration as well as growth drastically in the library screen. PTPN1, also known as protein-

tyrosine phosphatase 1B (PTP1B) is the founding member of the protein tyrosine phosphatase (PTP) family. PTPN1 is important in mammalian metabolism, where it negatively regulates the insulin signaling pathway. It has been considered as a promising therapeutic target for type 2 diabetes, in addition to several cancers [51]. PTPN1 has been shown to induce the growth of breast cancer tumors in mice [52], while breast cancer cell invasion and metastasis can be inhibited using small molecule inhibitors by downregulating PTPN1 [53,54]. We have shown here that siRNA against PTPN1 can inhibit breast cancer cell migration, while combinational siRNA therapy with CDC20 siRNA inhibited cell growth as well as migration.

LHPP (phospholysine phosphohistidine inorganic pyrophosphate phosphatase) is an inorganic pyrophosphatase that hydrolyzes phospholysine and phosphohistidine, and has a broad substrate specificity. Inorganic pyrophosphatase controls the level of inorganic pyrophosphate produced by biosynthesis of protein, RNA, and DNA. Over-expression of LHPP is known to be associated with hyperthyroidism [55]. No studies have been reported so far about the involvement of LHPP in cancer, however, it has been suggested that over-expression of the protein in hyperthyroidism may contribute to carcinogenesis in the thyroid [55]. We observed relatively poor efficacy of LHPP siRNA to decrease the migration of MDA-MB-231 cells, but the combinational siRNA therapy of LHPP and CDC20 decreased cell migration and growth significantly.

DUPD1, also known as dual specificity phosphatase 27 (DUSP27), is a recently identified dual-specificity phosphatase that can dephosphorylate both phosphotyrosine and phosphoserine/threonine residues. It is a member of the protein-tyrosine phosphatase superfamily that cooperates with protein kinases to regulate cell proliferation and

differentiation. Although there is no clear involvement with cancer, DUPD1 is over-expressed in pancreatic cancer [56] and liver metastasis of colorectal cancer [57]. In the present study, DUPD1 siRNA showed the highest efficacy in terms of cell growth and migration inhibitions in the library screen. However, no cell migration inhibition was observed with DUPD1 siRNA in the validation studies nor the combinational siRNA therapy. This discrepancy is likely due to the lack of effective downregulation of the DUPD1 transcript by DUPD1 siRNA delivery **(Fig 4.10)**. The siRNA that was used in the validation study was dicer-substrate siRNA, which is 27-mer and expected to provide higher efficacy [58]. However, no downregulation of DUPD1 transcripts by siRNA indicates poor functional outcome of siRNA by failing the translational inhibition of DUPD1 mRNA when it was delivered to cytoplasm of MDA-MB-231 cells. Perhaps, a better siRNA design that has high functionality and specificity may resolve this paradox.

4.5 Conclusions

We have established a novel polymeric siRNA delivery carrier based on PEI-LA/HA that could serve as a viable platform to target breast cancer cells. As cellular uptake of siRNA greatly increased with the addition of HA into the delivery system, a more favorable interaction of siRNA/polymer complexes with the triple-negative breast cancer cells was evident compared to complexes without HA. The cell-surface receptor CD44 played a role in increased uptake, but that did not appear to be the sole mechanism for siRNA delivery into the cells, and improved physicochemical characteristics might have played a significant role. While CDC20 siRNA showed an excellent and consistent ability to inhibit triple-negative breast cancer cells, more validation of siRNAs against phosphatases is needed. This may include *in vivo* studies confirming the functional validity

of phosphatase siRNAs to inhibit cell migration and metastasis. The identified phosphatases could serve as potential targets to inhibit migration of highly aggressive breast cancer cells. Moreover, combinational siRNA delivery against cell cycle and phosphatases could be a promising strategy to inhibit both growth and migration of metastatic breast cancer cells. These could be further developed to treat other types of metastatic cancer.

4.6 Acknowledgements

Manoj Parmar is a recipient of Women and Children's Health Research Institute (WCHRI) and Alberta Innovates-Health Solutions (AIHS) Graduate Studentships. This study was supported by operating grants from Canadian Breast Cancer Foundation (CBCF) and Natural Sciences and Engineering Council of Canada (NSERC).

4.7 References

1. Weigelt B, Peterse JL, Veer LJ. Breast cancer metastasis: markers and models. *Nat. Rev. Cancer*, 2005, 5:591-602.
2. Rahman M, Mohammed S. Breast cancer metastasis and the lymphatic system. *Onco. Lett,* 2015, 10:1233-1239.
3. Ligresti G, Libra M, Militello L, Clementi S, Donia M, Imbesi R, Malaponte G, Cappellani A, McCubrey JA, Stivala F. Breast cancer: Molecular basis and therapeutic strategies. *Mol. Med. Rep,* 2008, 1:451-458.
4. Vici P, Pizzuti L, Natoli C, Gamucci T, Di Lauro L, Barba M, Sergi D, Botti C, Michelotti A, Moscetti L, Mariani L, Izzo F, D'Onofrio L, Sperduti I, Conti F, Rossi V, Cassano A, Maugeri-Saccà M, Mottolese M, Marchetti P. Triple positive breast cancer: a distinct subtype? *Cancer Treat. Rev*, 2015, 41:69-76.
5. Dent R, Trudeau M, Pritchard K, Hanna WM, Kahn HK, Sawka CA, Lickley LA, Rawlinson E, Sun P, Narod SA. Triple-negative breast cancer: clinical features and patterns of recurrence. *Clin. Cancer Res*, 2007, 13:4429-4434.
6. McManus MT, Sharp PA. Gene silencing in mammals by small interfering RNAs. *Nat. Rev. Genet*, 2002, 3:737-747.
7. Wilson RC, Doudna JA. Molecular mechanisms of RNA interference. *Annu. Rev. Biophys,* 2013, 42:217-239.
8. Pecot CV, Calin GA, Coleman RL, Lopez-Berestein G, Sood AK. RNA interference in the clinic: Challenges and future directions. *Nat. Rev. Cancer*, 2011, 11:59–67.

9. Aliabadi HM, Landry B, Sun C, Tang T, Uludag H. Supramolecular assemblies in functional siRNA delivery: where do we stand? *Biomaterials*, 2012, 33:2546–2569.

10. Aliabadi HM, Landry B, Bahadur RK, Neamnark A, Suwantong O, Uludag H. Impact of lipid substitution on assembly and delivery of siRNA by cationic polymers. *Macromol. Biosci*, 2011, 11:662–672.

11. KC RB, Kucharski C, Uludag H. Additive nanocomplexes of cationic lipopolymers for improved non-viral gene delivery to mesenchymal stem cells. *J. Mater. Chem. B,* 2015, 3:3972–3982.

12. Fraser JR, Laurent TC, Laurent UB. Hyaluronan: its nature, distribution, functions and turnover. *J. Intern. Med*, 1997, 242:27-33.

13. Aruffo A, Stamenkovic I, Melnick M, Underhill CB, Seed B. CD44 is the principal cell surface receptor for hyaluronate. *Cell*, 1990, 61:1303-1313.

14. Mattheolabakis G, Milane L, Singh A, Amiji MM. Hyaluronic acid targeting of CD44 for cancer therapy: from receptor biology to nanomedicine. *J. Drug. Target*, 2015, 23:605-618.

15. Idowu MO, Kmieciak M, Dumur C, Burton RS, Grimes MM, Powers CN, Manjili MH. $CD44^{+}/CD24^{-/low}$ cancer stem/progenitor cells are more abundant in triple-negative invasive breast carcinoma phenotype and are associated with poor outcome. *Hum. Pathol*, 2012, 43:364-373.

16. Sandhu C, Slingerland J. Deregulation of the cell cycle in cancer. *Cancer Detect. Prev*, 2000, 24:107–118.

17. Parmar MB, Aliabadi HM, Mahdipoor P, Kucharski C, Maranchuk R, Hugh JC, Uludag H. Targeting cell cycle proteins in breast cancer cells with siRNA by using lipid-substituted polyethylenimines. *Front. Bioeng. Biotechnol*, 2015, 3:14.

18. Kimata Y, JE, Fry AM, Yamano H. A role for the Fizzy/ Cdc20 family of proteins in activation of the APC/C distinct from substrate recruitment. *Mol. Cell*, 2008, 32:576–583.

19. Motiwala T, Jacob ST. Role of protein tyrosine phosphatases in cancer. *Prog. Nucleic Acid Res. Mol. Biol*, 2006, 81:297–329.

20. Al-Aidaroos AQ, Zeng Q. PRL-3 phosphatase and cancer metastasis. *J. Cell. Biochem*, 2010, 111:1087-1098.

21. Bessette DC, Qiu D, Pallen CJ. PRL PTPs: mediators and markers of cancer progression. *Cancer Metastasis Rev*, 2008, 27:231-252.

22. Saha S, Bardelli A, Buckhaults P, Velculescu VE, Rago C, St Croix B, Romans KE, Choti MA, Lengauer C, Kinzler KW, Vogelstein B. A phosphatase associated with metastasis of colorectal cancer. *Science*, 2001, 294:1343-1346.

23. Lee ST, Feng M, Wei Y, Li Z, Qiao Y, Guan P, Jiang X, Wong CH, Huynh K, Wang J, Li J, Karuturi KM, Tan EY, Hoon DS, Kang Y,Yu Q. Protein tyrosine phosphatase UBASH3B is overexpressed in triple-negative breast cancer and promotes invasion and metastasis, *Proc. Natl. Acad. Sci. U.S.A*, 2013, 110:11121-11126.

24. Spring K, Fournier P, Lapointe L, Chabot C, Roussy J, Pommey S, Stagg J, Royal I. The protein tyrosine phosphatase DEP-1/PTPRJ promotes breast cancer cell invasion and metastasis. *Oncogene*, 2015, 34:5536-5547.

25. Feng X, Wu Z, Wu Y, Hankey W, Prior TW, Li L, Ganju RK, Shen R, Zou X. CDC25A regulates matrix metalloprotease 1 through Foxo1 and mediates metastasis of breast cancer cells. *Mol. Cell. Biol*, 2011, 31:3457-3471.

26. Bahadur KC, Landry B, Aliabadi HM, Lavasanifar A, Uludag H. Lipid substitution on low molecular weight (0.6–2.0 kDa) polyethylenimine leads to a higher zeta potential of plasmid DNA and enhances transgene expression. *Acta. Biomater*, 2011, 7: 2209–2217.

27. Remant Bahadur KC, Uludag H. A comparative evaluation of disulfide-linked and hydrophobically-modified PEI for plasmid delivery. *J. Biomater. Sci. Polym. Ed*, 2011, 22:873–892.

28. Sumantran VN. Cellular chemosensitivity assays: An overview. *Methods Mol. Biol*, 2011, 731:219–236.

29. Liang CC, Park AY, Guan JL. *In vitro* scratch assay: a convenient and inexpensive method for analysis of cell migration *in vitro*. *Nat. Protoc*, 2007, 2:329-333.

30. Schneider CA, Rasband WS, Eliceiri KW. NIH Image to ImageJ: 25 years of image analysis. *Nat. Methods*, 2012, 9:671-675.

31. Gebäck T, Schulz MM, Koumoutsakos P, Detmar M. TScratch: a novel and simple software tool for automated analysis of monolayer wound healing assays. *Biotechniques*, 2009, 46:265-274.

32. Livak KJ, Schmittgen TD. Analysis of relative gene expression data using real-time quantitative PCR and the $2^{-\Delta\Delta C}{}_{T}$ method. *Methods*, 2001, 25:402-408.

33. Parmar MB, Arteaga Ballesteros BE, Fu T, KC RB, Montazeri Aliabadi H, Hugh JC, Löbenberg R, Uludağ H. Multiple siRNA delivery against cell cycle and anti-apoptosis proteins using lipid-substituted polyethylenimine in triple-negative breast cancer and nonmalignant cells. *J. Biomed. Mater. Res*. *A*, 2016, 104:3031-3044.

34. Sheridan C, Kishimoto H, Fuchs RK, Mehrotra S, Bhat-Nakshatri P, Turner CH, Jr Goulet R, Badve S, Nakshatri H. CD44+/CD24- breast cancer cells exhibit enhanced invasive properties: an early step necessary for metastasis. *Breast Cancer Res*, 2006, 8:R59.

35. Shen H, Shi S, Zhang Z, Gong T, Sun X. Coating solid lipid nanoparticles with hyaluronic acid enhances antitumor activity against melanoma stem-like cells. *Theranostics*, 2015, 5:755-771.

36. Yang C, He Y, Zhang H, Liu Y, Wang W, Du Y, Gao F. Selective killing of breast cancer cells expressing activated CD44 using CD44 ligand-coated nanoparticles *in vitro* and *in vivo*. *Oncotarget*, 2015, 6:15283-15296.

37. Aliabadi HM, Maranchuk R, Kucharski C, Mahdipoor P, Hugh J, Uludağ H. Effective response of doxorubicin-sensitive and -resistant breast cancer cells to combinational siRNA therapy. *J. Control. Release*, 2013, 172:219-228.

38. Takakura S, Kohno T, Manda R, Okamoto A, Tanaka T, Yokota J. Genetic alterations and expression of the protein phosphatase 1 genes in human cancers. *Int. J. Oncol*, 2001, 18:817-824.

39. Harima Y, Ikeda K, Utsunomiya K, Shiga T, Komemushi A, Kojima H, Nomura M, Kamata M, Sawada S. Identification of genes associated with progression and metastasis of advanced cervical cancers after radiotherapy by cDNA microarray analysis. *Int. J. Radiat. Oncol. Biol. Phys*, 2009, 175:232-1239.

40. Negro R, Gobessi S, Longo PG, He Y, Zhang ZY, Laurenti L, Efremov DG. Overexpression of the autoimmunity-associated phosphatase PTPN22 promotes survival of antigen-stimulated CLL cells by selectively activating AKT. *Blood*, 2012, 119:6278–6287.

41. Cancer Genome Atlas Network, Comprehensive molecular portraits of human breast tumors. *Nature*, 2012, 490:61-70.

42. Fasching PA, Brucker SY, Fehm TN, Overkamp F, Janni W, Wallwiener M, Hadji P, Belleville E, Häberle L, Taran FA, Lüftner D, Lux MP, Ettl J, Müller V, Tesch H, Wallwiener D, Schneeweiss A. Biomarkers in patients with metastatic breast cancer and the PRAEGNANT study network. *Geburtshilfe Frauenheilkd*, 2015, 75:41-50.

43. Qiao YN, He WQ, Chen CP, Zhang CH, Zhao W, Wang P, Zhang L, Wu YZ, Yang X, Peng YJ, Gao JM, Kamm KE, Stull JT, Zhu MS. Myosin phosphatase target subunit 1 (MYPT1) regulates the contraction and relaxation of vascular smooth muscle and maintains blood pressure. *J. Biol. Chem*, 2014, 289:22512-22523.

44. Wakatsuki T, Wysolmerski RB, Elson EL. Mechanics of cell spreading: role of myosin II. *J. Cell. Sci*, 2003, 116:1617-1625.

45. Kaneko K, Satoh K, Masamune A, Satoh A, Shimosegawa T. Myosin light chain kinase inhibitors can block invasion and adhesion of human pancreatic cancer cell lines. *Pancreas*, 2002, 24:34-41.

46. Xia D, Stull JT, Kamm KE. Myosin phosphatase targeting subunit 1 affects cell migration by regulating myosin phosphorylation and actin assembly. *Exp. Cell. Res*, 2005, 304:506-517.

47. Totsukawa G, Wu Y, Sasaki Y, Hartshorne DJ, Yamakita Y, Yamashiro S, Matsumura F. Distinct roles of MLCK and ROCK in the regulation of membrane protrusions and focal adhesion dynamics during cell migration of fibroblasts. *J. Cell. Biol,* 2004, 164:427-439.

48. Cuadros M, Cano C, López FJ, López-Castro R. A. Concha, Expression profiling of breast tumors based on human epidermal growth factor receptor 2 status defines migration-related genes. *Pathobiology*, 2013, 80:32-40.

49. Van den Broeck A, Vankelecom H, Van Eijsden R, Govaere O, Topal B. Molecular markers associated with outcome and metastasis in human pancreatic cancer. *J. Exp. Clin. Cancer. Res,* 2012, 31:68.

50. Zhang C, Li A, Li H, Peng K, Wei Q, Lin M, Liu Z, Yin L, Li J. PPP1R12A copy number is associated with clinical outcomes of stage III CRC receiving oxaliplatin-based chemotherapy. *Mediators. Inflamm,* 2015, 2015:417184.

51. Lessard L, Stuible M, Tremblay ML. The two faces of PTP1B in cancer. *Biochim. Biophys. Acta*, 2010, 1804:613-619.

52. Bentires-Alj M, Neel BG. Protein-tyrosine phosphatase 1B is required for HER2/Neu-induced breast cancer. *Cancer Res*, 2007, 67:2420-2424.

53. Julien SG, Dubé N, Read M, Penney J, Paquet M, Han Y, Kennedy BP, Muller WJ, Tremblay ML. Protein tyrosine phosphatase 1B deficiency or inhibition delays ErbB2-induced mammary tumorigenesis and protects from lung metastasis. *Nat. Genet*, 2007, 39:338-346.

54. Cortesio CL, Chan KT, Perrin BJ, Burton NO, Zhang S, Zhang ZY, Huttenlocher A. Calpain 2 and PTP1B function in a novel pathway with Src to regulate invadopodia dynamics and breast cancer cell invasion. *J. Cell. Biol*, 2008, 180:957-971.

55. Koike E, Toda S, Yokoi F, Izuhara K, Koike N, Itoh K, Miyazaki K, Sugihara H. Expression of new human inorganic pyrophosphatase in thyroid diseases: its intimate association with hyperthyroidism. *Biochem. Biophys. Res. Commun*, 2006, 341:691-696.

56. Pilarsky C, Ammerpohl O, Sipos B, Dahl E, Hartmann A, Wellmann A, Braunschweig T, Löhr M, Jesenofsky R, Friess H, Wente MN, Kristiansen G, Jahnke B, Denz A, Rückert F, Schackert HK,

Klöppel G, Kalthoff H, Saeger HD, Grützmann R. Activation of Wnt signaling in stroma from pancreatic cancer identified by gene expression profiling. *J. Cell. Mol. Med*, 2008, 12:2823-2835.

57. Sayagués JM, Corchete LA, Gutiérrez ML, Sarasquete ME, Del Mar Abad M, Bengoechea O, Fermiñán E, Anduaga MF, Del Carmen S, Iglesias M, Esteban C, Angoso M, Alcazar JA, García J, Orfao A, Muñoz-Bellvis L. Genomic characterization of liver metastases from colorectal cancer patients. *Oncotarget*, 2016, 7:72908-72922.

58. Kim DH, Behlke MA, Rose SD, Chang MS, Choi S, Rossi JJ. Synthetic dsRNA Dicer substrates enhance RNAi potency and efficacy. *Nat. Biotechnol*, 2005, 23:222–226.

5. Additive polyplexes to undertake siRNA therapy against CDC20 and survivin in breast cancer cells

A version of this chapter was published in:

Parmar MB, K.C. RB, Löbenberg R, Uludağ H. Additive polyplexes to undertake siRNA therapy against CDC20 and survivin in breast cancer cells. *Biomacromolecules*, 2018, 19:4193–4206.

5.1 Introduction

Breast cancer is one of the leading causes of death among women. Current breast cancer treatments, developed based on broadly acting chemotherapeutic agents, have many toxic side effects due to their non-specific actions on non-malignant cells [1,2]. The specific therapies developed to treat breast cancer are mainly targeting overexpressing estrogen receptor, progesterone receptor or human epidermal growth factor receptor 2 (HER2) on breast cancer cells [3,4]. However, another common sub-type of breast cancer is triple-negative breast cancer (TNBC; 12-17% of all breast cancers), where all the three protein receptors are absent [4]. The specific therapies are, therefore, not suitable to treat TNBC, which urgently warrant a search for novel targeted therapies that not only provide beneficial effects on breast cancer cells, but also show minimal side effects on normal cells.

RNA Interference (RNAi) has evolved into a promising strategy in recent years to specifically target cancer cells, where a synthetic small interfering RNA (siRNA) is delivered to silence an overexpressing gene that contributes to uncontrolled growth of the malignant cells [5]. Since siRNA is highly labile and anionic macromolecule, it needs a carrier that can transport it across plasma membrane into the cytoplasm [6]. We previously developed a library of cationic polymers based to polyethylenimine (PEI) for its safe transportation and protection from extracellular degradation [7,8]. High molecular weight PEI (>25 kDa) displays significant cell toxicity due to high cationic charge that has a capability to irreversibly disrupt cell membrane [9]. On the contrary, low molecular weight PEI (<2 kDa) shows minimal cytotoxicity due to weak interactions with plasma membrane, but they are ineffective as nucleic acid carriers. We observed that modifying <2 kDa PEI with lipid moieties makes them excellent transfection reagents, and a 1.2 kDa PEI modified

with linoleic acid (PEI-LA) has emerged as a leading carrier for the delivery of siRNA in breast cancer cells.

To further improve the siRNA delivery efficiency, we recently developed 'additive' polyplexes by incorporating hyaluronic acid (HA) along with siRNA during polyplex formation, and showed that such a formulation was superior in siRNA delivery efficiency [10]. Incorporating HA altered the physicochemical properties of the polyplexes, most significantly the ζ-potential and propensity for siRNA dissociation. Incorporating HA also provided a means for the polyplexes to bind to overexpressed cluster of differentiation-44 (CD44) cell surface receptor. However, the extent of CD44 involvement on the uptake of siRNA in breast cancer cells was not clearly evident [10]. Even though no major role of CD44 receptor was found for the uptake of HA formulated additive polyplexes, the higher efficacy of siRNA was consistently evident. Therefore, in this study, we investigated other polyanionic polymers such as polyacrylic acid (PA) and dextran sulfate (DS), and neutral polymer methyl cellulose (MC) to further probe the mechanism behind higher efficacy of additive siRNA polyplexes. HA is a natural polymer that is distributed widely throughout connective, epithelial, and neural tissues, and one of the main components of extracellular matrix, while PA is a synthetic anionic polymer that is widely used in pharmaceutical, cosmetic and paint industries [11,12]. DS is an anionic polysaccharide that is made up of anhydroglucose, and MC is a synthetic polymer without any charge that is mainly used in food and cosmetic products [13].

This study employed polymeric delivery of siRNA against cell cycle and anti-apoptosis proteins that were previously shown to be significant in reducing the proliferation of breast cancer cells [14]. Cell-division cycle protein 20 (CDC20) particularly is a key cell

cycle protein that is a potent therapeutic target for siRNA in breast cancer cells [10,14,15]. CDC20 is a key regulatory cell cycle protein that activates the anaphase-promoting complex (APC) during mitosis, leading to initiation of chromatid separation and entrance of cell cycle into anaphase [16]. CDC20 is found to be overexpressed in many cancer-types, including breast cancer [17]. Based on monitoring of 445 patients for up to 20 years, high CDC20 expression is found to be associated with aggressive course of breast cancer and short-term patient survival [18]. Since overexpressed CDC20 is correlated to extremely poor outcome of breast cancer patients, silencing its expression by siRNA could potentially lead to cell cycle arrest, thereby decreasing tumor cell growth. Cell cycle process is often coordinated with apoptotic proteins to maintain tissue homeostasis [19], thereby targeting cell cycle as well as anti-apoptotic proteins simultaneously may improve the therapeutic impact on breast cancer cells. We, therefore, targeted a key anti-apoptotic protein for cell survival, survivin, in this study. Survivin is a member of inhibitor of apoptosis proteins (IAP), which inhibits apoptosis by blocking caspase activation process [20]. It is found to be up-regulated in many types of cancer, although barely detectable in most of the terminally differentiated cells [20], making it an excellent target to decrease only cancer cells growth without affecting non-malignant cells.

The side effects of siRNA delivery on non-malignant cells are often overlooked by focusing mainly on the efficacy of the delivery in malignant cells. Here, we investigated siRNA effects on non-malignant cells along with breast cancer cells to determine non-specific effects of the siRNA delivery. Non-malignant breast cells are the first-line of cells that may be affected by siRNA delivery were investigated here along with endothelial cells that have some functional similarity with epithelial breast cancer cells, and have been

reported to cross-talk with breast cancer cells [21,22]. Cells from a potential site for breast cancer metastasis, bone marrow stromal cells, were also used to determine the effects of siRNA delivery. Finally, since kidney is one of the major organs where nanoparticles tend to accumulate, kidney fibroblast cells were additionally included to provide an insight about the siRNA effects at this site.

Here, we first determined the physicochemical characteristics and functional efficacy of additive siRNA polyplexes formulated with PEI-LA and HA/PA/DS/MC. We then determined the accessibility of pDNA delivery using same polyplexes that were developed for siRNA transfection. Lastly, the functional efficacy of CDC20/survivin siRNA delivery was accessed in breast cancer cells as well as side effects in non-malignant cells. We also identified some safe siRNA/polymer formulations that showed drastic impact on breast cancer cells while affecting poorly to non-malignant cells.

5.2 Materials and Methods

5.2.1 Materials

The amines of low molecular weight PEI (1.2 kDa) were substituted with linoleic acid via N-acylation (PEI-LA) and the degree of substitution on the polymer was 2.6 LA/PEI, determined by ^{1}H-NMR spectroscopy [23,24]. HA (~300 kDa), PA (2, 14, 100 and 250 kDa), DS (~500 kDa), MC (~14 kDa), MTT [3-(4 5-dimethylthiazol-2-yl)-2 5-diphenyltetrazolium] and dimethyl sulfoxide (DMSO) were purchased from Sigma-Aldrich (St. Louis, MO). Hank's Balanced Salt Solution (HBSS) was prepared in-house. SYBR™ Green I and Caspase-3 substrate (Ac-DEVD-AFC) were purchased from ThermoFisher Scientific (Waltham, MA) and Enzo Life Sciences (Farmingdale, NY), respectively. CDC20 siRNA (Cat. No. HSC.RNAi.N001255.12.1), survivin siRNA (Cat.

No. HSC.RNAI.N001012271.12.1), and negative control scrambled siRNA (Cat. No. DS NC1) were ordered from IDT (Coralville, IA). The 6-Carboxyfluorescein (FAM) labeled scrambled siRNA was purchased from IDT. The Green Fluorescent Protein (GFP) expressing gWiz-GFP and blank gWiz pDNA were purchased from Aldevron (Fargo, ND). The blank gWiz pDNA was labeled with Cy3 (Mirus Bio LLC, Madison, WI) for uptake studies according to manufacturer's recommendations. Primers for CDC20 (forward: CGCTATATCCCCCATCGCAG; reverse: GATGTTCCTTCTTGG TGGGC), survivin (forward: TGAGAACGAGCCAGACTTGG; reverse: ATGTTCCTCT ATGGGGTCGT), and Glyceraldehyde 3-phosphate dehydrogenase (GAPDH; forward: TCACTGTTCT CTCCCTCCGC; reverse: TACGACCAAATCCGTTGACTCC) were supplied by Sigma-Aldrich.

5.2.2 Cell culture

The TNBC cells MDA-MB-231, SUM149PT, MDA-MB-436, and estrogen/progesterone-positive cells MCF7 were cultured in DMEM/F12 medium with 10% fetal bovine serum (FBS), 100 U/mL penicillin and 100 µg/mL streptomycin. MDA-MB-231 and MCF7 cells were a generous gift from Dr. Judith Hugh, Department of Laboratory Medicine & Pathology, University of Alberta, while SUM149PT and MDA-MB-436 cells were gift from Dr. Afsaneh Lavasanifar, Faculty of Pharmacy and Pharmaceutical Sciences, University of Alberta. Non-malignant breast cells MCF10A, generous gift from Dr. Judith Hugh were cultured in DMEM/F12 medium with 500 ng/mL hydrocortisone, 20 ng/mL human epidermal growth factor (hEGF), 0.01 mg/mL human insulin, 100 ng/mL cholera toxin, 5% horse serum, 100 U/mL penicillin, and 100 mg/mL streptomycin. Human bone marrow stromal cells (hBMSC) were isolated from 21 years

old male patient as previously described [25] with informed consent and approval from the Research Ethics Board, University of Alberta. hBMSC cells were cultured in DMEM/F12 medium with 12% FBS, 2% GlutaMAX™ Supplement (ThermoFisher Scientific), 2% MEM Non-Essential Amino Acids (ThermoFisher Scientific), 100 U/mL penicillin and 100 mg/mL streptomycin. Human umbilical vein endothelial cells (HUVEC), generous gift from Dr. Janet A. W. Elliott, Department of Chemical and Materials Engineering, University of Alberta, were cultured on rat tail type I collagen coated culture flask with EGM-2 medium that was supplied with manufacturer's growth factor bulletkit, 10% FBS, 100 U/mL penicillin, and 100 mg/mL streptomycin. Human embryonic kidney cells HEK293T were cultured in DMEM/F12 medium with 10% FBS, 100 U/mL penicillin and 100 µg/mL streptomycin. All cells were maintained in a humidified atmosphere at 37 °C and 95/5% air/CO_2. All cell-lines were routinely tested for mycoplasma contamination by a PCR-based method as described by Young et al, 2010 [26]. All cells except hBMSC were authenticated by STR DNA profiling analysis at the Genetic Analysis Facility, The Centre for Applied Genomics, The Hospital for Sick Children (Toronto, ON).

5.2.3 Preparation of siRNA/polymer polyplexes

Additive siRNA/polymer polyplexes were prepared as described in Parmar et al., 2018 [10]. Briefly, additive polymer (HA/PA/DS/MC) was first added to siRNA at pre-specified concentrations followed by addition of the required volume of 150 mM NaCl. PEI-LA was then added to the siRNA/additive polymer solution to allow a final complexation process for 30 min.

5.2.4 Physicochemical characterization of siRNA/polymer polyplexes

To characterize the siRNA/polymer polyplexes, the hydrodynamic diameter (Z-average), polydispersity index (PDI) and surface charge (ζ-potential) of these complexes were determined in ddH_2O using Zetasizer Nano ZS (Malvern, UK). Additive polyplexes were prepared as described above using 0.6 µg of scrambled siRNA at 1:6:0 and 1:6:1 siRNA:PEI-LA:additive-polymer w/w/w ratios. The complexes were diluted to 1 mL ddH_2O before each measurement. To determine the dissociation of siRNA/polymer polyplexes, additive polyplexes were prepared as described here followed by addition of different amounts of heparin (0 to 70 U/mL) to dissociate the complexes. SYBR Green I was used to quantify dissociated siRNA.

5.2.5 siRNA uptake by flow cytometry and confocal microscopy

To determine siRNA delivery efficiency of polyplexes made with different additive polymers, MDA-MB-231 cells were transfected with FAM-labeled siRNA at 30 nM with 1:6:0 and 1:6:1 siRNA:PEI-LA:additive-polymer w/w/w ratios. As a negative control, non-labeled scrambled siRNA was used to make complexes at 1:6:0 and 1:6:1 siRNA:PEI-LA:HA w/w/w ratio (data not shown). After 24 h of siRNA transfection, cells were trypsinized and fixed with 3.7% formaldehyde. The uptake of siRNA was quantified using BD Accuri™ C6 Plus Flow Cytometer (BD Biosciences, Franklin Lakes, NJ). The mean fluorescence of the recovered cell population and the percentage of cells showing FAM-fluorescence were determined after gating of the cell population as such that auto-fluorescence of non-treated cells represented ~1% of the total cell population.

Confocal microscopy was performed to further investigate qualitative uptake of siRNA. After growing MDA-MB-231 cells on glass cover slips for 24 h, cells were transfected with 30 nM FAM-labeled scrambled siRNA polyplexes at 1:6:0 and 1:6:1

siRNA:PEI-LA:additive-polymer w/w/w ratios. As a negative control, non-labeled scrambled siRNA was used to make complexes at 1:6:1 siRNA:PEI-LA:HA w/w/w ratio. After 24 and 72 h of siRNA treatment, cover slips were washed with HBSS, fixed with 4% paraformaldehyde for 20 min and mounted on a slide using in-house prepared mounting medium (polyvinyl alcohol in glycerol) with 4',6-diamidino-2-phenylindole (DAPI, Life Technologies) to stain nuclei and wheat germ agglutinin, Texas Red conjugate (Invitrogen) to stain the cytoplasmic membrane. Confocal pictures were taken using ZEN 2011 software by implicating 40x 1.3 oil plan-Apochromat lens in a Laser Scanning Confocal Microscope (LSM710, Carl Zeiss AG, Oberkochen, Germany).

5.2.6 Cell growth inhibition by MTT assay

Additive polyplexes were formulated as described above using 20 and 40 nM of scrambled and CDC20 siRNA at 1:6:0, 1:6:0.3, 1:6:1 and 1:6:3 siRNA:PEI-LA:additive-polymer ratios. Scrambled siRNA was used as a negative control. MDA-MB-231 cells were treated with additive polyplexes, formulated using CDC20 siRNA, and the inhibition of cell growth was determined by MTT assay to evaluate a functional efficacy of siRNA/polymer polyplexes. After 72 h of treatment, MTT was added to the cells at 1 mg/mL final concentration in HBSS, and cells were incubated for 1 hr at 37 °C and 5% CO_2. The formazan crystals formed from soluble MTT because of cellular activity of live cells were dissolved in DMSO [27]. The optical density (OD) was measured at 570 nm and the ODs were summarized as a percentage of cell growth based on non-treated cells (taken as 100% cell growth).

To determine the effects of different molecular weight of PA in siRNA/polymer complexes, MDA-MB-231 cells were treated with additive polyplexes, formulated with 2,

14, 100 and 250 kDa polyacrylic acid, and MTT assay was performed after 72 h of CDC20 siRNA treatment. Additive polyplexes were formulated using 20 and 40 nM of scrambled and CDC20 siRNA at 1:6:0.3, 1:6:1 and 1:6:3 siRNA:PEI-LA:PA ratios.

5.2.7 pDNA delivery

To determine whether polymeric delivery system that was developed for siRNA transfection could also deliver pDNA, the uptake of Cy3-labeled gWiz in MDA-MB-231 cells was performed at 0.5 µg/mL pDNA with 1:6:0 and 1:6:1 pDNA:PEI-LA:additive-polymer w/w/w ratios. As negative controls, non-labeled gWiz pDNA was used to make complexes at 1:6:0 and 1:6:1 pDNA:PEI-LA:HA w/w/w ratio (data not shown). After 24 h of pDNA transfection, uptake of pDNA was quantified using BD Accuri™ C6 Plus Flow Cytometer (BD Biosciences) as described above.

The functional efficacy of pDNA delivery by determining GFP expression from gWiz-GFP pDNA was also performed using HA, PA, DS and MC as additive polymers in polyplexes formulation. MDA-MB-231 cells were transfected with gWiz-GFP pDNA at 0.5 µg/mL with 1:6:0 and 1:6:1 pDNA:PEI-LA:additive-polymer w/w/w ratios. GFP expression from gWiz-GFP pDNA was determined after 48 h of pDNA transfection using BD Accuri™ C6 Plus Flow Cytometer (BD Biosciences) as described above.

5.2.8 MTT assay for CDC20/Survivin siRNA delivery

To determine the functional efficacy of CDC20 and survivin siRNAs, breast cancer cells were transfected with individual and combinational CDC20/survivin siRNAs and inhibition of cells growth was determined by MTT assay. Individual CDC20 or survivin siRNA was delivered as 15 nM CDC20/survivin siRNA + 15 nM scrambled siRNA, while combinational siRNAs were delivered as 15 nM CDC20 siRNA + 15 nM survivin siRNA

at 1:3:0, 1:6:0, 1:9:0, 1:3:1, 1:6:1 and 1:9:1 siRNA:PEI-LA:HA/PA w/w/w ratios. To evaluate the side effects of siRNA delivery to non-malignant cells, MCF10A, hBMSC, HUVEC and HEK293T cells were transfected with CDC20/survivin siRNAs as described above and inhibition of cells growth was determined by MTT assay.

5.2.9 siRNA uptake in non-malignant cells

To determine transfection efficiency of additive polyplexes to non-malignant cells compared to breast cancer cells, MDA-MB-231, SUM149PT and all non-malignant cells were transfected with FAM-labeled siRNA at 30 nM with 1:6:0 and 1:6:1 siRNA:PEI-LA:HA/PA w/w/w ratios. As a negative control, non-labeled scrambled siRNA was used to make complexes at 1:6:0 and 1:6:1 siRNA:PEI-LA:HA w/w/w ratio (data not shown). After 24 h of siRNA transfection, uptake of siRNA was quantified as described above using BD Accuri™ C6 Plus Flow Cytometer (BD Biosciences).

5.2.10 Reverse transcription – quantitative PCR (RT-qPCR)

To determine the silencing efficiency of CDC20/survivin siRNAs in breast cancer cells and non-malignant cells, MDA-MB-231, SUM149PT, MCF10A and hBMSC cells were transfected with individual CDC20/survivin siRNA (15 nM individual siRNA + 15 nM scrambled siRNA) and combinational siRNAs (15 nM CDC20 siRNA + 15 nM survivin siRNA) at 1:6:1 siRNA:PEI-LA:HA/PA w/w/w ratio. After 48 h of siRNA treatment, total RNA was isolated from cells using TRIzol reagent (Invitrogen, Carlsbad, CA), and 2 μg of total RNA was converted into cDNA using M-MLV reverse transcriptase (Invitrogen) according to manufacturer's instruction. StepOne Real-Time PCR System (Applied Biosystems, Foster City, CA) was employed to perform qPCR with 15 ng of cDNA from each sample and a SYBR Green qPCR Mastermix (Molecular Biology Service

Unit, Department of Biological Sciences, University of Alberta, Edmonton, AB). All primers for CDC20, survivin and a reference gene GAPDH were designed using NCBI Primer-BLAST (http://www.ncbi.nlm.nih.gov/tools/primer-blast/). Template cDNA was omitted from qPCR reaction as a negative control. The qPCR results were analyzed using $2^{-\Delta\Delta C}{}_T$ method and presented as relative quantity of transcripts [28]. The qPCR conditions comprised an initial denaturation step for 10 min at 95.0 ºC, followed by 40 cycles at 95.0 ºC for 15 s (denaturation), and annealing and elongation at 60 ºC for 1 min.

5.2.11 Caspase activity assay

To evaluate the induction of caspase activity as a result of siRNA delivery, breast cancer cells (MDA-MB-231 and SUM149PT) and non-malignant cells (MCF10A and hBMSC) were transfected with individual CDC20/survivin siRNA (15 nM individual siRNA + 15 nM scrambled siRNA) and combinational siRNAs (15 nM CDC20 siRNA + 15 nM survivin siRNA) at 1:6:1 siRNA:PEI-LA:HA/PA w/w/w ratio. After 48 h of siRNA treatment, cells were washed with HBSS and collected using cell scraper followed by 3-4 times freeze-thaw cycles to lyse the cells. Cell lysate was collected after removing cell debris by centrifugation. Total protein concentration in cell lysate was determined using BCA Protein Assay kit (Thermo Fisher Scientific) according to manufacturer's instructions. Caspase-3-like activity was determined by incubating cell lysate at 37ºC with Caspase-3 substrate (Ac-DEVD-AFC) according to manufacturer's instructions. Caspase activity was expressed as increase of relative fluorescent units per hour and normalized with total protein content.

5.2.12 Statistical analysis

All results were presented as mean ± standard deviation (n=3). Results were analyzed by one-way ANOVA with tukey's multiple comparison post-hoc test, where an asterisk (*) indicated significantly different groups in figures. The significance ($p < 0.05$) was typically determined by comparing specific siRNA-treated groups to that of scrambled siRNA-treated group.

5.3 Results

5.3.1 Characterization of siRNA/polymer polyplexes

We previously developed additive polyplexes using PEI-LA to complex a mixture of siRNA and HA [10]. The incorporation of HA into polyplexes was beneficial in siRNA delivery, and changes in polyplexes features and HA affinity to CD44 were considered as likely reasons for the beneficial effect. To further elucidate the role of additives, we introduced two additional polyanionic polymers (PA and DS) and a neutral polymer (MC) in the polyplexes. The polyplexes were first characterized for hydrodynamic diameter, polydispersity and ζ-potential. The size of siRNA/PEI-LA complexes without any additive polymer was ~180 nm, which was similar with the HA or DS additives **(Fig 5.1A)**. However, the size was increased slightly ~220 nm with the PA additive, and was decreased slightly ~120 nm with the MC additive. The polydispersity index was between 0.2 and 0.3 for all the formulations **(Fig 5.1A)**. The surface charge of the polyplexes was +40 mV in the absence of additive polymer, which was decreased to +30 mV upon introduction of HA and DS into the polyplexes **(Fig 5.1B)**. The ζ-potential decreased dramatically to +5 mV when polyplexes were formulated with the PA additive. Similarly, a decreased surface charge (+25 mV) was recorded for MC formulated polyplexes.

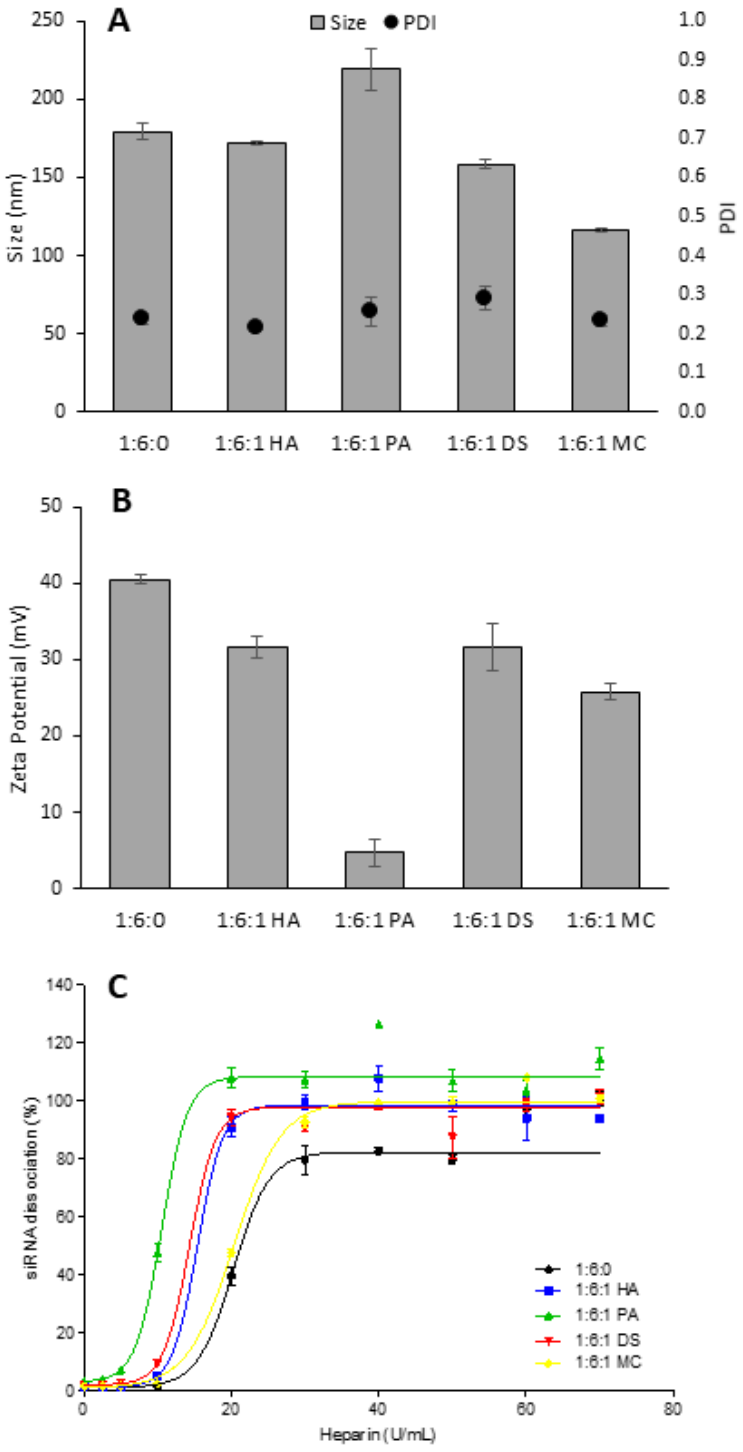

Fig 5.1: Physicochemical characteristics of additive polyplexes.

Size and PDI **(A**; mean ± SD**)**, ζ-potential **(B**; mean ± SD**)** and dissociation **(C)** of siRNA/polymer polyplexes were determined at 1:6:0 and 1:6:1 siRNA:PEI-LA:additive-polymer (w/w/w) ratios. Additive polymers used here were hyaluronic acid (HA), polyacrylic acid (PA), dextran sulfate (DS) and methyl cellulose (MC).

To determine the propensity of siRNA to be released from polyplexes, dissociation of siRNA polyplexes was performed for all additive polymers **(Fig 5.1C)**. The dissociation was induced by incubating polyplexes with varying concentrations of heparin. Polyplexes prepared without additive polymer and prepared with MC required a relatively higher heparin amount for siRNA release from the polyplexes compared to HA, PA and DS formulated polyplexes. Similar propensity of siRNA dissociation was observed with the HA and DS additives, while the most robust release of siRNA was evident with the PA additive.

5.3.2 Cellular uptake of siRNA in breast cancer cells

The MDA-MB-231 cells were employed to determine the cellular uptake of siRNA polyplexes. The polyplexes without any additive was able to deliver siRNA and transfect >90% cell population. However, the efficiency of transfection (mean siRNA fluorescence/cell) was markedly less compared to additive polyplexes formulated with HA, PA and DS **(Fig 5.2A)**. HA formulated additive polyplexes showed the highest siRNA uptake compared to other formulations. The siRNA uptake was similar for the neutral MC additive polyplexes and the polyplexes prepared without additive polymer.

Confocal microscopy further confirmed the uptake of siRNA polyplexes after 24 h of transfection **(Fig 5.2B)**. Similar to flow cytometry assessment, polyplexes formed with HA and PA additives showed increased siRNA delivery as compared to without additive polymer in polyplexes. The difference for the DS and MC additives were not immediately clear by confocal microscopy analysis. The retention of siRNA after 72 h of transfection was decreased dramatically for polyplexes without additive polymer **(Fig 5.2C)**. HA formulated polyplexes still showed the highest transfection of cells and retention of siRNA

compared to other groups at 72 h post-transfection. HA formulated polyplexes seemed to be aggregated inside cytoplasm, which may have contributed towards its longer retention until 72 h. The PA and DS formulated polyplexes were also able to retain siRNA until 72 h post-transfection. However, the efficiency to retain siRNA by the DS formulated polyplexes was less compared to HA and PA. The polyplexes with MC additive showed similar transfection to that of siRNA polyplexes without any additive, with no visible signs of siRNA intracellularly at 72 h post-transfection.

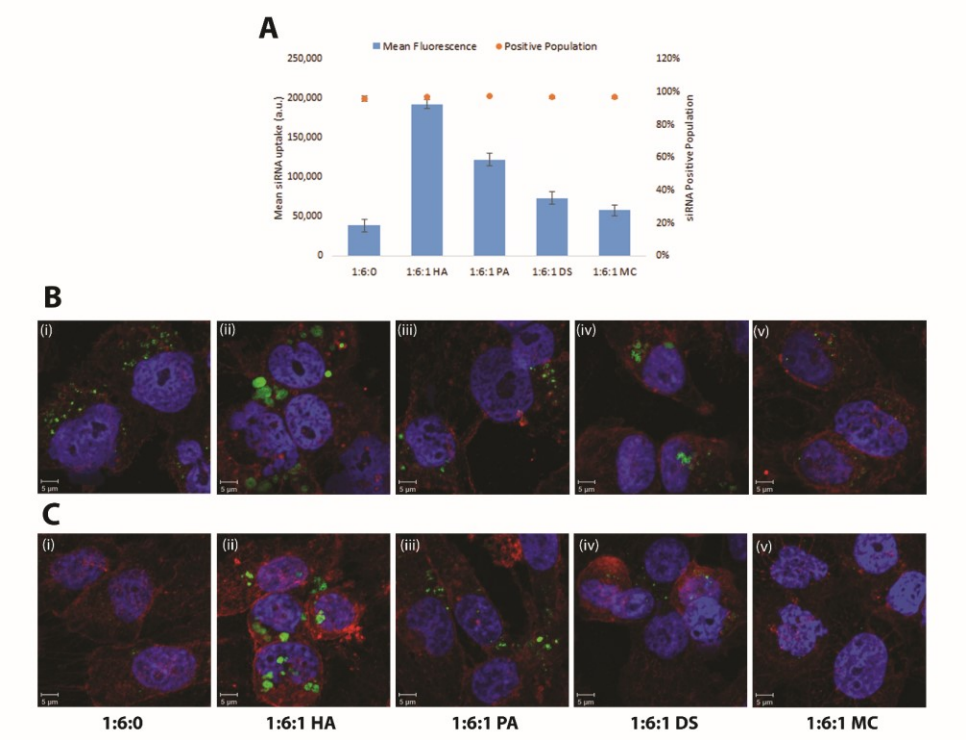

Fig 5.2: Cellular uptake of siRNA/polymer polyplexes.

Uptake of FAM-labeled siRNA was determined after 24 h of transfection in MDA-MB-231 cells by flow cytometry **(A)**, and summarized as the mean (±SD) siRNA fluorescence/cell and percentage of cells positive for siRNA. Confocal microscopy analysis after 24 **(B)** and 72 **(C)** h of transfection in MDA-MB-231 cells using 30 nM siRNA at 1:6:0 and 1:6:1 siRNA:PEI-LA:additive-polymer (w/w/w) ratios using HA, PA, DS and MC additives. As negative controls, non-labeled siRNA was delivered with 1:6:0 and 1:6:1 siRNA:PEI-LA:HA (w/w/w) ratios (data not shown).

5.3.3 Functional evaluation of additive polyplexes

Growth inhibition in MDA-MB-231 cells was determined after delivering CDC20 siRNA at 1:6:0, 1:6:0.3, 1:6:1 and 1:6:3 siRNA:PEI-LA:additive-polymer ratios. No cell growth inhibition was observed by polyplexes without additive polymer (1:6:0 ratio) at 20 nM CDC20 siRNA, while these polyplexes inhibited cell growth by ~20% at 40 nM siRNA **(Fig 5.3A)**. At 20 nM siRNA, the HA formulated polyplexes inhibited cell growth at the only 1:6:1 ratio, and decreased cell growth by 30-35% at all ratios with 40 nM siRNA concentration. Furthermore, 30-35% cell growth was inhibited by PA formulated polyplexes at 1:6:1 ratio with both 20 and 40 nM siRNA, while the cell growth was decreased by ~45% with the DS formulated polyplexes at 1:6:1 ratio with 40 nM siRNA. Interestingly, no cell growth inhibition was evident at 1:6:3 ratio with the PA and DS formulated polyplexes. No significant difference in cell growth inhibition was observed for MC formulated polyplexes at both 20 and 40 nM CDC20 siRNA.

The commercial polymers used as additives in polyplexes displayed different molecular weights, which could directly affect the obtained growth inhibitions. To determine the effects of additive polymer molecular weight on functional efficacy of siRNA/polymer polyplexes, 2, 14, 100 and 250 kDa PA was used to formulate PA polyplexes, and those were delivered to find MDA-MB-231 cell growth inhibition. All PA formulated polyplexes were able to inhibit cell growth at 1:6:0.3 and 1:6:1 ratios, while 1:6:3 ratio was ineffective to decrease cell growth **(Fig 5.3B)**, similar to the results in **Fig 5.3A**. No significant difference among different molecular weight PA formulated polyplexes was observed in functional efficacy of CDC20 siRNA.

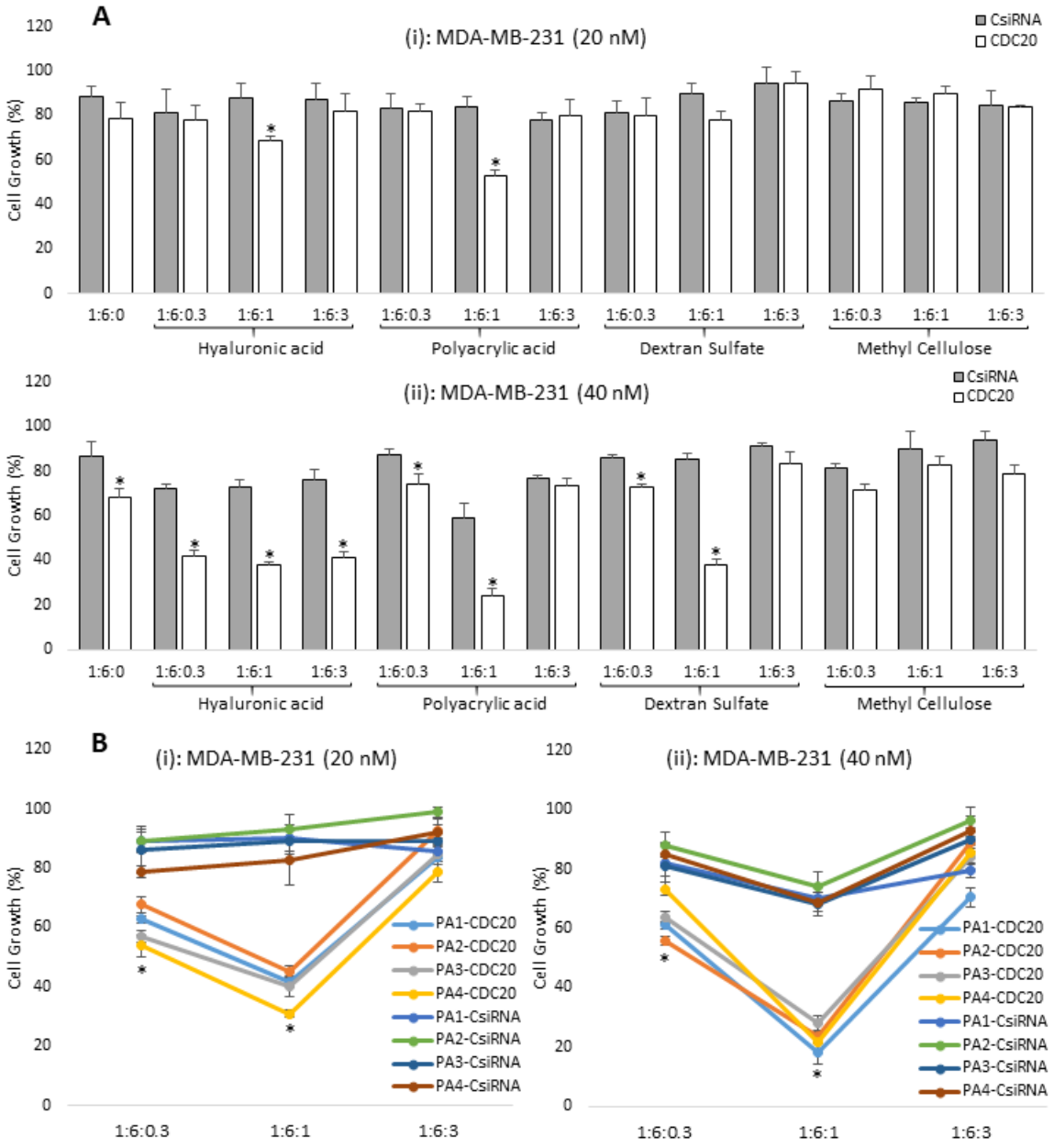

Fig 5.3: Functional evaluation of additive polyplexes using CDC20 siRNA to inhibit cell growth.

(A) MDA-MB-231 cells growth inhibition was determined with 20 and 40 nM of CDC20 siRNA at 1:6:0, 1:6:0.3, 1:6:1 and 1:6:3 siRNA:PEI-LA:additive-polymer (w/w/w) ratios using HA, PA, DS and MC additives. **(B)** PA1 (2 kDa), PA2 (14 kDa), PA3 (100 kDa) and PA4 (250 kDa) formulated additive polyplexes were evaluated to determine the effects of molecular weight of PA in the functional outcome of siRNA delivery. Scrambled siRNA (CsiRNA) was used as a negative control in all experiments. The asterisks represent the significant cell growth inhibition by CDC20 siRNA compared to CsiRNA ($p < 0.05$).

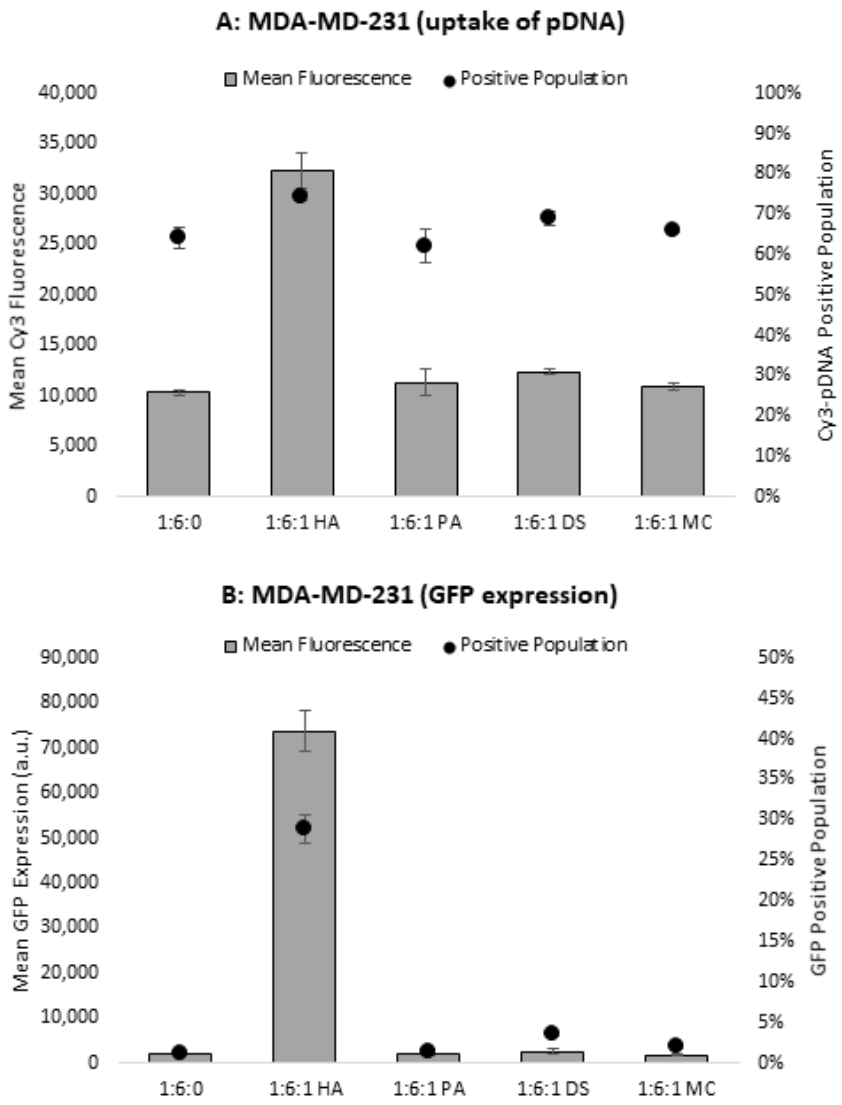

Fig 5.4: pDNA delivery using additive polyplexes.

Cellular uptake of Cy3-labeled gWiz pDNA was determined after 24 h of transfection **(A)**, while functional efficacy of GFP expression from gWiz-GFP pDNA was determined after 48 h of transfection **(B)** in MDA-MB-231 cells using 0.5 µg/mL pDNA at 1:6:0 and 1:6:1 pDNA:PEI-LA:additive-polymer (w/w/w) ratios using HA, PA, DS and MC additives. Non-labeled pDNA and gWiz without GFP gene were delivered with 1:6:0 and 1:6:1 pDNA:PEI-LA:HA (w/w/w) ratios as negative controls in **A** and **B**, respectively (not shown). The data was summarized as the mean (±SD) pDNA fluorescence/cell and percentage of cells positive for pDNA.

5.3.4 Additive polyplexes for pDNA delivery

To evaluate whether the additive polyplexes developed for siRNA delivery were also beneficial for delivery of pDNA, the uptake of additive pDNA polyplexes was determined in MDA-MB-231 cells. The HA formulated polyplexes showed the highest pDNA delivery compared to all other formulations **(Fig 5.4A)**. No benefits of PA, DS and MC in polyplexes were found as the uptake of pDNA was similar to polyplexes without additive polymer. The functional efficacy of pDNA delivery was evaluated by determining the GFP expression from pDNA-transfected cells. No GFP expression was observed by polyplexes without additive polymer as the mean fluorescence was similar to negative controls (data not shown). High GFP expression was found with the HA formulated polyplexes, while no GFP expression was observed with PA, DS and MC formulated polyplexes **(Fig 5.4B)**.

No difference in the size and PDI of additive polyplexes prepared with pDNA were found **(Fig 5.S1)**. The surface charge of the additive polyplexes prepared with polyanionic additive polymers (HA, PA and DS) decreased to +20-25 mV from +30-35 mV of without additive polymer and neutral MC additive. The dissociation of pDNA/polymer polyplexes seemed to be independent of the overall charge of the polyplexes as no clear pattern was detected that may have been dependent on surface charge **(Fig 5.S1)**. The PA formulated polyplexes seemed to have competed with pDNA to bind to PEI-LA as ~40% of pDNA release was detected without adding heparin.

5.3.5 CDC20/Survivin siRNA delivery in breast cancer cells

The siRNAs against CDC20 and survivin were delivered individually and in combination to several breast cancer cells, MDA-MB-231, SUM149PT, MDA-MB-436

and MCF7 **(Fig 5.5)**. The growth of MDA-MB-231 cells was inhibited significantly by individual and combinational CDC20/survivin siRNAs when polyplexes were delivered at 1:3:0 and 1:3:1 (with HA) ratios. However, no cell growth inhibition was found with the PA formulated polyplexes at 1:3:1 ratio. CDC20 and survivin siRNAs delivered at 1:6:0 and 1:9:0 ratios were unable to inhibit MDA-MB-231 cells growth, while those siRNAs delivered at 1:6:1 and 1:9:1 with HA and PA formulated polyplexes decreased the cell growth significantly. Similar results were obtained with SUM149PT, MDA-MB-436 and MCF7 cells as well, where CDC20/survivin siRNAs delivered at 1:3:0 and 1:3:1 (with HA) ratios inhibited cells growth significantly, but PA formulated polyplexes were unable to inhibit the cells growth except individual CDC20 siRNA. In addition, 1:6:0 and 1:9:0 ratios were ineffective to inhibit SUM149PT, MDA-MB-436 and MCF7 cells growth, while 1:6:1 and 1:9:1 with HA/PA formulated polyplexes inhibited cell growth significantly. The levels of cell growth inhibition by CDC20/survivin siRNAs among TNBC cells (MDA-MB-231, SUM149PT and MDA-MB-436) and estrogen/progesterone-positive MCF7 cells seemed to be similar **(Fig 5.S2)**. Overall, the MDA-MB-436 cells were the most responsive cells among all breast cancer cells.

To determine any synergistic effects of CDC20 and survivin co-delivery, the data in **Fig 5.5** were re-analyzed to compare the effects from individual delivery of CDC20 and survivin siRNAs vs. the co-delivery. The sum of growth inhibition by individual CDC20 and survivin siRNA delivery was plotted against growth inhibition by co-delivery **(Fig 5.S3)**. Only 1:6:1 and 1:9:1 formulations with HA showed a synergistic effect with CDC20/survivin co-delivery compared to individual delivery, suggesting that individual CDC20 and survivin delivery may be adequate compared to co-delivery. Specific target

sensitivity was also determined for CDC20 and survivin by plotting individual siRNA delivery effects on breast cancer cell growth inhibition **(Fig 5.S3)**. Overall, CDC20 siRNA showed higher cell growth inhibition compared to survivin in all cells, which suggests that breast cancer cells were more sensitive to CDC20 silencing compared to survivin.

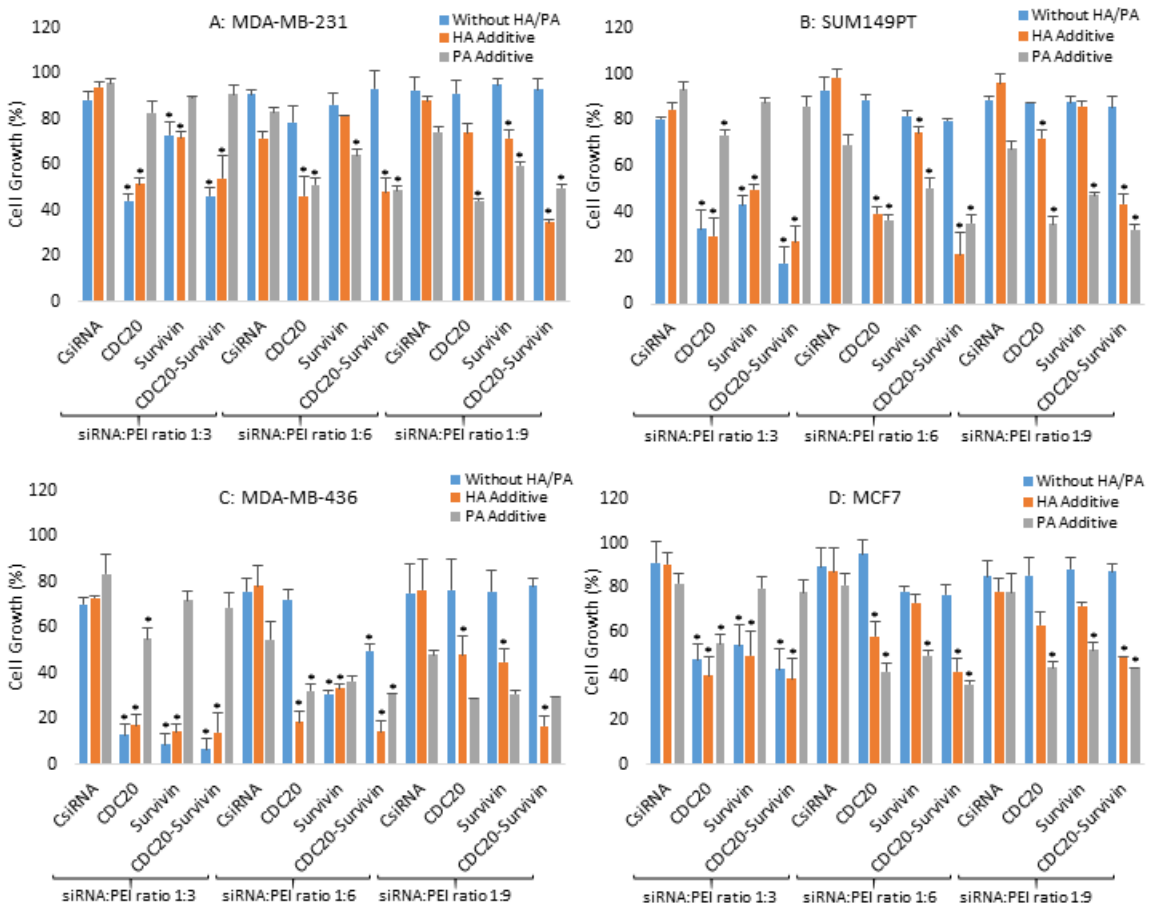

Fig 5.5: Delivery of CDC20 and survivin siRNA in breast cancer cells.

The CDC20 and survivin siRNAs were delivered individually or in combination with total 30 nM siRNAs (15 + 15 nM) at 1:3, 1:6 and 1:9 siRNA:PEI-LA (w/w) ratios with/without HA/PA additives. After 72 h of siRNA transfection, MDA-MB-231 **(A)**, SUM149PT **(B)**, MDA-MB-436 **(C)** and MCF7 **(D)** cells growth inhibition were determined, and presented as a percent cell growth compared to non-treated cells (taken as 100%). Scrambled siRNA (CsiRNA) was used as a negative control. The asterisks represent the significant cell growth inhibition by CDC20/survivin siRNA compared to CsiRNA ($p < 0.05$).

5.3.6 Effect of siRNA delivery on non-malignant cells

The growth inhibition in non-malignant cells was also performed to evaluate any damage to normal cells due to the delivery by the chosen siRNAs **(Fig 5.6)**. No growth inhibition in non-malignant breast cells MCF10A was observed when the polyplexes were delivered without additive polymer at all ratios. However, a significant decrease in cell growth was found with HA formulated polyplexes at all ratios, while the PA formulated polyplexes were unable to inhibit MCF10A cells growth. In addition, 1:3 siRNA:PEI-LA ratio seemed to show a toxicity of the carrier in MCF10A cells as 20-30% cells growth was inhibited by scrambled siRNA delivery with this formulation **(Fig 5.6A)**. No effects of siRNA delivery at all formulations was observed in primary cells hBMSC, while HUVEC were the most affected cells by siRNA delivery. Only co-delivery of CDC20/survivin siRNAs decreased HUVEC cells growth significantly at 1:3:0 and 1:3:1 (with HA) ratios. Similar to breast cancer cells, CDC20/survivin siRNAs formulated at 1:6:0 and 1:9:0 ratios were unable to inhibit HUVEC cells growth, while HA/PA additive with1:6:1 and 1:9:1 ratios inhibited the growth dramatically. HEK293T cells were also least affected cells among non-malignant cells tested, possibly indicating a lack of involvement of these two targets in controlling cell growth in kidney cells. Only co-delivery of CDC20/survivin siRNAs and the individual CDC20 siRNA delivery with PA additive at 1:6:1 and 1:9:1 ratios, respectively, inhibited HEK293T cells growth significantly.

Since CDC20/survivin siRNA delivery showed some inhibitory effects on non-malignant cells, relatively safe formulations that decreased breast cancer cells growth without affecting non-malignant cells needed to be identified. As such, the absolute growth inhibition by all formulations in non-malignant cells was plotted against breast cancer cells,

and siRNA formulations with little effect on non-malignant cells, but higher efficacy in breast cancer cells were highlighted **(Fig 5.S4)**. The ratios 1:3:0 and 1:3:1 with HA additive were mostly safe as these formulations inhibited all breast cancer cells dramatically while

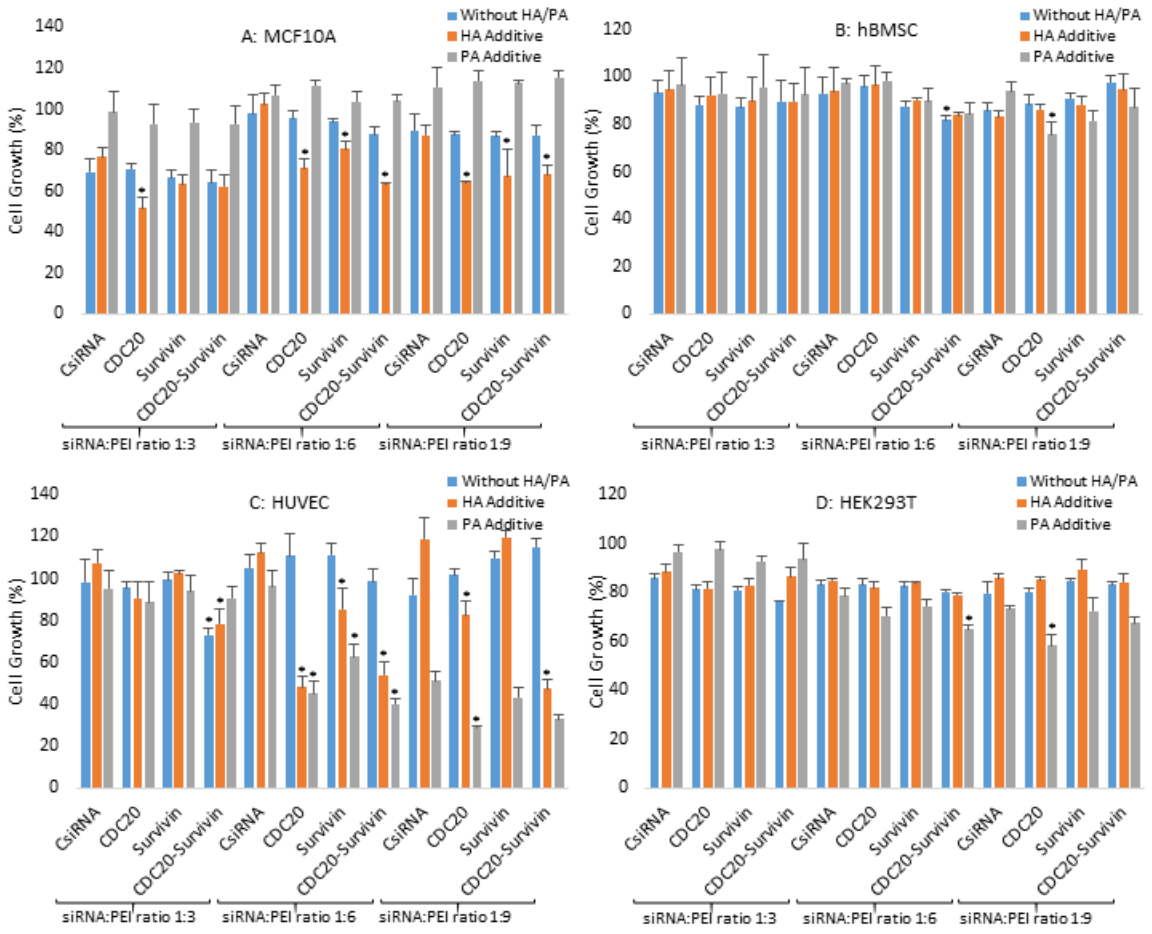

Fig 5.6: The effects of CDC20 and survivin siRNA delivery in non-malignant cells.

The CDC20 and survivin siRNAs were delivered individually or in combination with total 30 nM siRNAs (15 + 15 nM) at 1:3, 1:6 and 1:9 siRNA:PEI-LA (w/w) ratios with/without HA/PA additives. Growth inhibition in MCF10A **(A)**, hBMSC **(B)**, HUVEC **(C)** and HEK293T **(D)** cells were determined after 72 h of siRNA transfection (with reference to non-treated cells, taken as 0% inhibition). Scrambled siRNA (CsiRNA) was used as a negative control. The asterisks represent the significant cell growth inhibition by CDC20/survivin siRNAs compared to CsiRNA ($p < 0.05$).

least affecting all non-malignant cells tested here. The HA additive at 1:6:1 and 1:9:1 ratios also showed higher efficacy in breast cancer cells, but damaged MCF10A and HUVEC cells significantly higher compared to hBMSC and HEK293T cells. Polyplexes formulated without additive polymer at 1:6:0 ratio inhibited comparatively more sensitive MDA-MB-436 cells, but this ratio was ineffective in other breast cancer cells as well as non-malignant cells. Similarly, PA formulated polyplexes at 1:6:1 ratio inhibited MCF7 cells growth significantly, but this ratio inhibited MCF10A and HUVEC cells as well.

5.3.7 Comparative mechanistic effects of siRNA delivery on malignant and non-malignant cells

To further understand effects of siRNA therapy on non-malignant cells, cellular uptake of siRNA, target specific silencing and induction of apoptosis were evaluated in non-malignant cells compared to breast cancer cells. Cellular uptake of siRNA was the highest in MDA-MB-231 cells compared to other non-malignant cells for polyplexes formulated with HA and PA additives **(Fig 5.7)**. Higher uptake of siRNA was evident with HA and PA formulated polyplexes compared to polyplexes without any additives. Non-malignant MCF10A cells showed higher uptake of siRNA compared to other normal cells, perhaps, due to high morphological similarity with breast cancer cells. The hBMSC, HUVEC and HEK293T cells showed a poor uptake of siRNA compared to all other cells.

The silencing efficiency of specific siRNAs on mRNA levels was determined by the RT-qPCR. Breast cancer cells MDA-MB-231 and SUM149PT showed 80-90% CDC20/survivin silencing whether the specific siRNAs were delivered individually or in combination with HA/PA additives **(Fig 5.8)**. Similarly, non-malignant breast cells showed significant reduction of CDC20 and survivin mRNA by HA additive. However, the PA

formulated polyplexes showed poor efficacy to silence both targets in MCF10A. Moreover, primary cells hBMSC were the least affected by siRNA delivery as significant reduction in CDC20/survivin transcripts were only detected by individual siRNA delivery.

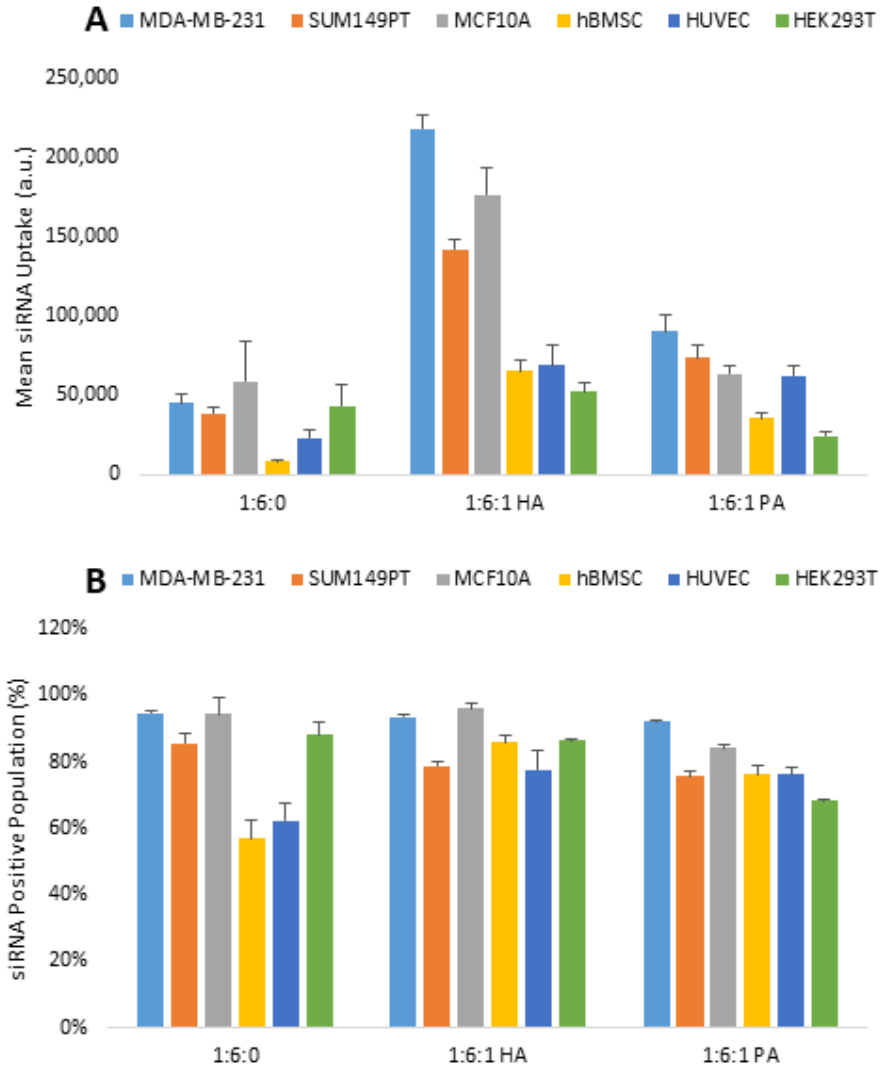

Fig 5.7: Cellular uptake of siRNA/polymer polyplexes.

Cellular uptake of siRNA/polymer polyplexes in non-malignant cells (MCF10A, hBMSC, HUVEC and HEK293T) compared to MDA-MB-231 and SUM149PT breast cancer cells. Mean FAM-labeled siRNA uptake **(A**; mean+SD**)** and siRNA positive cells **(B**; mean+SD**)** was determined after 24 h of transfection using 30 nM siRNA at 1:6:0 and 1:6:1 siRNA:PEI-LA:HA/PA (w/w/w) ratios. As negative controls, non-labeled siRNA was delivered with 1:6:0 and 1:6:1 siRNA:PEI-LA:HA (w/w/w) ratios (not shown).

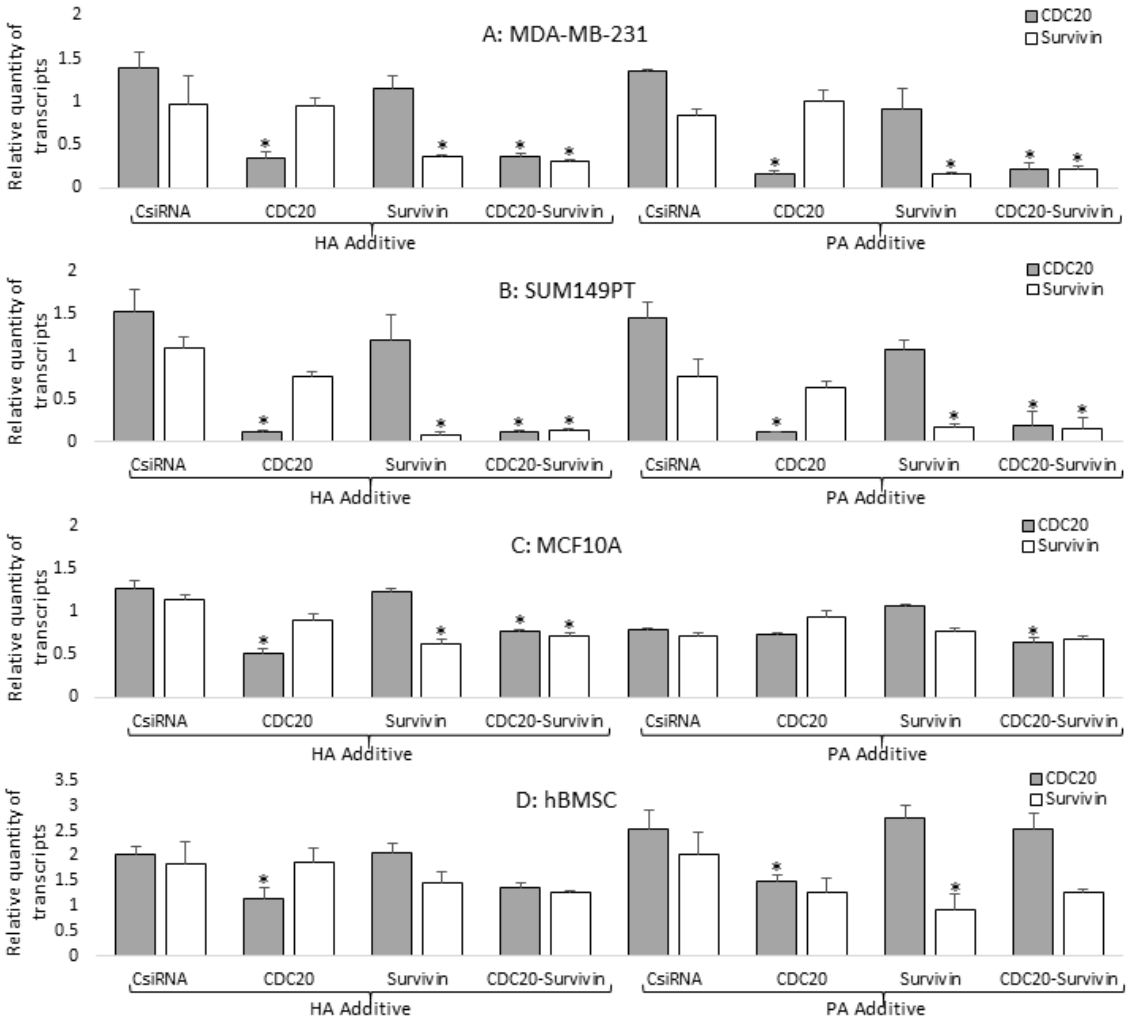

Fig 5.8: The RT-qPCR analysis in malignant and non-malignant cells.

The RT-qPCR analysis to determine the silencing efficiency of CDC20 and survivin siRNA delivery in breast cancer (MDA-MB-231 and SUM149PT) and non-malignant cells (MCF10A and hBMSC). Individual and combinational siRNAs at total 30 nM (15 + 15 nM) concentration with 1:6:1 siRNA:PEI-LA:HA/PA (w/w/w) ratio were delivered in MDA-MB-231 **(A)**, SUM149PT **(B)**, MCF10A **(C)** and hBMSC **(D)**. Scrambled siRNA (CsiRNA) was used as a negative control. The asterisks represent the significant silencing of CDC20/survivin transcripts by specific siRNAs compared to CsiRNA ($p < 0.05$).

Given the pro-survival role of survivin in the apoptotic pathway, silencing it with siRNA is expected to induce apoptosis. We already confirmed induction of apoptosis (TUNEL assay) by survivin silencing in breast cancer cells in a previous study [29]. Here

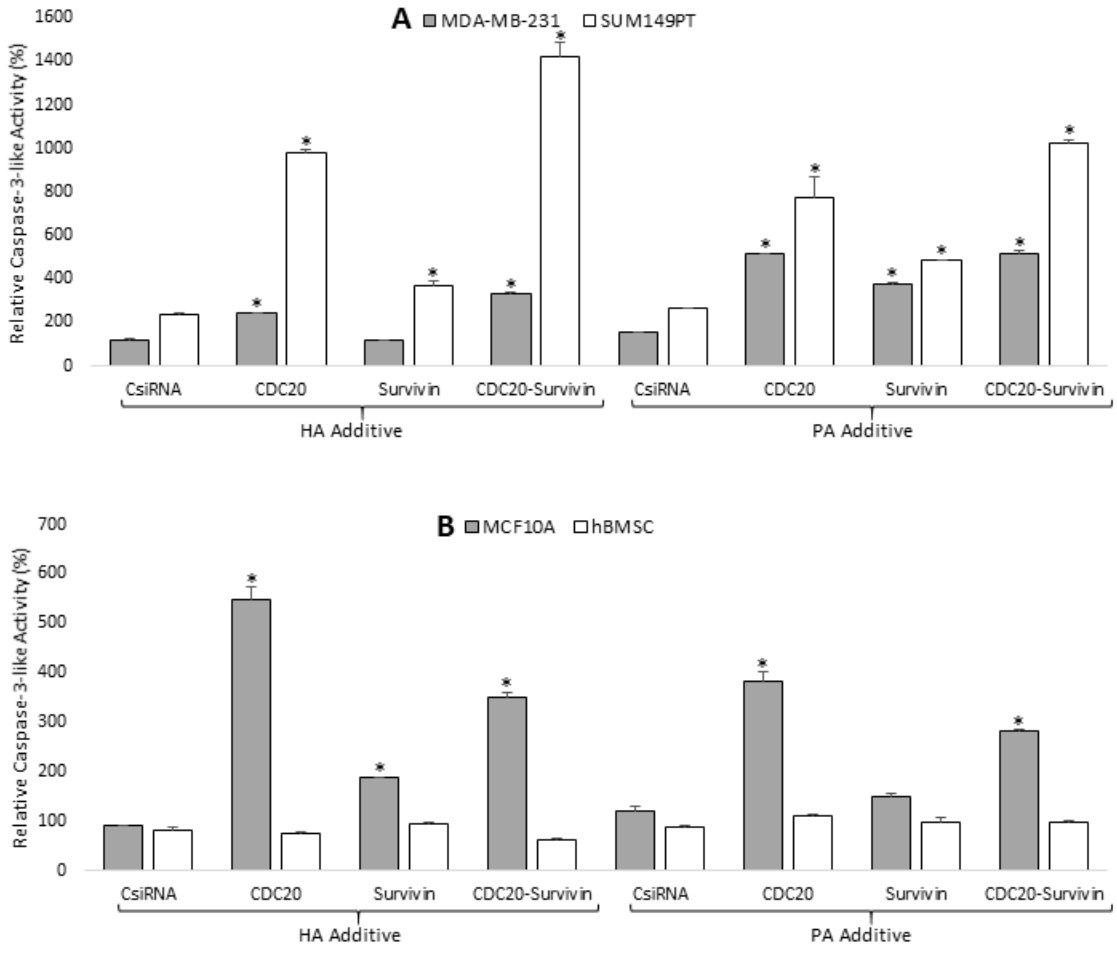

Fig 5.9: Induction of caspase-3 activity as a measure of cellular apoptosis by CDC20/survivin siRNA delivery.

Caspase activity assay was performed after delivering total 30 nM (15 + 15 nM) individual or combinational CDC20/survivin siRNAs at 1:6:1 siRNA:PEI-LA:HA/PA (w/w/w) ratio in breast cancer **(A**; MDA-MB-231 and SUM149PT**)** and non-malignant **(B**; MCF10A and hBMSC**)** cells. Scrambled siRNA (CsiRNA) was used as a negative control. The asterisks represent the significant increased caspase-3-like activity by CDC20/survivin siRNAs compared to CsiRNA ($p < 0.05$).

we detected induction of apoptosis by determining the levels of caspase-3 activity after survivin and CDC20 silencing **(Fig 5.9)**. Significantly increased caspase-3 activity was found in breast cancer cells MDA-MB-231 and SUM149PT with CDC20/survivin siRNAs

whether those were delivered individually or in combination using HA/PA formulated polyplexes. Similarly, MCF10A also showed higher caspase-3 activity upon delivery of CDC20/survivin siRNAs by HA/PA formulated polyplexes. However, hBMSC cells were again the least responsive to siRNA delivery and no significant increased caspase-3 activity was observed with CDC20/survivin siRNA delivery.

5.4 Discussion

Nucleic acid-based therapeutics are being actively explored as promising approaches to develop targeted therapies for several diseases, including breast cancer [30,31]. However, there are several challenges associated with development of nucleic acid-based therapeutics [32,33]. A major challenge is to develop a safe and non-toxic carrier for nucleic acid delivery, and whether the promising carrier developed for a particular nucleic acid could be deployed for other nucleic acid therapeutics. We have recently spent extensive efforts for development of PEI-based carriers for nucleic acid delivery, and successfully developed a library of carriers for the delivery of siRNA and pDNA [34]. Even though these PEI-based carriers can transfect cells and deliver functional outcomes, there is a continued demand to improve the efficiency of transfection and delivery. We recently improved the efficacy of siRNA transfection using additive polyplexes formulated with PEI-LA and HA [10]. Here we further explored the concept of additive polyplexes and formulated these polyplexes with other polyanionic and neutral polymers. Even though no significant difference in the size and PDI of polyplexes were observed upon additive polymer inclusion, a major difference in surface charge was evident that may have impacted the dissociation of siRNA/polymer complexes. Additive polyplexes prepared with polyanionic polymers HA, PA and DS showed more robust

release of siRNA from the polyplexes, presumably due to lower polyionic complexation of siRNA with the cationic PEI-LA, which may have increased the availability of siRNA inside cytoplasm for RISC assembly **(Fig 5.10)**.

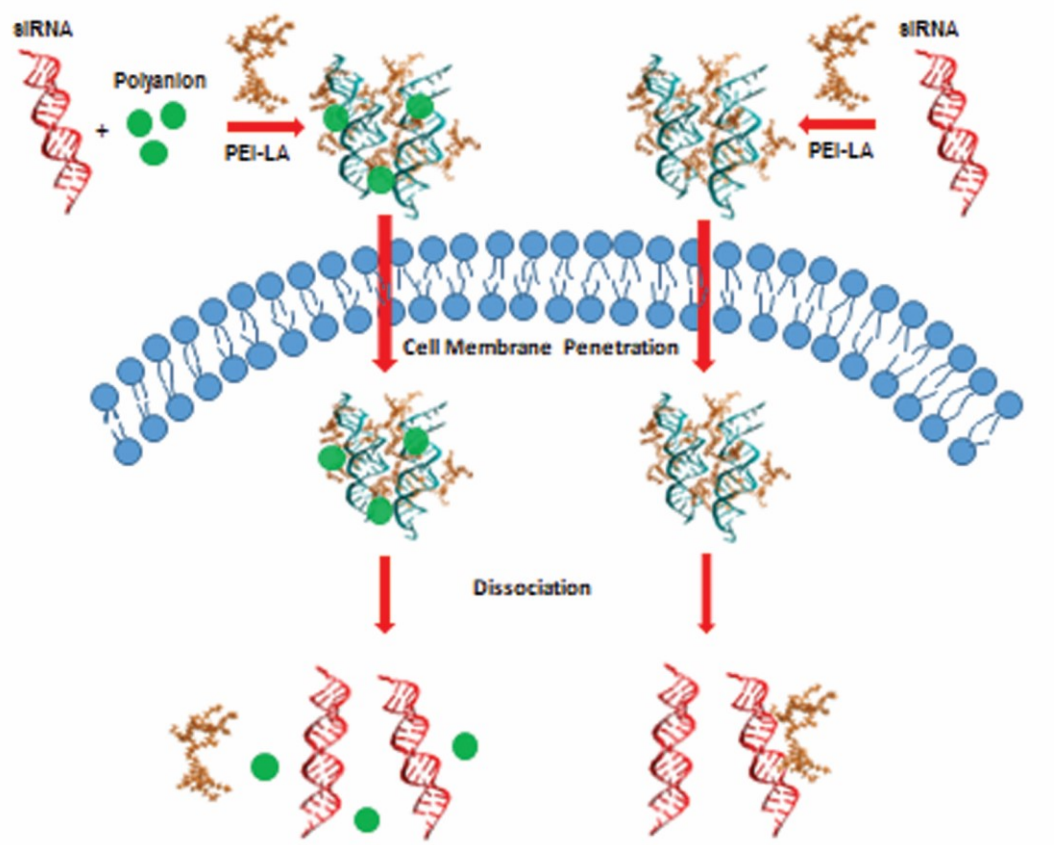

Fig 5.10: An illustration to summarize the mechanism by which higher efficacy of siRNA was achieved with additive polyplexes compared to polyplexes without polyanion.

A robust release of siRNA from additive polyplexes inside cytoplasm may have led to higher availability of siRNA for RISC assembly, leading to improved efficacy of siRNA.

A higher delivery of siRNA was also evident with additive polyplexes, clearly the increased propensity to dissociate with competing polyanionic molecules did not affect the uptake of the siRNA. Additionally, the retention time of siRNA particles inside cells was improved as well. The results from the siRNA/polymer dissociation assay might have

predicted a lower retention time due to increased dissociation inside cells, but our confocal microscopy observations were contrary to this expectation. It is possible that polyanionic polymers might have protected the siRNA inside cells against cytoplasmic nucleases and/or decreased interactions with de-stabilizing molecules due to lower cationic charge. Nevertheless, the longer presence of additive polyplexes ultimately led to higher functional efficacy of CDC20 and survivin siRNA delivery in breast cancer cells. The siRNA:additive-polymer ratio used to formulate the polyplexes had a dramatic effect on siRNA efficacy as 1:1 w/w ratio was the most effective ratios for all polyplexes, while lower (1:0.3) and higher (1:3) ratios provided less than optimal outcomes. The neutral polymer MC was universally ineffective as an additive, suggesting an importance of anionic charges for effective siRNA delivery. Furthermore, based on the results from the cell growth inhibition by PA additive polyplexes, the molecular weight of the additive polymer had no obvious effect on the functional outcomes.

Additive polyplexes were not only beneficial for siRNA efficacy, but also for pDNA delivery. We observed in the past that most of the polymeric carriers developed for cytoplasmic delivery of siRNA failed to achieve functional pDNA delivery, perhaps, due to their inability to deliver the pDNA cargo into the nucleus. We observed the same result here for PEI-LA as it was unable to express pDNA in breast cancer cells, while providing some efficacy with siRNA delivery. However, additive polyplexes of PEI-LA with HA expressed GFP successfully in the breast cancer cells. On the other hand, no GFP expression was detected with PA/DS/MC additives, suggesting that the choice of effective additive with the pDNA cargo was more restrictive, possibly reflecting the need to deliver the pDNA all the way to the nucleus. No influence of dissociation of pDNA/polymer

polyplexes was observed on functional outcome of pDNA delivery, as GFP expression was only found with HA additive.

Additive polyplexes formulated with HA and PA successfully increased cell growth arrest in all breast cancer cells. Since a similar response to siRNA delivery was seen for TNBC cells and estrogen/progesterone-positive MCF7 cells, the reported siRNA-based therapy seemed to be functionally independent of the phenotype of breast cancer cells. PEI-LA used without additive polymers at lower 1:3 siRNA:PEI-LA ratio and HA/PA formulated polyplexes at 1:3, 1:6 and 1:9 siRNA:PEI-LA ratios decreased the breast cancer cell growth significantly. However, no cell growth inhibition was observed at higher 1:6 and 1:9 siRNA:PEI-LA ratios without additive polymers, suggesting less dissociation of siRNA from the PEI-LA once complexes were in the cytoplasm at these higher ratios. Due to additional negative charges in the polyplexes introduced by HA/PA at the 1:6 and 1:9 siRNA:PEI-LA ratios, siRNA might have bound loosely to PEI-LA, ultimately releasing siRNA better once the polyplexes reached to cytoplasm.

With the delivery of multiple siRNAs, it is more preferable to derive synergistic activities from the delivered agents, provided that the targeting mechanism complement each other. Most of the obtained outcomes using the two targets CDC20 and survivin led to antagonistic effects of co-delivery in breast cancer cells. However, additive polyplexes with 1:6:1 and 1:9:1 siRNA:PEI-LA:HA ratios showed synergistic effects with co-delivery of CDC20/survivin siRNAs, suggesting that the specific formulation of the polyplexes can amplify the beneficial effect of the co-delivered siRNAs. In terms of target sensitivity, CDC20 siRNA delivery was more effective to retard cell growth compared to survivin siRNA, indicating that these cells may be more dependent on CDC20 activity for

proliferation. The normal levels of CDC20 transcripts were found to be higher compared to survivin transcripts **(Fig 5.S5)**, and induction of caspase-3 activity was around 2-fold higher by individual CDC20 siRNA delivery compared to survivin in breast cancer cells, which may be indicative of increased reliance on CDC20 protein for cell proliferation.

The efficacy of siRNA delivery was determined in non-malignant cells to observe any possible side-effects on normal cells. Non-malignant breast MCF10A cells and endothelial HUVEC cells were more sensitive to siRNA compared to hBMSC and kidney HEK293T cells. Since the siRNA polyplexes were designed for breast cancer cells, we expected to find some effects in MCF10A cells due to similarity in cell membrane structure with breast cancer cells. We observed in the past that PEI-based carriers that are developed for one-type of cells showed poor efficacy in others due to difference in the cell membrane composition, *e.g.,* carriers developed for adherent cells show poor transfection of siRNA to suspension cells [35]. The morphologies of hBMSC and HEK293T cells are quite different from breast cancer cells, which could be one of the reasons behind poor outcome of siRNA delivery in these cells. All non-malignant cells, in fact, were effectively transfected by additive polyplexes, but the uptake of siRNA was evidently lower in non-malignant cells compared to breast cancer cells, suggesting different efficiency of additive polyplexes to deliver siRNA based on types of cells being used for siRNA uptake. HUVEC cells, on the other hand, were affected by the specific siRNA delivery, perhaps due to some functional similarity with the epithelial breast cancer cells [21], and higher involvement of endothelial cells to cross-talk with breast cancer cells [22]. It is likely that HUVEC cells may also rely on CDC20 and/or survivin for proliferation and survival, so that higher effects were seen with the specific siRNAs used here. In addition to quantitative siRNA

delivery, we considered the possibility of target-specific silencing efficiency to have an impact on outcomes of siRNA delivery. The CDC20/survivin transcripts were found to be silenced less in non-malignant cells (10-50%) compared to breast cancer cells (80-90%). In hBMSC particularly, CDC20/survivin siRNAs not only showed poor silencing for targeted mRNAs, but also failed to induce apoptosis, making them the least affected cells by siRNA delivery. On the contrary, CDC20/survivin siRNAs reduced the transcripts levels significantly and induced apoptosis in MCF10A cells. Furthermore, the co-delivery of CDC20/survivin siRNAs silenced both targets at equal efficiency in breast cancer cells, suggesting no impediment of co-delivery in the silencing efficiency of each siRNA. While the promise of CDC20 and survivin as breast cancer targets were suggested in the literature [17,36], other targets with no activity in normal cells might still need to be identified based on our results.

Based on the overall results in this study, siRNA formulations strongly effective on breast cancer cells, but poorly effective on non-malignant cells were identified, namely polyplexes with 1:3 siRNA:PEI-LA ratio with/without HA additive. The siRNA:PEI-LA ratios 1:6 and 1:9 with HA were also quite effective on breast cancer cells, but showed some undesirable effects on certain non-malignant cells. The additive polyplexes described here might provide an additional degree of freedom to fine tune formulation features to minimize side effects of siRNA on non-malignant cells. In addition to naturally derived polyanion HA, the synthetic polyanion PA was also an effective additive that gave a longer retention of siRNA in cytoplasm and offered improved efficacy/safety profile with the additive polyplexes. However, additive complexes from HA was more universally effective based on the analysis in **Fig 5.S4**. In addition, HA additive polyplexes not only

delivered siRNA successfully, but also expressed GFP from pDNA, indicating that this formulation could easily be transferred to deliver other types of nucleic acids-based therapeutics; perhaps co-delivery of siRNA/pDNA may provide an improved therapeutic outcomes of nucleic acid delivery. Similarly, co-delivery of siRNA polyplexes and chemotherapeutic agents may result into improved efficacy of chemotherapy. Since HA is a natural polymer that is widely distributed in several tissues and extracellular matrix, this additive may be preferable for *in vivo* delivery of siRNA, which may potentially reduce immunogenicity and improved circulatory time by reducing renal clearance [37,38]. Validation of the siRNA delivery *in vivo* with additive polyplexes is required to determine the ideal additive and resultant functional outcomes.

5.5 Conclusions

The additive siRNA polyplexes formulated using PEI-LA with natural polymer HA and synthetic polymer PA showed an improved delivery of siRNA due to better dissociation of siRNA/polymer polyplexes, and could serve as a viable platform to develop nucleic acids-based therapeutics. Both siRNA and pDNA could be delivered with improved efficiency using the same additive polyplexes, indicating the possibility of applying these formulations to different types of nucleic acid therapeutics. The CDC20/survivin siRNAs delivered by additive polyplexes showed promising results in breast cancer cells to inhibit their growth, but undesirable effects were also evident in non-malignant cells. A careful formulation of additive siRNA/polymer polyplexes could potentially minimize side effects on normal cells, but similar studies need to be conducted in preclinical animal models to further validate the beneficial effect of additive polyplexes. Since the efficacy of siRNA delivery by additive polyplexes was independent of breast

cancer phenotypes, these polyplexes could be functional for a range of breast cancers and additionally in other types of cancers.

5.6 Acknowledgements

We thank Cezary Kucharski for his assistance in RT-qPCR. Manoj Parmar is a recipient of Women and Children's Health Research Institute (WCHRI) and Alberta Innovates-Health Solutions (AIHS) Graduate Studentships. This study was supported by operating grants from Canadian Breast Cancer Foundation (CBCF) and Natural Sciences and Engineering Council of Canada (NSERC). Equipment support (flow cytometry) was provided by Edmonton Civic Employees Charitable Assistance Fund (ECE-CAF).

5.7 References

1. Kayl AE, Meyers CA. Side-effects of chemotherapy and quality of life in ovarian and breast cancer patients. *Curr Opin Obstet Gynecol,* 2006, 18:24-28.
2. Tao JJ, Visvanathan K, Wolff AC. Long term side effects of adjuvant chemotherapy in patients with early breast cancer. *Breast,* 2015, 24:S149-S153.
3. Ligresti G, Libra M, Militello L, Clementi S, Donia M, Imbesi R, Malaponte G, Cappellani A, McCubrey JA, Stivala F. Breast cancer: Molecular basis and therapeutic strategies. *Mol Med Rep,* 2008, 1:451-458.
4. Vici P, Pizzuti L, Natoli C, Gamucci T, Di Lauro L, Barba M, Sergi D, Botti C, Michelotti A, Moscetti L, Mariani L, Izzo F, D'Onofrio L, Sperduti I, Conti F, Rossi V, Cassano A, Maugeri-Saccà M, Mottolese M, Marchetti P. Triple positive breast cancer: a distinct subtype? *Cancer Treat Rev,* 2015, 41:69-76.
5. McManus MT, Sharp PA. Gene silencing in mammals by small interfering RNAs. *Nat Rev Genet,* 2002, 3:737-747.
6. Pecot CV, Calin GA, Coleman RL, Lopez-Berestein G, Sood AK. RNA interference in the clinic: Challenges and future directions. *Nat Rev Cancer,* 2011, 11:59–67.
7. Aliabadi HM, Landry B, Sun C, Tang T, Uludağ H. Supramolecular assemblies in functional siRNA delivery: where do we stand? *Biomaterials,* 2012, 33:2546–2569.
8. Aliabadi HM, Landry B, Bahadur RK, Neamnark A, Suwantong O, Uludağ H. Impact of lipid substitution on assembly and delivery of siRNA by cationic polymers. *Macromol Biosci,* 2011, 11:662–672.
9. Moghimi SM, Symonds P, Murray JC, Hunter AC, Debska G, Szewczyk A. A two-stage poly(ethylenimine)-mediated cytotoxicity: implications for gene transfer/therapy. *Mol Ther,* 2005, 11:990-995.

10. Parmar MB, Meenakshi Sundaram DN, KC RB, Maranchuk R, Montazeri Aliabadi H, Hugh JC, Löbenberg R, Uludağ H. Combinational siRNA delivery using hyaluronic acid modified amphiphilic polyplexes against cell cycle and phosphatase proteins to inhibit growth and migration of triple-negative breast cancer cells. *Acta Biomater,* 2018, 66:294-309.

11. Fraser JR, Laurent TC, Laurent UB. Hyaluronan: its nature, distribution, functions and turnover. *J Intern Med,* 1997, 242:27-33.

12. Wiśniewska M, Urban T, Nosal-Wiercińska A, Zarko VI, Gun'ko VM. Comparison of stability properties of poly(acrylic acid) adsorbed on the surface of silica, alumina and mixed silica-alumina nanoparticles – application of turbidimetry method. *Cent Eur J Chem,* 2014, 12:476-479.

13. Rogers TL, Wallick D. Reviewing the use of ethylcellulose, methylcellulose and hypromellose in microencapsulation. *Drug Dev Ind Pharm,* 2012, 38:129-157.

14. Parmar MB, Arteaga Ballesteros BE, Fu T, KC RB, Montazeri Aliabadi H, Hugh JC, Löbenberg R, Uludağ H. Multiple siRNA delivery against cell cycle and anti-apoptosis proteins using lipid-substituted polyethylenimine in triple-negative breast cancer and nonmalignant cells. *J Biomed Mater Res A,* 2016, 104:3031-3044.

15. Parmar MB, Aliabadi HM, Mahdipoor P, Kucharski C, Maranchuk R, Hugh JC, Uludağ H. Targeting cell cycle proteins in breast cancer cells with siRNA by using lipid-substituted polyethylenimines. *Front Bioeng Biotechnol,* 2015, 3:14.

16. Kimata Y, Baxter JE, Fry AM, Yamano H. A role for the Fizzy/ Cdc20 family of proteins in activation of the APC/C distinct from substrate recruitment. *Mol Cell,* 2008, 32:576–583.

17. Wang L, Zhang J, Wan L, Zhou X, Wang Z, Wei W. Targeting Cdc20 as a novel cancer therapeutic strategy. *Pharmacol Ther,* 2015, 151:141-151.

18. Karra H, Repo H, Ahonen I, Löyttyniemi E, Pitkänen R, Lintunen M, Kuopio T, Söderström M, Kronqvist P. Cdc20 and securin overexpression predict short-term breast cancer survival. *Br J Cancer,* 2014, 110:2905-2913.

19. King KL, Cidlowski JA. Cell cycle regulation and apoptosis. *Annu Rev Physiol,* 1998, 60:601–617.

20. Sah NK, Khan Z, Khan GJ, Bisen PS. Structural, functional and therapeutic biology of survivin. *Cancer Lett,* 2006, 244:164–171.

21. Kinne RK. Endothelial and epithelial cells: general principles of selective vectorial transport. *Int J Microcirc Clin Exp,* 1997, 17:223-230.

22. Buchanan CF, Szot CS, Wilson TD, Akman S, Metheny-Barlow LJ, Robertson JL, Freeman JW, Rylander MN. Cross-talk between endothelial and breast cancer cells regulates reciprocal expression of angiogenic factors *in vitro*. *J Cell Biochem,* 2012, 113:1142-1151.

23. Bahadur KC, Landry B, Aliabadi HM, Lavasanifar A, Uludağ H. Lipid substitution on low molecular weight (0.6–2.0 kDa) polyethylenimine leads to a higher zeta potential of plasmid DNA and enhances transgene expression. *Acta Biomater,* 2011, 7:2209–2217.

24. Remant Bahadur KC, Uludağ H. A comparative evaluation of disulfide-linked and hydrophobically-modified PEI for plasmid delivery. *J Biomater Sci Polym Ed,* 2011, 22:873–892.

25. Jiang H, Secretan C, Gao T, Bagnall K, Korbutt G, Lakey J, Jomha NM. The development of osteoblasts from stem cells to supplement fusion of the spine during surgery for AIS. p 467-472. *In:* Uyttendaele D, Dangerfield PH (ed.). *Studies in Health Technology and Informatics: Research in Spinal Deformities*, 2006, IOS Press, Amsterdam, The Netherlands.

26. Young L, Sung J, Stacey G, Masters JR. Detection of mycoplasma in cell cultures. *Nat Protoc,* 2010, 5:929-934.

27. Sumantran VN. Cellular chemosensitivity assays: An overview. *Methods Mol Biol,* 2011, 731:219–236.

28. Livak KJ, Schmittgen TD. Analysis of relative gene expression data using real-time quantitative PCR and the $2^{-\Delta\Delta C}{}_T$ method. *Methods,* 2001, 25:402-408.

29. Montazeri Aliabadi H, Landry B, Mahdipoor P, Uludağ H. Induction of apoptosis by survivin silencing through siRNA delivery in a human breast cancer cell line. *Mol Pharm,* 2011, 8:1821-1830.

30. Opalinska JB, Gewirtz AM. Nucleic-acid therapeutics: basic principles and recent applications. *Nat Rev Drug Discov,* 2002, 1:503-514.

31. Alvarez-Salas LM. Nucleic acids as therapeutic agents. *Curr Top Med Chem,* 2008, 8:1379-1404.

32. Elsabahy M, Nazarali A, Foldvari M. Non-viral nucleic acid delivery: key challenges and future directions. *Curr Drug Deliv,* 2011, 8:235-244.

33. Hsu CY, Uludağ H. Nucleic-acid based gene therapeutics: delivery challenges and modular design of nonviral gene carriers and expression cassettes to overcome intracellular barriers for sustained targeted expression. *J Drug Target,* 2012, 20:301-328.

34. KC RB, Thapa B, Valencia-Serna J, Aliabadi HM, Uludağ H. Nucleic acid combinations: A new frontier for cancer treatment. *J Control Release,* 2017, 256:153-169.

35. Valencia-Serna J, Gul-Uludağ H, Mahdipoor P, Jiang X, Uludağ H. Investigating siRNA delivery to chronic myeloid leukemia K562 cells with lipophilic polymers for therapeutic BCR–ABL downregulation. *J Control Release,* 2013, 172:495–503.

36. Jha K, Shukla M, Pandey M. Survivin expression and targeting in breast cancer. *Surg Oncol,* 2012, 21:125-131.

37. Almalik A, Benabdelkamel H, Masood A, Alanazi IO, Alradwan I, Majrashi MA, Alfadda AA, Alghamdi WM, Alrabiah H, Tirelli N, Alhasan AH. Hyaluronic acid coated chitosan nanoparticles reduced the immunogenicity of the formed protein corona. *Sci Rep,* 2017, 7:10542.

38. Huang G, Huang H. Application of hyaluronic acid as carriers in drug delivery. *Drug Delivery,* 2018, 25:766-772.

6. Overall conclusions, discussion and future directions

6.1 Overall Conclusions

This dissertation explored cell cycle proteins as potential siRNA-mediated therapeutic targets for breast cancer therapy along with anti-apoptotic and phosphatase proteins. We also formulated tailored PEI-based siRNA delivery agents and showed the importance of formulation details while preparing the siRNA/polymer polyplexes. The review of literature stated clearly how crucial it is to find alternative and specific therapies for breast cancer due to side-effects of current therapeutics regimes (**Chapter 1**). RNAi-mediated targeting of deregulated cell cycle proteins has a great potential to decrease the growth of malignant cells. A critical APC activator protein, CDC20, has recently emerged to have an oncogenic role in several human malignancies, and silencing CDC20 with RNAi therapeutics is believed to be a promising strategy to decrease tumor growth. We further established that combinational therapy against cell cycle and anti-apoptotic/phosphatase proteins has higher beneficial role in cancer therapy compared to targeting single protein alone. Furthermore, we reviewed several strategies to engineer nanoparticle so that better tumor homing of therapeutic molecules and higher efficacy of cancer therapy could be achieved.

The screening of siRNA library led to the identification of CDC20, RAD51 and CHEK1 as promising targets among cell cycle proteins for non-viral RNAi therapy (**Chapter 2**). Although we expected the siRNA therapy against cell cycle proteins to sensitize the cells with chemotherapy, no such effect was evident when doxorubicin was employed as the chemotherapeutic drug. Nevertheless, CDC20 siRNA alone effectively decreased the growth of breast cancer xenografts in mice, when we used a linoleic acid-substituted 2 kDa PEI to deliver CDC20 siRNA in animals. This study highlighted the

importance of cell cycle protein targets in breast cancer therapy, and provided an effective siRNA delivery carrier to silence these targets.

Based on our literature search, we noted that the combination of cell cycle proteins (TTK and CDC20) and an anti-apoptotic protein, survivin could be promising targets for siRNA therapy to decrease the proliferation of triple-negative breast cancer cells (**Chapter 3**). This study has indicated improved therapeutic efficacy of siRNAs by employing combinational siRNAs against cell cycle and anti-apoptosis proteins in breast cancer cells. The engineered polymers such as PEI-LA employed here could be used to deliver multiple siRNAs against critical targets. Co-delivery of siRNAs did not impair the desired silencing efficiency observed with individual siRNAs. However, the siRNA therapy with the chosen targets showed significant non-specific effects on non-malignant cells *in vitro*. Non-specific effects of siRNA could be minimized with specific formulation of siRNA/polymer complexes.

In **Chapter 4**, we established a new polymeric siRNA delivery system based on PEI-LA/HA that could serve as a viable platform to target breast cancer cells. As cellular uptake of siRNA greatly increased with the addition of HA into the delivery system, a more favorable interaction of siRNA/polymer complexes with the triple-negative breast cancer cells was evident compared to complexes without HA. The cell-surface receptor CD44 played a role in increased uptake, but that did not appear to be the sole mechanism for siRNA delivery into the cells, and improved physicochemical characteristics might have played a significant role. The identified phosphatases could serve as potential targets to inhibit migration of highly aggressive breast cancer cells. Moreover, combinational siRNA delivery against cell cycle and phosphatases could be a promising strategy to inhibit both

growth and migration of metastatic breast cancer cells. These could be further developed to treat other types of metastatic cancer.

In **Chapter 5**, we formulated additive siRNA polyplexes using PEI-LA with natural polymer HA and synthetic polymer PA, which showed an improved delivery of siRNA due to better dissociation of siRNA/polymer polyplexes. Both siRNA and pDNA could be delivered with improved efficiency using the same additive polyplexes, indicating the possibility of applying these formulations to different types of nucleic acid therapeutics. The CDC20 and survivin siRNAs delivered by additive polyplexes showed promising results in breast cancer cells to inhibit their growth, but undesirable effects were also evident in non-malignant cells. A careful formulation of additive siRNA/polymer polyplexes could potentially minimize side effects on normal cells. Since the efficacy of siRNA delivery by additive polyplexes was independent of breast cancer phenotypes, these polyplexes could be functional for a range of breast cancers and additionally in other types of cancers.

6.2 Discussion and future directions on cell cycle protein targets

We established the importance of targeting deregulated cell cycle protein in breast cancer. Specifically, we focused on CDC20 and our results clearly indicated that silencing CDC20 with siRNA has a promising impact on breast cancer growth. Since CDC20 is a key regulatory protein in cell cycle modulation during transition from metaphase to anaphase, silencing CDC20 in breast cancer cells would have arrested cell cycle that ultimately would have led to cell growth inhibition. Several other proteins contributing to cell cycle regulation, such as CDKs, cyclins, kinesin protein family, cell division cycle proteins, checkpoint kinases, centromere proteins, RAD homolog proteins, *etc.* have also

been found to be deregulated in many cancer types [1-6]. These cell cycle proteins could also serve as potential targets for cancer treatment, and those should be further explored to determine whether they contribute to oncogenesis.

Combinational siRNA therapy against CDC20 and survivin showed synergistic effects of dual targeting. Several other anti-apoptotic proteins have also been found to be upregulated in cancer such as BCL2 family [7], which could be taken into account for the combinational siRNA therapy. Furthermore, animal study confirming the validity of dual targeting against cell cycle and anti-apoptotic proteins would make a strong case for this therapeutic strategy. Orthotopic animal models are more preferable for such studies compared to heterotopic models as they offer tissue site-specific pathology and are generally deemed more clinically relevant [8,9].

We further evaluated our therapeutic strategy to tackle metastatic breast cancer by targeting cell cycle and phosphatase proteins. We established this strategy based on our *in vitro* results of cell migration inhibition by phosphatase siRNA. However, *in vivo* study is needed to confirm this therapeutic strategy. Orthotopic animal models must be used for *in vivo* study as they allow studies of metastasis as well. Potential site of metastasis such as liver, spleen, lung, etc. should be evaluated after siRNA therapy. Circulating DNA and tumor cells could also serve as a potential biomarker of breast cancer metastasis [10].

If synthetic lethality relationship between two critical cell cycle proteins has been established, combinational targeting of these specific proteins may result in drastic impact of siRNA therapy. Synthetic lethality occurs when the simultaneous silencing of two critical proteins results in cell growth inhibition [11]. Two proteins are considered synthetic lethal only when cell death occurs with their simultaneous silencing. Synthetic lethality

relationship should be explored between cell cycle and anti-apoptotic/phosphatase proteins to increase the impact of siRNA therapy in breast cancer cells.

We observed non-specific effects of siRNA therapy in non-malignant cells *in vitro*, which should be evaluated *in vivo* as well. Since cell cycle protein targets explored here are also present in normal cells, there is a chance that these proteins could be silenced in normal cells, resulting in adverse effects of therapy. To nullify side-effects of siRNA therapy, mutated cell cycle proteins that contribute to oncogenesis could be identified and targeted by siRNA. Alternatively, deregulated cell cycle protein with the similar characteristics as survivin (*i.e.,* mostly absent in terminally differentiated cells) could be identified and targeted by siRNA.

In addition to siRNA, other RNAi therapeutics could be explored for cell cycle targeting as well. Several miRNA that target cell cycle proteins have been identified as potential therapeutic tools for cancer [12]. Multiple cell cycle proteins can be targeted with just one miRNA reagent due to its complementarity to several proteins. Another RNA therapeutic agent, piwi-interacting RNA (piRNA) has recently emerged as a potential cancer therapeutic agent [13]. The piRNA that specifically targets cell cycle proteins could be explored as well. Recently, mRNA delivery has been exploited in the development of novel therapeutics for genetic diseases and cancer [14,15]. mRNA therapeutics could be delivered to express specific protein in cancer cells, which could potentially contribute to halt the cell cycle. Even though we mainly focused here on siRNA delivery, other RNA therapeutics have a great potential and those may be considered for breast cancer therapy as well.

Cell cycle protein targets could be evaluated *ex vivo* as well. Breast cancer patient samples could be cultured [16] and specific siRNA therapy should be explored in patient-derived breast cancer cells. Alternatively, frozen tumor samples, normal adjacent tissues, and formalin fixed paraffin embedded tissues are available from Biobank [17]. These samples could be obtained to determine expression of specific target in tumor vs. normal adjacent tissues so that clinical relevance of the targeted protein could be established.

6.3 Discussion and future directions on siRNA delivery system

Here we used PEI modified with linoleic acid that showed higher transfection efficiency compared to non-modified PEI. We also determined the importance of formulation while preparing siRNA/polymer polyplexes as non-specific effects of siRNA could be minimized with specific formulation of siRNA/polymer complexes. Side-effects of siRNA were evident in endothelial and normal breast cell, while no effects of siRNA delivered by PEI-LA/HA was observed in bone marrow and kidney cells, suggesting a variability of PEI-LA/HA delivery system to transfect different cell-type. This could be advantageous and further explored to develop such a carrier that could potentially differentiate between malignant and non-malignant cells.

We characterized siRNA/polymer polyplexes extensively to understand the impact of improved physicochemical characteristics on breast cancer cells. HA-modified PEI-LA delivery system showed higher functional efficacy of siRNA compared to non-modified PEI-LA due to higher dissociation and better availability of siRNA inside cytoplasm rather than CD44 receptor-mediated uptake of polyplexes. Therefore, other polyanionic polymers such as poly(aspartic) acid should be explored to determine whether higher functional efficacy of siRNA could be achieved with other polymers. We observed better pDNA

delivery with PEI-LA/HA delivery system, which should be studied further to observe the promise of this delivery system for pDNA transfection. Perhaps, co-delivery of siRNA and pDNA could be performed to obtain higher efficacy of therapeutic treatment.

We have mainly performed *in vitro* studies with 2D cell culture and determined the outcome of siRNA delivery. Perhaps, siRNA delivery in 3D cell culture may reveal the distribution of siRNA/polymer complexes better as 3D cell culture can mimic the tumor microenvironment [18]. Breast cancer cell culture in 3D spheroids should be established and the efficacy of siRNA delivery and its distribution should be explored to obtain more physiologically relevant information. Apart from *in vitro* studies, bio-distribution and toxicity of siRNA delivery system need to be outlined *in vivo* to better understand pharmacokinetics of siRNA/polymer polyplexes. The importance of formulating siRNA/polymer polyplexes need to be defined in preclinical settings as well.

Overall, an ideal carrier or siRNA that could target cancer cells solely still remains to be conceptualized, designed and synthesized **(Fig 6.1)**. Studies for such systematic investigations remain to be conducted for deploying siRNA therapy for breast cancer.

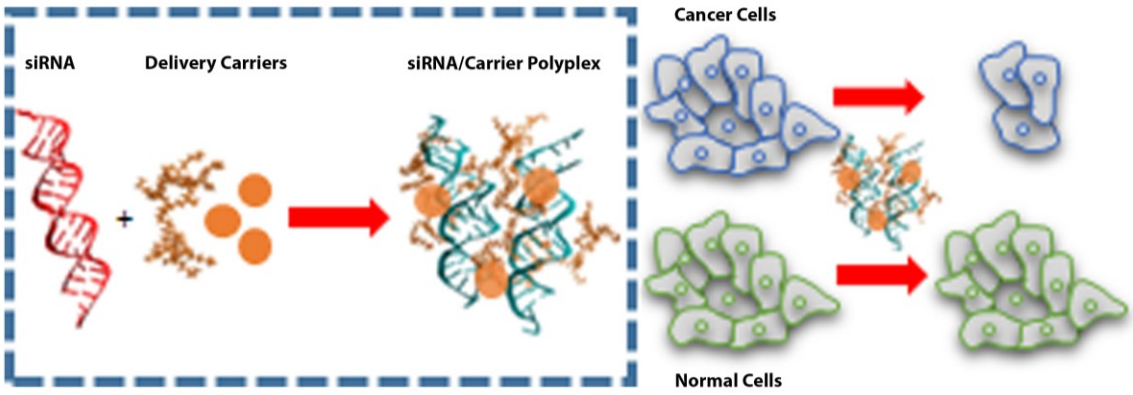

Fig 6.1: An illustration of an ideal siRNA or its delivery carrier that would target cancer cells solely without affecting normal cells.

6.4 References

1. Malumbres M, Carnero A. Cell cycle deregulation: a common motif in cancer. *Prog Cell Cycle Res*, 2003, 5:5-18.
2. Vermeulen K, Van Bockstaele DR, Berneman ZN. The cell cycle: a review of regulation, deregulation and therapeutic targets in cancer. *Cell Prolif*, 2003, 36:131-149.
3. Casimiro MC, Crosariol M, Loro E, Li Z, Pestell RG. Cyclins and cell cycle control in cancer and disease. *Genes Cancer*, 2012, 3:649-657.
4. Chong T, Sarac A, Yao CQ, Liao L, Lyttle N, Boutros PC, Bartlett JMS, Spears M. Deregulation of the spindle assembly checkpoint is associated with paclitaxel resistance in ovarian cancer. *J Ovarian Res*, 2018, 11:27.
5. Liao WT, Wang X, Xu LH, Kong QL, Yu CP, Li MZ, Shi L, Zeng MS, Song LB. Centromere protein H is a novel prognostic marker for human nonsmall cell lung cancer progression and overall patient survival. *Cancer*, 2009, 115:1507-1517.
6. Hannay JA, Liu J, Zhu QS, Bolshakov SV, Li L, Pisters PW, Lazar AJ, Yu D, Pollock RE, Lev D. Rad51 overexpression contributes to chemoresistance in human soft tissue sarcoma cells: a role for p53/activator protein 2 transcriptional regulation. *Mol Cancer Ther*, 2007, 6:1650-1660.
7. Yip KW, Reed JC. Bcl-2 family proteins and cancer. *Oncogene*, 2008, 27:6398-6406.
8. Paschall AV, Liu K. An orthotopic mouse model of spontaneous breast cancer metastasis. *J Vis Exp*, 2016, 114:54040.
9. Guo W, Zhang S, Liu S. Establishment of a novel orthotopic model of breast cancer metastasis to the lung. *Oncol Rep*, 2015, 33:2992-2998.
10. Rossi G, Mu Z, et al. Cell-free DNA and circulating tumor cells: comprehensive liquid biopsy analysis in advanced breast cancer. *Clin Cancer Res*, 2018, 24:560-568.
11. Nijman SM. Synthetic lethality: general principles, utility and detection using genetic screens in human cells. *FEBS Lett*, 2011, 585:1-6.
12. Hydbring P, Wang Y, Fassl A, et al. Cell-cycle-targeting MicroRNAs as therapeutic tools against refractory cancers. *Cancer Cell*, 2017, 31:576-590.
13. Assumpção CB, Calcagno DQ, Araújo TM, Santos SE, Santos ÂK, Riggins GJ, Burbano RR, Assumpção PP. The role of piRNA and its potential clinical implications in cancer. *Epigenomics*, 2015, 7:975-984.
14. Weissman D, Karikó K. mRNA: Fulfilling the promise of gene therapy. *Mol Ther*, 2015, 23:1416-1417.
15. Guan S, Rosenecker J. Nanotechnologies in delivery of mRNA therapeutics using nonviral vector-based delivery systems. *Gene Ther*, 2017, 24:133-143.
16. Nishikata T, Ishikawa M, Matsuyama T, Takamatsu K, Fukuhara T, Konishi Y. Primary culture of breast cancer: a model system for epithelial-mesenchymal transition and cancer stem cells. *Anticancer Res*, 2013, 33:2867-2873.
17. Castillo-Pelayo T, Babinszky S, LeBlanc J, Watson PH. The importance of biobanking in cancer research. *Biopreserv Biobank*, 2015, 13:172-177.
18. Edmondson R, Broglie JJ, Adcock AF, Yang L. Three-dimensional cell culture systems and their applications in drug discovery and cell-based biosensors. *Assay Drug Dev Technol*, 2014, 12:207-218.

Unified Bibliography

1.1 Joo WD, Visintin I, Mor G. Targeted cancer therapy - are the days of systemic chemotherapy numbered? *Maturitas*, 2013, 76:308-314.

1.2 Tannock IF. Conventional cancer therapy: promise broken or promise delayed? *Lancet*, 1998, 351 Suppl 2:SII9-SII16.

1.3 Abdelrahim M, Safe S, Baker C, Abudayyeh A. RNAi and cancer: Implications and applications. *J RNAi Gene Silencing*, 2006, 2:136-145.

1.4 Chakraborty C, Sharma AR, Sharma G, Doss CGP, Lee SS. Therapeutic miRNA and siRNA: moving from bench to clinic as next generation medicine. *Mol Ther Nucleic Acids*, 2017, 8:132-143.

1.5 Surakasula A, Nagarjunapu GC, Raghavaiah KV. A comparative study of pre- and post-menopausal breast cancer: Risk factors, presentation, characteristics and management. *J Res Pharm Pract*, 2014, 3:12-18.

1.6 Singh V, Saunders C, Wylie L, Bourke A. New diagnostic techniques for breast cancer detection. *Future Oncol*, 2008, 4:501-513.

1.7 Hon JD, Singh B, et al. Breast cancer molecular subtypes: from TNBC to QNBC. *Am J Cancer Res*, 2016, 6:1864-1872.

1.8 Mohamed A, Krajewski K, Cakar B, Ma CX. Targeted therapy for breast cancer. *Am J Pathol*, 2013, 183:1096-1112.

1.9 Aydiner A, Sen F, Karanlik H, Aslay I, Dincer M, İğci A. A Review of Local and Systemic Therapy in Breast Cancer. In: Aydiner A, İgci A, Soran A. (ed.) *Breast Disease*, 2016, Springer, Cham, Switzerland.

1.10 Miller E, Lee HJ, Lulla A, Hernandez L, Gokare P, Lim B. Current treatment of early breast cancer: adjuvant and neoadjuvant therapy. *F1000Res*, 2014, 3:198.

1.11 Karam A. Update on breast cancer surgery approaches. *Curr Opin Obstet Gynecol*, 2013, 25:74-80.

1.12 Joshi SC, Khan FA, Pant I, Shukla A. Role of radiotherapy in early breast cancer: an overview. *Int J Health Sci (Qassim)*, 2007, 1:259-264.

1.13 Brown LC, Mutter RW, Halyard MY. Benefits, risks, and safety of external beam radiation therapy for breast cancer. *Int J Womens Health*, 2015, 7:449-458.

1.14 Deng X, Wu H, Gao F, Su Y, Li Q, Liu S, Cai J. Brachytherapy in the treatment of breast cancer. *Int J Clin Oncol*, 2017, 22:641-650.

1.15 Monroe AT, Feigenberg SJ, Mendenhall NP. Angiosarcoma after breast-conserving therapy. *Cancer*, 2003, 97:1832-1840.

1.16 Apuri S. Neoadjuvant and Adjuvant Therapies for Breast Cancer. *South Med J*, 2017, 110:638-642.

1.17 Hassan MS, Ansari J, Spooner D, Hussain SA. Chemotherapy for breast cancer (Review). *Oncol Rep*, 2010, 24:1121-1131.

1.18 Partridge AH, Burstein HJ, Winer EP. Side effects of chemotherapy and combined chemohormonal therapy in women with early-stage breast cancer. *J Natl Cancer Inst Monogr*, 2001, 2001:135-142.

1.19 Abdulkareem IH, Zurmi IB. Review of hormonal treatment of breast cancer. *Niger J Clin Pract*, 2012, 15:9-14.

1.20 Tremont A, Lu J, Cole JT. Endocrine Therapy for Early Breast Cancer: Updated Review. *Ochsner J*, 2017, 17:405-411.

1.21 Wiseman LR, Goa KL. Toremifene. A review of its pharmacological properties and clinical efficacy in the management of advanced breast cancer. *Drugs*, 1997, 54:141-160.

1.22 Riemsma R, Forbes CA, Kessels A, Lykopoulos K, Amonkar MM, Rea DW, Kleijnen J. Systematic review of aromatase inhibitors in the first-line treatment for hormone sensitive advanced or metastatic breast cancer. *Breast Cancer Res Treat*, 2010, 123:9-24.

1.23 Loibl S, Gianni L. HER2-positive breast cancer. *Lancet*, 2017, 389:2415-2429.

1.24 Mayer EL. Targeting breast cancer with CDK inhibitors. *Curr Oncol Rep*, 2015, 17:443.

1.25 Amir E, Seruga B, Serrano R, Ocana A. Targeting DNA repair in breast cancer: a clinical and translational update. *Cancer Treat Rev*, 2010, 36:557-565.

1.26 Schafer KA. The cell cycle: a review. *Vet Pathol*, 1998, 35:461-478.

1.27 Vermeulen K, Van Bockstaele DR, Berneman ZN. The cell cycle: a review of regulation, deregulation and therapeutic targets in cancer. *Cell Prolif*, 2003, 36:131-149.

1.28 Ahmad A, Wang Z, Ali R, Bitar B, Logna FT, Maitah MY, Bao B, Ali S, Kong D, Li Y, Sarkar FH. Cell Cycle Regulatory Proteins in Breast Cancer: Molecular Determinants of Drug Resistance and Targets for Anticancer Therapies. In: Aft RL. (ed.) *Targeting New Pathways and Cell Death in Breast Cancer*, 2012, InTech, Rijeka, Croatia.

1.29 Stewart ZA, Westfall MD, Pietenpol JA. Cell-cycle dysregulation and anticancer therapy. *Trends Pharmacol Sci*, 2003, 24:139-145.

1.30 Maya-Mendoza A, Tang CW, Pombo A, Jackson DA. Mechanisms regulating S phase progression in mammalian cells. *Front Biosci*, 2009, 14:4199-4213.

1.31 Norbury C, Nurse P. Animal cell cycles and their control. *Annu Rev Biochem*, 1992, 61:441-470.

1.32 Lodish H, Berk A, Kaiser CA, Krieger M, Scott MP, Bretscher A, Ploegh H, Matsudaira P. *Molecular Cell Biology (6th edition)*, 2008, W.H. Freeman, New York, USA.

1.33 Morgan D. *Cell Cycle: Principles of Control*, 2007, New Science Press, London, UK.

1.34 Liskay RM. Absence of a measurable G2 phase in two Chinese hamster cell lines. *PNAS*, 1977, 74:1622-1625.

1.35 Hartwell LH, Weinert TA. Checkpoints: controls that ensure the order of cell cycle events. *Science*, 1989, 246:629-634.

1.36 Pardee AB. G1 events and regulation of cell proliferation. *Science*, 1989, 246:603-608.

1.37 Zetterberg A, Larsson O, Wiman KG. What is the restriction point? *Curr Opin Cell Biol*, 7:835-842.

1.38 Maller Jl, Gautier J, Langan TA, Lohka MJ, Shenoy S, Shalloway D, Nurse P. Maturation-promoting factor and the regulation of the cell cycle. *J Cell Sci Suppl*, 1989, 12:53-63.

1.39 Castro A, Bernis C, Vigneron S, Labbé JC, Lorca T. The anaphase-promoting complex: a key factor in the regulation of cell cycle. *Oncogene*, 2005, 24:314-325.

1.40 Kramer ER, Scheuringer N, Podtelejnikov AV, Mann M, Peters JM. Mitotic regulation of the APC activator proteins CDC20 and CDH1. *Mol Biol Cell*, 2000, 11:1555-1569.

1.41 Peters JM. SCF and APC: the Yin and Yang of cell cycle regulated proteolysis. *Curr Opin Cell Biol*, 1998, 10:759-768.

1.42 Foe I, Toczyski D. Structural biology: a new look for the APC. *Nature*, 2011, 470:182-183.

1.43 Chang L, Barford D. Insights into the anaphase-promoting complex: a molecular machine that regulates mitosis. *Curr Opin Struct Biol*, 2014, 29:1-9.

1.44 Chang LF, Zhang Z, Yang J, McLaughlin SH, Barford D. Molecular architecture and mechanism of the anaphase-promoting complex. *Nature*, 2014, 513:388-393.

1.45 Hartwell LH, Mortimer RK, Culotti J, Culotti M. Genetic control of the cell division cycle in yeast: v. genetic analysis of CDC mutants. *Genetics*, 1973, 74:267-286.

1.46 Morgan DO. The D box meets its match. *Mol Cell*, 2013, 50:609-610.

1.47 Jin L, Williamson A, Banerjee S, Philipp I, Rape M. Mechanism of ubiquitin-chain formation by the human anaphase-promoting complex. *Cell*, 2008, 133:653-665.

1.48 Di Fiore B, Davey NE, Hagting A, Izawa D, Mansfeld J, Gibson TJ, Pines J. The ABBA motif binds APC/C activators and is shared by APC/C substrates and regulators. *Dev Cell*, 2015, 32:358-372.

1.49 Petersen BO, Wagener C, et al. Cell cycle- and cell growth-regulated proteolysis ofmammalian CDC6 is dependent on APC-CDH1. *Genes Dev*, 2000, 14:2330–2343.

1.50 Littlepage LE, Ruderman JV. Identification of a new APC/C recognition domain, the A box, which is required for the Cdh1-dependent destruction of the kinase Aurora-A during mitotic exit. *Genes Dev*, 2002, 16:2274–2285.

1.51 Araki M, Wharton RP, Tang Z, Yu H, Asano M. Degradation of origin recognition complex large subunit by the anaphase-promoting complex in Drosophila. *EMBO J*, 2003, 22:6115–6126.

1.52 Reis A, Levasseur M, Chang HY, Elliott DJ, Jones KT. The CRY box: a second APCcdh1-dependent degron in mammalian cdc20. *EMBO Rep*, 2006, 7:1040–1045.

1.53 Hames RS, Wattam SL, Yamano H, Bacchieri R, Fry AM. APC/C-mediated destruction of the centrosomal kinase Nek2A occurs in early mitosis and depends upon a cyclin A-type D-box. *EMBO J*, 2001, 20:7117–7127.

1.54 Amador V, Ge S, Santamaria PG, Guardavaccaro D, Pagano M. APC/C(Cdc20) controls the ubiquitin-mediated degradation of p21 in prometaphase. *Mol Cell*, 2007, 27:462–473.

1.55 Harley ME, Allan LA, Sanderson HS, Clarke PR. Phosphorylation of Mcl-1 by CDK1-cyclin B1 initiates its Cdc20-dependent destruction during mitotic arrest. *EMBO J*, 2010, 29:2407–2420.

1.56 Wan L, Tan M, et al. APC(Cdc20) suppresses apoptosis through targeting Bim for ubiquitination and destruction. *Dev Cell*, 2014, 29:377–391.

1.57 Yu H. Cdc20: a WD40 activator for a cell cycle degradation machine. *Mol Cell*, 2007, 27:3–16.

1.58 Hu D, Qiao X, Wu G, Wan Y. The emerging role of APC/CCdh1 in development. *Semin Cell Dev Biol*, 2011, 22:579–585.

1.59 Penas C, Ramachandran V, Ayad NG. The APC/C ubiquitin ligase: from cell biology to tumorigenesis. *Front Oncol*, 2011, 1:60.

1.60 Wang Z, Wan L, et al. Cdc20: a potential novel therapeutic target for cancer treatment. *Curr Pharm Des*, 2013, 19:3210–3214.

1.61 Li M, York JP, Zhang P. Loss of Cdc20 causes a securin-dependent metaphase arrest in two-cell mouse embryos. *Mol Cell Biol*, 2007, 27:3481–3488.

1.62 Wang L, Zhang J, Wan L, Zhou X, Wang Z, Wei W. Targeting Cdc20 as a novel cancer therapeutic strategy. *Pharmacol Ther*, 2015, 151:141-151.

1.63 Li D, Zhu J, et al. Overexpression of oncogenic STK15/BTAK/Aurora A kinase in human pancreatic cancer. *Clin Cancer Res*, 2003, 9:991–997.

1.64 Wu WJ, Hu KS, et al. CDC20 overexpression predicts a poor prognosis for patients with colorectal cancer. *J Transl Med*, 2013, 11:142.

1.65 Kim JM, Sohn HY, et al. Identification of gastric cancer-related genes using a cDNA microarray containing novel expressed sequence tags expressed in gastric cancer cells. *Clin Cancer Res*, 2005, 11:473–482.

1.66 Li J, Gao JZ, Du JL, Huang ZX, Wei LX. Increased CDC20 expression is associated with development and progression of hepatocellular carcinoma. *Int J Oncol*, 2014, 45:1547-1555.

1.67 Chang DZ, Ma Y, et al. Increased CDC20 expression is associated with pancreatic ductal adenocarcinoma differentiation and progression. *J Hematol Oncol*, 2012, 5:15.

1.68 Kato T, Daigo Y, Aragaki M, Ishikawa K, Sato M, Kaji M. Overexpression of CDC20 predicts poor prognosis in primary non-small cell lung cancer patients. *J Surg Oncol*, 2012, 106:423–430.

1.69 Zaravinos A, Lambrou GI, Boulalas I, Delakas D, Spandidos DA. Identification of common differentially expressed genes in urinary bladder cancer. *PLoS One*, 2011, 6:e18135.

1.70 Mondal G, Sengupta S, Panda CK, Gollin SM, Saunders WS, Roychoudhury S. Overexpression of Cdc20 leads to impairment of the spindle assembly checkpoint and aneuploidization in oral cancer. *Carcinogenesis*, 2007, 28:81–92.

1.71 Rajkumar T, Sabitha K, et al. Identification and validation of genes involved in cervical tumourigenesis. *BMC Cancer*, 2011, 11:80.

1.72 Majumder P, Bhunia S, Bhattacharyya J, Chaudhuri A. Inhibiting tumor growth by targeting liposomally encapsulated CDC20 siRNA to tumor vasculature: therapeutic RNA interference. *J Control Release*, 2014, 180:100–108.

1.73 Yuan B, Xu Y, et al. Increased expression of mitotic checkpoint genes in breast cancer cells with chromosomal instability. *Clin Cancer Res*, 2006, 12:405–410.

1.74 Bièche I, Vacher S, et al. Expression analysis of mitotic spindle checkpoint genes in breast carcinoma: role of NDC80/HEC1 in early breast tumorigenicity, and a two-gene signature for aneuploidy. *Mol Cancer*, 2011, 10:23.

1.75 Karra H, Repo H, et al. Cdc20 and securin overexpression predict short-term breast cancer survival. *Br J Cancer*, 2014, 110:2905–2913.

1.76 Zeng X, Sigoillot F, et al. Pharmacologic inhibition of the anaphase-promoting complex induces a spindle checkpoint dependent mitotic arrest in the absence of spindle damage. *Cancer Cell*, 2010, 18:382–395.

1.77 Sackton KL, Dimova N, et al. Synergistic blockade of mitotic exit by two chemical inhibitors of the APC/C. *Nature*, 2014, 514:646–649.

1.78 Das T, Roy KS, Chakrabarti T, Mukhopadhyay S, Roychoudhury S. Withaferin A modulates the spindle assembly checkpoint by degradation of Mad2-Cdc20 complex in colorectal cancer cell lines. *Biochem Pharmacol*, 2014, 91:31–39.

1.79 Jiang J, Thyagarajan-Sahu A, Krchnak V, Jedinak A, Sandusky GE, Sliva D. NAHA, a novel hydroxamic acid-derivative, inhibits growth and angiogenesis of breast cancer *in vitro* and *in vivo*. *PLoS One*, 2012, 7:e34283.

1.80 Puliyappadamba VT, Wu W, et al. Antagonists of anaphase-promoting complex (APC)-2-cell cycle and apoptosis regulatory protein (CARP)-1 interaction are novel regulators of cell growth and apoptosis. *J Biol Chem*, 2011, 286:38000–38017.

1.81 Nasr T, Bondock S, Youns M. Anticancer activity of new coumarin substituted hydrazide–hydrazone derivatives. *Eur J Med Chem*, 2014, 76:539–548.

1.82 Taniguchi K, Momiyama N, Ueda M, Matsuyama R, Mori R, Fujii Y, Ichikawa Y, Endo I, Togo S, Shimada H. Targeting of CDC20 via small interfering RNA causes enhancement of the cytotoxicity of chemoradiation. *Anticancer Res*, 2008, 28:1559-1563.

1.83 Kidokoro T, Tanikawa C, Furukawa Y, Katagiri T, Nakamura Y, Matsuda K. CDC20, a potential cancer therapeutic target, is negatively regulated by p53. *Oncogene*, 2008, 27:1562-1571.

1.84 Liu M, Zhang Y, Liao Y, Chen Y, Pan Y, Tian H, Zhan Y, Liu D. Evaluation of the antitumor efficacy of RNAi-mediated inhibition of CDC20 and heparanase in an orthotopic liver tumor model. *Cancer Biother Radiopharm*, 2015, 30:233-239.

1.85 Li K, Mao Y, et al. Silencing of CDC20 suppresses metastatic castration-resistant prostate cancer growth and enhances chemosensitivity to docetaxel. *Int J Oncol*, 2016, 49:1679-1685.

1.86 Mukherjee A, Bhattacharyya J, Sagar MV, Chaudhuri A. Liposomally encapsulated CDC20 siRNA inhibits both solid melanoma tumor growth and spontaneous growth of intravenously injected melanoma cells on mouse lung. *Drug Deliv Transl Res*, 2013, 3:224-234.

1.87 Bhunia S, Radha V, Chaudhuri A. CDC20 siRNA and paclitaxel co-loaded nanometric liposomes of a nipecotic acid-derived cationic amphiphile inhibit xenografted neuroblastoma. *Nanoscale*, 2017, 9:1201-1212.

1.88 Parmar MB, Aliabadi HM, Mahdipoor P, Kucharski C, Maranchuk R, Hugh JC, Uludağ H. Targeting cell cycle proteins in breast cancer cells with siRNA by using lipid-substituted polyethylenimines. *Front Bioeng Biotechnol*, 2015, 3:14.

1.89 Parmar MB, Arteaga Ballesteros BE, Fu T, K.C. RB, Montazeri Aliabadi H, Hugh JC, Löbenberg R, Uludağ H. Multiple siRNA delivery against cell cycle and anti-apoptosis proteins using lipid-substituted polyethylenimine in triple-negative breast cancer and nonmalignant cells. *J Biomed Mater Res A*, 2016, 104:3031-3044.

1.90 Parmar MB, Meenakshi Sundaram DN, K.C. RB, Maranchuk R, Montazeri Aliabadi H, Hugh JC, Löbenberg R, Uludağ H. Combinational siRNA delivery using hyaluronic acid modified amphiphilic polyplexes against cell cycle and phosphatase proteins to inhibit growth and migration of triple-negative breast cancer cells. *Acta Biomater*, 2018, 66:294-309.

1.91 Parmar MB, K.C. RB, Löbenberg R, Uludağ H. Additive polyplexes to undertake siRNA therapy against CDC20 and survivin in breast cancer cells. *Biomacromolecules*, 2018, 19:4193–4206.

1.92 Xie Q, Wu Q, et al. CDC20 maintains tumor initiating cells. *Oncotarget*, 2015, 6:13241-13254.

1.93 Wang L, Hou Y, Yin X, Su J, Zhao Z, Ye X, Zhou X, Zhou L, Wang Z. Rottlerin inhibits cell growth and invasion via down-regulation of Cdc20 in glioma cells. *Oncotarget*, 2016, 7:69770-69782.

1.94 Paul D, Ghorai S, Dinesh US, Shetty P, Chattopadhyay S, Santra MK. Cdc20 directs proteasome-mediated degradation of the tumor suppressor SMAR1 in higher grades of cancer through the anaphase promoting complex. *Cell Death Dis*, 2017, 8:e2882.

1.95 Baumgarten AJ, Felthaus J, Wäsch R. Strong inducible knockdown of APC/C^{CDC20} does not cause mitotic arrest in human somatic cells. *Cell Cycle*, 2009, 8:643-646.

1.96 Yamanaka S, Campbell NR, An F, Kuo SC, Potter JJ, Mezey E, Maitra A, Selaru FM. Coordinated effects of microRNA-494 induce G_2/M arrest in human cholangiocarcinoma. *Cell Cycle*, 2012, 11:2729-2738.

1.97 Frenzel A, Grespi F, Chmelewskij W, Villunger A. Bcl2 family proteins in carcinogenesis and the treatment of cancer. *Apoptosis*, 2009, 14:584-596.

1.98 Wang S, Bai L, Lu J, Liu L, Yang CY, Sun H. Targeting inhibitors of apoptosis proteins (IAPs) for new breast cancer therapeutics. *J Mammary Gland Biol Neoplasia*, 2012, 17:217-228.

1.99 Krueger A, Baumann S, Krammer PH, Kirchhoff S. FLICE-inhibitory proteins: regulators of death receptor-mediated apoptosis. *Mol Cell Biol*, 2001, 21:8247-8254.

1.100 Safa AR. c-FLIP, a master anti-apoptotic regulator. *Exp Oncol*, 2012, 34:176-184.

1.101 Shamas-Din A, Kale J, Leber B, Andrews DW. Mechanisms of action of Bcl-2 family proteins. *Cold Spring Harb Perspect Biol*, 2013, 5:a008714.

1.102 Oberoi-Khanuja TK, Murali A, Rajalingam K. IAPs on the move: role of inhibitors of apoptosis proteins in cell migration. *Cell Death Dis*, 2013, 4:e784.

1.103 Mita AC, Mita MM, Nawrocki ST, Giles FJ. Survivin: key regulator of mitosis and apoptosis and novel target for cancer therapeutics. *Clin Cancer Res*, 2008, 14:5000-5005.

1.104 Khan S, Ferguson Bennit H, et al. Localization and upregulation of survivin in cancer health disparities: a clinical perspective. *Biologics*, 2015, 9:57-67.

1.105 Vader G, Kauw JJ, Medema RH, Lens SM. Survivin mediates targeting of the chromosomal passenger complex to the centromere and midbody. *EMBO Rep*, 2006, 71:85-92.

1.106 Sampath SC, Ohi R, Leismann O, Salic A, Pozniakovski A, Funabiki H. The chromosomal passenger complex is required for chromatin-induced microtubule stabilization and spindle assembly. *Cell*, 2004, 118:187-202.

1.107 Giodini A, Kallio MJ, et al. Regulation of microtubule stability and mitotic progression by survivin. *Cancer Res*, 2002, 62:2462-2467.

1.108 Altieri DC. The case for survivin as a regulator of microtubule dynamics and cell-death decisions. *Curr Opin Cell Biol*, 2006, 18:609-615.

1.109 Tamm I, Wang Y, et al. IAP-family protein survivin inhibits caspase activity and apoptosis induced by Fas (CD95), Bax, caspases, and anticancer drugs. *Cancer Res*, 1998, 5823:5315-5320.

1.110 Adida C, Berrebi D, Peuchmaur M, Reyes-Mugica M, Altieri DC. Anti-apoptosis gene, survivin, and prognosis of neuroblastoma. *Lancet*, 1998, 351:882-883.

1.111 ZhangT, Otevrel T, et al. Evidence that APC regulates survivin expression: a possible mechanism contributing to the stem cell origin of colon cancer. *Cancer Res*, 2001, 61:8664-8667.

1.112 Fukuda S, Pelus LM. Regulation of the inhibitorof- apoptosis family member survivin in normal cord blood and bone marrow CD34(+) cells by hematopoietic growth factors: implication of survivin expression in normal hematopoiesis. *Blood*, 2001, 98:2091-2100.

1.113 Gianani R, Jarboe E, et al. Expression of survivin innormal, hyperplastic, and neoplastic colonic mucosa. *Hum Pathol*, 2001, 32:119-125.

1.114 Altieri DC. Survivin, cancer networks and pathway-directed drug discovery. *Nat Rev Cancer*, 2008, 81:61-70.

1.115 Blanc-Brude OP, Mesri M, Wall NR, Plescia J, Dohi T, Altieri DC. Therapeutic targeting of the survivin pathway in cancer: initiation of mitochondrial apoptosis and suppression of tumor-associated angiogenesis. *Clin Cancer Res*, 2003, 97:2683-2692.

1.116 Tu SP, Jiang XH, et al. Suppression of survivin expression inhibits *in vivo* tumorigenicity and angiogenesis in gastric cancer. Cancer Res, 2003, 6322:7724-7732.

1.117 Pennati M, Folini M, Zaffaroni N. Targeting survivin in cancer therapy: fulfilled promises and open questions. *Carcinogenesis*, 2007, 286:1133-1139.

1.118 Ryan BM, O'Donovan N, Duffy MJ. Survivin: a new target for anti-cancer therapy. *Cancer Treat Rev*, 2009, 35:553-562.

1.119 Peery RC, Liu JY, Zhang JT. Targeting survivin for therapeutic discovery: past, present, and future promises. *Drug Discov Today*, 2017, 22:1466-1477.

1.120 Fernald K, Kurokawa M. Evading apoptosis in cancer. *Trends Cell Biol*, 2013, 23:620-633.

1.121 Tacar O, Sriamornsak P, Dass CR. Doxorubicin: an update on anticancer molecular action, toxicity and novel drug delivery systems. *J Pharm Pharmacol*, 2013, 65:157-170.

1.122 Horwitz SB. Taxol (paclitaxel): mechanisms of action. *Ann Oncol*, 1994, 5 Suppl 6:S3-S6.

1.123 Lee BS, Kim SH, Jin T, Choi EY, Oh J, Park S, Lee SH, Chung JH, Kang SM. Protective effect of survivin in Doxorubicin-induced cell death in h9c2 cardiac myocytes. *Korean Circ J*, 2013, 43:400-407.

1.124 Xiong H, Yu S, Zhuang L, Xiong H. Changes of survivin mRNA and protein expression during paclitaxel treatment in breast cancer cells. *J Huazhong Univ Sci Technolog Med Sci*, 2007, 27:65-67.

1.125 Dong H, Yao L, Bi W, Wang F, Song W, Lv Y. Combination of survivin siRNA with neoadjuvant chemotherapy enhances apoptosis and reverses drug resistance in breast cancer MCF-7 cells. J Cancer Res Ther, 2015, 11:717-722.

1.126 Colnaghi R, Wheatley SP. Liaisons between survivin and Plk1 during cell division and cell death. *J Biol Chem*, 2010, 285:22592-22604.

1.127 Seth S, Matsui Y, et al. RNAi-based therapeutics targeting survivin and PLK1 for treatment of bladder cancer. *Mol Ther*, 2011, 19:928-935.

1.128 Kedinger V, Meulle A, et al. Sticky siRNAs targeting survivin and cyclin B1 exert an antitumoral effect on melanoma subcutaneous xenografts and lung metastases. *BMC Cancer*, 2013, 13:338.

1.129 Zhao S, Sedwick D, Wang Z. Genetic alterations of protein tyrosine phosphatases in human cancers. *Oncogene*, 2015, 34:3885-3894.

1.130 Hardy S, Julien SG, Tremblay ML. Impact of oncogenic protein tyrosine phosphatases in cancer. *Anticancer Agents Med Chem*, 2012, 12:4-18.

1.131 Yu S, Li L, Wu Q, Dou N, Li Y, Gao Y. PPP2R2D, a regulatory subunit of protein phosphatase 2A, promotes gastric cancer growth and metastasis via mechanistic target of rapamycin activation. *Int J Oncol*, 2018, 52:2011-2020.

1.132 Luo W, Xu C, Ayello J, Dela Cruz F, Rosenblum JM, Lessnick SL, Cairo MS. Protein phosphatase 1 regulatory subunit 1A in ewing sarcoma tumorigenesis and metastasis. *Oncogene*, 2018, 37:798-809.

1.133 Tonks NK. Protein tyrosine phosphatases: from genes, to function, to disease. *Nat Rev Mol Cell Biol*, 2006, 7:833-846.

1.134 Zhang ZY. Protein tyrosine phosphatases: structure and function, substrate specificity, and inhibitor development. *Annu Rev Pharmacol Toxicol*, 2002, 42:209-234.

1.135 Mumby MC, Walter G. Protein serine/threonine phosphatases: structure, regulation, and functions in cell growth. *Physiol Rev*, 1993, 73:673-699.

1.136 Camps M, Nichols A, Arkinstall S. Dual specificity phosphatases: a gene family for control of MAP kinase function. *FASEB J*, 2000, 14:6-16.

1.137 Bäumer N, Mäurer A, Krieglstein J, Klumpp S. Expression of protein histidine phosphatase in *Escherichia coli*, purification, and determination of enzyme activity. *Methods Mol Biol*, 2007, 365:247-260.

1.138 Jiang Y. Regulation of the cell cycle by protein phosphatase 2A in *Saccharomyces cerevisiae*. *Microbiol Mol Biol Rev*, 2006, 70:440-449.

1.139 Cheng A, Ross KE, Kaldis P, Solomon MJ. Dephosphorylation of cyclin-dependent kinases by type 2C protein phosphatases. *Genes Dev*, 1999, 13:2946-2957.

1.140 Kim HS, Fernandes G, Lee CW. Protein Phosphatases Involved in Regulating Mitosis: Facts and Hypotheses. *Mol Cells*, 2016, 39:654-662.

1.141 Motiwala T, Jacob ST. Role of protein tyrosine phosphatases in cancer. *Prog Nucleic Acid Res Mol Biol*, 2006, 81:297-329.

1.142 Figueiredo J, da Cruz E Silva OA, Fardilha M. Protein phosphatase 1 and its complexes in carcinogenesis. *Curr Cancer Drug Targets*, 2014, 14:2-29.

1.143 Lee ST, Feng M, et al. Protein tyrosine phosphatase UBASH3B is overexpressed in triple-negative breast cancer and promotes invasion and metastasis. *Proc Natl Acad Sci USA*, 2013, 110:11121-11126.

1.144 Spring K, Fournier P, Lapointe L, Chabot C, Roussy J, Pommey S, Stagg J, Royal I. The protein tyrosine phosphatase DEP-1/PTPRJ promotes breast cancer cell invasion and metastasis. *Oncogene*, 2015, 34:5536-5547.

1.145 Hoekstra E, Peppelenbosch MP, Fuhler GM. The role of protein tyrosine phosphatases in colorectal cancer. *Biochim Biophys Acta*, 2012, 1826:179-188.

1.146 Nunes-Xavier CE, Mingo J, López JI, Pulido R. The role of protein tyrosine phosphatases in prostate cancer biology. *Biochim Biophys Acta Mol Cell Res*, 2019, 1866:102-113.

1.147 Ruvolo PP. Role of protein phosphatases in the cancer microenvironment. *Biochim Biophys Acta Mol Cell Res*, 2019, 1866:144-152.

1.148 Al-Aidaroos AQ, Zeng Q. PRL-3 phosphatase and cancer metastasis. *J Cell Biochem*, 2010, 111:1087-1098.

1.149 Feng X, Wu Z, Wu Y, Hankey W, Prior TW, Li L, Ganju RK, Shen R, Zou X. Cdc25A regulates matrix metalloprotease 1 through Foxo1 and mediates metastasis of breast cancer cells. *Mol Cell Biol*, 2011, 31:3457-3471.

1.150 Bollu LR, Mazumdar A, Savage MI, Brown PH. Molecular pathways: targeting protein tyrosine phosphatases in cancer. *Clin Cancer Res*, 2017, 23:2136-2142.

1.151 Scott LM, Lawrence HR, Sebti SM, Lawrence NJ, Wu J. Targeting protein tyrosine phosphatases for anticancer drug discovery. *Curr Pharm Des*, 2010, 16:1843-1862.

1.152 McConnell JL, Wadzinski BE. Targeting protein serine/threonine phosphatases for drug development. *Mol Pharmacol*, 2009, 75:1249-1261.

1.153 Liang F, Liang J, Wang WQ, Sun JP, Udho E, Zhang ZY. PRL3 promotes cell invasion and proliferation by down-regulation of Csk leading to Src activation. *J Biol Chem*, 2007, 282:5413-5419.

1.154 Csoboz B, Gombos I, Tatrai E, Tovari J, Kiss AL, Horvath I, Vigh L. Chemotherapy induced PRL3 expression promotes cancer growth via plasma membrane remodeling and specific alterations of caveolae-associated signaling. *Cell Commun Signal*, 2018, 16:51.

1.155 Xia ZS, Wu D, Zhong W, Lu XJ, Yu T, Chen QK. Wip1 gene silencing enhances the chemosensitivity of human colon cancer cells. *Oncol Lett*, 2017, 14:1875-1883.

1.156 Cao Y, Tu Y, Mei J, Li Z, Jie Z, Xu S, Xu L, Wang S, Xiong Y. RNAi-mediated knockdown of PRL-3 inhibits cell invasion and downregulates ERK 1/2 expression in the human gastric cancer cell line, SGC-7901. *Mol Med Rep*, 2013, 7:1805-1811.

1.157 Zimmerman MW, Homanics GE, Lazo JS. Targeted deletion of the metastasis-associated phosphatase Ptp4a3 (PRL-3) suppresses murine colon cancer. *PLoS One*, 2013, 8:e58300.

1.158 Wei M, Korotkov KV, Blackburn JS. Targeting phosphatases of regenerating liver (PRLs) in cancer. *Pharmacol Ther*, 2018, 2018, 190:128-138.

1.159 Fire A, Xu S, Montgomery MK, Kostas SA, Driver SE, Mello CC. Potent and specific genetic interference by double-stranded RNA in *Caenorhabditis elegans*. *Nature*, 1998, 391:806-811.

1.160 Hamilton AJ, Baulcombe DC. A species of small antisense RNA in posttranscriptional gene silencing in plants. *Science*, 1999, 286:950-952.

1.161 Bentwich I, et al. Identification of hundreds of conserved and nonconserved human microRNAs. *Nature Genet*, 2005, 37:766-770.

1.162 Moore CB, Guthrie EH, Huang MT, Taxman DJ. Short hairpin RNA (shRNA): design, delivery, and assessment of gene knockdown. *Methods Mol Biol*, 2010, 629:141-158.

1.163 Kim DH, Rossi JJ. Strategies for silencing human disease using RNA interference. *Nature Rev Genet*, 2007, 8:173-184.

1.164 Wilson RC, Doudna JA. Molecular mechanisms of RNA interference. *Annu Rev Biophys*, 2013, 42:217-239.

1.165 Leuschner PJ, Ameres SL, Kueng S, Martinez J. Cleavage of the siRNA passenger strand during RISC assembly in human cells. *EMBO Rep*, 2006, 7:314-320.

1.166 Preall JB, Sontheimer EJ. RNAi: RISC gets loaded. *Cell*, 2005, 123:543-545.

1.167 Wang Z, Rao DD, Senzer N, Nemunaitis J. RNA interference and cancer therapy. *Pharm Res*, 2011, 28:2983-2995.

1.168 Aliabadi HM, Landry B, Sun C, Tang T, Uludağ H. Supramolecular assemblies in functional siRNA delivery: where do we stand? *Biomaterials*, 2012, 33:2546-2569.

1.169 Meneksedag-Erol D, Tang T, Uludağ H. Molecular modeling of polynucleotide complexes. Biomaterials, 2014, 35:7068-7076.

1.170 Aliabadi HM, Landry B, Bahadur RK, Neamnark A, Suwantong O, Uludağ H. Impact of lipid substitution on assembly and delivery of siRNA by cationic polymers. *Macromol Biosci*, 2011, 11:662-672.

1.171 Wang J, Lu Z, Wientjes MG, Au JL. Delivery of siRNA therapeutics: barriers and carriers. *AAPS J*, 2010, 12:492-503.

1.172 Hashida M, Kawakami S, Yamashita F. Lipid carrier systems for targeted drug and gene delivery. *Chem Pharm Bull*, 2005, 53:871-880.

1.173 Boussif O, Lezoualc'h F, Zanta MA, Mergny MD, Scherman D, Demeneix B, Behr JP. A versatile vector for gene and oligonucleotide transfer into cells in culture and *in vivo*: polyethylenimine. *Proc Natl Acad Sci USA*, 1995, 92:7297-7303.

1.174 Gong D et al. Cyclin A2 regulates nuclear-envelope breakdown and the nuclear accumulation of cyclin B1. *Curr Biol*, 2007, 17:85-91.

1.175 Sakurai H et al. Comparison of gene expression efficiency and innate immune response induced by Ad vector and lipoplex. *J Control Release*, 2007, 117:430-437.

1.176 Gautam A, Densmore CL, Waldrep JC. Pulmonary cytokine responses associated with PEI-DNA aerosol gene therapy. *Gene Ther*, 2001, 8:254-257.

1.177 Sakurai H, Kawabata K, Sakurai F, Nakagawa S, Mizuguchi H. Innate immune response induced by gene delivery vectors. *Int J Pharm*, 2008 354:9-15.

1.178 Lechardeur D, Lukacs GL. Nucleocytoplasmic transport of plasmid DNA: a perilous journey from the cytoplasm to the nucleus. *Hum Gene Ther*, 2006, 17:882-889.

1.179 Zang L, Nishikawa M, Machida K, Ando M, Takahashi Y, Watanabe Y, Takakura Y. Inhibition of nuclear delivery of plasmid DNA and transcription by interferon γ: hurdles to be overcome for sustained gene therapy. *Gene Ther*, 2011, 18:891-897.

1.180 Ribeiro SC, Monteiro GA, Prazeres DM. The role of polyadenylation signal secondary structures on the resistance of plasmid vectors to nucleases. *J Gene Med*, 2004, 6:565-573.

1.181 Whitehead KA, Dahlman JE, Langer RS, Anderson DG. Silencing or stimulation? siRNA delivery and the immune system. *Annu Rev Chem Biomol Eng*, 2011, 2:77-96.

1.182 Bessis N, GarciaCozar FJ, Boissier MC. Immune responses to gene therapy vectors: influence on vector function and effector mechanisms. *Gene Ther*, 2004, 11:S10-S17.

1.183 Riu E, Chen ZY, Xu H, He CY, Kay MA. Histone modifications are associated with the persistence or silencing of vector-mediated transgene expression *in vivo*. *Mol Ther*, 2007, 15:1348-1355.

1.184 Pillai RS. MicroRNA function: multiple mechanisms for a tiny RNA? *RNA*, 2005, 11:1753-1761.

1.185 Baumann V, Winkler J. miRNA-based therapies: strategies and delivery platforms for oligonucleotide and non-oligonucleotide agents. *Future Med Chem*, 2014, 6:1967-1984.

1.186 Shaukat Z, Liu D, Choo A, Hussain R, O'Keefe L, Richards R, Saint R, Gregory SL. Chromosomal instability causes sensitivity to metabolic stress. *Oncogene*, 2015, 34:4044-4055.

1.187 Aagaard L, Rossi JJ. RNAi therapeutics: principles, prospects and challenges. *Adv Drug Deliv Rev*, 2007, 59:75-86.

1.188 Carter MG, Sharov AA, VanBuren V, Dudekula DB, Carmack CE, Nelson C, Ko MS. Transcript copy number estimation using a mouse whole-genome oligonucleotide microarray. *Genome Biol*, 2005, 6:R61.

1.189 Bao T, Davidson NE. Gene expression profiling of breast cancer. *Adv Surg*, 2008, 42:249-260.

1.190 Owens DE III, Peppas NA. Opsonization, biodistribution, and pharmacokinetics of polymeric nanoparticles. *Int J Pharm*, 2006, 307:93-102.

1.191 Chithrani BD, Ghazani AA, Chan WC. Determining the size and shape dependence of gold nanoparticle uptake into mammalian cells. *Nano Lett*, 2006, 6:662-668.

1.192 Toy R, Peiris PM, Ghaghada KB, Karathanasis E. Shaping cancer nanomedicine: the effect of particle shape on the *in vivo* journey of nanoparticles. *Nanomedicine (Lond)*, 2014, 9:121–134.

1.193 Agarwal R, Jurney P, Raythatha M, et al. Effect of shape, size, and aspect ratio on nanoparticle penetration and distribution inside solid tissues using 3D spheroid models. *Adv Healthc Mater*, 2015, 4:2269–2280.

1.194 Sun B, Ji Z, Liao YP, et al. Engineering an effective immune adjuvant by designed control of shape and crystallinity of aluminum oxyhydroxide nanoparticles. *ACS Nano*, 2013, 7:10834–10849.

1.195 Shen H, Shi S, Zhang Z, Gong T, Sun X. Coating solid lipid nanoparticles with hyaluronic acid enhances antitumor activity against melanoma stem-like cells. *Theranostics*, 2015, 5:755-771.

1.196 Veronese FM, Mero A. The impact of PEGylation on biological therapies. *BioDrugs*, 2008, 22:315-329.

1.197 Teesalu T, Sugahara KN, Ruoslahti E. Tumor-penetrating peptides. *Front Oncol*, 2013, 3:216.

1.198 Cardoso MM, Peça IN, Roque AC. Antibody-conjugated nanoparticles for therapeutic applications. *Curr Med Chem*, 2012, 19:3103-3127.

2.1 Luqmani YA. Mechanisms of drug resistance in cancer chemotherapy. *Med Princ Pract*, 2005, 14:35-48.

2.2 Gillet JP, Gottesman MM. Mechanisms of multidrug resistance in cancer. *Methods Mol Biol,* 2010, 596:47-76.

2.3 McManus MT, Sharp PA. Gene silencing in mammals by small interfering RNAs. *Nat Rev Genet*, 2002, 3:737-747.

2.4 Kim DH, Rossi JJ. Strategies for silencing human disease using RNA interference. *Nat Rev Genet*, 2007, 8:173-184.

2.5 Wilson RC, Doudna JA. Molecular mechanisms of RNA interference. *Ann. Rev. Biophys,* 2013, 42:217-239.

2.6 Pecot CV, Calin GA, Coleman RL, Lopez-Berestein G, Sood AK. RNA interference in the clinic: challenges and future directions. *Nat Rev Cancer*, 2011, 11: 59-67.

2.7 Bora RS, Gupta D, Mukkur TK, Saini KS. RNA interference therapeutics for cancer: challenges and opportunities. *Mol Med Rep*, 2012, 6:9-15.

2.8 Haupenthal J, Baehr C, Kiermayer S, Zeuzem S, Piiper A. Inhibition of RNAse A family enzymes prevents degradation and loss of silencing activity of siRNAs in serum. *Biochem Pharmacol,* 2006, 71: 702-710.

2.9 Aliabadi HM, Landry B, Bahadur RK, Neamnark A, Suwantong O, Uludağ H. Impact of lipid substitution on assembly and delivery of siRNA by cationic polymers. *Macromol Biosci*, 2011, 11:662-672.

2.10 Montazeri Aliabadi H, Landry B, Mahdipoor P, Uludağ H. Induction of apoptosis by survivin silencing through siRNA delivery in a human breast cancer cell line. *Mol Pharm*, 2011, 8:1821-1830.

2.11 Aliabadi HM, Mahdipoor P, Uludağ H. Polymeric delivery of siRNA for dual silencing of Mcl-1 and P-glycoprotein and apoptosis induction in drug-resistant breast cancer cells. *Cancer Gene Ther*, 2013, 20:169-177.

2.12 Aliabadi HM, Maranchuk R, Kucharski C, Mahdipoor P, Hugh J, Uludağ H. Effective response of doxorubicin-sensitive and -resistant breast cancer cells to combinational siRNA therapy. *J Cont Rel*, 2013, 172:219-228.

2.13 Aliabadi HM, Landry B, Sun C, Tang T, Uludağ H. Supramolecular assemblies in functional siRNA delivery: where do we stand? *Biomaterials,* 2012, 33:2546-2569.

2.14 Cooper GM. *The Cell: A Molecular Approach (2nd Ed.)*, 2000, ASM Press, Washington, DC.

2.15 Malumbres M, Carnero A. Cell cycle deregulation: a common motif in cancer. *Prog Cell Cycle Res,* 2003, 5:5-18.

2.16 Sandhu C, Slingerland J. Deregulation of the cell cycle in cancer. *Cancer Detect Prev,* 2000, 24:107-118.

2.17 Vermeulen K, Van Bockstaele DR, Berneman ZN. The cell cycle: a review of regulation, deregulation and therapeutic targets in cancer. *Cell Prolif*, 2003, 36:131-149.

2.18 Parmar MB, Uludağ H. Targeting cyclins and cyclin-dependent kinases involved in cell cycle regulation by RNAi as a potential cancer therapy. In: Braddock M. (ed.) *Nanomedicines: Design, Delivery and Detection,* 2016, Royal Society of Chemistry, London, UK.

2.19 Blangy A, Lane HA, d'Hérin P, Harper M, Kress M, Nigg EA. Phosphorylation by p34cdc2 regulates spindle association of human Eg5, a kinesin-related motor essential for bipolar spindle formation *in vivo. Cell*, 1995, 83:1159-1169.

2.20 Dagenbach EM, Endow SA. A new kinesin tree. *J Cell Sci*, 2004, 117:3-7.

2.21 Marra E, Palombo F, Ciliberto G, Aurisicchio L. Kinesin spindle protein siRNA slows tumor progression. *J Cell Physiol*, 2013, 228:58-64.

2.22 Tabernero J, Shapiro GI, LoRusso PM, Cervantes A, Schwartz GK, Weiss GJ, et al. First-in-humans trial of an RNA interference therapeutic targeting VEGF and KSP in cancer patients with liver involvement. *Cancer Discovery,* 2013, 3:406-417.

2.23 Amarzguioui M, Rossi JJ. Principles of dicer substrate (D-siRNA) design and function. *Methods Mol Biol*, 2008, 442:3-10.

2.24 Bahadur KC, Landry B, Aliabadi HM, Lavasanifar A, Uludağ H. Lipid substitution on low molecular weight (0.6-2.0 kDa) polyethylenimine leads to a higher zeta potential of plasmid DNA and enhances transgene expression. *Acta Biomater,* 2011, 7:2209 2217.

2.25 Remant Bahadur KC, Uludağ H. A comparative evaluation of disulfide-linked and hydrophobically-modified PEI for plasmid delivery. *J Biomater Sci Polym Ed*, 2011, 22:873-892.

2.26 Sumantran VN. Cellular chemosensitivity assays: an overview. *Methods Mol Biol*, 2011, 731:219-236.

2.27 Snead NM, Wu X, Li A, Cui Q, Sakurai K, Burnett JC, Rossi JJ. Molecular basis for improved gene silencing by Dicer substrate interfering RNA compared with other siRNA variants. *Nucleic Acids Res*, 2013, 41:6209-6221.

2.28 Satyanarayana A, Kaldis P. Mammalian cell-cycle regulation: several Cdks, numerous cyclins and diverse compensatory mechanisms. *Oncogene,* 2009, 28:2925-2939.

2.29 Schwartz GK, Shah MA. Targeting the cell cycle: a new approach to cancer therapy. *J Clin Oncol,* 2005, 23:9408-9421.

2.30 Weinstein J. Cell cycle-regulated expression, phosphorylation, and degradation of p55Cdc. A mammalian homolog of CDC20/Fizzy/slp1. *J Biol Chem,* 1997, 272:28501-28511.

2.31 Galkin VE, Wu Y, Zhang XP, Qian X, He Y, Yu X, Heyer WD, Luo Y, Egelman EH. The Rad51/RadA N-terminal domain activates nucleoprotein filament ATPase activity. *Structure,* 2006, 14:983-992.

2.32 Chen MS, Ryan CE, Piwnica-Worms H. Chk1 kinase negatively regulates mitotic function of Cdc25A phosphatase through 14-3-3 binding. *Mol Cell Biol,* 2003, 23:7488-7497.

2.33 Iacomino G, Medici MC, Napoli D, Russo GL. Effects of histone deacetylase inhibitors on p55CDC/Cdc20 expression in HT29 cell line. *J Cell Biochem*, 2006, 99:1122-1131.

2.34 Kim JM, Sohn HY, Yoon SY, Oh JH, Yang JO, Kim JH, et al. Identification of gastric cancer-related genes using a cDNA microarray containing novel expressed sequence tags expressed in gastric cancer cells. *Clin Cancer Res*, 2005, 11:473-482.

2.35 Ouellet V, Guyot MC, Le Page C, Filali-Mouhim A, Lussier C, Tonin PN, Provencher DM, Mes-Masson AM. Tissue array analysis of expression microarray candidates identifies markers associated with tumor grade and outcome in serous epithelial ovarian cancer. *Int J Cancer,* 2006, 119:599-607.

2.36 Kidokoro T, Tanikawa C, Furukawa Y, Katagiri T, Nakamura Y, Matsuda K. CDC20, a potential cancer therapeutic target, is negatively regulated by p53. *Oncogene,* 2008, 27:1562-1571.

2.37 Takahashi T, Haruki N, Nomoto S, Masuda A, Saji S, Osada H, Takahashi T. Identification of frequent impairment of the mitotic checkpoint and molecular analysis of the mitotic checkpoint genes, hsMAD2 and p55CDC, in human lung cancers. *Oncogene,* 1999, 18: 4295-4300.

2.38 Wang Z, Wan L, Zhong J, Inuzuka H, Liu P, Sarkar FH, Wei W. Cdc20: a potential novel therapeutic target for cancer treatment. *Curr Pharm Des*, 2013, 19:3210-3214.

2.39 Mondal G, Sengupta S, Panda CK, Gollin SM, Saunders WS, Roychoudhury S. Overexpression of Cdc20 leads to impairment of the spindle assembly checkpoint and aneuploidization in oral cancer. *Carcinogenesis*, 2007, 28:81-92.

2.40 Richardson C, Stark JM, Ommundsen M, Jasin M. Rad51 overexpression promotes alternative double-strand break repair pathways and genome instability. *Oncogene,* 200423:546-553.

2.41 Vispé S, Cazaux C, Lesca C, Defais M. Overexpression of Rad51 protein stimulates homologous recombination and increases resistance of mammalian cells to ionizing radiation. *Nucleic Acids Res*, 1998, 26:2859-2864.

2.42 Klein HL. The consequences of Rad51 overexpression for normal and tumor cells. *DNA Repair,* 2008, 7:686-693.

2.43 Syljuåsen RG, Sørensen CS, Hansen LT, Fugger K, Lundin C, Johansson F, et al. Inhibition of human Chk1 causes increased initiation of DNA replication, phosphorylation of ATR targets, and DNA breakage. *Mol Cell Biol*, 2005, 25:3553-3562.

2.44 Taniguchi K, Momiyama N, Ueda M, Matsuyama R, Mori R, Fujii Y, et al. Targeting of CDC20 via small interfering RNA causes enhancement of the cytotoxicity of chemoradiation. *Anticancer Res*, 2008, 28:1559-1563.

2.45 Tsai MS, Kuo YH, Chiu YF, Su YC, Lin YW. Down-regulation of Rad51 expression overcomes drug resistance to gemcitabine in human non-small-cell lung cancer cells. *J Pharmacol Exp Ther*, 2010, 335:830-840.

2.46 Kim DH, Behlke MA, Rose SD, Chang MS, Choi S, Rossi JJ. Synthetic dsRNA Dicer substrates enhance RNAi potency and efficacy. *Nat Biotechnol*, 2005, 23:222-226.

2.47 Behlke MA. Progress towards *in vivo* use of siRNAs. *Mol Ther.* 2006, 13:644-670.

2.48 AbuHammad S, Zihlif M. Gene expression alterations in doxorubicin resistant MCF7 breast cancer cell line. *Genomics,* 2013, 101:213-220.

2.49 Bonnet ME, Gossart JB, Benoit E, Messmer M, Zounib O, Moreau V, Behr JP, Lenne- Samuel N, Kedinger V, Meulle A, Erbacher P, Bolcato-Bellemin AL. Systemic delivery of sticky siRNAs targeting the cell cycle for lung tumor metastasis inhibition. *J Control Rel*, 2013, 170:183-190.

2.50 Christgen M, Lehmann U. MDA-MB-435: the questionable use of a melanoma cell line as a model for human breast cancer is ongoing. *Cancer Biol Ther*, 2007, 6:1355-1357.

2.51 Chambers AF. MDA-MB-435 and M14 cell lines: identical but not M14 melanoma? *Cancer Res*, 2009, 69:5292-5293.

3.1 Vici P, Pizzuti L, Natoli C, Gamucci T, Di Lauro L, Barba M, Sergi D, Botti C, Michelotti A, Moscetti L, Mariani L, Izzo F, D'Onofrio L, Sperduti I, Conti F, Rossi V, Cassano A, Maugeri-Saccà M, Mottolese M, Marchetti P. Triple positive breast cancer: a distinct subtype? *Cancer Treat Rev*, 2015, 41:69-76.

3.2 Hart CD, Migliaccio I, Malorni L, Guarducci C, Biganzoli L, Di Leo A. Challenges in the management of advanced, ER-positive, HER2-negative breast cancer. *Nat Rev Clin Oncol*, 2015, 12:541-552.

3.3 Tinoco G, Warsch S, Glück S, Avancha K, Montero AJ. Treating breast cancer in the 21st century: emerging biological therapies. *J Cancer*, 2013, 4:117-132.

3.4 Foulkes WD, Smith IE, Reis-Filho JS. Triple-negative breast cancer. *N Engl J Med*, 2010, 363:1938-1948.

3.5 Dent R, Trudeau M, Pritchard KI, Hanna WM, Kahn HK, Sawka CA, Lickley LA, Rawlinson E, Sun P, Narod SA. Triple-negative breast cancer: clinical features and patterns of recurrence. *Clin Cancer Res,* 2007, 13:4429-4434.

3.6 Reis-Filho JS, Tutt AN. Triple negative tumours: a critical review. *Histopathology*, 2008, 52:108-118.

3.7 McManus MT, Sharp PA. Gene silencing in mammals by small interfering RNAs. *Nat Rev Genet*, 2002, 3:737-747.

3.8 Kim DH, Rossi JJ. Strategies for silencing human disease using RNA interference. *Nat Rev Genet*, 2007, 8:173-184.

3.9 Wilson RC, Doudna JA. Molecular mechanisms of RNA interference. *Annu Rev Biophys,* 2013, 42:217-239.

3.10 Pecot CV, Calin GA, Coleman RL, Lopez-Berestein G, Sood AK. RNA interference in the clinic: challenges and future directions. *Nat Rev Cancer*, 2011, 11:59-67.

3.11 Bora RS, Gupta D, Mukkur TK, Saini KS. RNA interference therapeutics for cancer: challenges and opportunities. *Mol Med Rep,* 2012, 6:9-15.

3.12 Aliabadi HM, Landry B, Sun C, Tang T, Uludağ H. Supramolecular assemblies in functional siRNA delivery: where do we stand? *Biomaterials*, 2012, 33:2546-2569.

3.13 Aliabadi HM, Landry B, Bahadur RK, Neamnark A, Suwantong O, Uludağ H. Impact of lipid substitution on assembly and delivery of siRNA by cationic polymers. *Macromol Biosci*, 2011, 11:662-672.

3.14 KC RB, Kucharski C, Uludağ H. Additive nanocomplexes of cationic lipopolymers for improved non-viral gene delivery to mesenchymal stem cells. *J Mat Chem B*, 2015, 3:3972-3982.

3.15 Sandhu C, Slingerland J. Deregulation of the cell cycle in cancer. *Cancer Detect Prev*, 2000, 24:107-118.

3.16 Malumbres M, Carnero A. Cell cycle deregulation: a common motif in cancer. *Prog Cell Cycle Res*, 2003, 5:5-18.

3.17 Mills GB, Schmandt R, McGill M, Amendola A, Hill M, Jacobs K, May C, Rodricks AM, Campbell S, Hogg D. Expression of TTK, a novel human protein kinase, is associated with cell proliferation. *J Biol Chem*, 1992, 267:16000-16006.

3.18 Hiruma Y, Sacristan C, Pachis ST, Adamopoulos A, Kuijt T, Ubbink M, von Castelmur E, Perrakis A, Kops GJ. Competition between MPS1 and microtubules at kinetochores regulates spindle checkpoint signaling. *Science*, 2015, 348:1264-1267.

3.19 Lo YL, Yu JC, Chen ST, Hsu GC, Mau YC, Yang SL, Wu PE, Shen CY. Breast cancer risk associated with genotypic polymorphism of the mitotic checkpoint genes: a multigenic study on cancer susceptibility. *Carcinogenesis*, 2007, 28:1079-1086.

3.20 Vaclavicek A, Bermejo JL, Wappenschmidt B, Meindl A, Sutter C, Schmutzler RK, Kiechle M, Bugert P, Burwinkel B, Bartram CR, Hemminki K, Försti A. Genetic variation in the major mitotic checkpoint genes does not affect familial breast cancer risk. *Breast Cancer Res Treat*, 2007, 106:205-213.

3.21 Ahn CH, Kim YR, Kim SS, Yoo NJ, Lee SH. Mutational analysis of TTK gene in gastric and colorectal cancers with microsatellite instability. *Cancer Res Treat*, 2009, 41:224-228.

3.22 Kaistha BP, Honstein T, Müller V, Bielak S, Sauer M, Kreider R, Fassan M, Scarpa A, Schmees C, Volkmer H, Gress TM, Buchholz M. Key role of dual specificity kinase TTK in proliferation and survival of pancreatic cancer cells. *Br J Cancer*, 2014, 111:1780-1787.

3.23 Kimata Y, Baxter JE, Fry AM, Yamano H. A role for the Fizzy/Cdc20 family of proteins in activation of the APC/C distinct from substrate recruitment. *Mol Cell*, 2008, 32:576-583.

3.24 Tipton AR, Ji W, Sturt-Gillespie B, Bekier ME, Wang K, Taylor WR, Liu ST. Monopolar spindle 1 (MPS1) kinase promotes production of closed MAD2 (C-MAD2) conformer and assembly of the mitotic checkpoint complex. *J Biol Chem*, 2013, 288:35149-35158.

3.25 Maciejowski J, George KA, Terret ME, Zhang C, Shokat KM, Jallepalli PV. Mps1 directs the assembly of Cdc20 inhibitory complexes during interphase and mitosis to control M phase timing and spindle checkpoint signaling. *J Cell Biol*, 2010, 190:89-100.

3.26 King KL, Cidlowski JA. Cell cycle regulation and apoptosis. *Annu Rev Physiol*, 1998, 60:601-617.

3.27 Reed JC. Mechanisms of apoptosis. *Am J Pathol*, 2000, 157:1415-1430.

3.28 Small S, Keerthivasan G, Huang Z, Gurbuxani S, Crispino JD. Overexpression of survivin initiates hematologic malignancies *in vivo*. *Leukemia,* 2010, 24:1920-1926.

3.29 Shi Z, Liang YJ, Chen ZS, Wang XH, Ding Y, Chen LM, Fu LW. Overexpression of Survivin and XIAP in MDR cancer cells unrelated to P-glycoprotein. *Oncol Rep*, 2007, 17:969-976.

3.30 Peroukides S, Bravou V, Alexopoulos A, Varakis J, Kalofonos H, Papadaki H. Survivin overexpression in HCC and liver cirrhosis differentially correlates with p-STAT3 and E-cadherin. *Histol Histopathol*, 2010, 25:299-307.

3.31 Sah NK, Khan Z, Khan GJ, Bisen PS. Structural, functional and therapeutic biology of survivin. *Cancer Lett*, 2006, 244:164-171.

3.32 Carvalho A, Carmena M, Sambade C, Earnshaw WC, Wheatley SP. Survivin is required for stable checkpoint activation in taxol-treated HeLa cells. *J Cell Sci*, 2003, 116:2987-2998.

3.33 Lens SM, Wolthuis RM, Klompmaker R, Kauw J, Agami R, Brummelkamp T, Kops G, Medema RH. Survivin is required for a sustained spindle checkpoint arrest in response to lack of tension. *EMBO J*, 2003, 22:2934-2947.

3.34 Bahadur KC, Landry B, Aliabadi HM, Lavasanifar A, Uludağ H. Lipid substitution on low molecular weight (0.6-2.0 kDa) polyethylenimine leads to a higher zeta potential of plasmid DNA and enhances transgene expression. *Acta Biomater*, 2011, 7:2209-2217.

3.35 Remant Bahadur KC, Uludağ H. A comparative evaluation of disulfide-linked and hydrophobically-modified PEI for plasmid delivery. *J Biomater Sci Polym Ed,* 2011, 22:873-892.

3.36 Jiang H, Secretan C, Gao T, Bagnall K, Korbutt G, Lakey J, Jomha NM. The development of osteoblasts from stem cells to supplement fusion of the spine during surgery for AIS. p 467-472. *In:* Uyttendaele D, Dangerfield PH (ed.). *Studies in Health Technology and Informatics: Research in Spinal Deformities*, 2006, IOS Press, Amsterdam, The Netherlands.

3.37 Sumantran VN. Cellular chemosensitivity assays: an overview. *Methods Mol Biol*, 2011, 731:219-236.

3.38 Moghimi SM, Symonds P, Murray JC, Hunter AC, Debska G, Szewczyk A. A two-stage poly(ethylenimine)-mediated cytotoxicity: implications for gene transfer/therapy. *Mol Ther*, 2005, 11:990-995.

3.39 Parmar MB, Aliabadi HM, Mahdipoor P, Kucharski C, Maranchuk R, Hugh JC, Uludağ H. Targeting cell cycle proteins in breast cancer cells with siRNA by using lipid-substituted polyethylenimines. *Front Bioeng Biotechnol*, 2015, 3:14.

3.40 Maire V, Baldeyron C, Richardson M, Tesson B, Vincent-Salomon A, Gravier E, Marty-Prouvost B, De Koning L, Rigaill G, Dumont A, Gentien D, Barillot E, Roman-Roman S, Depil S, Cruzalegui F, Pierré A, Tucker GC, Dubois T. TTK/hMPS1 is an attractive therapeutic target for triple-negative breast cancer. *PLoS One*, 2013, 8:e63712.

3.41 Liang XD, Dai YC, Li ZY, Gan MF, Zhang SR, Yin-Pan, Lu HS, Cao XQ, Zheng BJ, Bao LF, Wang DD, Zhang LM, Ma SL. Expression and function analysis of mitotic checkpoint genes identifies TTK as a potential therapeutic target for human hepatocellular carcinoma. *PLoS One*, 2014, 9:e97739.

3.42 Dahlman KB, Parker JS, Shamu T, Hieronymus H, Chapinski C, Carver B, Chang K, Hannon GJ, Sawyers CL. Modulators of prostate cancer cell proliferation and viability identified by short-hairpin RNA library screening. *PLoS One*, 2012, 7:e34414.

3.43 Malefyt AP, Wu M, Vocelle DB, Kappes SJ, Lindeman SD, Chan C, Walton SP. Improved asymmetry prediction for short interfering RNAs. *FEBS J*, 2014, 281:320-330.

3.44 Noland CL, Doudna JA. Multiple sensors ensure guide strand selection in human RNAi pathways. *RNA*, 2013, 19:639-648.

3.45 Kim DH, Behlke MA, Rose SD, Chang MS, Choi S, Rossi JJ. Synthetic dsRNA Dicer substrates enhance RNAi potency and efficacy. *Nat Biotechnol*, 2005, 23:222-226.

3.46 Montazeri Aliabadi H, Landry B, Mahdipoor P, Uludağ H. Induction of apoptosis by survivin silencing through siRNA delivery in a human breast cancer cell line. *Mol Pharm*, 2011, 8:1821-1830.

3.47 Pietenpol JA, Stewart ZA. Cell cycle checkpoint signaling: cell cycle arrest versus apoptosis. *Toxicology,* 2002, 181-182:475-481.

3.48 Castedo M, Perfettini JL, Roumier T, Andreau K, Medema R, Kroemer G. Cell death by mitotic catastrophe: a molecular definition. *Oncogene,* 2004, 23:2825-2837.

3.49 Harley ME, Allan LA, Sanderson HS, Clarke PR. Phosphorylation of Mcl-1 by CDK1-cyclin B1 initiates its Cdc20-dependent destruction during mitotic arrest. *EMBO J*, 2010, 29:2407-2420.

3.50 Saintigny Y, Dumay A, Lambert S, Lopez BS. A novel role for the Bcl-2 protein family: specific suppression of the RAD51 recombination pathway. *EMBO J*, 2001, 20:2596-2607.

3.51 Valencia-Serna J, Gul-Uludağ H, Mahdipoor P, Jiang X, Uludağ H. Investigating siRNA delivery to chronic myeloid leukemia K562 cells with lipophilic polymers for therapeutic BCR-ABL down-regulation. *J Control Release*, 2013, 172:495-503.

3.52 Mishra P, Nayak B, Dey RK. PEGylation in anti-cancer therapy: An overview. *Asian Journal of Pharmaceutical Sciences*, 2015, 11:337-348.

3.53 Martens TF, Remaut K, Deschout H, Engbersen JF, Hennink WE, van Steenbergen MJ, Demeester J, De Smedt SC, Braeckmans K. Coating nanocarriers with hyaluronic acid facilitates intravitreal drug delivery for retinal gene therapy. *J Control Release*, 2015, 202:83-92.

4.1 Weigelt B, Peterse JL, Veer LJ. Breast cancer metastasis: markers and models. *Nat. Rev. Cancer*, 2005, 5:591-602.

4.2 Rahman M, Mohammed S. Breast cancer metastasis and the lymphatic system. *Onco. Lett,* 2015, 10:1233-1239.

4.3 Ligresti G, Libra M, Militello L, Clementi S, Donia M, Imbesi R, Malaponte G, Cappellani A, McCubrey JA, Stivala F. Breast cancer: Molecular basis and therapeutic strategies. *Mol. Med. Rep,* 2008, 1:451-458.

4.4 Vici P, Pizzuti L, Natoli C, Gamucci T, Di Lauro L, Barba M, Sergi D, Botti C, Michelotti A, Moscetti L, Mariani L, Izzo F, D'Onofrio L, Sperduti I, Conti F, Rossi V, Cassano A, Maugeri-Saccà M, Mottolese M, Marchetti P. Triple positive breast cancer: a distinct subtype? *Cancer Treat. Rev*, 2015, 41:69-76.

4.5 Dent R, Trudeau M, Pritchard K, Hanna WM, Kahn HK, Sawka CA, Lickley LA, Rawlinson E, Sun P, Narod SA. Triple-negative breast cancer: clinical features and patterns of recurrence. *Clin. Cancer Res*, 2007, 13:4429-4434.

4.6 McManus MT, Sharp PA. Gene silencing in mammals by small interfering RNAs. *Nat. Rev. Genet*, 2002, 3:737-747.

4.7 Wilson RC, Doudna JA. Molecular mechanisms of RNA interference. *Annu. Rev. Biophys,* 2013, 42:217-239.

4.8 Pecot CV, Calin GA, Coleman RL, Lopez-Berestein G, Sood AK. RNA interference in the clinic: Challenges and future directions. *Nat. Rev. Cancer*, 2011, 11:59–67.

4.9 Aliabadi HM, Landry B, Sun C, Tang T, Uludag H. Supramolecular assemblies in functional siRNA delivery: where do we stand? *Biomaterials*, 2012, 33:2546–2569.

4.10 Aliabadi HM, Landry B, Bahadur RK, Neamnark A, Suwantong O, Uludag H. Impact of lipid substitution on assembly and delivery of siRNA by cationic polymers. *Macromol. Biosci*, 2011, 11:662–672.

4.11 KC RB, Kucharski C, Uludag H. Additive nanocomplexes of cationic lipopolymers for improved non-viral gene delivery to mesenchymal stem cells. *J. Mater. Chem. B,* 2015, 3:3972–3982.

4.12 Fraser JR, Laurent TC, Laurent UB. Hyaluronan: its nature, distribution, functions and turnover. *J. Intern. Med*, 1997, 242:27-33.

4.13 Aruffo A, Stamenkovic I, Melnick M, Underhill CB, Seed B. CD44 is the principal cell surface receptor for hyaluronate. *Cell*, 1990, 61:1303-1313.

4.14 Mattheolabakis G, Milane L, Singh A, Amiji MM. Hyaluronic acid targeting of CD44 for cancer therapy: from receptor biology to nanomedicine. *J. Drug. Target*, 2015, 23:605-618.

4.15 Idowu MO, Kmieciak M, Dumur C, Burton RS, Grimes MM, Powers CN, Manjili MH. $CD44^{+}/CD24^{-/low}$ cancer stem/progenitor cells are more abundant in triple-negative invasive breast carcinoma phenotype and are associated with poor outcome. *Hum. Pathol*, 2012, 43:364-373.

4.16 Sandhu C, Slingerland J. Deregulation of the cell cycle in cancer. *Cancer Detect. Prev*, 2000, 24:107–118.

4.17 Parmar MB, Aliabadi HM, Mahdipoor P, Kucharski C, Maranchuk R, Hugh JC, Uludag H. Targeting cell cycle proteins in breast cancer cells with siRNA by using lipid-substituted polyethylenimines. *Front. Bioeng. Biotechnol*, 2015, 3:14.

4.18 Kimata Y, JE, Fry AM, Yamano H. A role for the Fizzy/ Cdc20 family of proteins in activation of the APC/C distinct from substrate recruitment. *Mol. Cell*, 2008, 32:576–583.

4.19 Motiwala T, Jacob ST. Role of protein tyrosine phosphatases in cancer. *Prog. Nucleic Acid Res. Mol. Biol*, 2006, 81:297–329.

4.20 Al-Aidaroos AQ, Zeng Q. PRL-3 phosphatase and cancer metastasis. *J. Cell. Biochem*, 2010, 111:1087-1098.

4.21 Bessette DC, Qiu D, Pallen CJ. PRL PTPs: mediators and markers of cancer progression. *Cancer Metastasis Rev*, 2008, 27:231-252.

4.22 Saha S, Bardelli A, Buckhaults P, Velculescu VE, Rago C, St Croix B, Romans KE, Choti MA, Lengauer C, Kinzler KW, Vogelstein B. A phosphatase associated with metastasis of colorectal cancer. *Science*, 2001, 294:1343-1346.

4.23 Lee ST, Feng M, Wei Y, Li Z, Qiao Y, Guan P, Jiang X, Wong CH, Huynh K, Wang J, Li J, Karuturi KM, Tan EY, Hoon DS, Kang Y,Yu Q. Protein tyrosine phosphatase UBASH3B is overexpressed in triple-negative breast cancer and promotes invasion and metastasis, *Proc. Natl. Acad. Sci. U.S.A*, 2013, 110:11121-11126.

4.24 Spring K, Fournier P, Lapointe L, Chabot C, Roussy J, Pommey S, Stagg J, Royal I. The protein tyrosine phosphatase DEP-1/PTPRJ promotes breast cancer cell invasion and metastasis. *Oncogene*, 2015, 34:5536-5547.

4.25 Feng X, Wu Z, Wu Y, Hankey W, Prior TW, Li L, Ganju RK, Shen R, Zou X. CDC25A regulates matrix metalloprotease 1 through Foxo1 and mediates metastasis of breast cancer cells. *Mol. Cell. Biol*, 2011, 31:3457-3471.

4.26 Bahadur KC, Landry B, Aliabadi HM, Lavasanifar A, Uludag H. Lipid substitution on low molecular weight (0.6–2.0 kDa) polyethylenimine leads to a higher zeta potential of plasmid DNA and enhances transgene expression. *Acta. Biomater*, 2011, 7: 2209–2217.

4.27 Remant Bahadur KC, Uludag H. A comparative evaluation of disulfide-linked and hydrophobically-modified PEI for plasmid delivery. *J. Biomater. Sci. Polym. Ed*, 2011, 22:873–892.

4.28 Sumantran VN. Cellular chemosensitivity assays: An overview. *Methods Mol. Biol*, 2011, 731:219–236.

4.29 Liang CC, Park AY, Guan JL. *In vitro* scratch assay: a convenient and inexpensive method for analysis of cell migration *in vitro*. *Nat. Protoc*, 2007, 2:329-333.

4.30 Schneider CA, Rasband WS, Eliceiri KW. NIH Image to ImageJ: 25 years of image analysis. *Nat. Methods*, 2012, 9:671-675.

4.31 Gebäck T, Schulz MM, Koumoutsakos P, Detmar M. TScratch: a novel and simple software tool for automated analysis of monolayer wound healing assays. *Biotechniques*, 2009, 46:265-274.

4.32 Livak KJ, Schmittgen TD. Analysis of relative gene expression data using real-time quantitative PCR and the $2^{-\Delta\Delta C}{}_T$ method. *Methods*, 2001, 25:402-408.

4.33 Parmar MB, Arteaga Ballesteros BE, Fu T, KC RB, Montazeri Aliabadi H, Hugh JC, Löbenberg R, Uludağ H. Multiple siRNA delivery against cell cycle and anti-apoptosis proteins using lipid-substituted polyethylenimine in triple-negative breast cancer and nonmalignant cells. *J. Biomed. Mater. Res*. *A*, 2016, 104:3031-3044.

4.34 Sheridan C, Kishimoto H, Fuchs RK, Mehrotra S, Bhat-Nakshatri P, Turner CH, Jr Goulet R, Badve S, Nakshatri H. CD44+/CD24- breast cancer cells exhibit enhanced invasive properties: an early step necessary for metastasis. *Breast Cancer Res*, 2006, 8:R59.

4.35 Shen H, Shi S, Zhang Z, Gong T, Sun X. Coating solid lipid nanoparticles with hyaluronic acid enhances antitumor activity against melanoma stem-like cells. *Theranostics*, 2015, 5:755-771.

4.36 Yang C, He Y, Zhang H, Liu Y, Wang W, Du Y, Gao F. Selective killing of breast cancer cells expressing activated CD44 using CD44 ligand-coated nanoparticles *in vitro* and *in vivo*. *Oncotarget*, 2015, 6:15283-15296.

4.37 Aliabadi HM, Maranchuk R, Kucharski C, Mahdipoor P, Hugh J, Uludağ H. Effective response of doxorubicin-sensitive and -resistant breast cancer cells to combinational siRNA therapy. *J. Control. Release*, 2013, 172:219-228.

4.38 Takakura S, Kohno T, Manda R, Okamoto A, Tanaka T, Yokota J. Genetic alterations and expression of the protein phosphatase 1 genes in human cancers. *Int. J. Oncol*, 2001, 18:817-824.

4.39 Harima Y, Ikeda K, Utsunomiya K, Shiga T, Komemushi A, Kojima H, Nomura M, Kamata M, Sawada S. Identification of genes associated with progression and metastasis of advanced cervical cancers after radiotherapy by cDNA microarray analysis. *Int. J. Radiat. Oncol. Biol. Phys*, 2009, 175:232-1239.

4.40 Negro R, Gobessi S, Longo PG, He Y, Zhang ZY, Laurenti L, Efremov DG. Overexpression of the autoimmunity-associated phosphatase PTPN22 promotes survival of antigen-stimulated CLL cells by selectively activating AKT. *Blood*, 2012, 119:6278–6287.

4.41 Cancer Genome Atlas Network, Comprehensive molecular portraits of human breast tumors. *Nature*, 2012, 490:61-70.

4.42 Fasching PA, Brucker SY, Fehm TN, Overkamp F, Janni W, Wallwiener M, Hadji P, Belleville E, Häberle L, Taran FA, Lüftner D, Lux MP, Ettl J, Müller V, Tesch H, Wallwiener D, Schneeweiss A. Biomarkers in patients with metastatic breast cancer and the PRAEGNANT study network. *Geburtshilfe Frauenheilkd*, 2015, 75:41-50.

4.43 Qiao YN, He WQ, Chen CP, Zhang CH, Zhao W, Wang P, Zhang L, Wu YZ, Yang X, Peng YJ, Gao JM, Kamm KE, Stull JT, Zhu MS. Myosin phosphatase target subunit 1 (MYPT1) regulates the contraction and relaxation of vascular smooth muscle and maintains blood pressure. *J. Biol. Chem*, 2014, 289:22512-22523.

4.44 Wakatsuki T, Wysolmerski RB, Elson EL. Mechanics of cell spreading: role of myosin II. *J. Cell. Sci*, 2003, 116:1617-1625.

4.45 Kaneko K, Satoh K, Masamune A, Satoh A, Shimosegawa T. Myosin light chain kinase inhibitors can block invasion and adhesion of human pancreatic cancer cell lines. *Pancreas*, 2002, 24:34-41.

4.46 Xia D, Stull JT, Kamm KE. Myosin phosphatase targeting subunit 1 affects cell migration by regulating myosin phosphorylation and actin assembly. *Exp. Cell. Res*, 2005, 304:506-517.

4.47 Totsukawa G, Wu Y, Sasaki Y, Hartshorne DJ, Yamakita Y, Yamashiro S, Matsumura F. Distinct roles of MLCK and ROCK in the regulation of membrane protrusions and focal adhesion dynamics during cell migration of fibroblasts. *J. Cell. Biol,* 2004, 164:427-439.

4.48 Cuadros M, Cano C, López FJ, López-Castro R. A. Concha, Expression profiling of breast tumors based on human epidermal growth factor receptor 2 status defines migration-related genes. *Pathobiology*, 2013, 80:32-40.

4.49 Van den Broeck A, Vankelecom H, Van Eijsden R, Govaere O, Topal B. Molecular markers associated with outcome and metastasis in human pancreatic cancer. *J. Exp. Clin. Cancer. Res,* 2012, 31:68.

4.50 Zhang C, Li A, Li H, Peng K, Wei Q, Lin M, Liu Z, Yin L, Li J. PPP1R12A copy number is associated with clinical outcomes of stage III CRC receiving oxaliplatin-based chemotherapy. *Mediators. Inflamm,* 2015, 2015:417184.

4.51 Lessard L, Stuible M, Tremblay ML. The two faces of PTP1B in cancer. *Biochim. Biophys. Acta*, 2010, 1804:613-619.

4.52 Bentires-Alj M, Neel BG. Protein-tyrosine phosphatase 1B is required for HER2/Neu-induced breast cancer. *Cancer Res*, 2007, 67:2420-2424.

4.53 Julien SG, Dubé N, Read M, Penney J, Paquet M, Han Y, Kennedy BP, Muller WJ, Tremblay ML. Protein tyrosine phosphatase 1B deficiency or inhibition delays ErbB2-induced mammary tumorigenesis and protects from lung metastasis. *Nat. Genet*, 2007, 39:338-346.

4.54 Cortesio CL, Chan KT, Perrin BJ, Burton NO, Zhang S, Zhang ZY, Huttenlocher A. Calpain 2 and PTP1B function in a novel pathway with Src to regulate invadopodia dynamics and breast cancer cell invasion. *J. Cell. Biol*, 2008, 180:957-971.

4.55 Koike E, Toda S, Yokoi F, Izuhara K, Koike N, Itoh K, Miyazaki K, Sugihara H. Expression of new human inorganic pyrophosphatase in thyroid diseases: its intimate association with hyperthyroidism. *Biochem. Biophys. Res. Commun*, 2006, 341:691-696.

4.56 Pilarsky C, Ammerpohl O, Sipos B, Dahl E, Hartmann A, Wellmann A, Braunschweig T, Löhr M, Jesenofsky R, Friess H, Wente MN, Kristiansen G, Jahnke B, Denz A, Rückert F, Schackert HK, Klöppel G, Kalthoff H, Saeger HD, Grützmann R. Activation of Wnt signaling in stroma from pancreatic cancer identified by gene expression profiling. *J. Cell. Mol. Med*, 2008, 12:2823-2835.

4.57 Sayagués JM, Corchete LA, Gutiérrez ML, Sarasquete ME, Del Mar Abad M, Bengoechea O, Fermiñán E, Anduaga MF, Del Carmen S, Iglesias M, Esteban C, Angoso M, Alcazar JA, García J, Orfao A, Muñoz-Bellvis L. Genomic characterization of liver metastases from colorectal cancer patients. *Oncotarget*, 2016, 7:72908-72922.

4.58 Kim DH, Behlke MA, Rose SD, Chang MS, Choi S, Rossi JJ. Synthetic dsRNA Dicer substrates enhance RNAi potency and efficacy. *Nat. Biotechnol*, 2005, 23:222–226.

5.1 Kayl AE, Meyers CA. Side-effects of chemotherapy and quality of life in ovarian and breast cancer patients. *Curr Opin Obstet Gynecol,* 2006, 18:24-28.

5.2 Tao JJ, Visvanathan K, Wolff AC. Long term side effects of adjuvant chemotherapy in patients with early breast cancer. *Breast,* 2015, 24:S149-S153.

5.3 Ligresti G, Libra M, Militello L, Clementi S, Donia M, Imbesi R, Malaponte G, Cappellani A, McCubrey JA, Stivala F. Breast cancer: Molecular basis and therapeutic strategies. *Mol Med Rep,* 2008, 1:451-458.

5.4 Vici P, Pizzuti L, Natoli C, Gamucci T, Di Lauro L, Barba M, Sergi D, Botti C, Michelotti A, Moscetti L, Mariani L, Izzo F, D'Onofrio L, Sperduti I, Conti F, Rossi V, Cassano A, Maugeri-Saccà M, Mottolese M, Marchetti P. Triple positive breast cancer: a distinct subtype? *Cancer Treat Rev,* 2015, 41:69-76.

5.5 McManus MT, Sharp PA. Gene silencing in mammals by small interfering RNAs. *Nat Rev Genet,* 2002, 3:737-747.

5.6 Pecot CV, Calin GA, Coleman RL, Lopez-Berestein G, Sood AK. RNA interference in the clinic: Challenges and future directions. *Nat Rev Cancer,* 2011, 11:59–67.

5.7 Aliabadi HM, Landry B, Sun C, Tang T, Uludağ H. Supramolecular assemblies in functional siRNA delivery: where do we stand? *Biomaterials,* 2012, 33:2546–2569.

5.8 Aliabadi HM, Landry B, Bahadur RK, Neamnark A, Suwantong O, Uludağ H. Impact of lipid substitution on assembly and delivery of siRNA by cationic polymers. *Macromol Biosci,* 2011, 11:662–672.

5.9 Moghimi SM, Symonds P, Murray JC, Hunter AC, Debska G, Szewczyk A. A two-stage poly(ethylenimine)-mediated cytotoxicity: implications for gene transfer/therapy. *Mol Ther,* 2005, 11:990-995.

5.10 Parmar MB, Meenakshi Sundaram DN, KC RB, Maranchuk R, Montazeri Aliabadi H, Hugh JC, Löbenberg R, Uludağ H. Combinational siRNA delivery using hyaluronic acid modified amphiphilic polyplexes against cell cycle and phosphatase proteins to inhibit growth and migration of triple-negative breast cancer cells. *Acta Biomater,* 2018, 66:294-309.

5.11 Fraser JR, Laurent TC, Laurent UB. Hyaluronan: its nature, distribution, functions and turnover. *J Intern Med,* 1997, 242:27-33.

5.12 Wiśniewska M, Urban T, Nosal-Wiercińska A, Zarko VI, Gun'ko VM. Comparison of stability properties of poly(acrylic acid) adsorbed on the surface of silica, alumina and mixed silica-alumina nanoparticles – application of turbidimetry method. *Cent Eur J Chem,* 2014, 12:476-479.

5.13 Rogers TL, Wallick D. Reviewing the use of ethylcellulose, methylcellulose and hypromellose in microencapsulation. *Drug Dev Ind Pharm,* 2012, 38:129-157.

5.14 Parmar MB, Arteaga Ballesteros BE, Fu T, KC RB, Montazeri Aliabadi H, Hugh JC, Löbenberg R, Uludağ H. Multiple siRNA delivery against cell cycle and anti-apoptosis proteins using lipid-substituted polyethylenimine in triple-negative breast cancer and nonmalignant cells. *J Biomed Mater Res A,* 2016, 104:3031-3044.

5.15 Parmar MB, Aliabadi HM, Mahdipoor P, Kucharski C, Maranchuk R, Hugh JC, Uludağ H. Targeting cell cycle proteins in breast cancer cells with siRNA by using lipid-substituted polyethylenimines. *Front Bioeng Biotechnol,* 2015, 3:14.

5.16 Kimata Y, Baxter JE, Fry AM, Yamano H. A role for the Fizzy/ Cdc20 family of proteins in activation of the APC/C distinct from substrate recruitment. *Mol Cell,* 2008, 32:576–583.

5.17 Wang L, Zhang J, Wan L, Zhou X, Wang Z, Wei W. Targeting Cdc20 as a novel cancer therapeutic strategy. *Pharmacol Ther,* 2015, 151:141-151.

5.18 Karra H, Repo H, Ahonen I, Löyttyniemi E, Pitkänen R, Lintunen M, Kuopio T, Söderström M, Kronqvist P. Cdc20 and securin overexpression predict short-term breast cancer survival. *Br J Cancer,* 2014, 110:2905-2913.

5.19 King KL, Cidlowski JA. Cell cycle regulation and apoptosis. *Annu Rev Physiol,* 1998, 60:601–617.

5.20 Sah NK, Khan Z, Khan GJ, Bisen PS. Structural, functional and therapeutic biology of survivin. *Cancer Lett,* 2006, 244:164–171.

5.21 Kinne RK. Endothelial and epithelial cells: general principles of selective vectorial transport. *Int J Microcirc Clin Exp,* 1997, 17:223-230.

5.22 Buchanan CF, Szot CS, Wilson TD, Akman S, Metheny-Barlow LJ, Robertson JL, Freeman JW, Rylander MN. Cross-talk between endothelial and breast cancer cells regulates reciprocal expression of angiogenic factors *in vitro*. *J Cell Biochem,* 2012, 113:1142-1151.

5.23 Bahadur KC, Landry B, Aliabadi HM, Lavasanifar A, Uludağ H. Lipid substitution on low molecular weight (0.6–2.0 kDa) polyethylenimine leads to a higher zeta potential of plasmid DNA and enhances transgene expression. *Acta Biomater,* 2011, 7:2209–2217.

5.24 Remant Bahadur KC, Uludağ H. A comparative evaluation of disulfide-linked and hydrophobically-modified PEI for plasmid delivery. *J Biomater Sci Polym Ed,* 2011, 22:873–892.

5.25 Jiang H, Secretan C, Gao T, Bagnall K, Korbutt G, Lakey J, Jomha NM. The development of osteoblasts from stem cells to supplement fusion of the spine during surgery for AIS. p 467-472. *In:* Uyttendaele D, Dangerfield PH (ed.). *Studies in Health Technology and Informatics: Research in Spinal Deformities*, 2006, IOS Press, Amsterdam, The Netherlands.

5.26 Young L, Sung J, Stacey G, Masters JR. Detection of mycoplasma in cell cultures. *Nat Protoc,* 2010, 5:929-934.

5.27 Sumantran VN. Cellular chemosensitivity assays: An overview. *Methods Mol Biol,* 2011, 731:219–236.

5.28 Livak KJ, Schmittgen TD. Analysis of relative gene expression data using real-time quantitative PCR and the $2^{-\Delta\Delta C}{}_{T}$ method. *Methods,* 2001, 25:402-408.

5.29 Montazeri Aliabadi H, Landry B, Mahdipoor P, Uludağ H. Induction of apoptosis by survivin silencing through siRNA delivery in a human breast cancer cell line. *Mol Pharm,* 2011, 8:1821-1830.

5.30 Opalinska JB, Gewirtz AM. Nucleic-acid therapeutics: basic principles and recent applications. *Nat Rev Drug Discov,* 2002, 1:503-514.

5.31 Alvarez-Salas LM. Nucleic acids as therapeutic agents. *Curr Top Med Chem,* 2008, 8:1379-1404.

5.32 Elsabahy M, Nazarali A, Foldvari M. Non-viral nucleic acid delivery: key challenges and future directions. *Curr Drug Deliv,* 2011, 8:235-244.

5.33 Hsu CY, Uludağ H. Nucleic-acid based gene therapeutics: delivery challenges and modular design of nonviral gene carriers and expression cassettes to overcome intracellular barriers for sustained targeted expression. *J Drug Target,* 2012, 20:301-328.

5.34 KC RB, Thapa B, Valencia-Serna J, Aliabadi HM, Uludağ H. Nucleic acid combinations: A new frontier for cancer treatment. *J Control Release,* 2017, 256:153-169.

5.35 Valencia-Serna J, Gul-Uludağ H, Mahdipoor P, Jiang X, Uludağ H. Investigating siRNA delivery to chronic myeloid leukemia K562 cells with lipophilic polymers for therapeutic BCR–ABL downregulation. *J Control Release,* 2013, 172:495–503.

5.36 Jha K, Shukla M, Pandey M. Survivin expression and targeting in breast cancer. *Surg Oncol,* 2012, 21:125-131.

5.37 Almalik A, Benabdelkamel H, Masood A, Alanazi IO, Alradwan I, Majrashi MA, Alfadda AA, Alghamdi WM, Alrabiah H, Tirelli N, Alhasan AH. Hyaluronic acid coated chitosan nanoparticles reduced the immunogenicity of the formed protein corona. *Sci Rep,* 2017, 7:10542.

5.38 Huang G, Huang H. Application of hyaluronic acid as carriers in drug delivery. *Drug Delivery,* 2018, 25:766-772.

6.1 Malumbres M, Carnero A. Cell cycle deregulation: a common motif in cancer. *Prog Cell Cycle Res*, 2003, 5:5-18.

6.2 Vermeulen K, Van Bockstaele DR, Berneman ZN. The cell cycle: a review of regulation, deregulation and therapeutic targets in cancer. *Cell Prolif*, 2003, 36:131-149.

6.3 Casimiro MC, Crosariol M, Loro E, Li Z, Pestell RG. Cyclins and cell cycle control in cancer and disease. *Genes Cancer*, 2012, 3:649-657.

6.4 Chong T, Sarac A, Yao CQ, Liao L, Lyttle N, Boutros PC, Bartlett JMS, Spears M. Deregulation of the spindle assembly checkpoint is associated with paclitaxel resistance in ovarian cancer. *J Ovarian Res*, 2018, 11:27.

6.5 Liao WT, Wang X, Xu LH, Kong QL, Yu CP, Li MZ, Shi L, Zeng MS, Song LB. Centromere protein H is a novel prognostic marker for human nonsmall cell lung cancer progression and overall patient survival. *Cancer*, 2009, 115:1507-1517.

6.6 Hannay JA, Liu J, Zhu QS, Bolshakov SV, Li L, Pisters PW, Lazar AJ, Yu D, Pollock RE, Lev D. Rad51 overexpression contributes to chemoresistance in human soft tissue sarcoma cells: a role for p53/activator protein 2 transcriptional regulation. *Mol Cancer Ther*, 2007, 6:1650-1660.

6.7 Yip KW, Reed JC. Bcl-2 family proteins and cancer. *Oncogene*, 2008, 27:6398-6406.

6.8 Paschall AV, Liu K. An orthotopic mouse model of spontaneous breast cancer metastasis. *J Vis Exp*, 2016, 114:54040.

6.9 Guo W, Zhang S, Liu S. Establishment of a novel orthotopic model of breast cancer metastasis to the lung. *Oncol Rep*, 2015, 33:2992-2998.

6.10 Rossi G, Mu Z, et al. Cell-free DNA and circulating tumor cells: comprehensive liquid biopsy analysis in advanced breast cancer. *Clin Cancer Res*, 2018, 24:560-568.

6.11 Nijman SM. Synthetic lethality: general principles, utility and detection using genetic screens in human cells. *FEBS Lett*, 2011, 585:1-6.

6.12 Hydbring P, Wang Y, Fassl A, et al. Cell-cycle-targeting MicroRNAs as therapeutic tools against refractory cancers. *Cancer Cell*, 2017, 31:576-590.

6.13 Assumpção CB, Calcagno DQ, Araújo TM, Santos SE, Santos ÂK, Riggins GJ, Burbano RR, Assumpção PP. The role of piRNA and its potential clinical implications in cancer. *Epigenomics*, 2015, 7:975-984.

6.14 Weissman D, Karikó K. mRNA: Fulfilling the promise of gene therapy. *Mol Ther*, 2015, 23:1416-1417.

6.15 Guan S, Rosenecker J. Nanotechnologies in delivery of mRNA therapeutics using nonviral vector-based delivery systems. *Gene Ther*, 2017, 24:133-143.

6.16 Nishikata T, Ishikawa M, Matsuyama T, Takamatsu K, Fukuhara T, Konishi Y. Primary culture of breast cancer: a model system for epithelial-mesenchymal transition and cancer stem cells. *Anticancer Res*, 2013, 33:2867-2873.

6.17 Castillo-Pelayo T, Babinszky S, LeBlanc J, Watson PH. The importance of biobanking in cancer research. *Biopreserv Biobank*, 2015, 13:172-177.

6.18 Edmondson R, Broglie JJ, Adcock AF, Yang L. Three-dimensional cell culture systems and their applications in drug discovery and cell-based biosensors. *Assay Drug Dev Technol*, 2014, 12:207-218.

Appendix

A. Supplementary information for Chapter 2

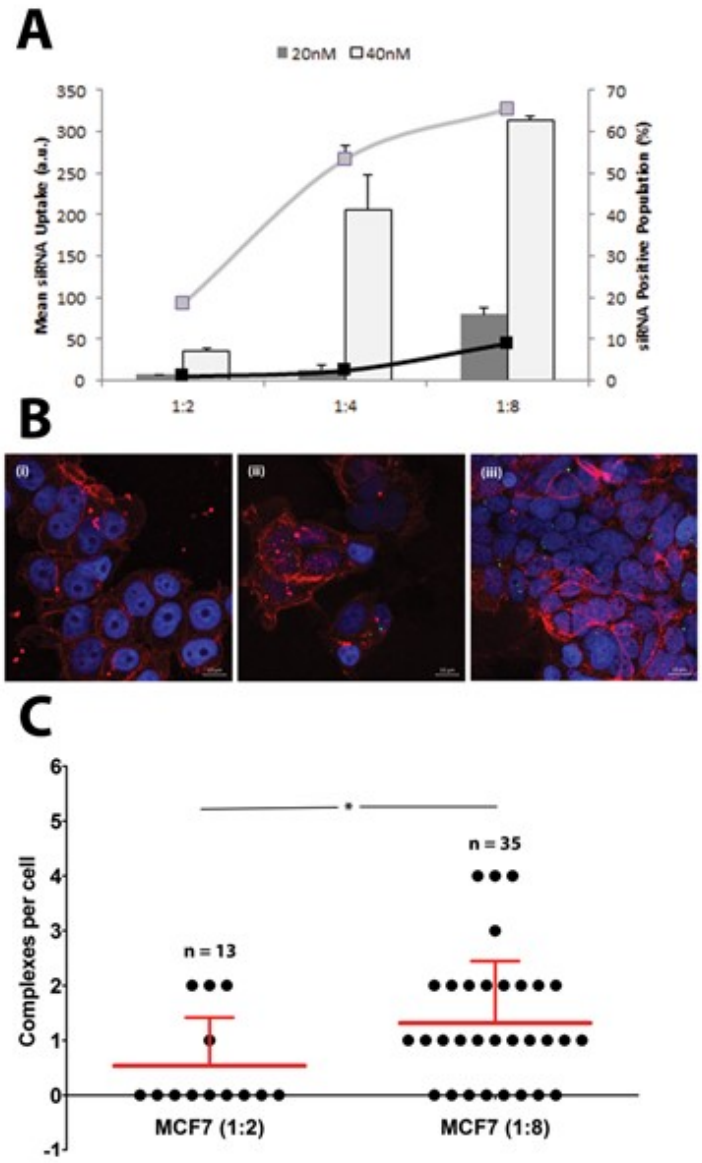

Fig 2.S1: Cellular uptake of FAM-labeled siRNA in MCF7 Cells.
(A) Uptake of FAM-labeled siRNA complexes by flow cytometry at 20 nM and 40 nM siRNA using 1:2, 1:4 and 1:8 siRNA:PEI-LA ratios after 24 hrs treatment in MCF7 cells. The results are summarized as mean FAM-siRNA uptake (bars) and as percentage of FAM-siRNA positive cell population (lines). **(B)** Confocal microscopy to determine the uptake of FAM-labeled siRNA complexes at 40 nM siRNA with 1:2 (ii) and 1:8 (iii) siRNA:PEI-LA ratios after 24 hrs treatment. Purple, red and green colors represent nuclei, cytoplasm and siRNA complexes, respectively. Non-labeled scrambled siRNA was transfected as a control (i). **(C)** The number of visible complexes per cell (as quantitated from confocal microscopy images) at 1:2 and 1:8 siRNA:PEI-LA ratios. The uptake was significantly different between 1:2 and 1:8 ratios (* at $p<0.05$).

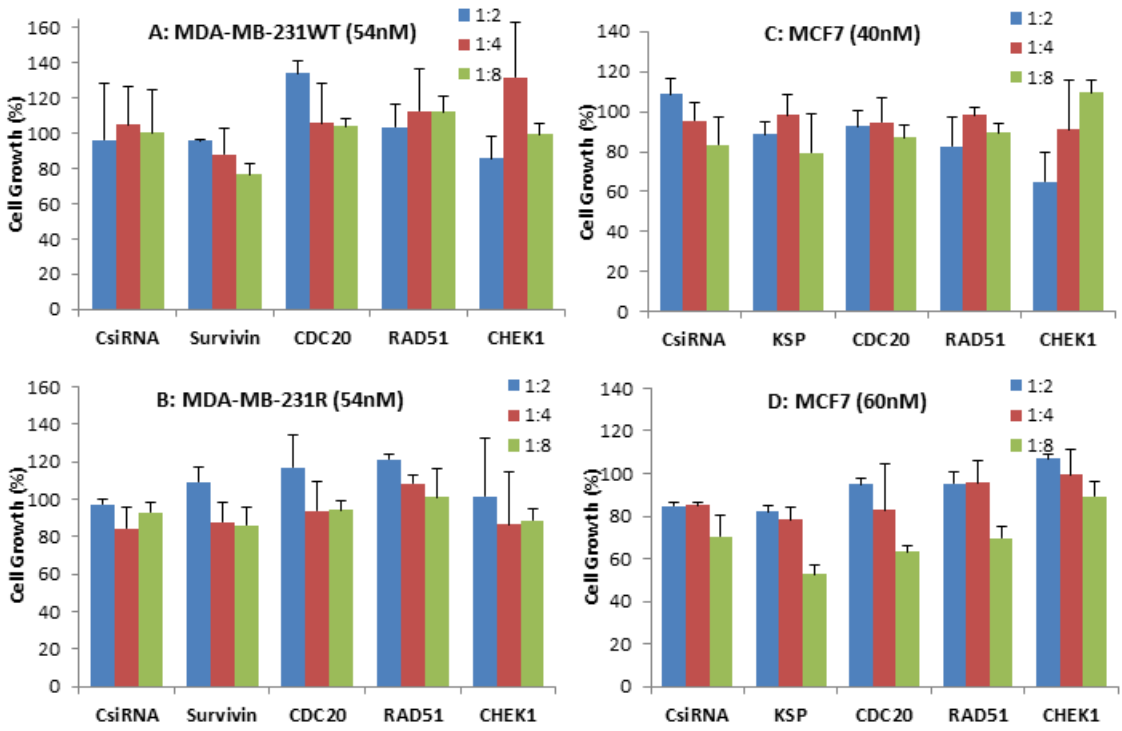

Fig 2.S2: siRNA delivery against cell cycle proteins in MDA-MB-231 and MCF7 cells.
The effects of cell cycle protein specific siRNAs in MDA-MB-231 (wild type, WT and multidrug resistant, R) at 54 nM and in MCF7 cells at 40 nM and 60 nM siRNA. In addition to KSP, CDC20, RAD51 and CHEK1 specific siRNAs, a specific siRNA against the anti-apoptosis protein, survivin was delivered using PEI-LA at 1:2, 1:4 and 1:8 siRNA:polymer ratios. The inhibition of cell growth by MTT assay indicated that the specific siRNA treatments were not effective in MDA-MB-231 and MCF7 compared to scrambled siRNA (CsiRNA).

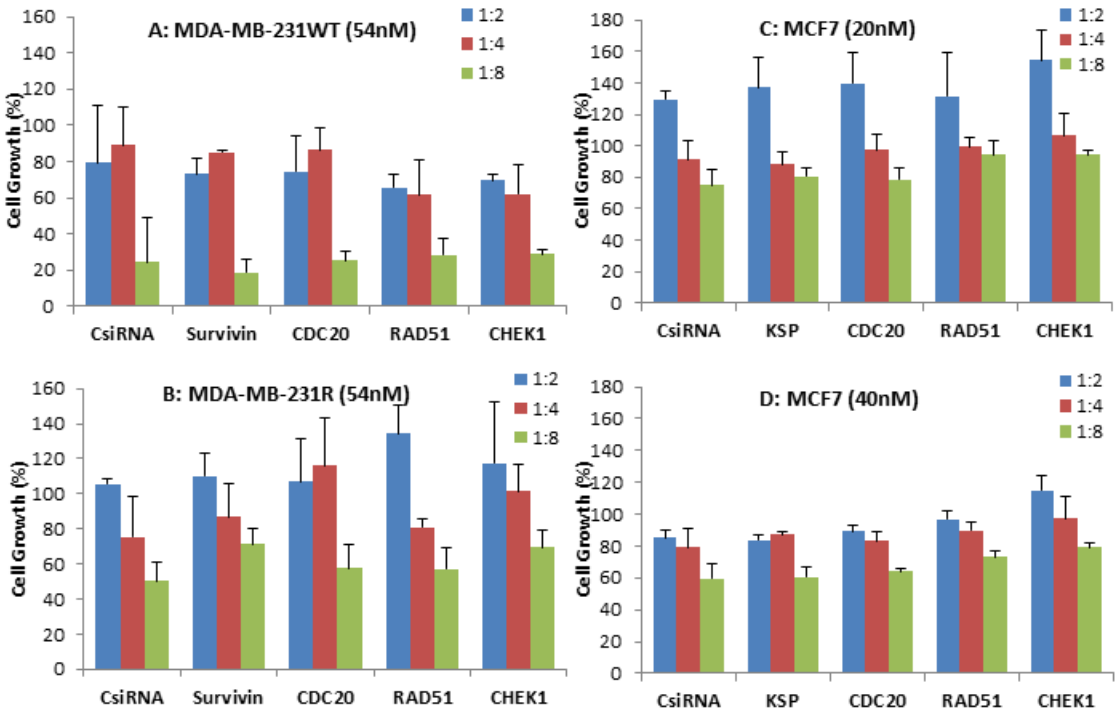

Fig 2.S3: siRNA delivery against cell cycle proteins and survivin in MDA-MB-231 and MCF7 cells. The cell cycle proteins, KSP, CDC20, RAD51 and CHEK1 with survivin were validated using PEI-CA in MDA-MB-231 (wild type, WT and multidrug resistant, R) at 54 nM siRNA, and in MCF7 at 20 nM and 40 nM siRNA concentrations. The results of the inhibition of cell growth assay by MTT indicated that the siRNA treatments were not effective in MDA-MB-231 and MCF7 compared to scrambled siRNA (CsiRNA).

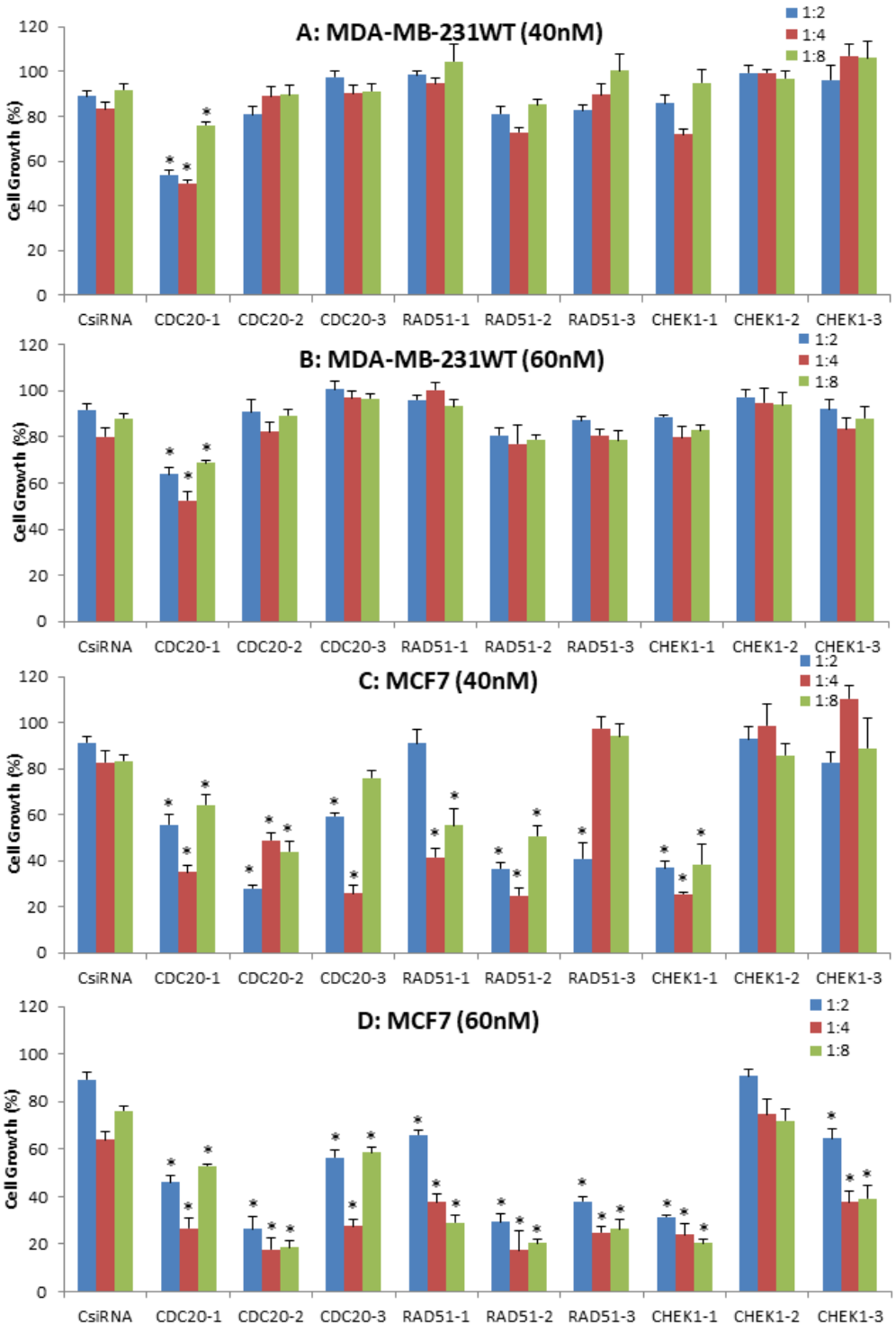

Fig 2.S4: Cell growth inhibition by DsiRNAs in MDA-MB-231WT and MCF7 cells.
Inhibition of cell growth using DsiRNAs against CDC20, RAD51 and CHEK1 at 40 nM and 60 nM DsiRNA concentrations with different DsiRNA:PEI-LA ratios in MDA-MB-231WT and MCF7. For each target proteins, three different DsiRNA isoforms were used. The significance (*) at $p<0.05$ was calculated for specific DsiRNA treated group based on scrambled DsiRNA (CsiRNA).

B. Supplementary information for Chapter 3

Table 3.S1: Synthesized polymers using low molecular weight PEIs.
The amines of PEIs were substituted with Linoleic Acid (LA) using various LA/PEI mol/mol feed ratios to obtain different degree of substitutions (*i.e.*, number of lipid molecules per PEI).

Polymer	Molecular Weight of PEI (kDa)	Feed-ratio (Lipid/PEI)	Degree of Substitution
0.6 PEI LA 1	0.6	1	0.36
0.6 PEI LA 2	0.6	2	0.71
0.6 PEI LA 4	0.6	4	1.09
1.2 PEI LA 0.5	1.2	0.5	0.11
1.2 PEI LA 1	1.2	1	0.31
1.2 PEI LA 2	1.2	2	1.20
1.2 PEI LA 4	1.2	4	1.62
1.2 PEI LA 6	1.2	6	2.55
1.2 PEI LA 8	1.2	8	4.00
2.0 PEI LA 0.75	2.0	0.75	0.20
2.0 PEI LA 1.5	2.0	1.5	0.57
2.0 PEI LA 3	2.0	3	1.95
2.0 PEI LA 6	2.0	6	2.31
2.0 PEI LA 9	2.0	9	3.20

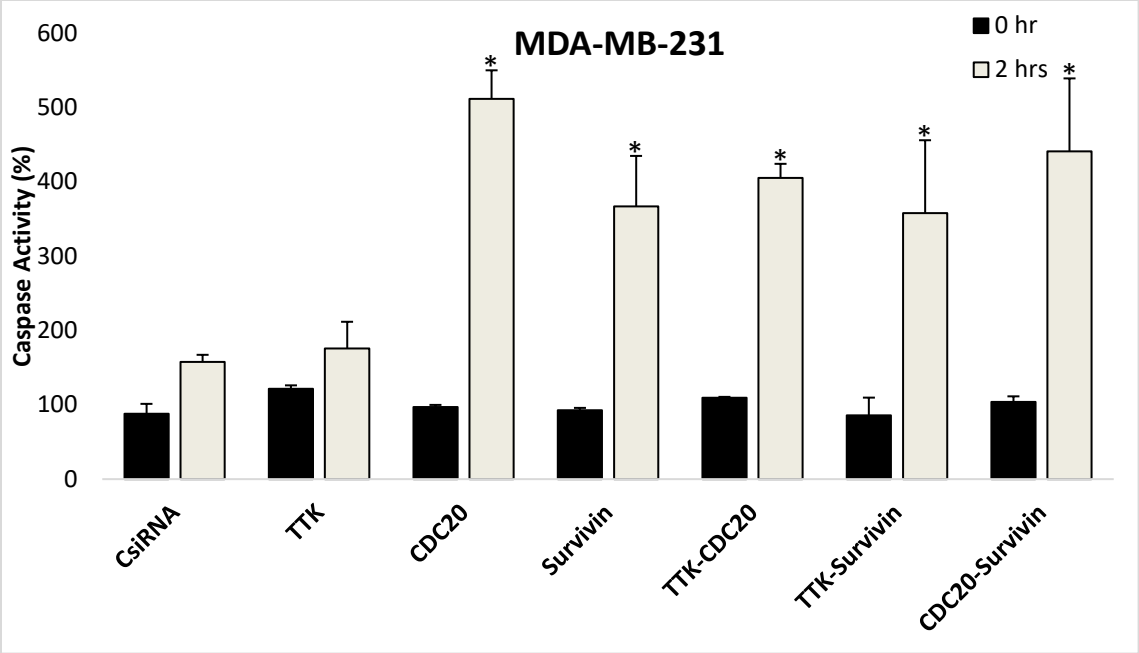

Fig 3.S1: Caspase activity assay for MDA-MB-231 cells with combinational siRNA therapy.
MDA-MB-231 cells were transfected with 30 nM siRNA at 1:4 siRNA:1.2PEI-LA-6 ratio. Caspase activity was assessed at 0 hr and 2 hrs of incubation at 37°C with the substrate and presented as the percentage compared to non-treated cells (taken as 100%). Asterisks represent the significant increase in the caspase activity after 2 hrs of incubation compared to CsiRNA and 0 hr of incubation ($p < 0.05$).

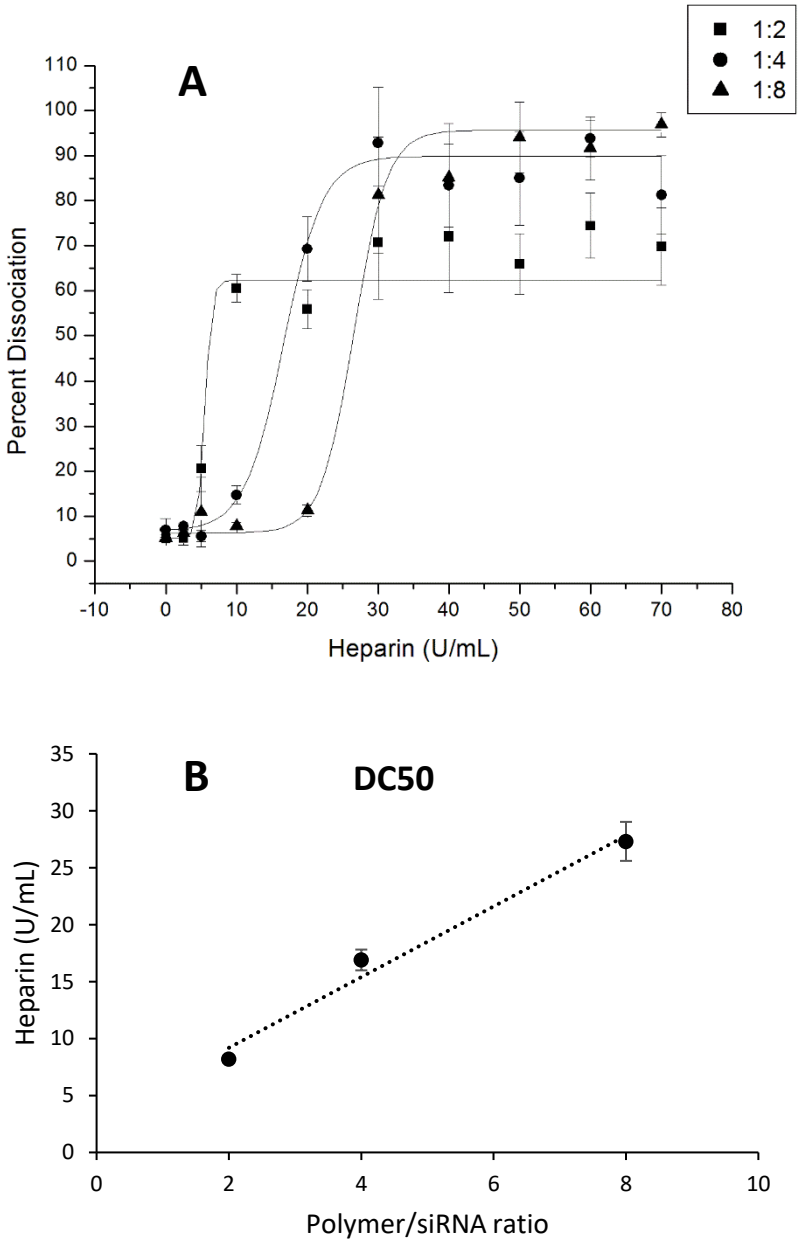

Fig 3.S2: Dissociation of siRNA/polymer complexes with heparin.
siRNA/polymer complexes were prepared with 0.6 µg of scrambled siRNA at 1:4 siRNA:polymer ratio and different amount of heparin was added to dissociate the complexes. The dissociated siRNA was quantitated with SYBR Green II (Cat. No. 50522; Cambrex Bio Sciences Rockland Inc., Rockland, ME) and results were presented as percentage dissociation with addition of heparin **(A)**. The concentration of heparin needed to dissociate 50% of siRNA from polymer (DC50) is calculated for all ratios **(B)**. It was obvious that the DC50 was less for low amount of polymer compared to higher amount of polymer added for complexation.

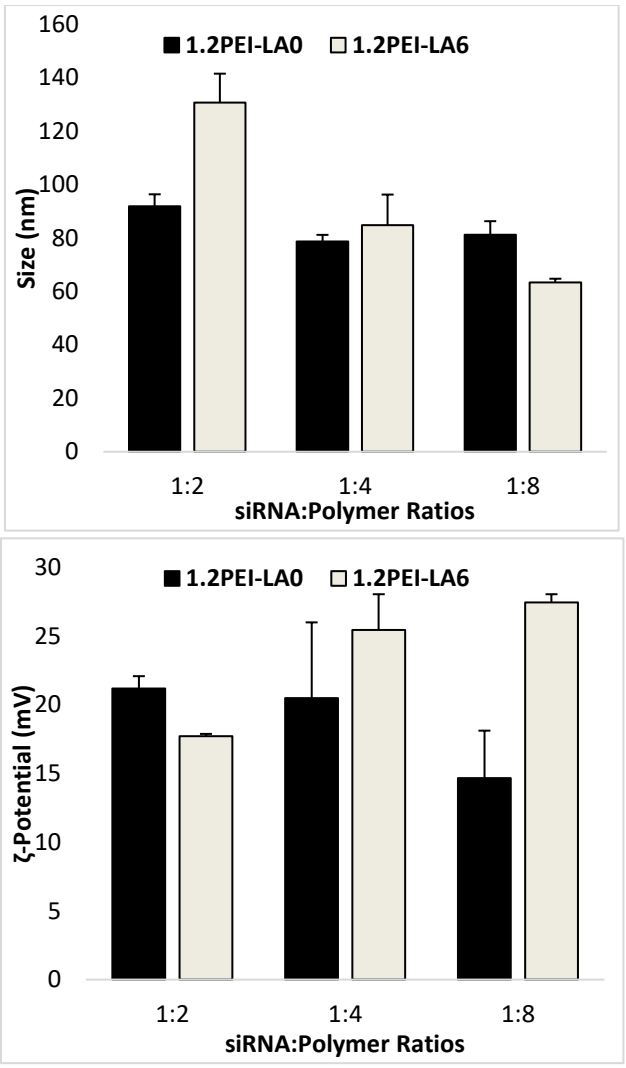

Fig 3.S3: Size and ζ-potential of complexes with different siRNA/polymer ratios.
To characterize complexes based on different siRNA/polymer ratios, hydrodynamic diameter (size) and surface charge (ζ-potential) of these complexes were determined in ddH_2O through dynamic light scattering (DLS) and electrophoretic light scattering (ELS) using Zetasizer Nano ZS (Malvern, UK). The complexes were prepared with 0.6 µg of scrambled siRNA at 1:2, 1:4 and 1:8 siRNA:polymer ratios and were diluted to 1 mL ddH_2O before each measurement. No difference in size of complexes with different ratios was observed with non-modified 1.2 kDa PEI, while it was decreased as the amount of 1.2PEI-LA6 has been increased in complexes. Similarly, surface charge of complexes with 1.2PEI-LA6 was increased as siRNA/polymer ratio was increased, suggesting an important role of amount of polymer during complexation process.

C. Supplementary information for Chapter 4

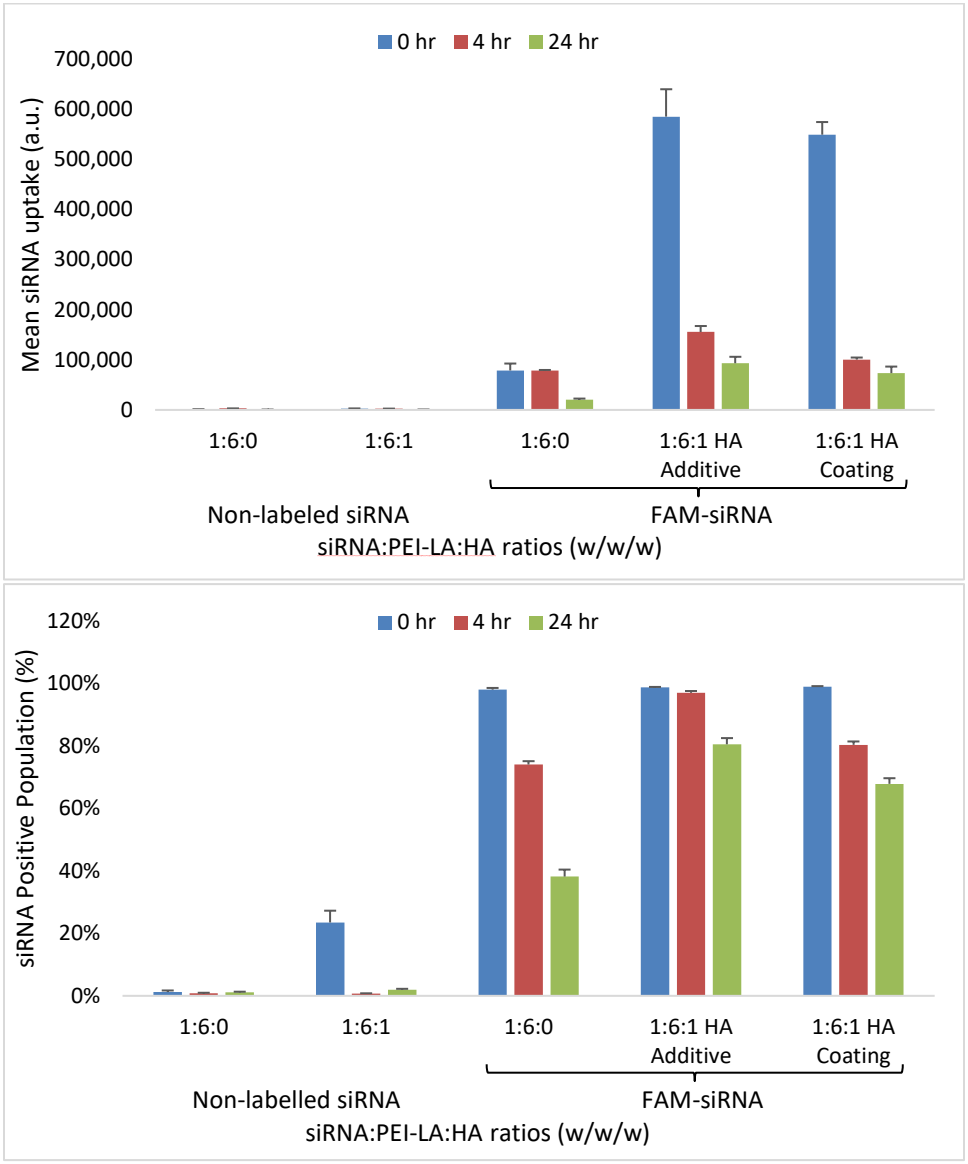

Fig 4.S1: Stability of siRNA in culture medium.
The complexes were incubated in cell culture medium for 0, 4 and 24 hr at 37°C. The uptake of FAM-labeled siRNA used to prepare these complexes was then determined using BD Accuri™ C6 Plus Flow Cytometer (BD Biosciences) as described in the Materials and Methods.

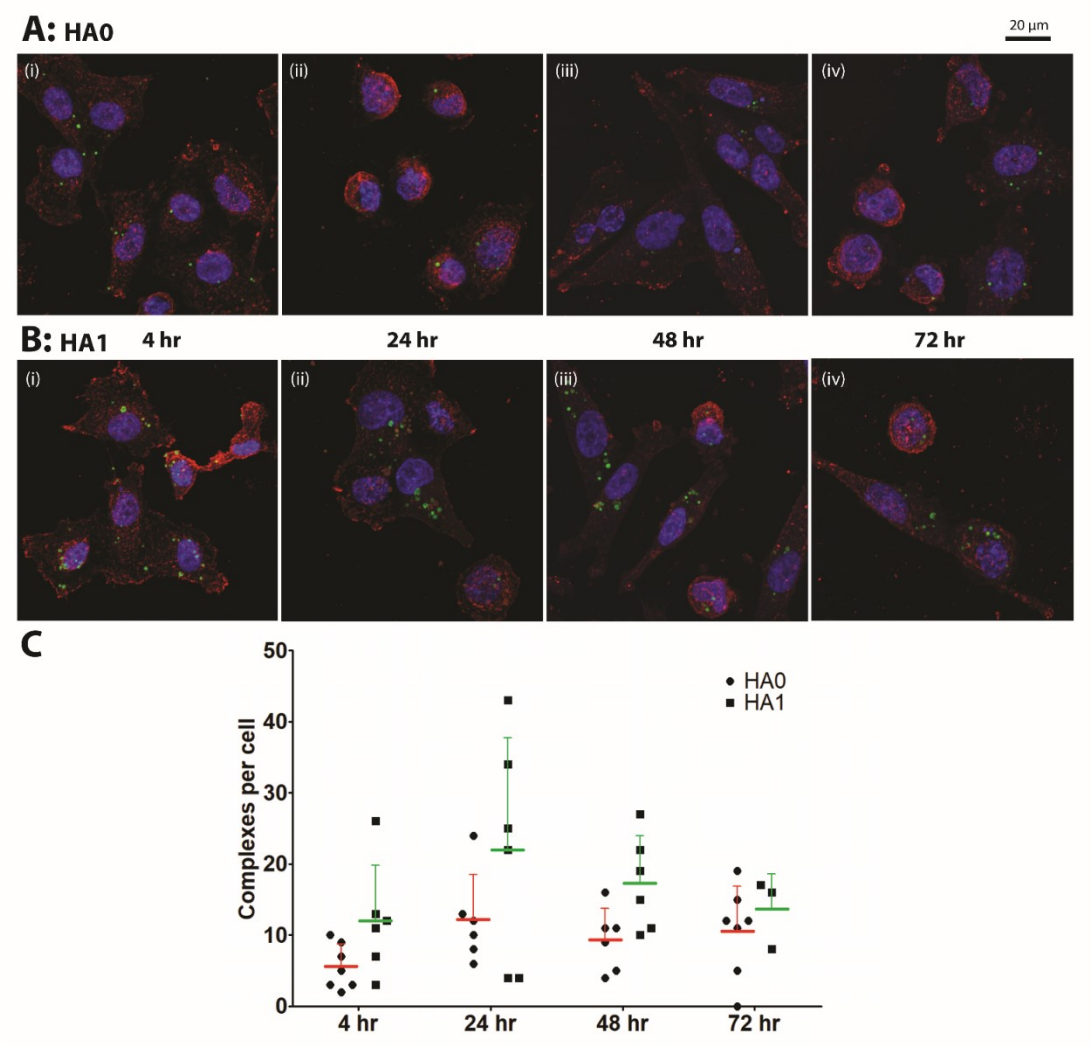

Fig 4.S2: Comparison of cellular uptake of siRNA/polymer complexes with and without HA at different time-points.

MDA-MB-231 cells were transfected with siRNA/PEI-LA without HA **(A)** and siRNA/PEI-LA/HA **(B)** complexes at 1:6:0 and 1:6:1 ratios, respectively. Confocal microscopy was performed after 4, 24, 48 and 72 hr of transfection. The number of complexes per cell was quantitated from confocal microscopy images for each time-point and presented for individual cells as well as the average number of particles in a cell with standard deviation (red and green lines; **C**). Purple, red and green colors in confocal microscopy images represent nuclei, cytoplasm and FAM-labeled siRNA complexes, respectively.

D. Supplementary information for Chapter 5

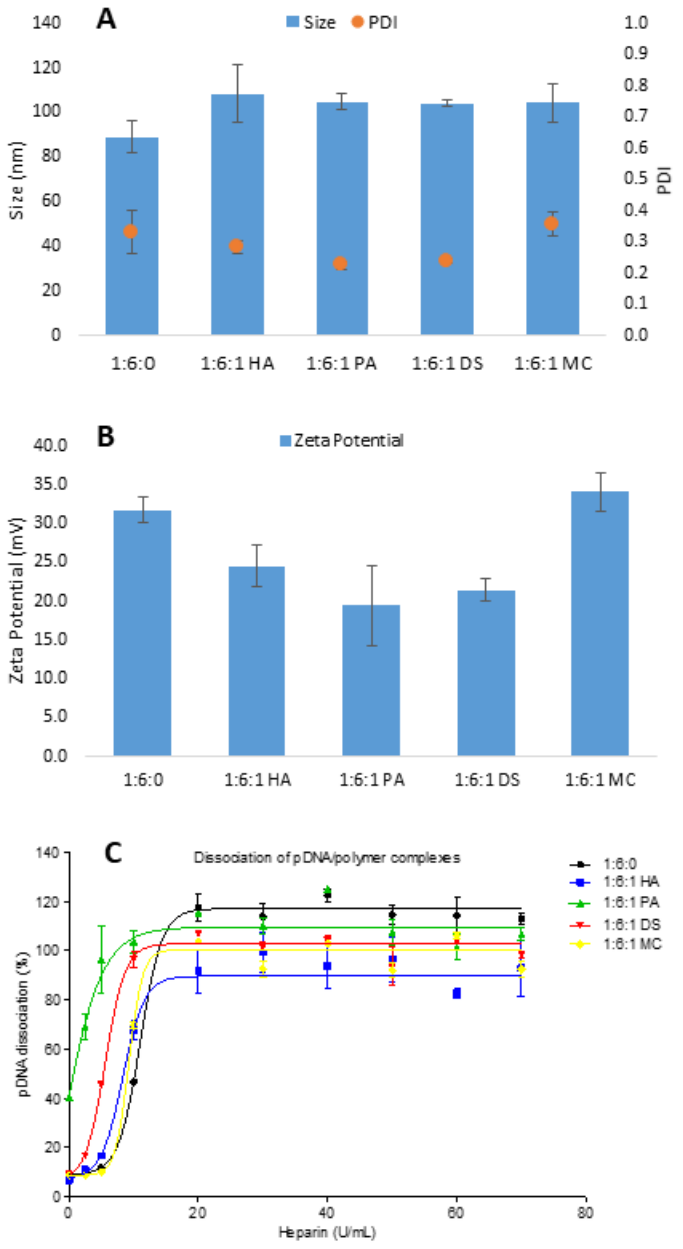

Fig 5.S1: Physicochemical characteristics of pDNA polyplexes.
Size, PDI **(A)**, ζ-potential **(B)** and dissociation **(C)** of pDNA/polymer polyplexes were determined at 1:6:0 and 1:6:1 pDNA:PEI-LA:additive-polymer w/w/w ratios. Additive polymers used here are hyaluronic acid (HA), polyacrylic acid (PA), dextran sulfate (DS) and methyl cellulose (MC).

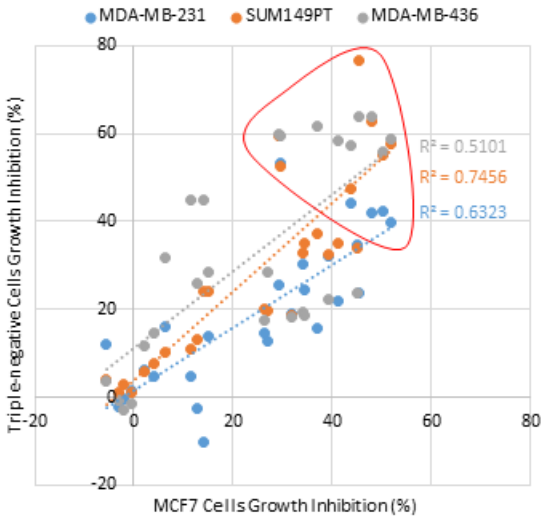

Fig 5.S2: Comparison of siRNA delivery in TNBC vs estrogen/progesterone-positive MCF7 cells.
To determine whether siRNA therapy depends on specific phenotype of cells, the growth inhibition of individual TNBC cells (MDA-MB-231, SUM149PT and MDA-MB-436) was plotted against growth inhibition of MCF7 cells by CDC20 and survivin siRNAs. Dashed lines fit linear regression with indicated R^2 values and points enclosed in the red triangle represent the most effective formulations in both phenotypes.

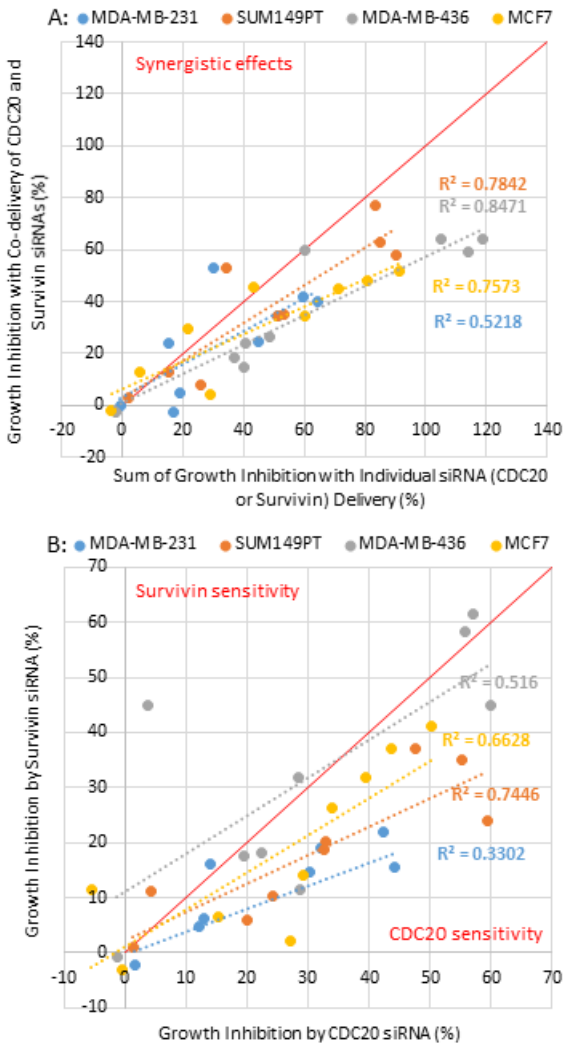

Fig 5.S3: Analysis of CDC20 and survivin correlation in breast cancer cells.
(A) The data from Fig 6 were re-plotted by summing the effects of individual siRNA treatments (as x-axis) vs the effect of co-delivery (y-axis). The synergistic effects were revealed by the data above the red 1:1 line. **(B)** To determine target-specific sensitivity to breast cancer cells, growth inhibition was plotted for individual delivery of CDC20 vs survivin siRNAs.

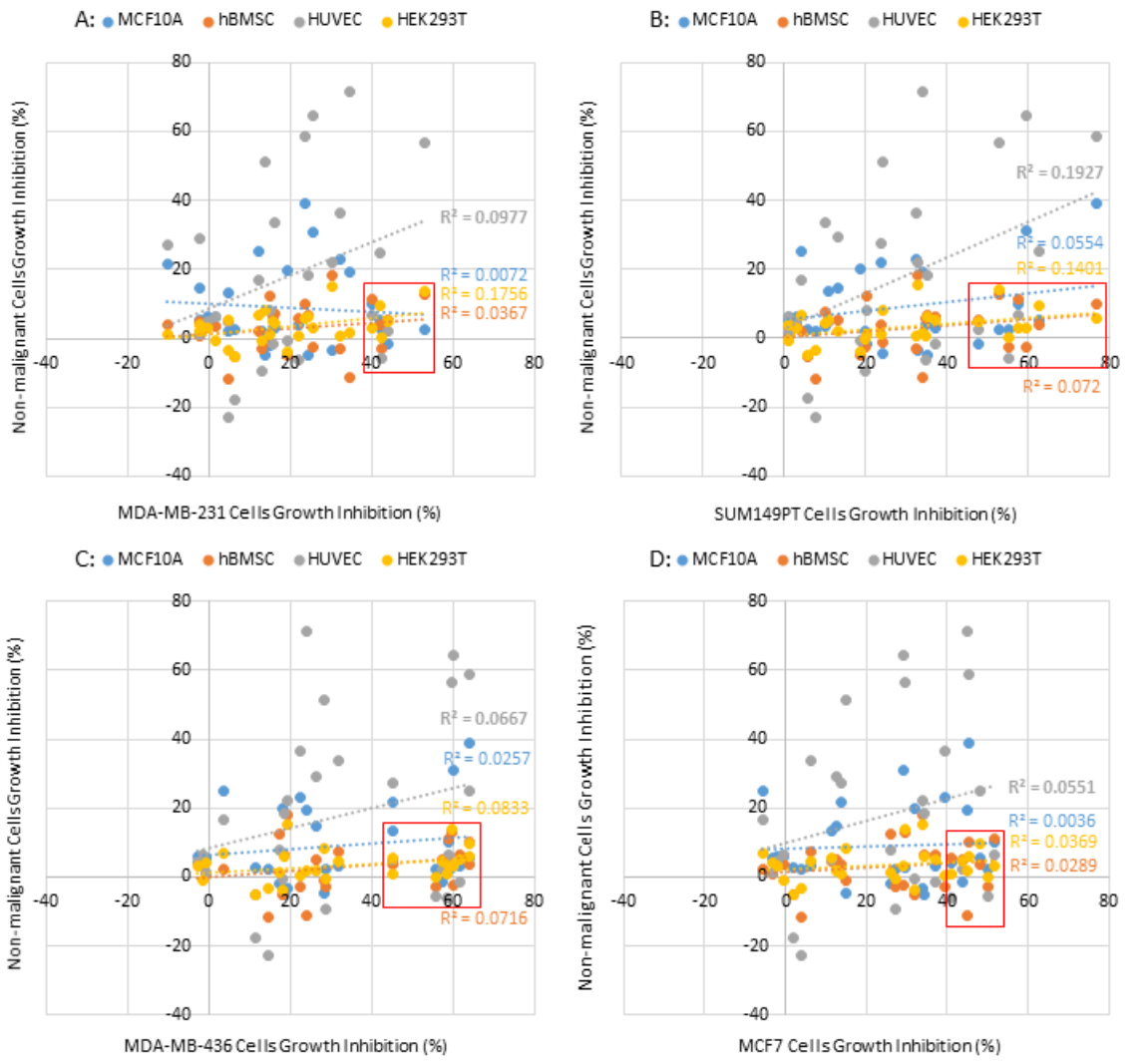

E: Formulations of siRNA/polymer polyplexes that correspond to dots highlighted in red rectangles above. CDC20 | Survivin | CDC20-Survivin

	MDA-MB-231			SUM149PT			MDA-MB-436			MCF7			MCF10A			hBMSC			HUVEC			HEK293T		
1:3:0																								
1:6:0																								
1:9:0																								
1:3:1 HA																								
1:6:1 HA																								
1:9:1 HA																								
1:3:1 PA																								
1:6:1 PA																								
1:9:1 PA																								

Fig 5.S4: Correlation between breast cancer and non-malignant cell growth inhibition.
MDA-MB-231 **(A)**, SUM149PT **(B)**, MDA-MB-436 **(C)** and MCF7 **(D)** cells growth inhibition were plotted against non-malignant cells (MCF10A, hBMSC, HUVEC and HEK293T cells) to identify formulation that decreased the breast cancer cells growth drastically, but poorly affected the growth of non-malignant cells. The identified formulations were shown in red rectangles in **A**, **B**, **C** and **D**, and further highlighted in the table with specific siRNA delivery **(E)**.

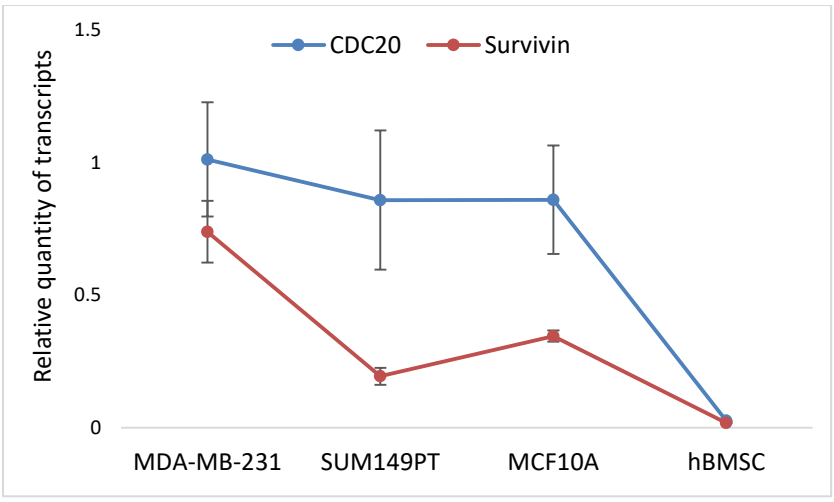

Fig 5.S5: CDC20/Survivin transcripts levels without any treatments.
The transcripts levels were determined in breast cancer (MDA-MB-231 and SUM149PT) and non-malignant (MCF10A and hBMSC) cells.

E. Content License for Fig 1.3

ELSEVIER LICENSE
TERMS AND CONDITIONS

Sep 05, 2018

This Agreement between Mr. Manoj Parmar ("You") and Elsevier ("Elsevier") consists of your license details and the terms and conditions provided by Elsevier and Copyright Clearance Center.

License Number	4422610206253
License date	Sep 05, 2018
Licensed Content Publisher	Elsevier
Licensed Content Publication	Biomaterials
Licensed Content Title	Molecular modeling of polynucleotide complexes
Licensed Content Author	Deniz Meneksedag-Erol,Tian Tang,Hasan Uludağ
Licensed Content Date	Aug 1, 2014
Licensed Content Volume	35
Licensed Content Issue	25
Licensed Content Pages	9
Start Page	7068
End Page	7076
Type of Use	reuse in a thesis/dissertation
Portion	figures/tables/illustrations
Number of figures/tables/illustrations	1
Format	both print and electronic
Are you the author of this Elsevier article?	No
Will you be translating?	No
Original figure numbers	figure 1
Title of your thesis/dissertation	Polymeric delivery of siRNA for breast cancer therapy
Expected completion date	Dec 2018
Estimated size (number of pages)	400
Requestor Location	Mr. Manoj Parmar 8308 - 114 St NW RTF 2-021 Edmonton, AB T6G2V2 Canada Attn: Mr. Manoj Parmar
Publisher Tax ID	GB 494 6272 12
Total	0.00 CAD
Terms and Conditions	